USGS
science for a changing world

MISSISSIPPI ALABAMA FLORIDA

200 m

1,000 m

2,000 m

LOCATION MAP

TEXAS LOUISIANA MISSISSIPPI ALABAMA GEORGIA FLORIDA

AREA SHOWN

Gulf of Mexico

Northeastern Gulf of Mexico Coastal and Marine Ecosystem Program: Ecosystem Monitoring, Mississippi/Alabama Shelf; Third Annual Interim Report

U.S. Department of the Interior
U.S. Geological Survey
Biological Resources Division

MMS

U.S. Department of the Interior
Minerals Management Service
**Gulf of Mexico OCS Region**

USGS
science for a changing world

Contractor Report
USGS/BRD/CR-1999-0005
OCS Study MMS 99-0055

Northeastern Gulf of Mexico Coastal and Marine Ecosystem Program: Ecosystem Monitoring, Mississippi/Alabama Shelf; Third Annual Interim Report

October 1999

PROJECT COOPERATION

This study was procured to meet information needs identified by the Minerals Management Service (MMS) in concert with the U.S. Geological Survey, Biological Resources Division (BRD).

DISCLAIMER

This report was prepared under contract between the U.S. Geological Survey, Biological Resources Division (BRD) and Continental Shelf Associates, Inc. This report has been technically reviewed by the BRD and the MMS, and has been approved for publication. Approval does not signify that the contents necessarily reflect the views and policies of the BRD or MMS, nor does mention of trade names or commercial products constitute endorsement or recommendation for use.

REPORT AVAILABILITY

Extra copies of this report may be obtained from:

U.S. Department of the Interior
U.S. Geological Survey
Biological Resources Division
Eastern Regional Office
1700 Leetown Road
Kearneysville, WV 25430

Telephone: (304) 725-8461 (ext. 675)

U.S. Department of the Interior
Minerals Management Service
Gulf of Mexico OCS Region
Public Information Office (MS 5034)
1201 Elmwood Park Boulevard
New Orleans, LA 70123-2394

Telephone: (504) 736-2519 or
1-800-200-GULF

SUGGESTED CITATION

Contributors

Program Management

Program Manager	David A. Gettleson[1]
Deputy Program Manager	Mahlon C. Kennicutt II[2]
Field Logistics Coordinator	Frederick B. Ayer II[1]
Data Manager	Alan D. Hart[1]
Deputy Data Manager	Gary A. Wolff[2]

Report Editor and Authors

Editor	Neal W. Phillips[1]
Geological Characterization	William W. Sager[2]
	William W. Schroeder[6]
Sediment Dynamics	Ian D. Walsh[5]
Geochemistry	Mahlon C. Kennicutt II[2]
Physical Oceanography/Hydrography	Frank J. Kelly[2]
	Norman L. Guinasso, Jr.[2]
Hard Bottom Communities	Dane D. Hardin[3]
	Keith D. Spring[1]
	Bruce D. Graham[1]
	Stephen T. Viada[1]
Fish Communities	David B. Snyder[1]
Companion Study: Micro-Habitat Studies	Ian R. MacDonald[2]
	Michael Peccini[2]
Companion Study: Epibiont Recruitment	Paul A. Montagna[4]
	Tara Holmberg[4]

Report Production

Technical Editor	Melody B. Powell[1]
Administrative Assistant	Debbie Paul[2]
Word Processing	Deborah V. Raffel[1]
Graphics	Suzanne R. Short[1]
Clerical	Deborah M. Cannon[1]
	Caroline M. Simpson[1]

---

[1]Continental Shelf Associates, Inc.
[2]Texas A&M University
[3]Applied Marine Sciences
[4]University of Texas at Austin
[5]Oregon State University
[6]Independent consultant

Contents

Contents
(continued)

Contents
(continued)

Figures

Figures
(continued)

Tables

Tables
(continued)

Tables
(continued)

Acronyms and Abbreviations

ADCP	Acoustic Doppler Current Profiler
AVHRR	Advanced Very High Resolution Radiometer
BLM	Bureau of Land Management
BP	before present
COTR	Contracting Officer's Technical Representative
CTD	conductivity/temperature/depth
CVAAS	cold vapor atomic absorption spectrophotometry
DO	dissolved oxygen
EOM	extractable organic matter
EPA	Environmental Protection Agency
FAAS	flame atomic absorption spectrophotometry
GC/FID	gas chromatography/flame ionization detection
GC/MS	gas chromatography/mass spectrometry
GFAAS	graphite furnace or flameless atomic absorption spectrophotometry
GIS	geographic information system
GPS	Global Positioning System
INAA	instrumental neutron activation analysis
LATEX	Texas-Louisiana Shelf Circulation and Transport Process Program
LSS	light scattering sensor
mab	meters above bottom
MAFLA	Mississippi-Alabama-Florida
MAMES	Mississippi-Alabama Marine Ecosystems Study
MASPTHMS	Mississippi-Alabama Shelf Pinnacle Trend Habitat Mapping Study
MDL	method detection limit
MMS	Minerals Management Service
NOAA	National Oceanic and Atmospheric Administration
NODC	National Oceanographic Data Center
NTU	nephelometric turbidity unit
OBS	optical backscatter
OCS	outer continental shelf
PAH	polycyclic aromatic hydrocarbon
PAR	photosynthetically active radiation
QA/QC	quality assurance/quality control
RLM	reef-like mound
ROV	remotely operated vehicle
SIM	selected ion monitoring
SOP	standard operating procedure
TAMU	Texas A&M University
TIC	total inorganic carbon
TOC	total organic carbon
TPH	total petroleum hydrocarbons
UCM	uresolved complex mixture
USGS	U.S. Geological Survey
UTC	Coordinated Universal Time

Chapter 1
Executive Summary

This Annual Interim Report summarizes the third year of a four-year program to characterize and monitor hard bottom features on the Mississippi/Alabama outer continental shelf (OCS). The "Northeastern Gulf of Mexico Coastal and Marine Ecosystems Program: Ecosystem Monitoring, Mississippi/Alabama Shelf" is being conducted by Continental Shelf Associates, Inc. and the Geochemical and Environmental Research Group of Texas A&M University, for the U.S. Geological Survey (USGS), Biological Resources Division.

The program consists of an integrated suite of reconnaissance, baseline characterization, monitoring, and process-oriented "companion studies." Based on previous studies and new geophysical reconnaissance, nine hard bottom sites in the Mississippi-Alabama pinnacle trend area have been selected for study (Fig. 1.1). The central focus of the program is monitoring of hard bottom community structure and dynamics. The potential sensitivity of these communities to OCS oil and gas industry activities is of interest to the Minerals Management Service (MMS), the client agency for whom the USGS is administering this program. Other monitoring components (geological and oceanographic processes) are needed to provide an understanding of the dominant environmental processes that control or influence hard bottom community distributional patterns, establishment, and development. These may include substrate characteristics such as relief, microtopography, sedimentology, and contaminant levels, as well as water column characteristics such as temperature, salinity, dissolved oxygen, near-bottom current patterns, and the presence and extent of bottom nepheloid layers. In addition, two companion studies have been designed to complement monitoring by providing information on benthic recruitment and micro-habitat environmental influences on community structure and dynamics.

Objectives

The overall goal of this program is to characterize and monitor biological communities and environmental conditions at carbonate mounds along the Mississippi-Alabama OCS. Specific objectives are as follows:

- To describe and monitor seasonal and interannual changes in community structure and zonation and relate these to changes in environmental conditions (i.e., dissolved oxygen, turbidity, temperature, salinity, etc.); and

- To characterize the geological, chemical, and physical environment of the mounds as an aid in understanding their origin, evolution, present-day dynamics, and long-term fate.

1

Fig. 1.1. Locations of final monitoring sites.
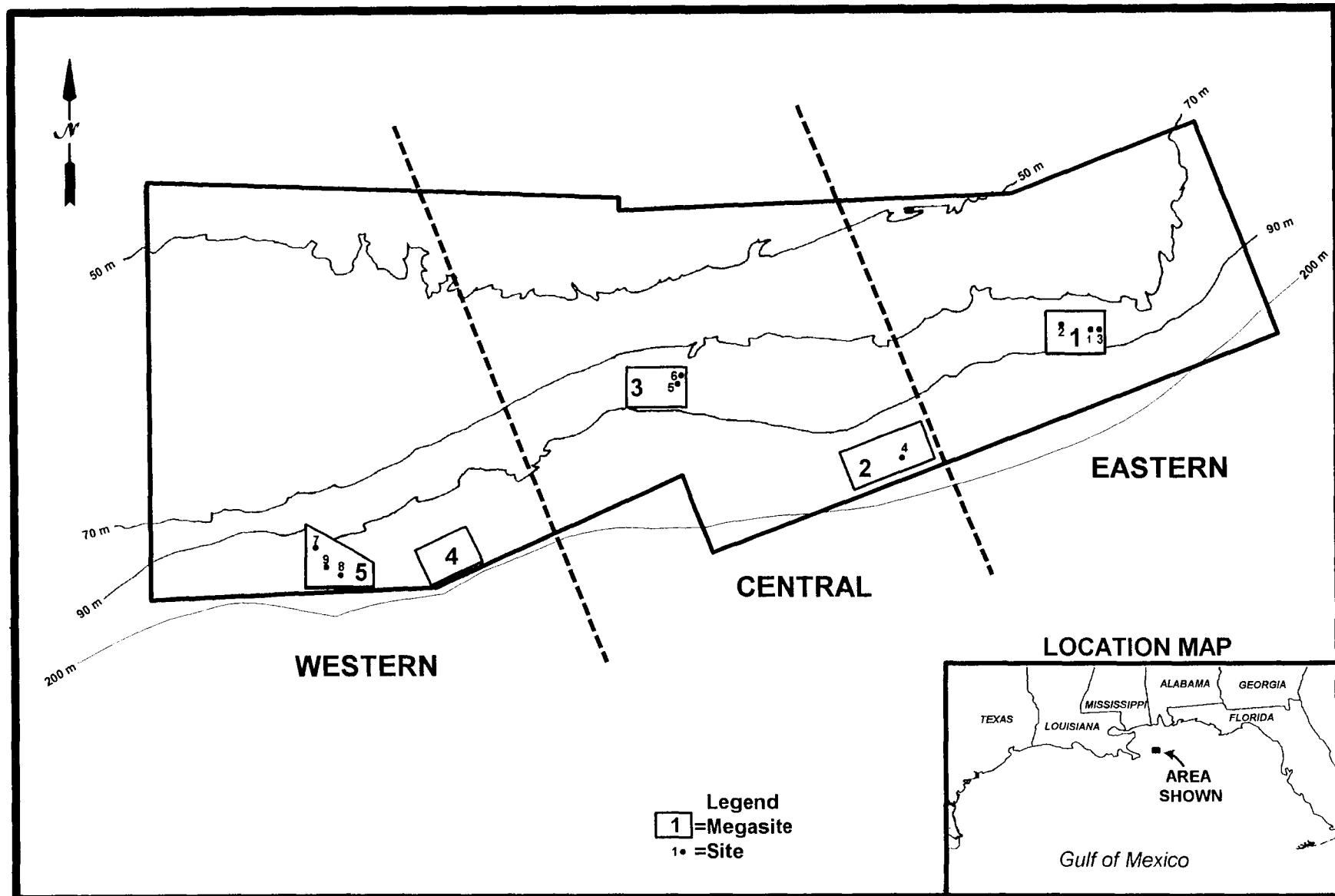
Phases and Cruise Scheduling

The program consists of four phases, each lasting approximately 12 months:

- Phase 1: Reconnaissance, Site Selection, Baseline Characterization, Monitoring, and Companion Studies;
- Phase 2: Monitoring and Companion Studies;
- Phase 3: Monitoring and Companion Studies; and
- Phase 4: Final Synthesis.

Phase 1 included three cruises. Cruise 1A (November 1996) was a geophysical reconnaissance of five megasites containing potential monitoring sites. Cruise 1B (March 1997) was a visual reconnaissance to provide further data on a few candidate sites that had little or no previous video or photographic data. The cruise also field tested the remotely operated vehicle (ROV) and monitoring techniques. Cruise 1C (May 1997), which was conducted after nine final study sites had been selected and approved, was the first of four cruises during which monitoring and companion studies are to be conducted. Activities during this first monitoring cruise included establishing fixed stations, collecting samples and data, and deploying oceanographic and biological moorings.

Phase 2 included two monitoring cruises that revisited the stations established during Cruise 1C. These were Cruise M2 (October 1997) and Cruise M3 (April-May 1998). (Cruise M3 began in April but operations were suspended due to weather delays; it was completed in August 1998.) In addition, mooring service cruises were conducted in July 1997 (S1), January 1998 (S2), and July 1998 (S3).

Phase 3 concluded the field sampling program with two additional mooring service cruises (S4, October 1998; and S5, January-February 1999) and one final monitoring cruise (M4), conducted in two legs. The first leg of Cruise M4 was conducted in April 1999 and included hydrographic profiling and retrieval of all oceanographic moorings. The second leg, completed in July-August 1999, included video and grab sampling of all monitoring stations and retrieval of all remaining biological moorings.

This report is the last of three Annual Interim Reports summarizing the methods and results of Phases 1-3. During Phase 4, a Final Synthesis Report will be produced in which all findings will be summarized, analyzed, synthesized, and discussed in relation to historical data from the region.

Site Selection

The contract specified that a total of nine sites be selected, including high (>10 m), medium (5 to 10 m), and low (<5 m) relief sites in the eastern, central, and western portions of the study area. Other factors considered in site selection were representativeness, availability of existing video and photographic data, and previous oil and gas industry activities. Site selection during Phase 1 involved the following steps:

- *Megasite Selection.* Prior to Cruise 1A, five large areas ("megasites") were selected for geophysical reconnaissance. The selection of the five megasites was based on geophysical data collected during the Mississippi-Alabama Marine Ecosystems Study (MAMES; Brooks 1991) and the Mississippi-Alabama Shelf Pinnacle Trend Habitat Mapping Study (MASPTHMS; Continental Shelf Associates, Inc. 1992). The megasites were selected because they were known to contain numerous features of varying relief (candidate sites) and could be surveyed within the time and financial constraints of the contract.

- *Geophysical Reconnaissance and Preliminary Site Selection.* During Cruise 1A, the five megasites were surveyed using swath bathymetry, high-resolution side-scan sonar, and subbottom profiler to produce detailed maps. After the initial survey of all five megasites, small subsets were chosen for higher resolution mapping. After the cruise, a list of candidate high, medium, and low relief features within the megasites was prepared and the historical video and photographic data were tabulated. At this point, three high relief and two medium relief sites were tentatively selected.

- *Visual Reconnaissance.* Three low relief sites and one medium relief site with little or no previous video or photographic data were identified as needing visual reconnaissance. During Cruise 1B, these features were briefly surveyed using an ROV to determine whether a hard bottom community was present. All of the sites visited during Cruise 1B were ultimately chosen as final sites.

- *Final Site Selection.* After the completion of Cruises 1A and 1B, the program managers and key principal investigators prepared a final site list. Site selection was discussed and approved during a teleconference with the USGS Contracting Officer's Technical Representative, the Scientific Review Board, and the program principal investigators.

Overview of Sampling Program

An overview of the sampling program, including mooring deployments and retrievals at the monitoring sites, is provided in Table 1.1. During Cruise 1C (May 1997), subbottom profiling was conducted to geophysically characterize each site in more detail than was possible with the broad-scale geophysical reconnaissance (Cruise 1A). Grab samples were collected for geological and geochemical analyses (see Chapters 4 and 6). Hydrographic profiling was also conducted at each station, including conductivity/temperature/depth (CTD), dissolved oxygen (DO), photosynthetically active radiation (PAR), transmissivity, and optical backscatter (OBS) (see Chapter 7). Hard bottom and fish community monitoring was conducted at each site using the ROV (see Chapters 8 and 9). Monitoring included random video/photographic transects and stations and establishment of fixed video/photoquadrats. Voucher specimens were also collected at some sites to aid in species identification.

Table 1.1. Summary of activities conducted on each monitoring cruise and mooring service cruise.

Site	1C (May 1997)	S1 (Jul 1997)	M2 (Oct 1997)	S2 (Jan 1998)	M3 (Apr-May 1998)	M3 (Aug 1998)	S3 (Jul 1998)	S4 (Oct 1998)	S5 (Jan-Feb 1999)	M4 Apr 1999	M4 July-Aug 1999
1	P H G V D(3) d(1)	H S(3)	H G V S(3)	H S(3) d(1)	H G V S(1) R(2)	r(1)	H S(1)	H S(1)	H S(1)	H R(1)	H G V r(1)
2	P H G V	--	H G V	--	H G	V					H G V
3	P H G V	--	H G V	--	H G	V					H G V
4	P H G V D(1) d(8)	H S(1)	H G V S(1) r(1)	H S(1) d(1)	H G S(1)	V r(3)^a	H S(1)	H S(1)	H S(1)	H R(1)	H G V r(4)
5	P H G V D(1) d(1)	H S(1)	H G V S(1)	H S(1) d(1)	H S(1) D(2)	G	H S(3)	H S(3)	H S(2) D(1)^b	H R(3)	H G V r(2)^c
6	P H G V	--	H G V	--	H	G					H G V
7	P H G V	--	H G V	--	H	G V					H G V
8	P H G V	--	H G V	--	H	G V					H G V
9	P H G V D(1) d(1)	H S(1)	H G V S(1)	H S(1) d(1)	H S(1)	G V r(1)	H S(1)	H S(1)	H S(1)	H R(1)	H G V r(1)

Abbreviations: P = subbottom profiling D(#) = deploy oceanographic mooring(s) d(#) = deploy biomooring(s)
H = hydrographic profiling S(#) = service oceanographic mooring(s) r(#) = retrieve biomooring(s)
G = grab sampling R(#) = remove oceanographic mooring(s) V = video and photography

^{a} A fourth biomooring was not recovered because it was visibly damaged (no plates remaining).
^{b} Array not recoverable, replacement deployed. Top current meter subsequently found by a fishing boat; data recovered.
^{c} Includes one biomooring that could not be retrieved on Cruise M3 due to turbidity.

The overall program consisted of repeating the Cruise 1C sampling on three subsequent monitoring cruises (M2, M3, and M4). The only exception is the subbottom profiling at each site, which was not repeated.

Six physical oceanographic/sediment dynamics moorings were installed during Cruise 1C (see Chapter 7). Three moorings were installed at Site 1, and one each at Sites 4, 5, and 9. Each site has had at least one oceanographic mooring in place throughout the study. Two of the three moorings at Site 1 were "re-locatable" and were subsequently redeployed at Site 5 on Cruise M3. Each mooring included current meters at 4 and 16 meters above bottom (mab), sediment traps at 2, 7, and 15 mab, and an instrument at 2 mab that measured temperature, conductivity, DO, and turbidity.

Eleven "biomoorings" (moorings containing sets of settling plates) were also deployed during Cruise 1C as part of the companion study of epibiont recruitment (see Chapter 11). Eight were deployed at Site 4 and one each at Sites 1, 5, and 9. The biomoorings at Sites 1 and 9 were retrieved during the second leg of Cruise M3 (August 1998); turbidity prevented retrieval of the Site 5 biomooring. Another set of biomoorings was deployed at the same sites on Cruise S2 (January 1998) and was recovered on the second leg of Cruise M4 (July-August 1999). The eight biomoorings at Site 4 are a "time-series" experiment; the original plan was to retrieve one on each subsequent service cruise and monitoring cruise until all eight were retrieved. However, this was changed so that all biomoorings could be retrieved on monitoring cruises when the ROV was present to cut the anchor line. One Site 4 mooring was retrieved on Cruise M2 (October 1997) and redeployed on Cruise S2 (January 1998). On the second leg of Cruise M3 (August 1998), three of the original Site 4 moorings were recovered, one was found to be damaged (no plates remaining), and the remaining four were recovered on the second leg of Cruise M4 (July-August 1999).

Chapter Summaries

The main body of the Annual Interim Report consists of Chapters 2 to 11. Chapter 2 (Introduction) discusses the rationale and historical background for the program and summarizes program objectives, phases, components, and report contents and organization. Site selection, a sampling program overview, cruise summaries, and data management are described in Chapter 3. The remainder of the report consists of chapters describing the individual components of the program. One-page summaries for Chapters 4 through 11 are presented on the following pages.

Investigators
W. Sager, W. Schroeder

Objectives	Methods
• Characterize the geology and morphology of carbonate mounds • Characterize monitoring sites (bathymetry, topography, sediment texture, etc.)	• Geophysical surveys (high-resolution side-scan sonar, swath bathymetry, subbottom profiler) • Grain size analysis of grab samples • Visual analysis of ROV photographs and videotapes

Data Sets Discussed in this Report

- Geophysical data from Cruises 1A (November 1996) and 1C (May 1997)
- Grain size data from grab samples from Cruise 1C (May 1997), M2 (October 1997), and M3 (April-May and August 1998)
- Geological analysis of ROV photos and videos from Cruise 1C (May 1997), M2 (October 1997), and M3 (April-May and August 1998)

Results and Discussion

The chapter presents summaries of megasite and monitoring site bathymetry, megasite side-scan sonar mosaics, and subbottom profiles. Monitoring sites are characterized geologically based on photos, videotapes, and grab samples. Mound morphology and characteristics are discussed.

From prior MMS-funded surveys, it was known that carbonate mounds were often clustered with sizes ranging from several meters on a side to hundreds of meters wide and 10 to 18 m high. It was also known that areas of high acoustic backscatter were associated with many mounds and that in some cases these areas were preferentially located to the southwest of the mounds. This new study emphasizes and broadens these findings. In addition, a better understanding of the relationship of backscatter to the mounds and the sediment characteristics is being developed.

Although it was known previously that many of the carbonate mounds are subcircular in plan view, new side-scan sonar data show the details of mound flanks and co-occurrences with far-greater resolution than ever before. The data also show that the shelf-edge "pinnacle" mounds are unlike the shallower mounds in that the pinnacle mounds are often irregular or linear in plan view whereas the shallower mounds are usually subcircular in plan view and often made up of clusters of smaller subcircular "unit" mounds. The data also imply a third class of mounds: low, wide, carbonate hard bottoms hundreds of meters in diameter but only a few meters in height. These mounds often have tops with features a few meters or less in height that make them appear to be made up of many smaller "mini-mounds" and in this sense they are similar to many of the other, shallower subcircular mounds.

The morphologic differences among mounds suggest differences in development. The low, wide carbonate hard bottoms imply slow upward growth over a large area, perhaps indicating stable sea level or slow sea level rise. It was previously speculated that such mounds grew at the shelf-edge during the slow sea level rise after the last ice age, but now they are known to be even more widespread. The tall, steep-sided "pinnacle" mounds suggest rapid growth during faster sea level rise. The widely-dispersed, shallower mounds, which are highly variable in size and height, may represent a short period of sea level stabilization in the middle of the deglaciation.

The data also give insights about the location of mound formation. Prior data implied the mounds formed atop erosional unconformities on the two deltas in the MAMES survey area. The new data support this observation. The data also imply that in some places, larger mound groups formed on bathymetric scarps or atop carbonate hard bottoms, implying that the mounds formed where suitable substrates were available.

Subbottom profiles over the mounds frequently show asymmetric profiles, another clue to mound formation. Often large mounds have a peak at the seaward edge and have sediments dammed up on their landward sides. These characteristics suggest that mound growth was most intense on the side facing the sea, where perhaps nutrients are highest and sediments least. This is similar to the formation of coral reefs and lends credence to the hypothesis that mounds were formed by biologic action in shallow water.

Sediments at the monitoring sites are mainly sand, with a small and variable amount of clay. The sand-silt-clay ternary diagram implies two end-members, sand and clay, that are intermixed. Since the sediments currently being deposited in the region are fine clays, this could occur due to resuspension events that mix clay with sand in sediments. A third component consists of gravel-sized fragments, usually shell fragments or other biogenic debris. Gravel content is usually highest near mounds, indicating them as a source or suggesting mound proximity as an important factor controlling the presence of organisms.

Sediment Dynamics (Chapter 5)

Investigator
I. Walsh

Objectives	Methods
• Provide quantitative and qualitative measurements of the extent and occurrence of the nepheloid layer • Determine sedimentation and resuspension rates • Determine how topographic highs affect present-day sedimentation • Determine temporal variations in sediment texture • Relate short-term sediment dynamics to long-term sediment accumulation	• Vertically separated sediment traps (2 m, 7 m, and 15 m above bottom [mab]) • CTD/transmissometer/OBS profiles on each cruise • OBS instruments on current meter arrays • Trace metal, grain size and TOC/TIC analysis of sediment trap samples • ROV observations

Data Sets Discussed in this Report

- Water column profiles: selected data
- Sediment trap data: Bulk fluxes from eight deployment periods, Cruise 1C (May 1997) through M4 Leg 1 (April 1999)

Results and Discussion

The study site is an area of high spatial and temporal variability in particle flux. Some regional trends are apparent. The surface layer was characterized by low salinity and a local maximum in the particle concentration reflecting biological activity during both the October 1997 and January 1998 cruises, with lower salinity and higher particle concentrations encountered in a westward direction. A benthic nepheloid layer (BNL) was present at all sites in all casts, though its intensity as measured by the beam attenuation and the vertical gradient in attenuation was variable. The BNL increased as bottom water temperatures decreased.

Sediment trap results reflect the influence of resuspension at the study sites, with fluxes increasing toward the bottom for all moorings and time periods. The dominant temporal signal in the data set is the extremely high fluxes recorded during period 6 (21 July to 13 October 1998). During this period, Hurricane Georges passed near the mooring sites and energetic currents were recorded. Fluxes during this period were the highest recorded for each site and depth during the study, and ranged from 4 to 70 times the average fluxes exclusive of period 6.

Average fluxes during the study, excluding period 6, ranged from 1.5 to 6 g m^{-2} d^{-1} in the traps 15 mab to 6.7 to 29.3 g m^{-2} d^{-1} in the 2.5 mab traps. Comparing between the sites, the study average fluxes increased from Site 1 to Site 4 to Site 5, with Site 9 essentially the same as Site 5 at 15 and 7 mab but with a lower average flux at 2.5 mab. This trend of increasing fluxes towards the west reflects the trend in the water column particle load discussed above. No seasonal trends are apparent over the study period, which may reflect the dominance of storm and event driven resuspension. Integration of the sediment trap results and the complete water column and physical oceanographic data sets should help constrain the relative importance of the physical forcing functions and seasonality to sedimentation in the study area.

Geochemistry (Chapter 6)

Investigator
M. C. Kennicutt II

Objectives	Methods
• Document the degree of hydrocarbon and trace metal contamination in the benthic environment at each site • Characterize the benthic abiotic environment at each site to aid in determining the origins of sediment and to define the relationship between sediment texture and biological patterns	• Analysis of hydrocarbons [total petroleum hydrocarbons (TPH), extractable organic matter (EOM), polycyclic aromatic hydrocarbons (PAH)], and trace metals (Al, Ba, Cd, Cr, Fe, Hg, Pb, and Zn) in grab samples (Cruise 1C only) • Analysis of total organic carbon (TOC) and total inorganic carbon (TIC) in grab samples • Trace metal and TOC/TIC analysis of sediment trap samples

Data Sets Discussed in this Report

- Grab samples from Cruise 1C (May 1997) analyzed for hydrocarbons and trace metals
- Grab samples from Cruise 1C (May 1997), Cruise M2 (October 1997) and M3 (April-May and August 1998) analyzed for TOC/TIC

Results and Discussion

Measures of sediment hydrocarbons at the sites were low and relatively uniform. Little or no evidence of petroleum related hydrocarbons was observed at any of the nine study sites. The slight increase in EOM and PAH towards the west most likely represents a general fining of sediments. Trace metals indicative of contamination were observed to be at or near background levels at all sites as well. In particular, barium, a tracer of drill mud discharges, was observed to be at background levels with only a very few samples that might be interpreted as slightly elevated. The slight increase in a few metals (Ba, Cr, Fe, Zn) towards the west also most likely represents a general fining of sediments. In conclusion, the sediments collected at the study sites exhibited little or no evidence of a significant history of contamination from drilling related or other activities and only a slight geographic trend in concentrations.

TOC in sediments at the study sites during Cruises 1C, M2, and M3 was low and relatively uniform. In most instances, TOC was less than 0.5%, occasionally reaching 1.0% or more. Sedimentary carbon was primarily in the form of carbonate. TIC ranged from ~3.5% to more than 8% (pure calcium carbonate would be 12% carbon). Carbonate content decreased from east to west by nearly a factor of two, reflecting proximity to riverine inputs of particulate matter.

Investigators	
F. Kelly, N. Guinasso, Jr.	
Objectives	**Methods**
• Characterize regional and local current dynamics • Determine the dynamics of important environmental parameters including temperature, salinity, dissolved oxygen, and turbidity • Define the relationship of current dynamics and environmental parameters to the geological and biological processes of the pinnacle features	• Moored instrument arrays (currents, conductivity, temperature, dissolved oxygen, turbidity, sediment traps) • CTD/DO/transmissivity/PAR/OBS profiles • Collateral data (satellite imagery, meteorological observations, etc.)

Data Sets Discussed in this Report

- Selected hydrographic profiles from Cruise 1C (May 1997) through Cruise M4 Leg 1 (April 1999)
- Selected instrument mooring data from all intervals (May 1997 through April 1999)

Results and Discussion

Current meters at 16 meters above bottom (mab) measured the mesoscale flow just above the pinnacles. Across the entire pinnacle study region there was substantial similarity in the observed flow fields. For the first year, the most frequent direction octant and the direction of the vector mean current were northeast. The most frequent speed range was 5 to 10 cm/s, reflecting the normal tidal influence. Strong currents, i.e., greater than 35 cm/s, were most frequently directed to the southwest. Maximum currents at 16 mab approached 50 cm/s during the first year. The near-bottom (4 mab) flow was more site specific. Bottom friction and the local topography influenced flow. The most frequent direction octants were those with a southerly component. Average scalar speeds were comparable at times to those at 16 mab, and mean vector speeds sometimes exceeded the overlying flow because of greater directionality.

September 1998 was the most unusual month because of several events. Hurricane Earl crossed the eastern side of the study area on September 3 and the eye of Hurricane Georges passed over Site 5 on September 29. Currents were strongest during Hurricane Georges. At 16 mab, speed reached 96.7 cm/s at Site 1. The direction of hurricane driven currents was mainly southwest at Sites 1 and 4, and shifted between southwest and northwest at Sites 5 and 9. Hurricane Earl, which moved more quickly across the shelf, forced a response of about half the intensity forced by Hurricane Georges. Between the two events, an oceanic circulation feature may have intruded onto the shelf. Currents were persistently southwestward during September 11-21 at Sites 1 and 4, with speeds of 15-20 cm/s. This signature was also observed at Site 5 and Site 9 for briefer periods. In the near-bottom currents (4 mab), the response to Hurricane Earl was strongest at Site 1, reaching about 50 cm/s, and almost nonexistent at Site 4. During Hurricane Georges, the near-bottom response was strongest at Site 4, reaching 60 cm/s. The intrusion event between the hurricanes was most evident at Site 4, where current speed at 4 mab exceeded 20 cm/s for eight days. Only during the hurricanes did turbidity values exceed normal background ranges.

Salinity and temperature profiles showed an annual pattern. In May 1997, salinity reached a maximum of about 36.5, which is typical for upper waters of much of the Gulf of Mexico. In the upper water column, profiles at the shallower Sites 5 and 6 exhibited the coolest and freshest water, while profiles at Sites 7, 8, and 9, which are closest to the Mississippi Delta, showed warmer fresh water. In July 1997, all sites showed little influence from fresh water. Fresher waters were again present in October 1997, and all sites showed evidence of cooling. Colder waters in the upper layers were found at Sites 7, 8, and 9 and at Site 4. Warmer fresher waters were found at the other sites. By January 1998, all water temperatures were below 21°C, and maximum salinities also decreased. Bottom salinities at many stations were below 36.0. This correlates well with the lower salinities recorded by the current meters during the third deployment period. In April 1998, the upper waters were slightly warmer and much fresher. The annual pattern was repeated during the second year, except in near surface waters, where salinity variability is large due to the influence of river discharge.

Hard Bottom Communities (Chapter 8)

Investigators
D. Hardin, K. Spring, B. Graham, S. Viada

Objectives	Methods
• Describe hard bottom community structure and seasonal dynamics at each site • Identify differences in hard bottom community structure among sites differing in relief (high/med/low) and location (east/central/west) • Understand relationships between community structure and environmental parameters	• Random video/photographic transects and stations (ROV) • Fixed video/photoquadrats (ROV) • Collection of voucher specimens (ROV)

Data Sets Discussed in this Report

- Videotapes and photographs from Cruises 1C (May 1997) and M2 (October 1997)

Results and Discussion

A total of 1,675 random photoquadrats have been analyzed from Cruises 1C and M2 for the numbers and percent cover of hard bottom organisms. All sites had at least 85 random photoquadrats for analysis from each cruise, except for Site 9 on Cruise 1C, where all but 6 samples were rejected due to turbidity.

Among the 42 numerically dominant taxa, Cnidaria was the most-represented phylum with 10 taxa of octocorals, 5 of ahermatypic corals, 4 of antipatharians, and single taxa of hermatypic corals and actinarians (anemones). Porifera was represented by 7 taxa, followed by Ectoprocta with 5. Among the 40 cover dominants, Cnidaria was represented by 10 taxa of octocorals, 4 of antipatharians, 3 of ahermatypic corals, and a single taxon of hermatypic corals. Porifera was represented by 6 taxa, followed by Echinodermata with 4. Although octocorals were represented by the most taxa in both density and cover, ahermatypic corals had the highest mean abundances (279.33 per m^2) and cover (5.62%), due to the dominance of *Rhizopsammia manuelensis*. Octocorals had the second highest mean density (13.60 per m^2) and cover (3.00%).

Cover varied substantially among sites but not much between cruises. Mean percent cover for ahermatypic corals ranged from 0.03 at Site 1 to 10.96 at Site 7. For antipatharians, cover ranged from 0.04 at Site 1 to 16.18 at Site 4. Octocorals, poriferans, and ectoprocts varied less among sites. Only at Site 6 was there a noticeable difference between Cruises 1C and M2, with an apparent large reduction in the coverage of ectoprocts between cruises. Abundances at high relief sites (Sites 1, 5, and 7) were neither obviously greater nor more diverse than at sites with lower relief.

Little of the biological variation among sites is apparently due to consistent effects of habitat relief. Some taxa were abundant in all relief categories and others varied inconsistently. *R. manuelensis* dominated all relief categories for both cover and density, although it was more abundant in medium and high relief. None of the other dominant taxa in any of the relief categories varied among categories consistent with an effect of relief.

ANOVAs for the effects of relief and region revealed numerous significant effects of each factor, but very few were absent significant interactions, indicating that the effects of relief differed among regions. The only results suggesting a gradient from high to low relief were for cover of all taxa combined. The only results suggesting a gradient from west to east were for densities of *R. manuelensis* and all ahermatypic corals combined.

The lack of significant effects of relief substantiates preliminary results noted in the Second Annual Interim Report. These results contradict those of several previous studies. However, the physical and biological variations within sites may be nearly as large as those between sites. Therefore, an important objective in future analyses will be to account for this within-site variation. While it is likely that physical variables affect the distribution and abundances of hard bottom biota on scales smaller than the defined sampling sites, it is puzzling that the data reveal so few possible effects on broader scales. Future analyses will address these questions.

11

Fish Communities (Chapter 9)

Investigator
D. Snyder

Objectives	Methods
• Describe fish community composition and temporal dynamics at each site • Identify differences in fish community composition among sites differing in relief and location • Understand relationships between fish communities and environmental parameters such as small-scale habitat variability, rock type, sediment cover, etc. • Identify trophic relationships among fishes, as well as between fishes and the epibenthic community	• Analysis of video and photographs from hard bottom community monitoring • Literature review of trophic relationships (in synthesis report)

Data Sets Discussed in this Report

- Videotapes and photographs from Cruises 1C (May 1997), M2 (October 1997), and M3 (April-May and August 1998)

Results and Discussion

Analysis of videotapes and still photographs revealed a total of 73 fish taxa from 32 families. Cruise 1C yielded 44 taxa, Cruise M2 produced 67 taxa, and Cruise M3 produced 63 taxa.

The most speciose families were sea basses (Serranidae), squirrelfishes (Holocentridae), lizardfishes (Synodontidae), jacks (Carangidae), wrasses (Labridae), and butterflyfishes (Chaetodontidae). The most frequently occurring taxa in video transects for the combined cruises were roughtongue bass (*Pronotogrammus martinicensis*), short bigeye (*Pristigenys alta*), bank butterflyfish (*Chaetodon aya*), and red barbier (*Hemanthias vivanus*). Streamer basses (e.g., roughtongue bass and red barbier) probably numerically dominate the pinnacle habitats. These species feed upon plankton and were commonly observed hovering above the substrate picking plankton from the water column. Streamer basses provide forage for a number of piscivorous species (e.g., amberjacks, groupers, sharks, and mackerels).

Although pelagic (e.g., sharks, jacks, bluefish, and king mackerel) and demersal (flounders) fishes also were observed, the ichthyofauna consists primarily of reef fishes. Commonly seen species represent the deep reef fish assemblage reported for water depths of 50 to 100 m in the western Atlantic. Similar species have been reported by previous investigations of the pinnacle features, off the southeastern U.S., within the lower portion of the Algal-Sponge Zone of the West Flower Garden Banks in the northwestern Gulf of Mexico, and near the head of De Soto Canyon. The total number of taxa represents about half of the fish fauna known from the hard banks and reefs of the northern Gulf of Mexico.

The influence of relief category (high, medium, and low relief), location (east, central, west), water depth, and distance from the Mississippi River mouth on fish assemblage composition was examined by correspondence analysis. Overall, there were no strong, consistent relationships. Site 1 had the most distinct species composition and supported the highest richness of reef species. Site 1 is in the high relief category, is the farthest from the Mississippi River mouth, and more importantly, is the shallowest of the study sites. Many fishes observed here, but not at other sites, commonly occur in shallow waters. The different species composition and richness at Site 1 may be due simply to shallow water depth or other unmeasured correlates of shallow water depth rather than distance from the Mississippi River mouth, or relief category.

Companion Study: GIS and Micro-Habitat Studies (Chapter 10)

Investigators
I. MacDonald, M. Peccini

Objectives	Methods
• Integrate physical measurements with biological observations on a micro-habitat scale within study sites • Provide uniform mapping products and geographic tools in support of the overall program	• Geographic information system (GIS) techniques were used to integrate data into consistent map formats and standardized displays • Subsets of bathymetric data were compiled in 300 by 300 m areas centered on the pinnacle(s) within each site. Data were fitted to a 1 m grid. The grids were contoured to provide base maps of each site. • A substratum classification scheme was developed and applied to Site 7 photographs

Data Sets Discussed in this Report
• Video and photographic observations of substrate types and two octocoral species for Site 7 on Cruises 1C (May 1997), M2 (October 1997), and M3 (April-May and August 1998)

Results and Discussion

A substrate classification scheme was applied to all photographs taken during the 1C, M2, and M3 surveys of Site 7, a medium relief site. The objective was to develop a method that adequately and repeatably describes processes which potentially influence faunal distributions and associations within microhabitats. The classification, which is being evaluated and refined, will also be applied to Site 9, a low relief site.

Two octocoral species were chosen for preliminary analysis of substrate associations: *Bebryce* sp., a fan-shaped gorgonian with sparse, stiff arms, and *Antipathes atlantica*, an alcyonarian with a brush-like array of flexible, many-branched arms. These colonial animals were common at Site 7, were readily identifiable in the photos and, due to their different growth form, they might be expected to occupy different microhabitats. Using the GIS, colony numbers of *Bebryce* sp. and *A. atlantica* in random photo stations at Site 7 were plotted, and bathymetric contours at 1-m intervals were overlain with regions of contiguous substrata. The numbers of *Bebryce* sp. colonies were higher than those of *A. atlantica*. Both species were almost entirely absent from the sedimented flat region surrounding the Site 7 pinnacle and had the greatest density in the continuous hard bottom region on the pinnacle top.

Substrate associations were tested objectively by examining the spatial distribution of the two octocoral species within Site 7. Indices that distinguish clumped from random distribution were calculated, first for the total area of Site 7, then for photos from combined subareas of "continuous hard bottom and monolithic outcrops," then separately for subareas of "continuous hard bottom" and "monolithic outcrops." Neither species approached a random distribution of individuals, with *Bebryce* showing greater clumping than *A. atlantica*. Individuals of *Bebryce* were clumped in all subareas. One index (Ludwig and Reynolds '*d*') suggested that *A. atlantica* had a random distribution within the region of "continuous hard bottom" at Site 7, which approximates the pinnacle top. The interpretation is that the "continuous hard bottom" designation adequately describes the microhabitat for *A. atlantica*. The distribution of *Bebryce* colonies appeared less clumped within the "continuous hard bottom" subarea than in Site 7 as a whole, but still was not random. Therefore, *Bebryce* appears to have some preference which is not captured by the substrate classification.

13

Companion Study: Epibiont Recruitment (Chapter 11)

Investigators
P. Montagna, T. Holmberg

Objectives	Methods
• Document the process of larval settlement, growth, and community development of hard bottom epibiota • Test hypotheses about the effects of location, height above bottom, duration of deployment, surface texture, predation, and water flow on recruitment	Settling plates are attached to "biomoorings." Major elements of the settling plate experiment studies are: 1. Spatial study with biomoorings at four sites (1, 4, 5, and 9) from May 1997 to August 1998 and again from January 1998 to July-August 1999 2. Time series study at Site 4, with eight biomoorings deployed initially (May 1997), one retrieved in October 1997 and redeployed in January 1998, four retrieved in August 1998, and the remaining four retrieved in July-August 1999 3. Two settling surface treatments: hard and soft 4. Three heights above bottom (0 m, 2 m, 13 m) 5. Three settling plate treatments: uncaged (U), caged (C), and partially caged (P)

Data Sets Discussed in this Report
• 6 month deployment at Site 4 -- Cruise 1C (May 1997) to Cruise M2 (October 1997). • 16 month deployment at Sites 4 and 9 -- Cruise 1C (May 1997) to Cruise M3 (August 1998)

Results and Discussion

Preliminary analyses of temporal and spatial differences have been completed. Due to misidentification of a hydroid as a bryozoan, many of the samples will have to be reanalyzed and have not been included in this report. All samples from Site 9 and several from Site 4 have been completed and are reported, although no firm statistics have been performed for the second year due to an insufficient number of total samples. Also, due to shackle failure, all of the biomoorings retrieved to date have been recovered from the seafloor. Therefore, no analysis of the effect of height above bottom is possible.

The results of the first 6-month exposure at Site 4 are reported again here due to reanalysis of the samples. There were no significant differences in coverage between treatments except for molluscs, which had higher coverage in caged and partially caged treatments. The category 'uncolonized' accounted for much of the total coverage of the plates after 6 months. Densities were also analyzed for several solitary organisms.

Comparisons of 6-month and 16-month data at Site 4 indicate that significant changes took place in mean coverages. All organisms occupied more space by the second year, except for the stolons of the colonial organisms. There was no uncolonized space free for recruitment by the second year. Abundant categories in the 16-month data from Site 4 were stolons (of colonial organisms), bryozoans, rhizopods, and annelids.

The 16-month biomoorings at Site 4 and Site 9 were compared to evaluate spatial differences among sites. The only striking differences are for annelids, which were four times greater at Site 4, and molluscs, which were almost 10 times greater at Site 9. Anthozoans were consistently present only at Site 9.

Mathematical combinations of the experimental treatments were used calculate the effects on rates of recruitment by ecological processes of predation, water flow, and gross recruitment. Ecological processes do not seem to have very similar effects among sites, but final statistical analysis of all the corrected samples are necessary to determine final conclusions.

Chapter 2
Introduction

This Annual Interim Report summarizes the third year of a four-year program to characterize and monitor hard bottom features on the Mississippi/Alabama outer continental shelf (OCS). The study area is shown in Fig. 2.1. The "Northeastern Gulf of Mexico Coastal and Marine Ecosystems Program: Ecosystem Monitoring, Mississippi/Alabama Shelf" is being conducted by Continental Shelf Associates, Inc. and the Geochemical and Environmental Research Group of Texas A&M University, for the U.S. Geological Survey (USGS), Biological Resources Division.

The program consists of an integrated suite of reconnaissance, baseline characterization, monitoring, and process-oriented "companion studies." Based on previous studies and new geophysical reconnaissance, nine hard bottom sites in the Mississippi-Alabama pinnacle trend area were selected for monitoring. The central focus of the program is monitoring of hard bottom community structure and dynamics. The potential sensitivity of these communities to OCS oil and gas industry activities is of interest to the Minerals Management Service (MMS), the client agency for whom the USGS is administering this program. Other monitoring components (geological and oceanographic processes) provide an understanding of the dominant environmental processes that control or influence hard bottom communities. These include substrate characteristics such as relief, microtopography, sedimentology, and contaminant levels, as well as water column characteristics such as temperature, salinity, dissolved oxygen, near-bottom current patterns, and the presence and extent of the bottom nepheloid layer. In addition, two companion studies complement monitoring by providing information on key ecological processes such as benthic recruitment, growth, and community dynamics.

Objectives

The overall goal of this program was to characterize and monitor biological communities and environmental conditions at carbonate mounds along the Mississippi-Alabama OCS. Specific objectives were as follows:

- To describe and monitor seasonal and interannual changes in community structure and zonation and relate these to changes in environmental conditions (i.e., dissolved oxygen, turbidity, temperature, salinity, etc.); and

- To characterize the geological, chemical, and physical environment of the mounds as an aid in understanding their origin, evolution, present-day dynamics, and long-term fate.
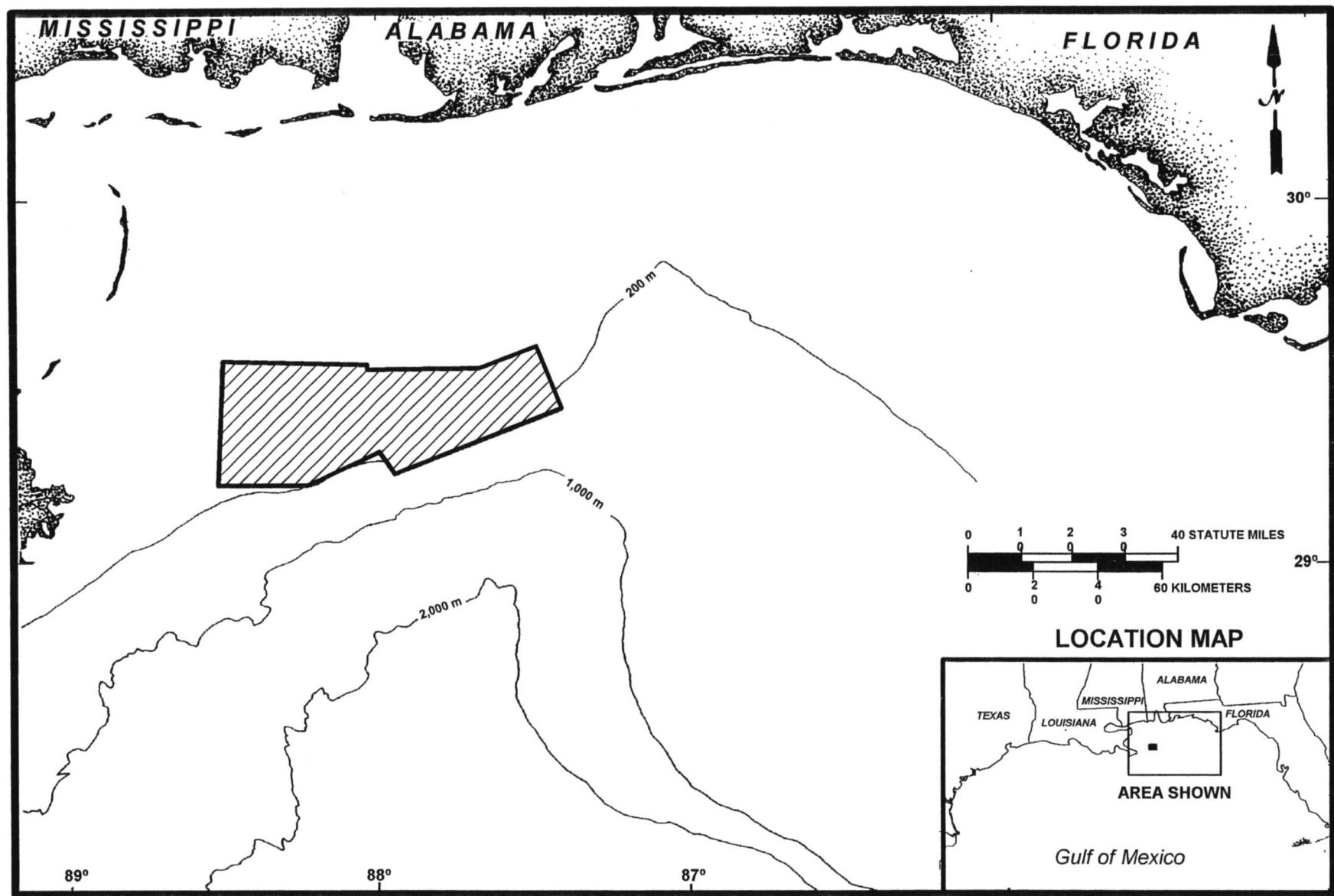
Fig. 2.1. Study area.

Phases

The program consists of four phases, each lasting approximately 12 months:

- Phase 1: Reconnaissance, Site Selection, Baseline Characterization, Monitoring, and Companion Studies;
- Phase 2: Monitoring and Companion Studies;
- Phase 3: Monitoring and Companion Studies; and
- Phase 4: Final Synthesis.

The flow of events is summarized in Fig. 2.2 and the schedule is given in Fig. 2.3. Phase 1 included two reconnaissance cruises (Cruise 1A, November 1996; and Cruise 1B, March 1997) followed by final site selection (April 1997) and the initiation of monitoring and companion studies on Baseline Characterization and Monitoring Cruise 1C (May 1997).

Phase 2 included two monitoring cruises, M2 (October 1997) and M3 (April-May 1998). (Cruise M3 began in April but was shut down due to weather delays; it was completed in August 1998.) In addition, mooring service cruises were conducted in July 1997 (S1), January 1998 (S2), and July 1998 (S3).

Phase 3 concluded the field sampling program with two additional mooring service cruises (S4, October 1998; and S5, January-February 1999) and one final monitoring cruise (M4), conducted in two legs. The first leg of Cruise M4 was conducted in April 1999 and included hydrographic profiling and retrieval of all oceanographic moorings. The second leg, conducted in July-August 1999, included video and grab sampling of all monitoring stations and retrieval of all remaining biological moorings.

This report is the last of three Annual Interim Reports summarizing the methods and results of Phases 1-3. During Phase 4, a Final Synthesis Report will be produced in which all findings will be summarized, analyzed, synthesized, and discussed in relation to historical data from the region.

Components

The program consists of an integrated suite of monitoring and process-oriented companion studies conducted at the nine sites during Monitoring Cruises 1C, M2, M3, and M4. Table 2.1 summarizes the monitoring components and companion studies, including objectives, methods, and principal investigators.

Four monitoring components form the core of the program. These are hard bottom communities, fish communities, geology/sediment dynamics/geochemistry, and physical oceanography/hydrography. Hard bottom and fish community monitoring consists mainly of video and photographic sampling at each site. Geophysical surveys and data from laboratory analysis of grab samples and rock collections are being used to

PHASE 1

Reconnaissance and Site Selection

Cruise 1A

Cruise 1B

Final Site Selection

Data Analysis and Interpretation

First Annual Interim Report

Baseline Characterization

Cruise 1C

preliminary

PHASE 2

Monitoring and Companion Studies

Cruise M2

Cruise M3

preliminary

Data Analysis and Interpretation

Second Annual Interim Report

PHASE 3

Cruise M4

preliminary

Data Analysis and Interpretation

Third Annual Interim Report

PHASE 4

Final Synthesis

Synthesis Meeting

Final Data Analysis and Interpretation

Final Synthesis Report

Fig. 2.2. Program flow chart.

MILESTONE	1996	1997	1998	1999	2000	2001
	O N D	J F M A M J J A S O N D	J F M A M J J A S O N D	J F M A M J J A S O N D	J F M A M J J A S O N D	J F
Contract Award	●					
Phase 1 - Reconnaissance, Baseline, and Monitoring		PHASE 1				
Cruise 1A - (Reconnaissance - Geophysical Mapping)						
Cruise 1B - (Reconnaissance - Visual)						
Final Site Selection						
Baseline Characterization and Monitoring Cruise 1C						
Mooring Service Cruise S1						
Draft/Final Annual Interim Report (Year 1)						
Phase 2 - Monitoring			PHASE 2			
Monitoring Cruise M2						
Mooring Service Cruise S2						
Monitoring Cruise M3 (two legs)						
Mooring Service Cruise S3						
Draft/Final Annual Interim Report (Year 2)						
Phase 3 - Monitoring				PHASE 3		
Mooring Service Cruise S4						
Mooring Service Cruise S5						
Monitoring Cruise M4 (two legs)						
Draft/Final Annual Interim Report (Year 3)						
Phase 4 - Final Interpretation and Synthesis					PHASE 4	
Synthesis Meeting						
Final Data Interpretation/Synthesis						
Draft/Proof/Final Synthesis Report						

Fig. 2.3. Program schedule and milestones.

Table 2.1. Summary of program components.

Component	Objectives	Methods	Principal Investigators
Geology/Sediment Dynamics/Geochemistry			
Site Characterization	• Define seafloor topography at/around each site • Determine how topographic highs affect sediment distribution • Geologic characterization of sites, including composition, origin, probable fate, roughness, and friability • Determine subtle differences of orientation, size, and morphology • Characterize substrate • Determine the distribution of sediment types	• Geophysical surveys (high-resolution side-scan sonar, swath bathymetry, subbottom profiler) • Grain size analysis of grab samples • Visual and laboratory analysis of photographs and rock samples • Analysis of rock samples (thin section petrography, x-ray diffractometry, scanning electron microscopy, electron microprobe, stable isotopes, ^{14}C dating)	W. Sager W. Schroeder D. Benson
Mound History	• Determine the origin of calcareous mounds • Determine developmental history of the mounds • Predict the future fate of the mounds	• ROV rock collections • Analyze using thin section petrography, x-ray diffractometry, scanning electron microscopy, electron microprobe, stable isotopes, ^{14}C dating	W. Sager W. Schroeder
Sediment Dynamics	• Provide quantitative and qualitative measurements of the extent and occurrence of the nepheloid layer • Determine sedimentation and resuspension rates • Determine how topographic highs affect present-day sedimentation • Determine temporal variations in sediment texture • Relate short-term sediment dynamics to long-term sediment accumulation	• Vertically separated sediment traps • CTD/transmissometer/OBS profiles • Optical instruments on moored arrays • ROV observations • Trace metal and grain size analysis of sediment trap samples	I. Walsh
Sediment Geochemistry	• Degree of hydrocarbon and trace metal contamination in the benthic environment at each site	• Hydrocarbon and trace metal analysis of grab samples (Phase 1) • TOC/TIC analysis of grab samples and sediment trap samples	M. Kennicutt
Physical Oceanography/ Hydrography	• Characterize the regional and local current dynamics in the study area • Determine the dynamics of important environmental parameters including temperature, salinity, dissolved oxygen, and turbidity. • Define the relationship of the current dynamics and environmental parameters to the geological and biological processes of the pinnacle features.	• Moored instrument arrays (currents, suspended sediments, conductivity, temperature, and dissolved oxygen, sed. traps) • CTD/DO/transmissivity/OBS profiles • Meteorological observations • Collateral data (satellite imagery, etc.)	F. Kelly N. Guinasso

Table 2.1. (continued).

Component	Objectives	Methods	Principal Investigators
Hard Bottom Communities	• Describe hard bottom community structure and seasonal dynamics at each site • Describe differences in hard bottom community structure among sites differing in relief (high/med/low) and location (east/central/west) • Describe relationships between community structure and environmental parameters such as small-scale habitat variability, rock type, sediment cover, turbidity, and other geologic and oceanographic variables	• Random video/photographic transects and stations (ROV) • Fixed video/photoquadrats (ROV) • Collection of voucher specimens (ROV)	D. Hardin K. Spring B. Graham S. Viada
Fish Communities	• Describe fish community composition and temporal dynamics at each monitoring site • Identify differences in fish community composition among sites differing in relief and location • Identify relationships between fish communities and environmental parameters such as small-scale habitat variability, rock type, sediment cover, etc. • Identify trophic relationships among fishes, as well as between fishes and the epibenthic community	• Analysis of video and photographs from hard bottom community monitoring (ROV) • Literature review of trophic relationships	D. Snyder
Companion Study #1 Micro-Habitat Studies	• Improved understanding of relationships between hard bottom epibiota and microhabitat factors (e.g., microtopography, orientation, substrate characteristics, small-scale current patterns)	• Use of GIS to integrate and analyze biotic and abiotic data collected during hard bottom community monitoring	I. MacDonald M. Peccini
Companion Study #2 Epibiont Recruitment	• Document process of larval settlement, growth, and community development of hard bottom epibiota	• Settling plates on moored arrays; experimental enclosures to evaluate predation and disturbance	P. Montagna T. Holmberg

Abbreviations: CTD = conductivity/temperature/depth; DO = dissolved oxygen; OBS = optical backscatter; ROV = remotely operated vehicle.

characterize the seafloor topography, sedimentology, and geochemistry (including contaminant levels) at each site and to help understand the origin, developmental history, and probable fate of the pinnacle features. The geological component also includes monitoring of nepheloid layer dynamics using sediment traps, transmissometer and optical backscatter profiles, and optical instruments on moored arrays. Physical oceanographic and hydrographic data are also collected to help understand the geological and biological processes of the pinnacle features. Data from moored instrument arrays, hydrographic profiles, and collateral sources provide a basis for characterization of regional and local current dynamics and help to understand the dynamics of important environmental parameters including temperature, salinity, dissolved oxygen, and turbidity. Currents and hydrographic variables are potentially important direct and indirect influences on hard bottom communities and could account for differences both within and between sites.

The two companion studies are designed to complement monitoring by providing information on key ecological processes such as benthic recruitment, growth, and community dynamics. The first, Micro-Habitat Studies, involves independent analysis of photographs and video collected during hard bottom community monitoring in relation to geological and oceanographic data. The analysis focuses on fine-scale factors such as microtopography, orientation, substrate characteristics, small-scale current patterns, and gradients in chemical contaminants. Techniques include statistical analysis, modeling, and fine-scale mapping using geographic information systems (GIS). The second companion study focuses on Epibiont Recruitment. Through the use of settlement plates deployed on moored arrays, this study documents the process of larval settlement, growth, and community development of hard bottom epibiota. Experimental enclosures were used to evaluate effects of predation and disturbance.

Report Contents and Organization

This report covers the approach, rationale, and methods for all work to date and includes data that have been analyzed and interpreted as of July 1999. This includes results from Monitoring Cruises 1C (May 1997), M2 (October 1997), M3 (April and August 1998), and the first leg of M4 (April 1999), as well as mooring retrievals on Service Cruises S1 (July 1997) and S2 (January 1998), S3 (July 1998), S4 (October 1998), and S5 (January-February 1999). Data from the second leg of Cruise M4 (July-August 1999) were not available in time for this report.

Following this introduction, Chapter 3 describes Site Selection and General Methods. Subsequent chapters present the rationale, field and laboratory methods, results, and discussion for each monitoring component and companion study.

Chapter 3
Site Selection and General Methods

Detailed methods for each program component are included in the individual chapters. As a general framework, this chapter first discusses site selection. An overview of the sampling program is then presented, followed by cruise summaries for Phase 3. Finally, data management is discussed.

Site Selection

The contract specified that a total of nine sites be selected, including high (>10 m), medium (5 to 10 m), and low (<5 m) relief sites in the eastern, central, and western portions of the study area. Other factors considered in site selection were representativeness, availability of existing video and photographic data, and previous oil and gas industry activities. Site selection during Phase 1 involved the following steps:

- *Megasite Selection.* Prior to Cruise 1A, five large areas ("megasites") were selected for geophysical reconnaissance (Fig. 3.1). The selection of the five megasites was based on geophysical data collected during the Mississippi-Alabama Marine Ecosystems Study (MAMES; Brooks 1991) and the Mississippi-Alabama Shelf Pinnacle Trend Habitat Mapping Study (MASPTHMS; Continental Shelf Associates, Inc. 1992). The megasites were selected because they were known to contain numerous features of varying relief (candidate sites) and could be surveyed within the time and financial constraints of the contract.

- *Geophysical Reconnaissance and Preliminary Site Selection.* During Cruise 1A, the five megasites were surveyed using swath bathymetry, high-resolution side-scan sonar, and subbottom profiler to produce detailed maps. After the initial survey of all five megasites, small subsets were chosen for higher resolution mapping. After the cruise, a list of candidate high, medium, and low relief features within the megasites was prepared and the historical video and photographic data were tabulated. At this point, three high relief and two medium relief sites were tentatively selected.

- *Visual Reconnaissance.* Three low relief sites and one medium relief site with little or no previous video or photographic data were identified as needing visual reconnaissance. During Cruise 1B, these features were briefly surveyed using a remotely operated vehicle (ROV) to determine whether a hard bottom community was present. All sites visited during Cruise 1B were ultimately chosen as final sites.

- *Final Site Selection.* After the completion of Cruises 1A and 1B, the program managers and key principal investigators prepared a final site list. Site selection was discussed and approved during a teleconference with the USGS Contracting Officer's Technical Representative, the Scientific Review Board, and the program principal investigators. The final sites are shown in Fig. 3.2 and summarized in Table 3.1.
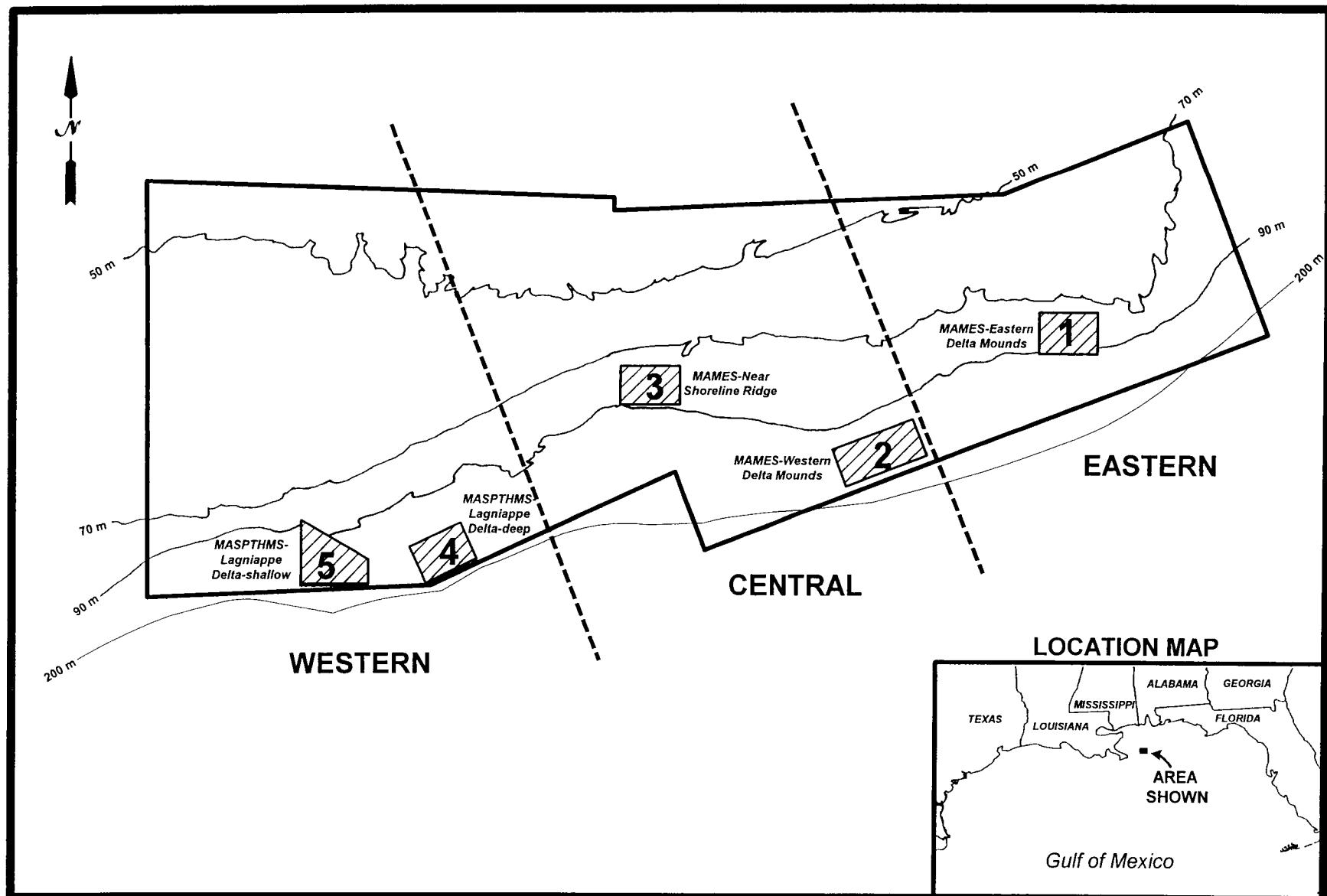
Fig. 3.1. Geographic locations of megasites surveyed during Cruise 1A.

WESTERN

CENTRAL

EASTERN

50 m

70 m

90 m

70 m

90 m

50 m

200 m

200 m

LOCATION MAP

TEXAS

LOUISIANA

MISSISSIPPI

ALABAMA

GEORGIA

FLORIDA

AREA
SHOWN

Gulf of Mexico

Legend

1 =Megasite

1• =Site
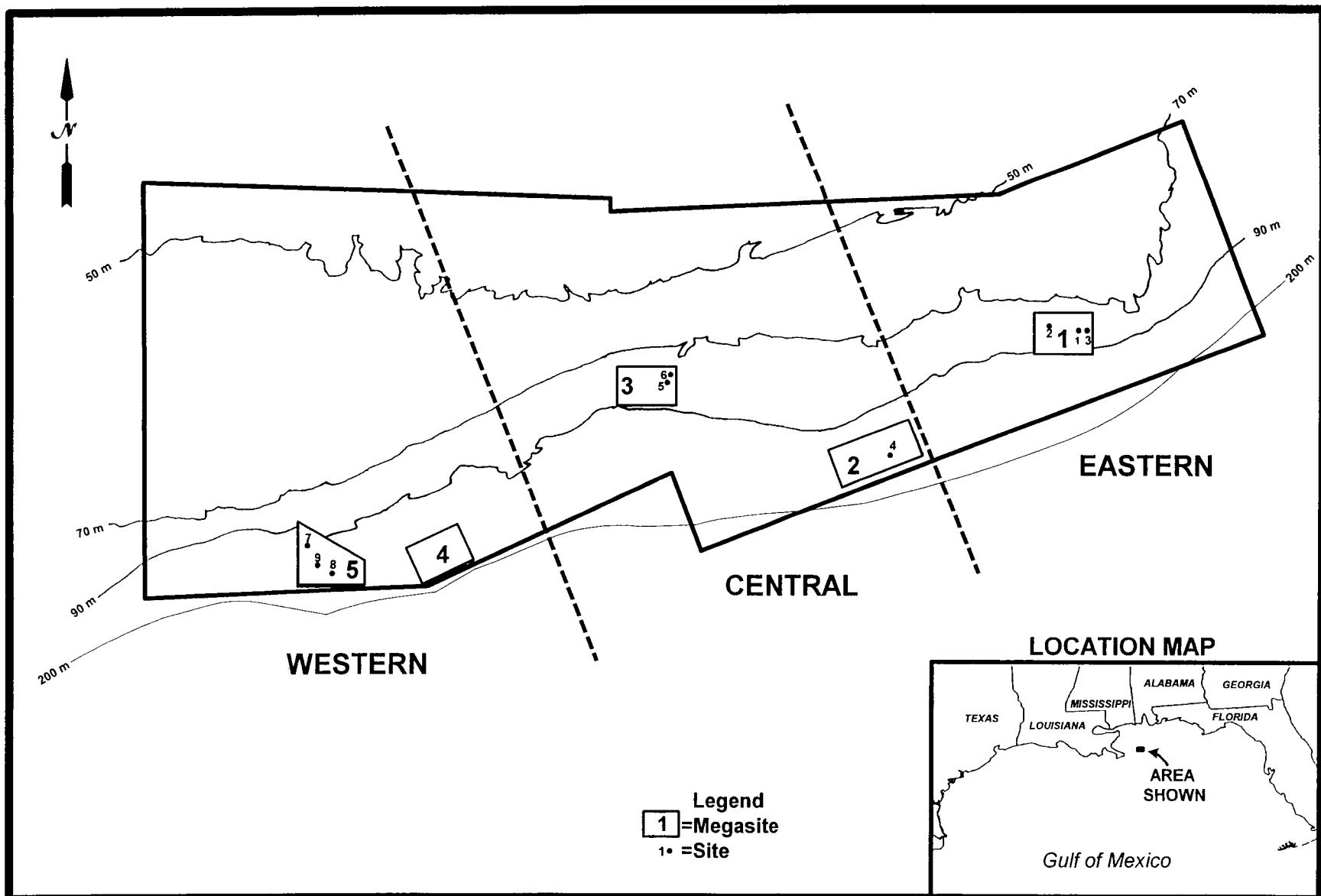
Fig. 3.2. Locations of final monitoring sites.

Table 3.1. Final monitoring sites.

Site	Area and Megasite	Relief Category	Water Depth and Lat/Long	OCS Lease Block	Previous Video and/or Photographic Data	Notes
1	Eastern (Megasite 1)	High	63-76.5 m 29°26'19.131"N 87°34'27.273"W	Destin Dome Block 533	MAMES Video Stations 13 and 14	Site diameter 200 m. Large, flat-top feature known as 40 Fathom Fishing Grounds. Site extends across top of mound and down the steep northeastern flank toward a flat seafloor
2	Eastern (Megasite 1)	Medium	69.5-81.5 m 29°26'41.053"N 87°36'26.512"W	Destin Dome Block 532	None	Site diameter 120 m. Bathymetry data show a mainly flat seafloor at a depth of about 77 to 78 m with a medium-sized mound about 50 m in diameter along the southern edge of the site. The mound is more than 5 m in height
3	Eastern (Megasite 1)	Low	76-80.3 m 29°26'15.901"N 87°34'15.266"W	Destin Dome Block 533	None. First visited during Cruise 1B on 24 March 1997	Site diameter 150 m. Patchy low relief rock outcrops with diameters ranging from 1 to 10 m and relief ranging from <1 to 4.5 m
4	Central (Megasite 2)	Medium	95-107 m 29°19'39.041"N 87°46'7.849"W	Destin Dome Block 661	MAMES Video Station 18 is in general area	Site diameter 140 m. Mound is about 10 m in height with a northwest trending ridge on its northwest side and a relatively flat top. On top, hard bottom with thin sand veneer and low relief rock outcrops (0.5 to 2 m)
5	Central (Megasite 3)	High	62-78 m 29°23'35.930"N 87°58'51.055"W	Main Pass Block 223	MAMES Video Station 8 is in general area	Site diameter 160 m. Tall, flat-top mound near the center and a lower mound at the southwest edge of the area. Smaller outcrops along edges of mound

Table 3.1. (continued).

Site	Area and Megasite	Relief Category	Water Depth and Lat/Long	OCS Lease Block	Previous Video and/or Photographic Data	Notes
6	Central (Megasite 3)	Low	75-78 m 29°23'52.887"N 87°58'42.610"W	Main Pass Block 249	None. First visited during Cruise 1B on 23 March 1997	Site diameter 150 m. Extensive areas of low-relief rock features ranging up to about 1 m in height on a relatively flat seafloor and covered with a thin layer of fine sediments
7	Western (Megasite 5)	High	69.5-88 m 29°15'24.844"N 88°20'21.455"W	Main Pass Block 286	MAMES Video Station 33; MASPTHMS ROV Dives 1, 2, and 3	Site diameter 200 m. Large, flat top mound known as 36 Fathom Ridge, elongated north-south. Feature has more irregular edges than the two other flat top mounds (Sites 1 and 5)
8	Western (Megasite 5)	Medium	88-96 m 29°13'53.857"N 88°19'01.565"W	Main Pass Block 285	None. First visited during Cruise 1B on 23 March 1997	Site diameter 100 m. Rugged feature near center of site with numerous crevices and overhangs. Relief 8 to 9 m
9	Western (Megasite 5)	Low	89-95.5 m 29°14'19.499"N 88°19'36.859"W	Main Pass Block 286	None. First visited during Cruise 1B on 21 March 1997	Site diameter 150 m. Small mounds and outcrops, generally 0.5 to 2 m in height with diameters of 10 to 15 m. A few features with up to 5 m relief with ledges, overhangs, and crevices

Abbreviations: MAMES = Mississippi-Alabama Marine Ecosystems Study; MASPTHMS = Mississippi-Alabama Shelf Pinnacle Trend Habitat Mapping Study; ROV = remotely operated vehicle.

Overview of Sampling Program

Table 3.2 is an overview of the sampling program, including mooring deployments and retrievals at the monitoring sites. During Cruise 1C (May 1997), subbottom profiling was conducted to geophysically characterize each site in more detail than was possible with the broad-scale geophysical reconnaissance (Cruise 1A). Grab samples were collected for geological and geochemical analyses (see Chapters 4 and 6). Hydrographic profiling was also conducted at each station, including conductivity/temperature/depth (CTD), dissolved oxygen (DO), photosynthetically available radiation (PAR), transmissivity, and optical backscatter (OBS) (see Chapter 7). Hard bottom and fish community monitoring was conducted at each site using the ROV (see Chapter 8). Monitoring included random video/photographic transects and stations and establishment of fixed video/photoquadrats. Voucher specimens were also collected at some sites to aid in species identification.

The overall program consisted of repeating the Cruise 1C sampling on three subsequent monitoring cruises (M2, M3, and M4). The only exception was the subbottom profiling at each site, which was not repeated.

Six physical oceanographic/sediment dynamics moorings were installed during Cruise 1C (see Chapter 7). Three moorings were installed at Site 1, and one each at Sites 4, 5, and 9. Each site has had at least one oceanographic mooring in place throughout the study. Two of the three moorings initially placed at Site 1 were subsequently redeployed at Site 5 on Cruise M3. Each mooring included current meters at 4 and 16 m above bottom (mab), sediment traps at 2, 7, and 15 mab, and an instrument that measures temperature, conductivity, DO, and turbidity.

Eleven "biomoorings" (moorings containing sets of settling plates) were also deployed during Cruise 1C as part of the companion study of epibiont recruitment (see Chapter 11). Eight were deployed at Site 4 and one each at Sites 1, 5, and 9. The biomoorings at Sites 1 and 9 were retrieved during the second leg of Cruise M3 (August 1998); turbidity prevented retrieval of the Site 5 biomooring. Another set of biomoorings was deployed at the same sites on Cruise S2 (January 1998) and was recovered on the second leg of Cruise M4 (July-August 1999). The eight biomoorings at Site 4 are a "time-series" experiment; the original plan was to retrieve one on each subsequent service cruise and monitoring cruise until all eight were retrieved. However, this was changed so that all biomoorings could be retrieved on monitoring cruises when the ROV was present to cut the anchor line. One Site 4 mooring was retrieved on Cruise M2 (October 1997) and redeployed on Cruise S2 (January 1998). On the second leg of Cruise M3 (August 1998), three of the original Site 4 moorings were recovered and one was found to be damaged (no plates remaining); the remaining four were recovered on the second leg of Cruise M4 (July-August 1999).

Table 3.2. Summary of activities conducted on each monitoring cruise and mooring service cruise.

Site	1C (May 1997)	S1 (Jul 1997)	M2 (Oct 1997)	S2 (Jan 1998)	M3 (Apr-May 1998)	M3 (Aug 1998)	S3 (Jul 1998)	S4 (Oct 1998)	S5 (Jan-Feb 1999)	M4 Apr 1999	M4 July-Aug 1999
1	P H G V D(3) d(1)	H S(3)	H G V S(3)	H S(3) d(1)	H G V S(1) R(2)	r(1)	H S(1)	H S(1)	H S(1)	H R(1)	H G V r(1)
2	P H G V	--	H G V	--	H G	V					H G V
3	P H G V	--	H G V	--	H G	V					H G V
4	P H G V D(1) d(8)	H S(1)	H G V S(1) r(1)	H S(1) d(1)	H G S(1)	V r(3)[a]	H S(1)	H S(1)	H S(1)	H R(1)	H G V r(4)
5	P H G V D(1) d(1)	H S(1)	H G V S(1)	H S(1) d(1)	H S(1) D(2)	G	H S(3)	H S(3)	H S(2) D(1)[b]	H R(3)	H G V r(2)[c]
6	P H G V	--	H G V	--	H	G					H G V
7	P H G V	--	H G V	--	H	G V					H G V
8	P H G V	--	H G V	--	H	G V					H G V
9	P H G V D(1) d(1)	H S(1)	H G V S(1)	H S(1) d(1)	H S(1)	G V r(1)	H S(1)	H S(1)	H S(1)	H R(1)	H G V r(1)

Abbreviations:
P = subbottom profiling   D(#) = deploy oceanographic mooring(s)   d(#) = deploy biomooring(s)
H = hydrographic profiling   S(#) = service oceanographic mooring(s)   r(#) = retrieve biomooring(s)
G = grab sampling   R(#) = remove oceanographic mooring(s)   V = video and photography

[a] A fourth biomooring was not recovered because it was visibly damaged (no plates remaining).
[b] Array not recoverable, replacement deployed. Top current meter subsequently found by a fishing boat; data recovered.
[c] Includes one biomooring that could not be retrieved on Cruise M3 due to turbidity.

Phase 3 Cruise Summaries

Phase 3 included one monitoring cruise, M4, which was conducted in two legs. During the first part (April 1999), oceanographic moorings were retrieved and hydrographic profiling was conducted at the four mooring stations. During the second leg (July-August 1999), video and grab sampling were conducted and the remaining biomoorings were retrieved. In addition, mooring service cruises were conducted in October 1998 (S4) and January-February 1999 (S5). The survey vessel for all cruises was the R/V TOMMY MUNRO. A Magnavox MX300 differential GPS was used for navigation. The cruises were staged out of Ocean Springs, MS.

The ROV used during monitoring cruises was the Benthos Openframe SeaROVER with a Python multifunction manipulator arm. Video, photographic, and ancillary equipment included a Sony high-resolution videocamera, DeepSea Power & Light Micro-SeaCam 2000 color videocamera, Photosea 1000 still camera and strobe, DeepSea Power & Light lasers, and a Simrad MS900 color imaging sonar.

Cruise S4

Mooring Service Cruise S4 was conducted during 13 to 14 October 1998. All six oceanographic moorings were successfully serviced (retrieved and redeployed) and 12 CTD casts were made.

Cruise S5

Mooring Service Cruise S5 began on 24 to 25 January 1999, but the generator on the TOMMY MUNRO broke less than six hours after departure and the ship had to return to the dock. The cruise was completed during 9 to 10 February 1999. Five of the six oceanographic moorings were successfully serviced and 12 CTD casts were made. Mooring C5C7 would not surface and a replacement mooring was deployed in its place. The flotation and top (Aanderaa) current meter were found by a charter fishing boat off Destin, Florida in late May and returned to the principal investigators. The data set was good through about the beginning of February 1999. The ROV attempted to locate and recover the bottom instruments and acoustic release on the second leg of Cruise M4 (July-August 1999), but they were not found.

Cruise M4

The first part of Cruise M4 was conducted from 13 to 14 April 1999. All six of the oceanographic moorings were retrieved and six CTD profiles were made at the mooring sites. During the second part of Cruise M4 (July-August 1999), ROV and grab sampling and CTD profiling were conducted at all nine monitoring sites. All remaining biomoorings were retrieved at Sites 1, 4, 5, and 9.

30

Data Management

A data management program has been established to monitor, control, and facilitate data flow and ensure the integrity of the data through each phase of the program. As part of this process, a program data management plan has been developed which consists of four interrelated elements: (1) data administration; (2) data control; (3) data utilization; and (4) data archiving submission.

The purpose of data administration is to ensure continuous tracking and custody of samples and data. Evidence of data possession, comparison, and security with signatures, dates, times, and location of data are noted. This element also ensures proper formatting and reporting of all data and distribution of data as required among the principal investigators.

Data control consists of monitoring the progress of data flow to identify data gaps and to facilitate further processing. The data control procedures adopted for the data management plan document data availability, data reduction, and data analysis.

Data utilization includes processing and validating data as they are submitted. The processed data are then made available to all study participants.

Available data are being routinely archived to ensure permanency.

Data types, formats, and procedures have been established to insure reliable and accurate data receipt and distribution. Sample inventories from the completed cruises have been developed, and a master inventory of samples received and analyses required is being maintained. A sample inventory for all project components has been finalized. This includes expected cruise dates, sampling schedules, and standardized cruise, site, and station nomenclature for all work elements, ensuring the smooth acquisition of data into the project database.

An inventory of the expected program data has been developed to ensure appropriate data processing and availability. Data that have been submitted to data management are presented in Table 3.3.

Table 3.3. Data submitted to data management.

Data Description	Cruise and Date	Media
Detailed Mosaics for Sites 1 and 2	Cruise 1A (Nov 96)	Tape
Bathymetric Observations	Cruise 1C (May 97)	Electronic
Bathymetric Observations	Cruise M2 (Oct 97)	Electronic
Survey Videotapes	Cruise 1C (May 97)	Videotape
Survey Videotapes	Cruise M2 (Oct 97)	Videotape
Survey Videotapes	Cruise M3 (Apr/Aug 98)	Videotape
Random Photo Locations	Cruise 1C (May 97)	Electronic
Random Photo Locations	Cruise M2 (Oct 97)	Electronic
Random Photo Locations	Cruise M3 (Apr/Aug 98)	Electronic
Random Photos	Cruise 1C (May 97)	CD ROM
Random Photos	Cruise M2 (Oct 97)	CD ROM
Random Photos	Cruise M3 (Apr/Aug 98)	CD ROM
Still Photo Logs	Cruise 1C (May 97)	Electronic
Still Photo Logs	Cruise M2 (Oct 97)	Electronic
Still Photo Logs	Cruise M3 (Apr/Aug 98)	Electronic
Random Photo Percent Cover Data	Cruise 1C (May 97)	Electronic
Random Photo Percent Cover Data	Cruise M2 (Oct 97)	Electronic
Random Photo Occurrence Data	Cruise 1C (May 97)	Electronic
Random Photo Occurrence Data	Cruise M2 (Oct 97)	Electronic
Sediment Grab Locations	Cruise 1C (May 97)	Electronic
Sediment Grab Locations	Cruise M2 (Oct 97)	Electronic
Sediment Grab Locations	Cruise M3 (Apr/Aug 98)	Electronic
Sediment Grain Size	Cruise 1C (May 97)	Electronic
Sediment Trace Metals	Cruise 1C (May 97)	Electronic
Sediment PAHs	Cruise 1C (May 97)	Electronic
Sediment TPH, EOM, TOC, and TIC	Cruise 1C (May 97)	Electronic
Sediment TOC and TIC	Cruise M2 (Oct 97)	Electronic
Sediment TOC and TIC	Cruise M3 (Apr/Aug 98)	Electronic
Sediment Trap Trace Metals	Cruise 1C (May 97)	Electronic
Sediment Trap Trace Metals	Cruise M2 (Oct 97)	Electronic
Sediment Trap TOC	Cruise 1C (May 97)	Electronic
Sediment Trap TOC	Cruise M2 (Oct 97)	Electronic

Abbreviations: EOM = extractable organic matter; TIC = total inorganic carbon; TOC = total organic carbon; TPH = total petroleum hydrocarbons; PAH = polycyclic aromatic hydrocarbons.

Chapter 4
Geologic Characterization

Introduction

The purpose of the geologic characterization segment of this program was to investigate the geology and morphology of carbonate mounds and surrounding sediments on the Mississippi-Alabama OCS. These mounds formed in an unknown manner at lower sea level stands of the Pleistocene-Holocene transgression (Ludwick and Walton 1957; Sager et al. 1992) and they have become a substrate upon which a diverse marine ecosystem has evolved (Gittings et al. 1992).

Much of our current geological knowledge of the Mississippi-Alabama carbonate mounds and their environs come from two prior MMS-funded studies: Mississippi-Alabama Marine Ecosystems Study (MAMES; Brooks 1991) and Mississippi-Alabama Shelf Pinnacle Trend Habitat Mapping Study (MASPTHMS; Continental Shelf Associates, Inc. 1992), both of which mapped the occurrence of carbonate mounds and the distribution of surficial sediments. Thousands of carbonate mounds ranging from less than a few meters in diameter to nearly a kilometer were found arrayed mostly in two isobath-parallel bands (Sager et al. 1992). Isobath-parallel ridges were also mapped in the shallower of these two depth zones. Both features are thought to be related to sea level stillstands during the last deglaciation. Surficial sediments are largely related to three late Pleistocene deltas, the Lagniappe Delta (Kindinger 1988; 1989) in the western part of the present study area (Fig. 4.1) and the "eastern" and "western" deltas in the original MAMES study area (Sager et al. 1999). These delta sediments were deposited during sea level lowstands or in the case of the "eastern delta," during the early part of the last deglaciation (Sager et al. 1999). Atop these sediments is a thin, variable-thickness layer, consisting mostly of sand, that is thought to have been deposited by reworking of shelf sediments near sea level as it rose across the shelf during the last deglacial transgression (Sager et al. 1999).

The goal of the geologic characterization subtask has been to derive as detailed a physical picture of the mounds as can be done with conventional geophysical and geologic data, in effect, to bridge the gap between prior broad-scale surveys and seafloor observations made in other elements of this program. The MAMES and MASPTHMS surveys were reconnaissance in nature, defining the broad distribution and setting of the Mississippi-Alabama OCS mounds. This project has sought to provide greater detail in the characterization of the mounds and their geologic environment. Target areas were mapped using four different data types: (1) high-resolution side-scan sonar images, (2) high-frequency subbottom profiles, (3) grab samples, and (4) ROV videos. High-resolution side-scan sonar mapping was used to construct acoustic images of the seafloor, which yield large-scale physical characteristics, such as shape, location, and large-scale roughness. Swath bathymetry data were derived from the side-scan and also give a rough measure of morphology. High-resolution subbottom profiler records and grab samples have been used to examine surrounding sediments and long term sedimentation. ROV videos were used to provide geologic characteristics at an even smaller scale (down to centimeters).
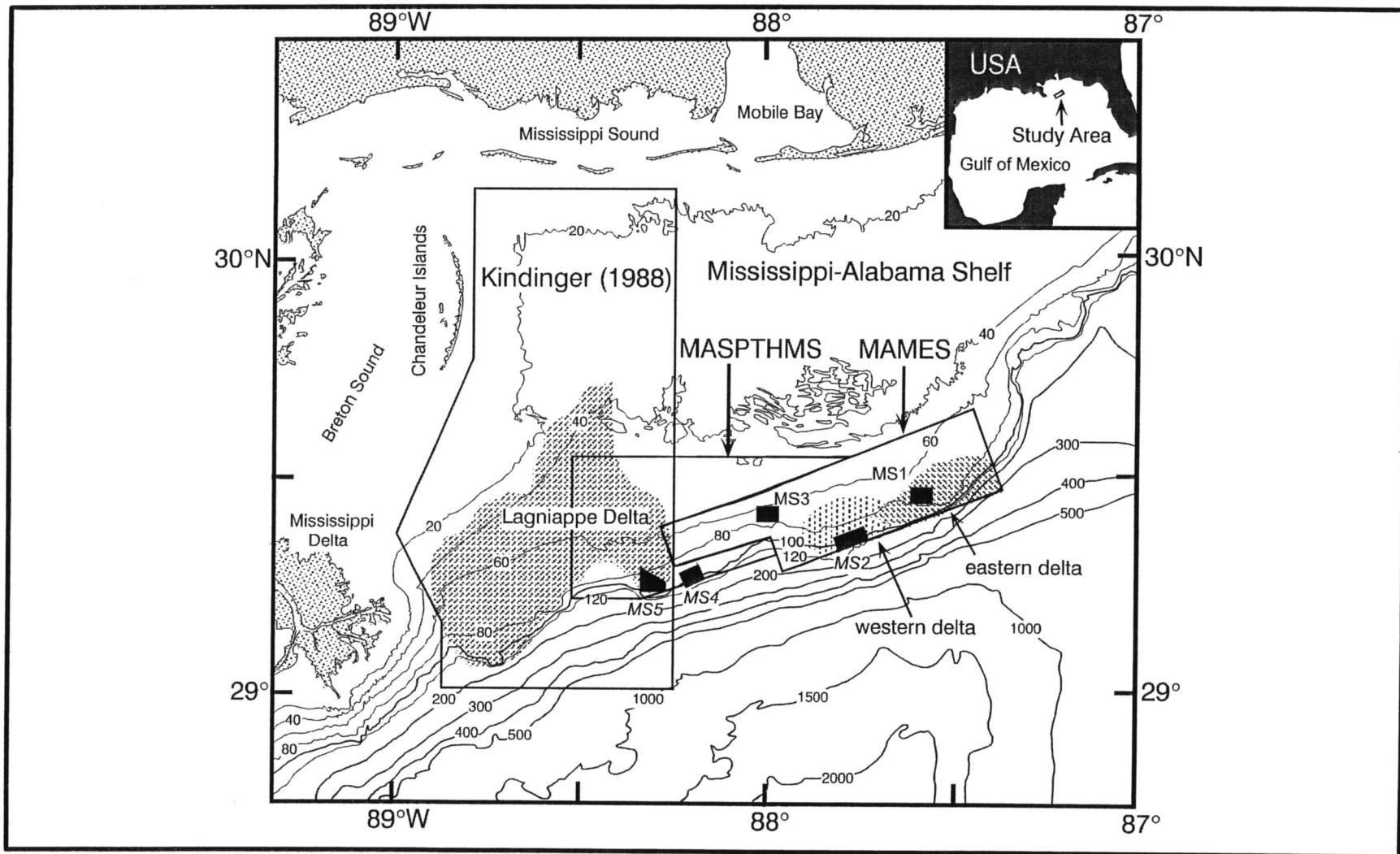
Fig. 4.1. Locations of MAMES, MASPTHMS, USGS study, and Megasites 1-5. Boxes show areas surveyed by MMS-funded MAMES and MASPTHMS studies along with area encompassed by USGS survey (Kindinger 1988; 1989). Small, numbered black boxes show megasite survey areas from this study. Hachured areas show locations of shelf-edge fluvial deltas mapped with high-resolution seismic reflection data (Kindinger 1988; 1989; Sager et al. 1999). Isobaths at 20 m intervals to 120 m and 100 m for deeper depths are shown for reference.

Methods

High-Resolution Geophysical Baseline Cruise (1A)

The purpose of the high-resolution geophysical baseline cruise was to gather large-scale geophysical images of the five megasites (Fig. 4.1). Two geophysical tools, a digital 72 kHz $TAMU^2$ side-scan sonar and an X-Star 2-12 kHz chirp sonar profiler, were employed to produce three different data types: (1) sonar seafloor images, (2) swath bathymetry, and (3) subbottom acoustic reflection profiles.

One hundred eighty track lines, totaling 797 km in length and covering an area of 144.5 km^2 with side-scan sonar swaths, were collected at the five megasites with the side-scan sonar and chirp sonar. Ship's tracks were spaced 175 m apart and the ship's speed was approximately 5.5 knots with a sonar layback of about 85 m continuously measured with an ultra-short baseline acoustic tracking system. Navigation was done using *Skyfix* differential GPS, with an accuracy of better than 5 m. On these tracks, which were either oriented at a heading of 0° or 30°, an image swath of 400 m was used to provide ~228% coverage of the seafloor. This allowed features directly beneath the sonar on one ship track to be imaged by adjacent tracks. This duplication was important because features have different appearances depending on the incidence angle of the acoustic waves and because the $TAMU^2$ sonar has a "blind spot" directly beneath the track. Because the sonar bathymetry swath is limited to 3.4 times water depth, the bathymetry swaths overlapped by 25% to 50% in these surveys.

The sonar digitization rate was typically 1,650 pixels per ping at a ping rate of 2.5 per second. This configuration implies that each pixel is representative of an area of seafloor 1.25 by 0.24 m. In addition to these data, slightly higher resolution data were also collected during Cruise 1A on tracks oriented perpendicular to the main survey tracks over areas of particular interest. These "detailed" surveys typically had track spacings of 150 m, sonar swath widths of 200 m, and were digitized with 3,300 pixels per ping, and at up to 5 pings per second. The goal was to provide higher resolution images of likely sites for more detailed study. In all, 34.7 km of data were collected on these "detailed survey" lines covering an area of 5.6 km^2 with side-scan swaths.

Other Cruises (1C, M2, M3)

Grab samples were collected for geologic analysis on the ROV baseline cruise (1C) and subsequent monitoring cruises. In total, 94 grabs were collected at the nine monitoring sites on Cruise 1C and 5 grabs at each site were collected on subsequent cruises for a total of 45 samples for each cruise (see Appendix Table 4.A at the end of this chapter for locations of grab samples through Cruise M3).

Additional chirp sonar data were collected on Cruise 1C. A grid of perpendicular lines was acquired between the lines collected over the "detailed" survey sites from Cruise 1A. Because the original grid had tracks with an east-west spacing of 175 m and north-south spacing of 150 m, the Cruise 1C data filled in the grids at spacings of 87.5 and 75 m.

Cruise 1C subbottom lines were positioned by differential GPS with an accuracy of about 5 m. The total length of subbottom data collected on Cruise 1C was 199.8 km.

TAMU^2 Sonar Data Interpretation

Sonar backscatter mosaics were produced by C&C Technologies, Inc. using proprietary image manipulation software. Images for each track were imported, georeferenced, and adjusted for sonar layback. The entire mosaic was built up of images for each of the component lines. Data gaps at the sonar nadir were filled with data from adjacent tracks. Owing to limitations of the proprietary image manipulation software, typical pixel sizes are about 1 m x 5 m. Subsequent analysis of the sonar mosaics has been carried out using ERMapper, a GIS analysis software package.

Bathymetry grids were also produced by C&C Technologies, Inc. Using proprietary software, sonar acoustic raypath takeoff angles were computed from phase angles measured at the sonar acoustic arrays. Takeoff angles and acoustic wave round-trip travel times were used to compute a depth profile perpendicular to the sonar track for each sonar ping. Depth locations and raypaths were corrected for variations in sound speed determined from periodic CTD casts made during the survey. Depth values were binned and plotted using the public domain GMT software package (Wessel and Smith 1995). Megasite bathymetry grids were binned at 15-m intervals whereas detailed survey bathymetry data were binned at 1-m intervals.

The analysis of *TAMU^2* images and mosaics is similar to geologic interpretation of aerial photographs. These images give a high-detail acoustic picture of seabottom morphology and surface texture. The sonar builds an image based on the amplitude of acoustic return ("backscatter") from the seafloor and this is related to morphology, roughness, and volume scattering within near-surface sediments (Johnson and Helferty 1990). Other data, such as swath bathymetry, subbottom profiles, and seafloor grabs, give different characteristics or ground-truth data (the grabs) that have been used to understand and interpret the images collected by the sonar. Using megasite sonar mosaics, backscatter patterns are classified and characterized to assist in constructing interpretative maps of geologic features. Sonar images have also been used to describe mound morphology in a variety of ways: classifying mound shapes, calculating mound size distributions, and calculating mound aspect ratio variations.

TAMU^2 bathymetry data have been used to make large and small-scale contour maps of each megasite and each monitoring site. These have been used to examine seafloor topography and mound morphology, orientation, and large scale roughness.

Subbottom Profile Interpretation

Data from the chirp echosounder have been used to examine thickness and character variations of shallow sediments in the study areas. The profiles have been analyzed using standard seismic stratigraphic techniques (e.g., Mitchum and Vail 1977). This involves

(1) recognition and correlation of acoustic reflectors by their characteristics and
(2) mapping and interpretation of seismic facies. The latter step assumes that sediments
of different sedimentary facies give a common, recognizable acoustic response. In
addition, the subbottom records have been an invaluable tool for interpreting the side-
scan sonar mosaics because they show seafloor topography and sediment layers that can
be compared with the sonar images.

Sediment Grain Size Analysis

Grain size measurements have been made on grab samples using standard techniques
(Folk 1974). Samples are homogenized, treated with bleach to oxidize organic matter,
and washed with distilled water to remove soluble salts. Sodium hexametaphosphate is
added to deflocculate each sample before wet-sieving with a 62.5 micron (4ϕ) sieve to
separate the sand and gravel from the mud fraction. The sand and gravel fraction is
dried, weighed, and sieved at $1/2\phi$ intervals from -1.5ϕ to 4.0ϕ. Each fraction is
examined for aggregates and those found are disaggregated. Sample fractions are
weighed to three significant figures. The mud fraction is analyzed for particle size by the
pipette settling method at intervals of 4.5ϕ, 5.0ϕ, 5.5ϕ, 6.0ϕ, 7.0ϕ, 8.0ϕ, 9.0ϕ, and 10.0ϕ.

ROV Videos and Photos

ROV videotapes and still photographs have been collected during Cruises 1C, M2, and
M3. These data provide valuable geologic information concerning seafloor features,
sediment types, and texture. Tapes and photos from Cruise 1C were viewed and
characterized for all sites using the descriptors in Table 4.1. As a first-cut, only the
random photo stations were characterized as they constituted the most uniform data set,
since all photos were taken at the same distance from the sea bottom (0.7 m). However,
it became apparent that the geologic context was difficult to assess solely from the photos
owing to the small area covered by each (approximately 0.75 m x 0.75 m).
Consequently, transects between photostations are now being analyzed to determine a
broader geologic setting.

The set of descriptor terms (Table 4.1) was selected to describe the morphology,
roughness, and sediment cover of the sea bottom viewed by the ROV. These terms are an
attempt to assess qualitative features that might be significant to biologic populations for
comparison with biologic data collected in other aspects of this program.

After these initial characterizations were carried out for all sites, a more detailed and
comprehensive analysis was undertaken for some sites. At the time of this report, only
Site 7 has been finished. For Site 7, still photos (at 400 random photo stations) and
between-station videos from Cruises 1C, M2, and M3 have been viewed and
characterized using a set of modified micro-habitat descriptors (Table 4.2). Using a GIS
program (ARCView), the photo stations and video transects were plotted and continuous
boundaries between morphological regions were approximated.

Table 4.1. Seafloor geologic descriptors for ROV photo stations.

General	Morphology (large scale)	RLM part	Relief (scale m)	Roughness (scale cm)	Sediment Texture	Sediment Cover
No rock visible	not desc	not desc	Flat Depression Mound	not desc	Fine Coarse Shell Hash Rubble	not desc
Rock outcrop	Boulder Ridge RLM	Base Face Top Flat Overhang	Low Medium High	Low Medium High	Fine Coarse Shell Hash Rubble	None Partial Complete

Abbreviations: RLM = reef-like mound.

Table 4.2. Modified seafloor geologic descriptors for Site 7 ROV photos and videos.

General	Morphology (large scale)	Relief (scale m)	Texture (scale cm)	Sediment Texture (Fine)	Sediment Texture (Coarse)
Relief present (outcrop)	Mound Monolith Hard bottom	Vertical Moderate Near-Horizontal	Small (10s cm) Medium (50-100 cm)	Thin Moderate Thick	None Part burial Near-complete burial
Flat area (no outcrop)	Open Channel Terrace	Not desc.	Not desc.	Not desc.	Not desc.

The modified descriptors (Table 4.2) were an attempt to better characterize the mound and hard bottom geology. As in the initial characterization, seafloor was characterized by the presence or absence of outcrop. However, because rock outcrop is often covered by a veneer of sediments, the presence or absence of outcrop was determined by seafloor relief or lack thereof. Flat areas were mainly described by their surroundings: open, channel, and terrace. Outcrop areas were characterized in a number of ways. Relief was described as near-vertical, moderate, or near-horizontal. Outcrops were classified by size: small outcrops (~meter size) were termed mounds, large isolated rocks were termed monoliths, whereas extensive hard substrates were termed hard bottoms. In this context, the top of a large mound would be described as a hard bottom. Where a station was on an outcrop that rose above an area of flat sediments, the height was estimated. Sediment cover was described on outcrop areas in two ways. At Site 7, fine-grained sediments tend to make a veneer whereas coarse sediments and shell hash usually filled depressions. The descriptors thin, moderate, and thick were applied to the veneer of fine grain sediments. For coarse sediments, the degree of burial was estimated (none, partial, near

38

complete). The surfaces of outcrops often show small-scale texture or pitting, probably owing to dissolution or bioerosion. When present, this texture was classified as small (tens of cm) or medium (~50-100 cm).

Results

Megasite Bathymetry

The bathymetry data produced from the $TAMU^2$ sonar far exceed previous data sets as far as accuracy and coverage. Nevertheless, several limitations are obvious in the bathymetry maps produced. To obtain greater depth precision, adjacent data values were averaged, so mounds have rounded shapes in comparison to the shapes seen in the sonar backscatter images. Furthermore, small mounds do not appear in the data because averaging smoothes them out. Overlapping data from adjacent tracks are typically offset by some 10 to 15 m (and sometimes more), owing to navigation uncertainties, so a small mound on one track can be averaged with a flat patch of seafloor on an adjacent track. Furthermore, smaller mounds are usually averaged with adjacent flat seafloor when their size is much smaller than the depth value bin size. As a result of this smoothing, the megasite bathymetry maps typically show only those mounds greater than about 25 m in diameter. In the detailed survey bathymetry, features with diameters greater than about half that size are preserved.

Two additional artifacts are noted by their along-track trends. First, the data occasionally display offsets of ~1 m from data collected on one track to those adjacent. In some instances this may be a "roll bias" in which the values on one side of the cross-track depth profile are slightly too great or too small. It is most obvious when examining the data in minute detail in small areas around the monitoring sites. The second artifact may be related. It appears as a crenulation of the contours in a track-parallel direction caused by the cross-track depth profile being bowed upwards in the center. This is probably a result of imperfect corrections for the refractive effects of sound-velocity variations in the water column because it is more dramatic at some sites (e.g., Megasites 1, 2, and 5) than others (e.g., Megasites 3 and 4). To understand this effect, recall that depths near the track lines are calculated from acoustic waves that travel nearly vertically through the water column and are therefore less affected by refraction. In contrast, depth soundings near the edge of the sonar swath leave the sonar at shallow angles, so their paths are affected by refraction to a greater degree. Consequently, a small error in determining water velocity versus depth profiles can translate to a greater error in determining depth at the edges of the sonar swath. At Megasite 1, for example, the crenulations typically appear as variations of about ±150 m in the lateral position of a particular contour in "flat" areas. The regional slope is about 0.17°, so this suggests an error of about ±0.45 m in depth, which is in turn 0.6% of the water depth in Megasite 1. Thus, the bathymetry data are better than "hydrographic" precision (<1% of water depth), yet because the slope is very shallow, the bathymetry contours appear irregular. For presentation purposes, the large scale bathymetry maps in the following sections were hand-smoothed and redigitized.

39

Megasite 1

Megasite 1 (Fig. 4.2) shows two large mound clusters near the shelf edge in water depths of 68 to 90 m. The western cluster is subcircular, approximately 600 m in diameter, and contains several smaller, steep-sided mounds. The other cluster is a crescentic band, approximately 800 m wide and 3,000 m long, located in the northeast part of the megasite. It contains two large flat-top mounds, approximately 300 to 400 m in diameter, and about a dozen smaller mounds. The large features are part of the "40-Fathom Fishing Ground" mound cluster that has been studied in prior MMS projects. One of these is the location of Site 1. The seafloor around the mounds is nearly flat, with a shallow slope to the south. Contours suggest that there is a 3 to 5 m depth difference from north to south across the crescentic mound band. This is in part owing to sediments tending to pile up on the north sides of these features.

Megasite 2

Depths in Megasite 2 range from 93 to 200 m and show numerous mounds at the shelf edge (Fig. 4.3). Seafloor north of the mounds is flat and is at about 100 to 103 m depth. To the south, the shelf edge at about 115 m depth separates the mounds from the steeper upper slope to the south. The mounds are subcircular to linear in plan view and seem to have two distinct morphologies. One type occurs as broad, low, round flat-topped topographic features several hundred meters in diameter. The others appear as taller, steeper, less-rounded features. The latter are the "pinnacles" described by Ludwick and Walton (1957) whereas the low features appear to be carbonate platforms. The bathymetry shows that these low platforms are typically flush with the seafloor on their north sides whereas the south sides usually have a drop of 3 to 5 m. The bathymetric map shows that the steepest and tallest mounds are clustered in the central and eastern part of the megasite, whereas those mounds in the western part tend to be dominantly the low, hard bottom type.

Megasite 3

Megasite 3 shows a gently sloping area of the outer shelf with depths of 64 to 86 m (Fig. 4.4). The main feature is a bulge in the contours which represents a broad, thin dome of sediments surrounding several groups of mounds. One mound group, in the western part of the megasite, is linear with a south-southeast trend. This linear feature is asymmetric, with a shallow slope on its north side and a steeper slope on its south side. To the north and southeast of this linear feature, two other smaller mounds have similar trends, implying some relationship. In the eastern half of the megasite, about a dozen medium mounds appear in several clusters. These are associated with a broad, low mound similar to those in Megasite 2. This broad mound is about 400 x 800 m in dimension and like others in Megasite 2, it shows a 2 to 3 m drop off on its south edge, whereas its northern edge is flush with the surrounding seafloor. The side-scan sonar mosaics also show a larger, but less obvious, low hard bottom in the central region of Megasite 3. This is seen in the bathymetry contours by slightly steeper slopes on its south edge, in the south-central part of the megasite.
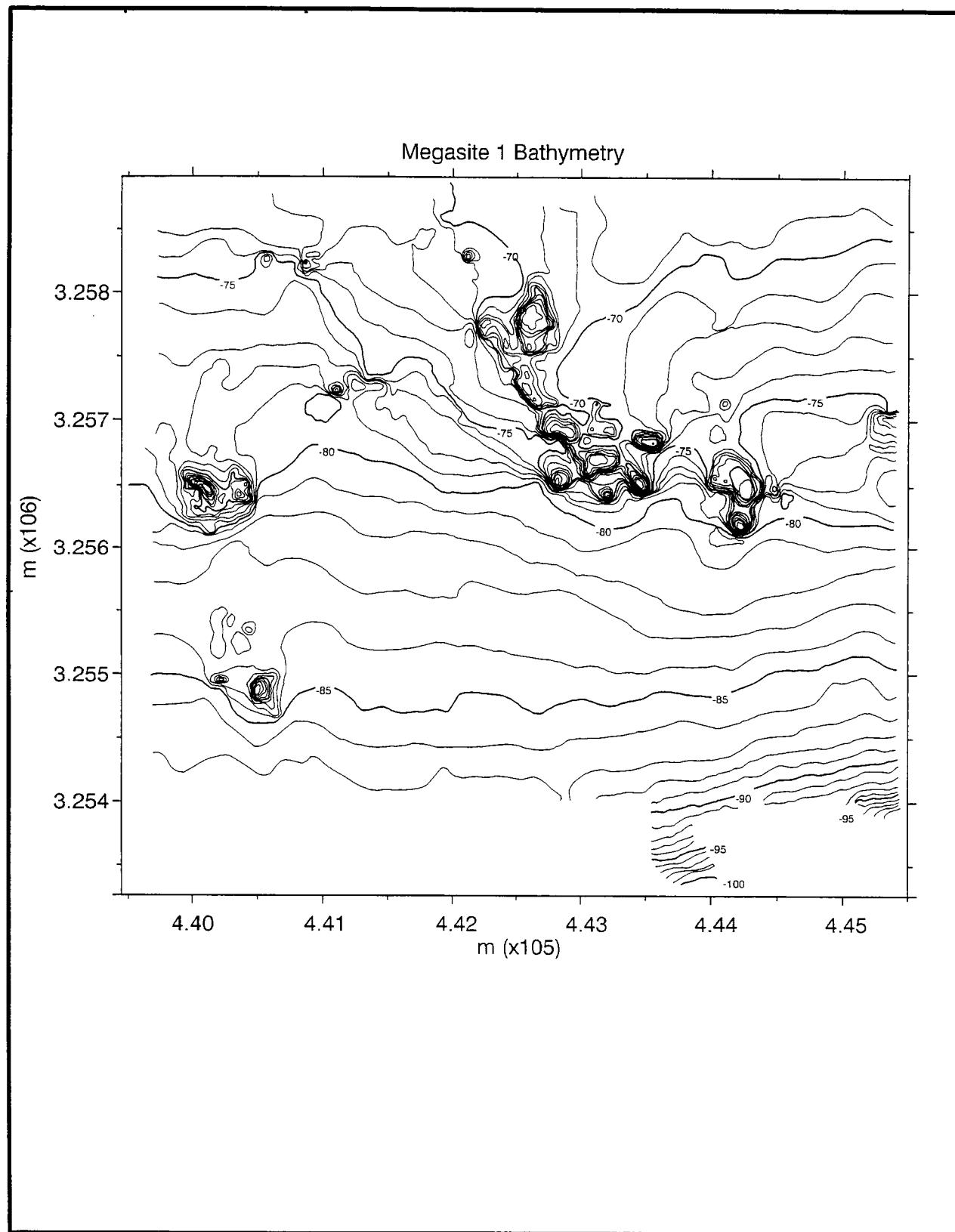
Fig. 4.2. Bathymetry of Megasite 1, derived from $TAMU^2$ sonar data. Contours shown at 1-m intervals with 5-m contours bold. UTM plot with axes labeled in meters.
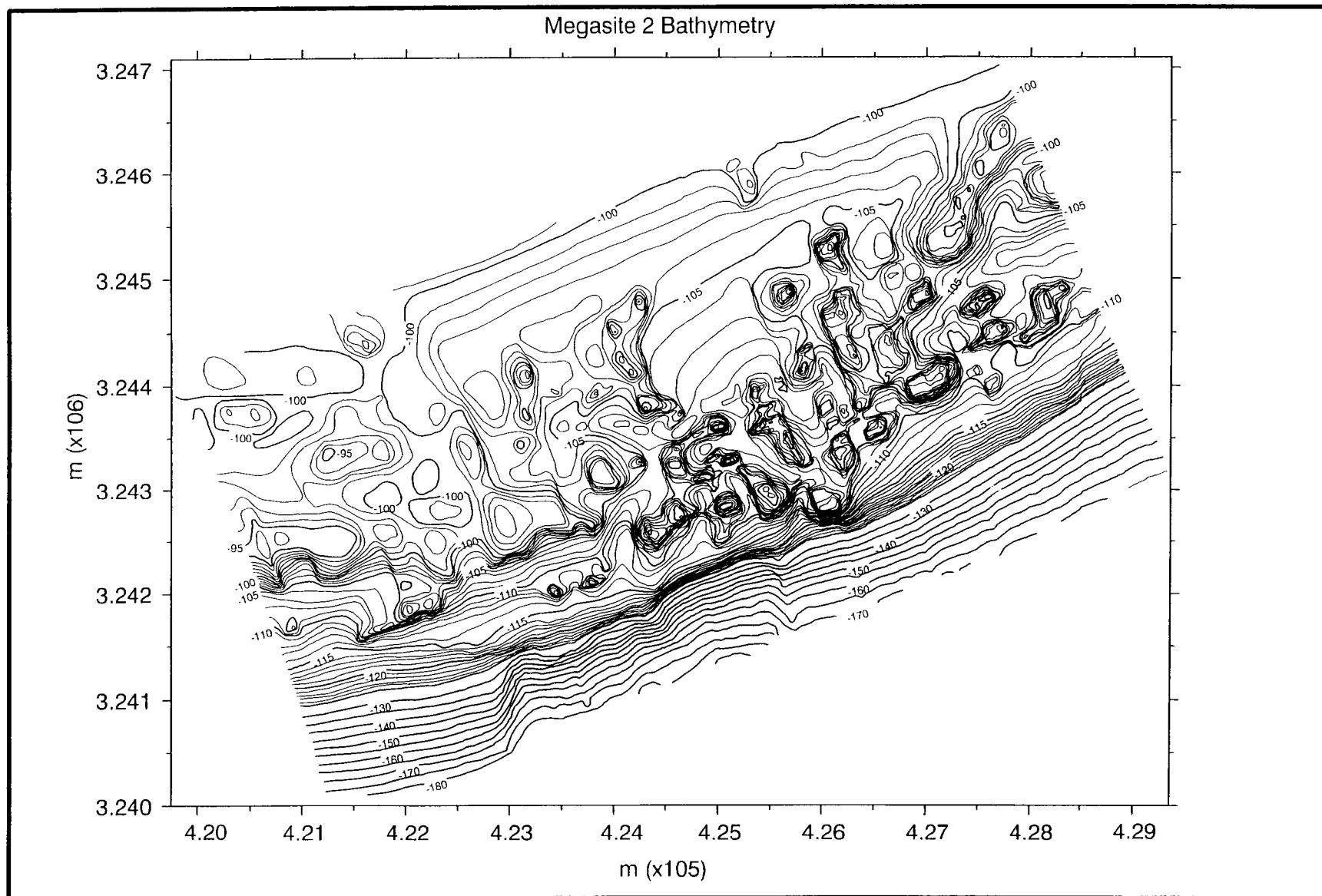
Fig. 4.3. Bathymetry of Megasite 2, derived from *TAMU²* sonar data. Conventions as in Fig. 4.2.
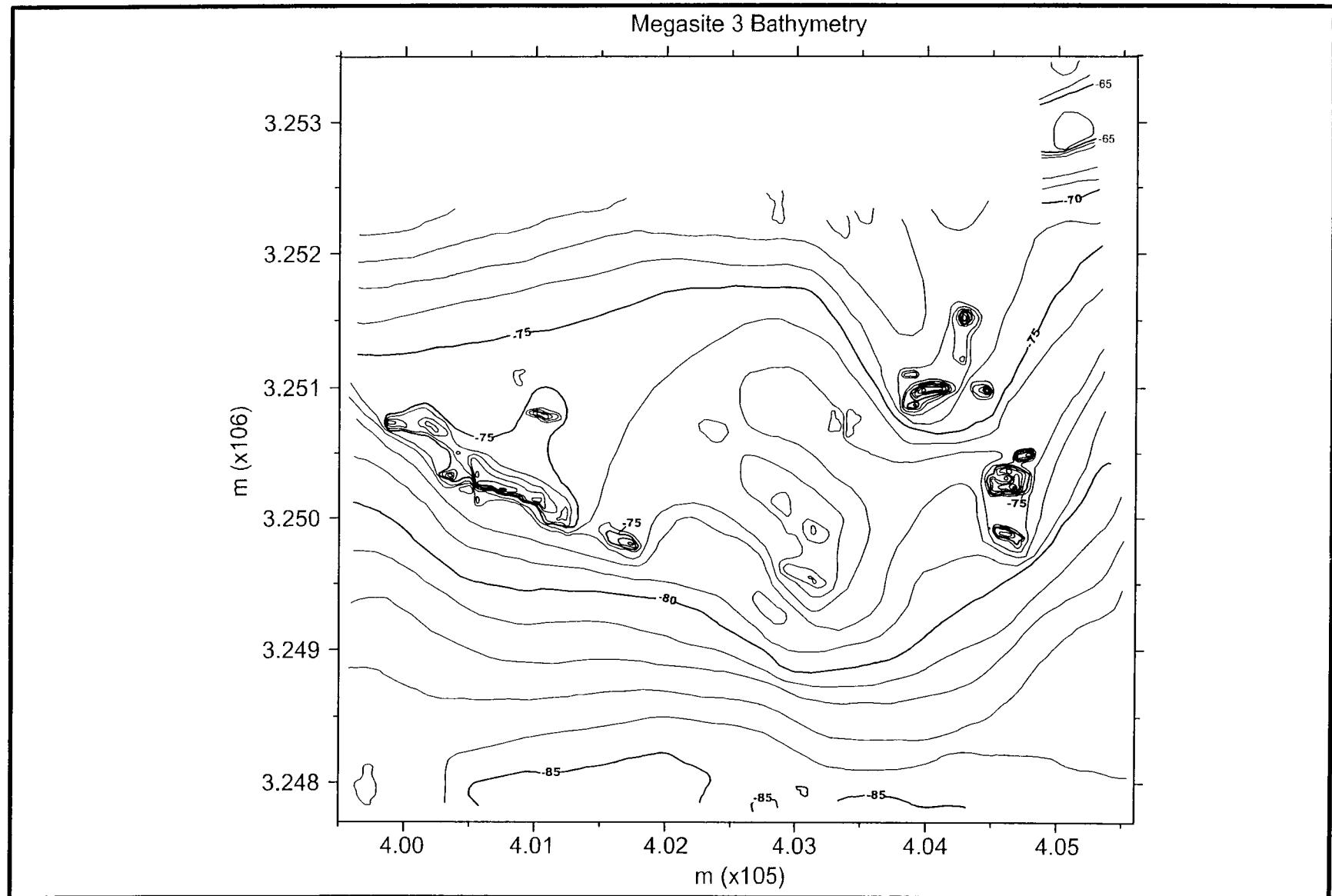
Fig. 4.4. Bathymetry of Megasite 3, derived from *TAMU²* sonar data. Conventions as in Fig. 4.2.

Megasite 4

Depths in Megasite 4 range from 93 to 189 m (Fig. 4.5). This site is similar to Megasite 2 in its shelf-edge position. Slopes in Megasite 4 are somewhat steeper than the others, being about 0.7° landward of the 120 m isobath. The main bathymetric features are curvilinear areas of steeper slope that appear to be the edges of fluvial deltas. The most prominent feature runs from west to east across the southern part of the megasite at depths of 112 to 133 m. Another obvious feature of the bathymetry in Megasite 4 is the lack of large mounds. This implies that all of the mounds are too small to be seen in the 15-m bathymetry grid.

Megasite 5

The shelf edge is also a prominent feature in the Megasite 5 bathymetry map, which shows depths ranging from 69 to 161 m (Fig. 4.6). Most of the northern two-thirds of the megasite is relatively flat seafloor. Superimposed is a curvilinear mound group that stretches from northwest to southeast across almost the entire megasite. The bathymetry shows several large mounds and numerous smaller mounds and mound groups. An extraordinary feature is the tall, linear mound at the northwest end of the mound group, which is the location of Site 7. Across the curvilinear mound group, the contours often show a depth offset of about 2 to 4 m. Seaward of the mound lineation is a flat bench at a depth of about 95 m, adjacent to the shelf edge.

Monitoring Site Bathymetry

Site 1

Site 1 contains the large flat-topped mound in Megasite 1 and seems well represented in the bathymetry data. The data show a large flat-topped feature with a top depth of about 63 m, a steep flank, and flat seafloor to the northeast at depths of about 75 to 76 m (Fig. 4.7).

Site 2

Bathymetry data from Site 2 show a mainly flat seafloor at a depth of about 77 to 78 m with a medium-sized mound approximately 50 m in diameter along the southern edge of the site (Fig. 4.7). The contours indicate the mound is more than 5 m in height.

Site 3

Bathymetry contours sat Site 3 show no evidence of the small mounds in the area (Fig. 4.7). Instead, the depths reflect a relatively flat seafloor, at depths of 78 to 79 m.
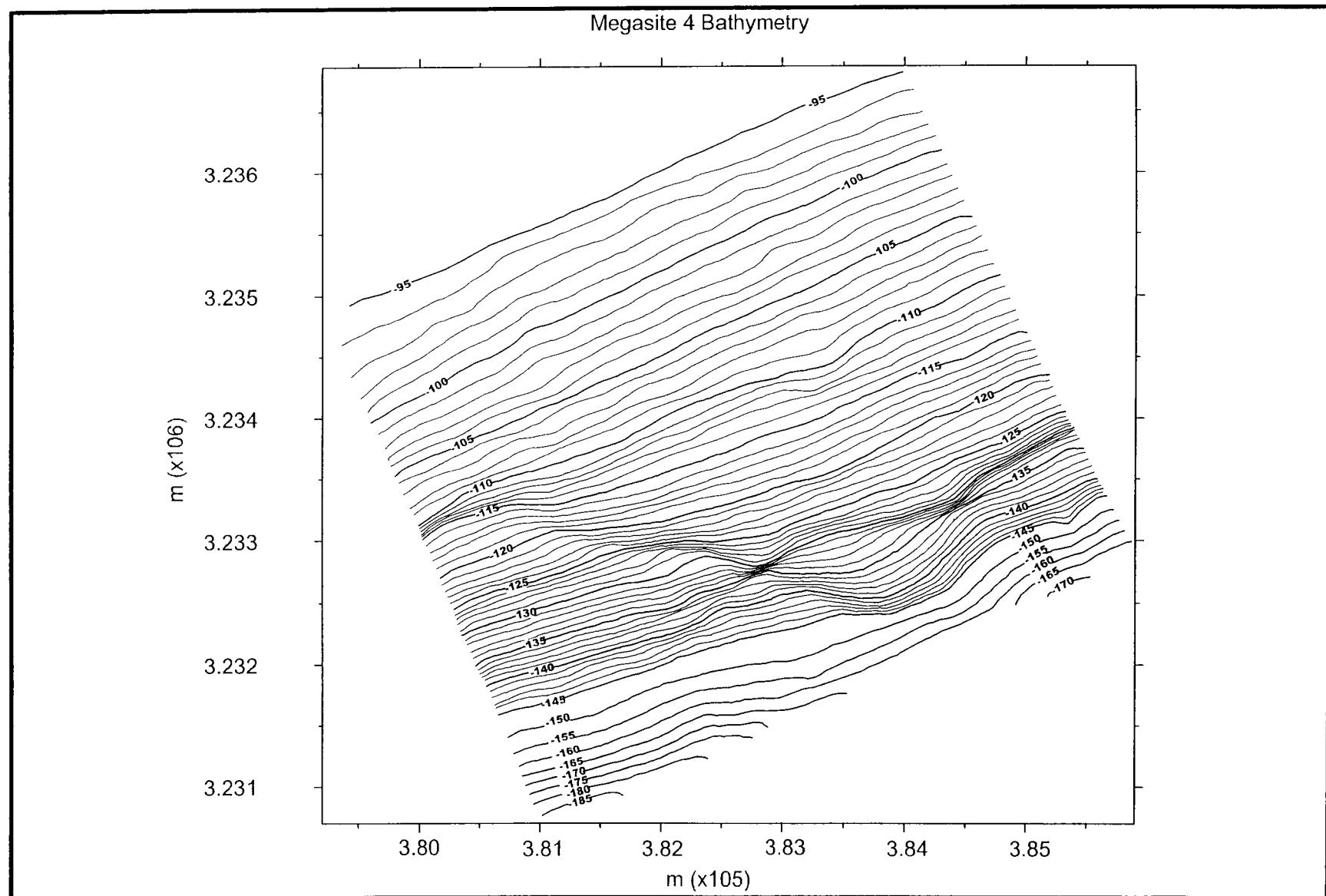
Fig. 4.5. Bathymetry of Megasite 4, derived from *TAMU²* sonar data. Conventions as in Fig. 4.2.
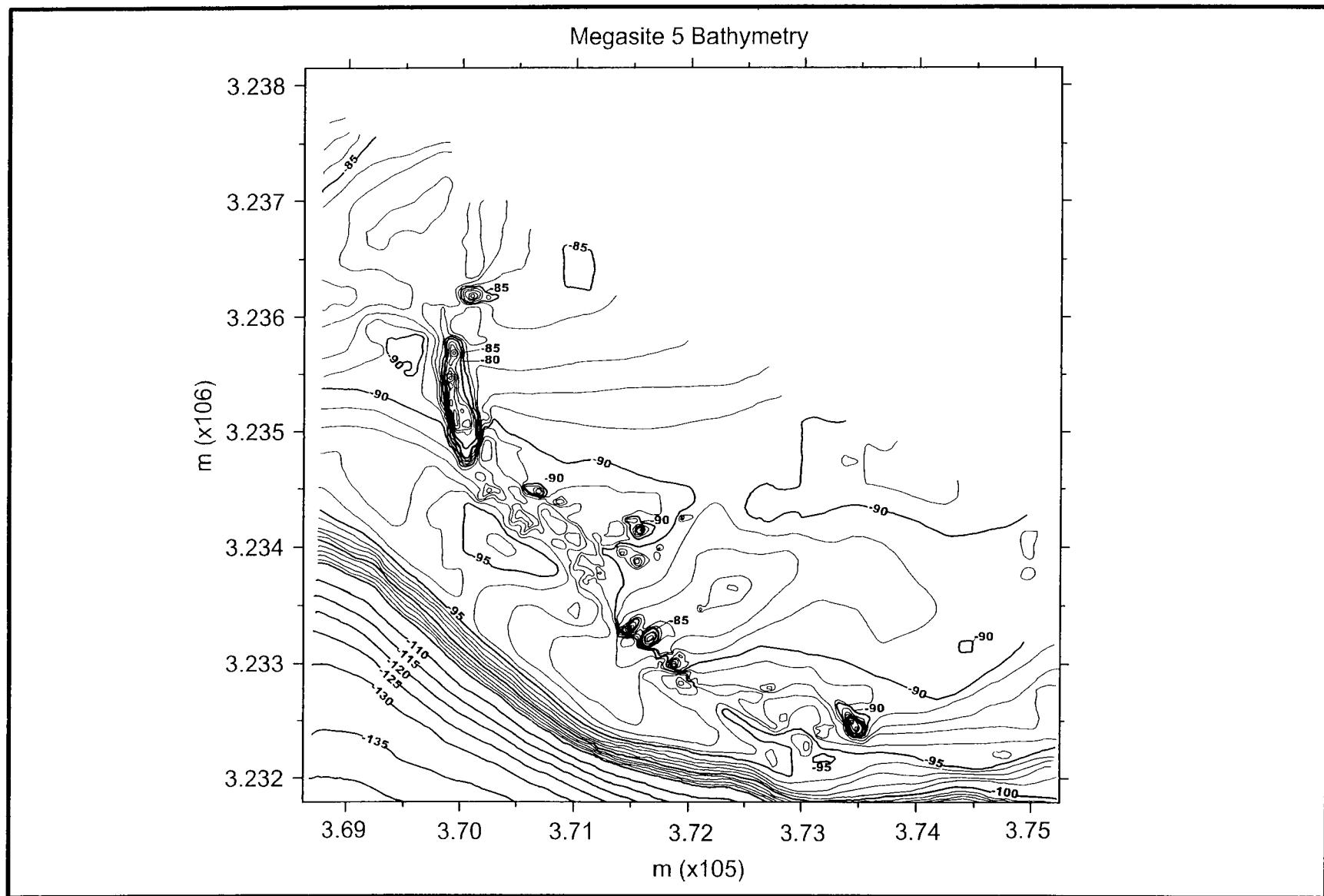
Fig. 4.6. Bathymetry of Megasite 5, derived from *TAMU²* sonar data. Conventions as in Fig. 4.2.
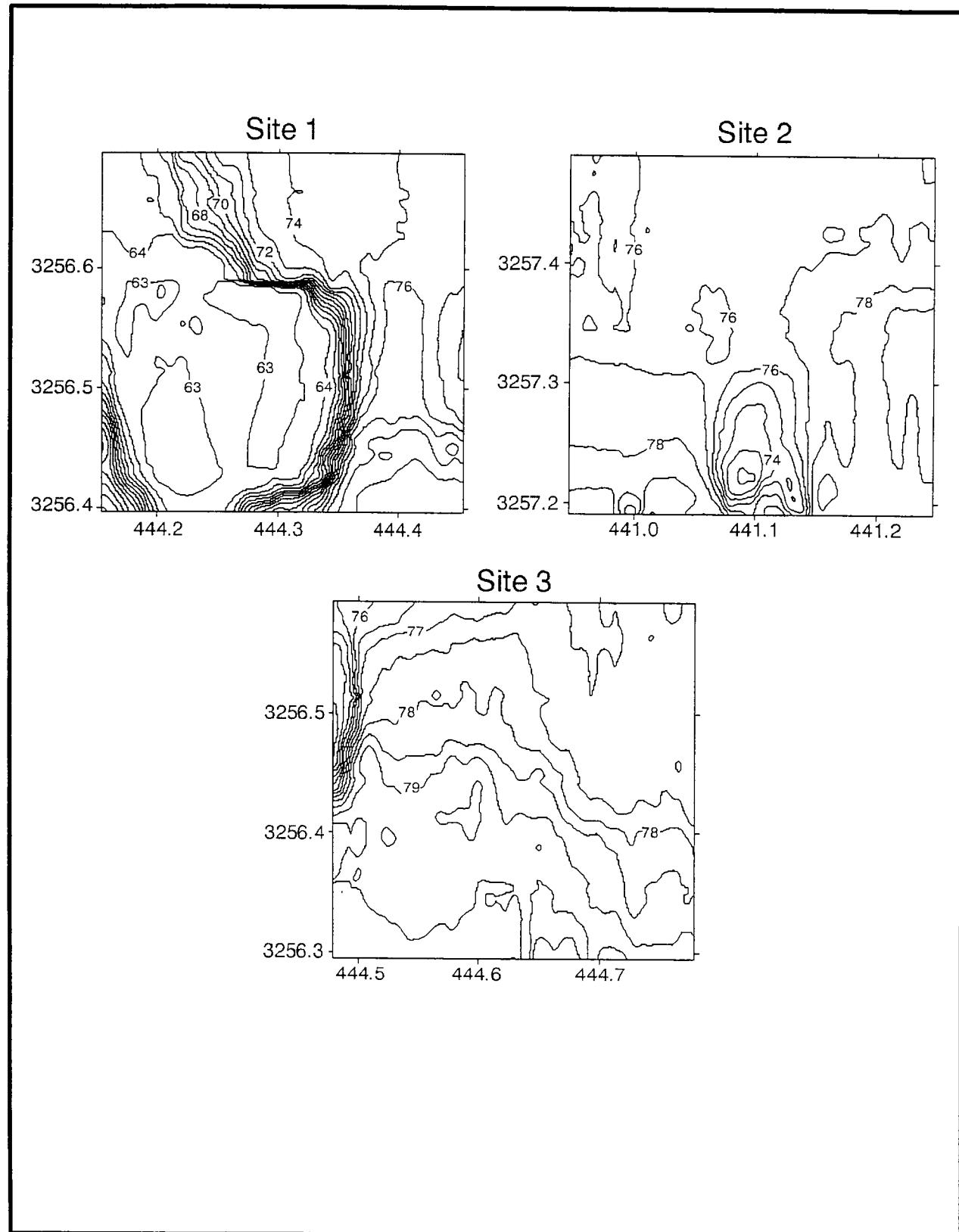
Fig. 4.7. Bathymetry of monitoring Sites 1-3, derived from $TAMU^2$ sonar data. Contours in Sites 1 and 2 are at 1-m intervals. Extra 0.5-m contours are shown in Site 3 for clarity. UTM plots with axes labeled in kilometers.

Site 4

Bathymetry data at Site 4 show a wide, medium-height mound with a northwest trending ridge on its northwest side (Fig. 4.8). Contours indicate the mound is about 10 m in height, but has a relatively flat top.

Site 5

Bathymetry data at Site 5 show a tall mound near the center and a lower mound at the southwest edge of the area (Fig. 4.8). The large mound seems to have a constriction in the middle, but comparison with the side-scan images indicates that this is an artifact caused by a navigation error in combining bathymetry data from two adjacent tracks.

Site 6

Contours at Site 6 are mainly unclosed, indicating a lack of relief at the site. The seafloor is relatively flat at a depth of about 74 m (Fig. 4.8).

Site 7

As at Site 1, the high relief of Site 7 lends itself to bathymetric mapping. The contours show a large, flat-topped mound, elongated north-south, with summit depths of about 70 m and bottom depths of about 86 to 87 m (Fig. 4.9).

Site 8

Bathymetry data at Site 8 show two closed contours around a medium-sized mound near the center of the site (Fig. 4.9). The mound appears subcircular and several meters in height.

Site 9

Relief at Site 9 is low, so the contours mostly wander unclosed at depths of about 90 m (Fig. 4.9). Several closed contours in the northeast quadrant indicate the presence of a small mound that is several meters in height.

Megasite Side-scan Sonar Mosaics

Mosaics made from *TAMU²* side-scan sonar data contain images constructed from the merging of backscatter image strips from individual ship's tracks. The side-scan sonar sends out a fan-shaped acoustic pulse that is narrow and parallel to the ship's track and wide in the orthogonal direction. The sonar then plots a "scan" depicting the amplitude of the backscattered signal for that particular pulse. By sequentially plotting many scans from subsequent pulses, an image is constructed. Typically the image is transformed to appear as if made by an "aerial photograph" illuminated from the ship's track, i.e., "light" areas face the sonar and shadows are on the opposite sides. Usually little of the returned acoustic energy comes from reflection because the incidence angle is such that most such
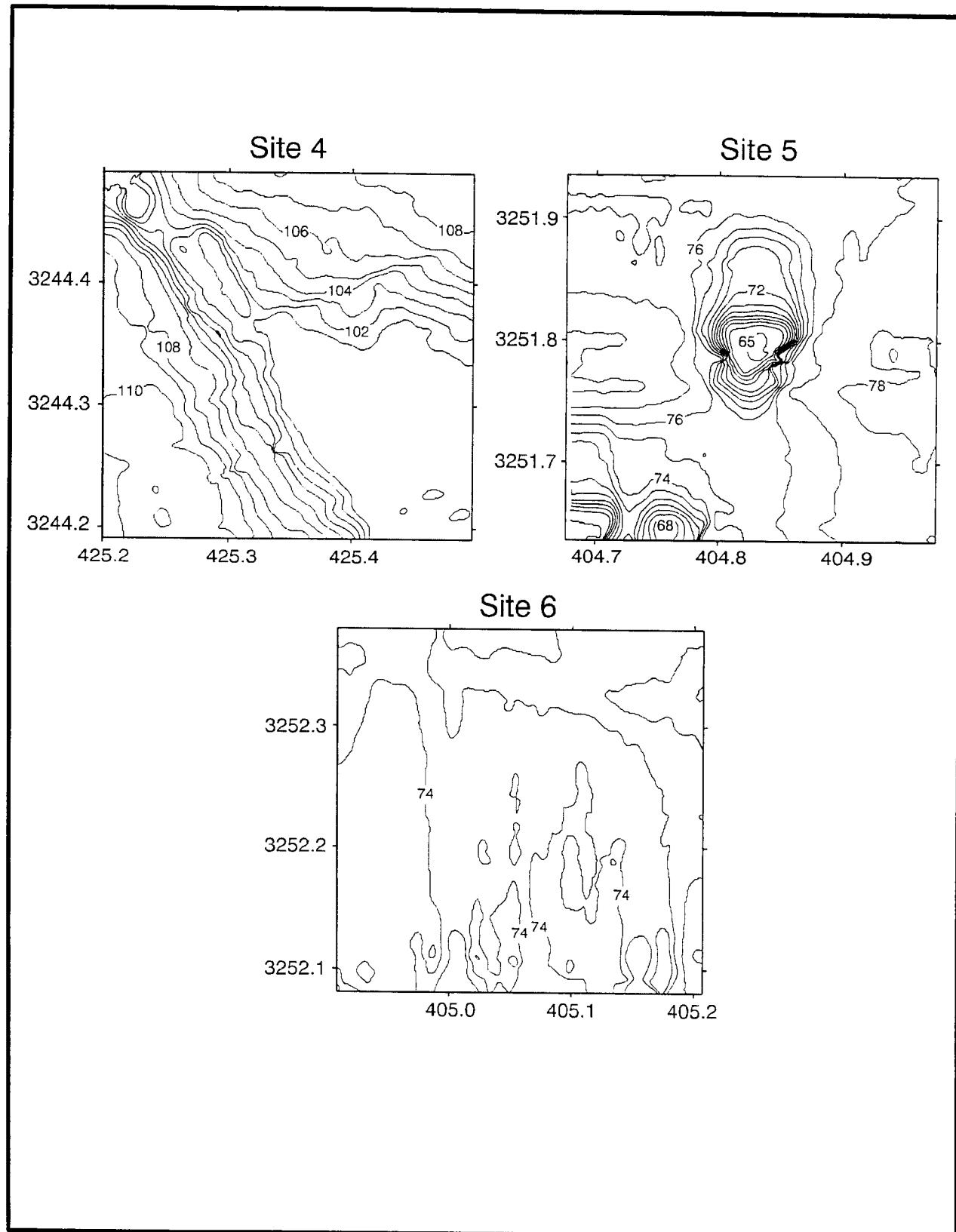
Fig. 4.8. Bathymetry of monitoring Sites 4-6, derived from *TAMU²* sonar data. Contours are at 1-m intervals. UTM plots with axes labeled in kilometers.
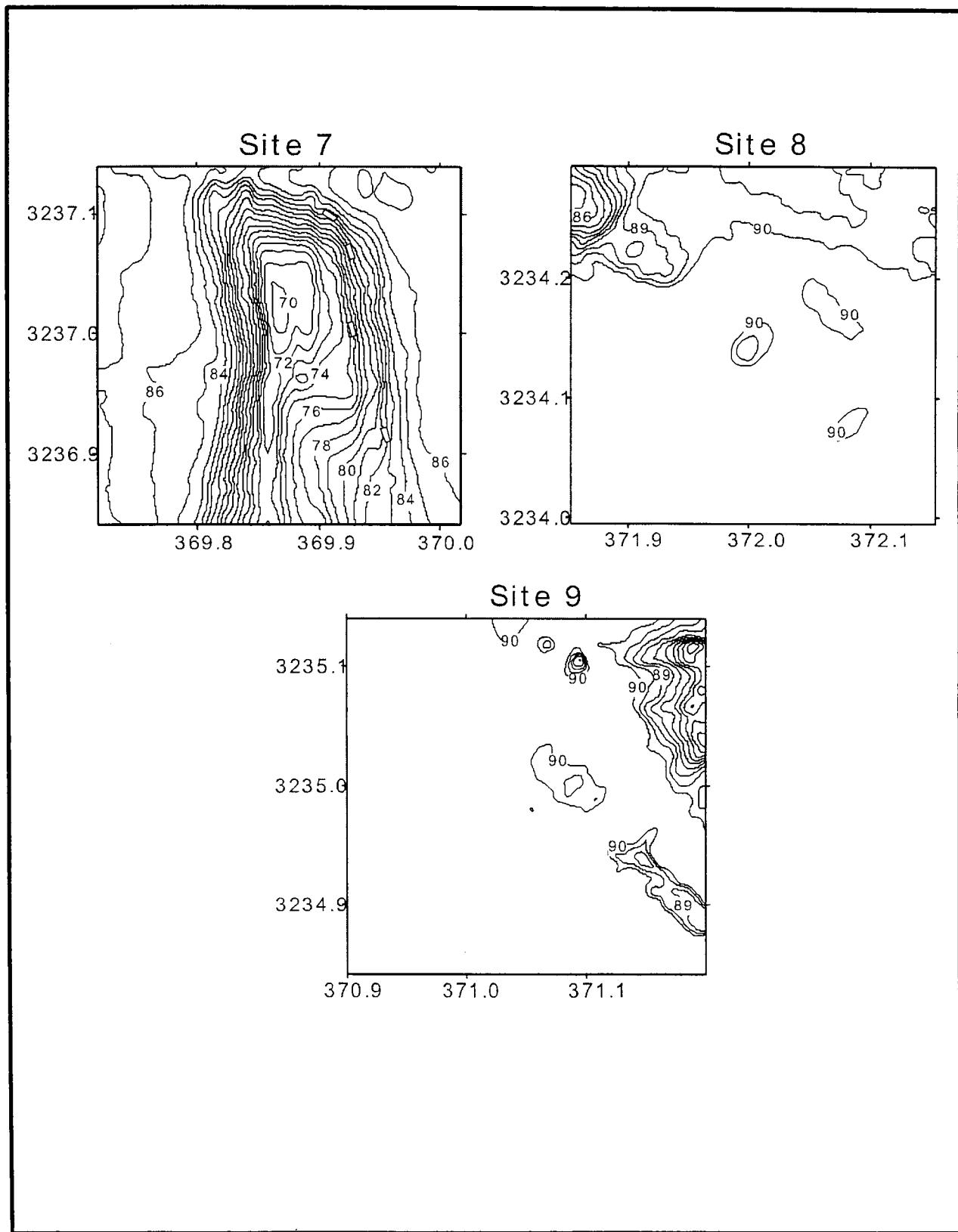
Fig. 4.9. Bathymetry of monitoring Sites 7-9, derived from *TAMU²* sonar data. Contours are at
1-m intervals in Sites 7 and 8. Extra 0.5-m contours are shown in Site 9 for clarity.
UTM plots with axes labeled in kilometers.

50

energy continues to propagate away from the sonar. Most of the returned energy is "backscattered," a process that includes diffraction from microtopography and scattering of energy from particles in the uppermost sediments (so called "volume scattering"; (Johnson and Helferty 1990). In the images, strong echoes are plotted dark whereas weak returns and shadows are light. Much of the returned acoustic signal appears to be related to mound topography and roughness (i.e., shadows, strong returns from faces that are directed towards the sonar, and diffraction from rough areas) and backscatter variations are caused by sediment textural variations.

Megasite 1

Prominent in the Megasite 1 mosaic are numerous groups of medium to large mounds, principally located in the northern, central, and western parts of the survey area (Fig. 4.10). In contrast, much of the seafloor in the southern part of the survey is mostly featureless. The large mound group in the north-central part of the megasite contains several large, flat-top mounds greater than 100 m in diameter. One of these, in the east-central part of the site, is the location of Site 1, atop the flat-topped mound known as "40-Fathom Fishing Grounds." Numerous smaller mounds are associated with these larger mounds. Another large mound group appears at the western edge of the survey. Associated with all of the mounds are areas of high backscatter, which appear dark in these mosaics. These high backscatter features usually are located on the southwest sides of the large mounds and mound groups. In subbottom profiler records, these areas show some erosion of the surficial sediments, so they are probably a textural difference caused by current winnowing. Many small to medium mounds show high backscatter "tails" extending to the southwest (Fig. 4.11). These appear as shallow gullies in the subbottom profiler records, implying erosion by bottom currents (Fig. 4.11). In the northeast part of Megasite 1 are three linear to sub-linear high backscatter features that appear to be small buried ridges in the subbottom profiler records. The most linear is about 25 m wide by 300 m long. These may be related to the shoreline ridges noted in the original MAMES survey (Sager et al. 1992).

Megasite 2

The Megasite 2 mosaic shows numerous mound clusters in a broad band that trends southwest to northeast across the survey area (Fig. 4.12). In the western part of the survey, areas of medium backscatter define broad, low hard bottoms typically several hundreds of meters across. Detailed examination of the sonar records shows that small mounds, typically less than 10 to 15 m across, are associated with these features. These large features appear to be carbonate hard bottoms, which may consist of many smaller mounds. In the central and east-central part of the survey, taller mounds are evident as acoustic shadows. These are often irregular in shape and associated with subcircular regions of high backscatter. In the far-eastern part of the survey, small mound clusters are associated with subcircular areas of high backscatter. Subbottom profiler records suggest these small mounds are the outcropping parts of larger buried mounds. There is also a suggestion that some of the tall irregular mounds are associated with broad carbonate bases, as if they grew atop hard bottoms similar to those farther west. Unlike high backscatter features in other megasites, those in Megasite 2 are not linear and rarely

51
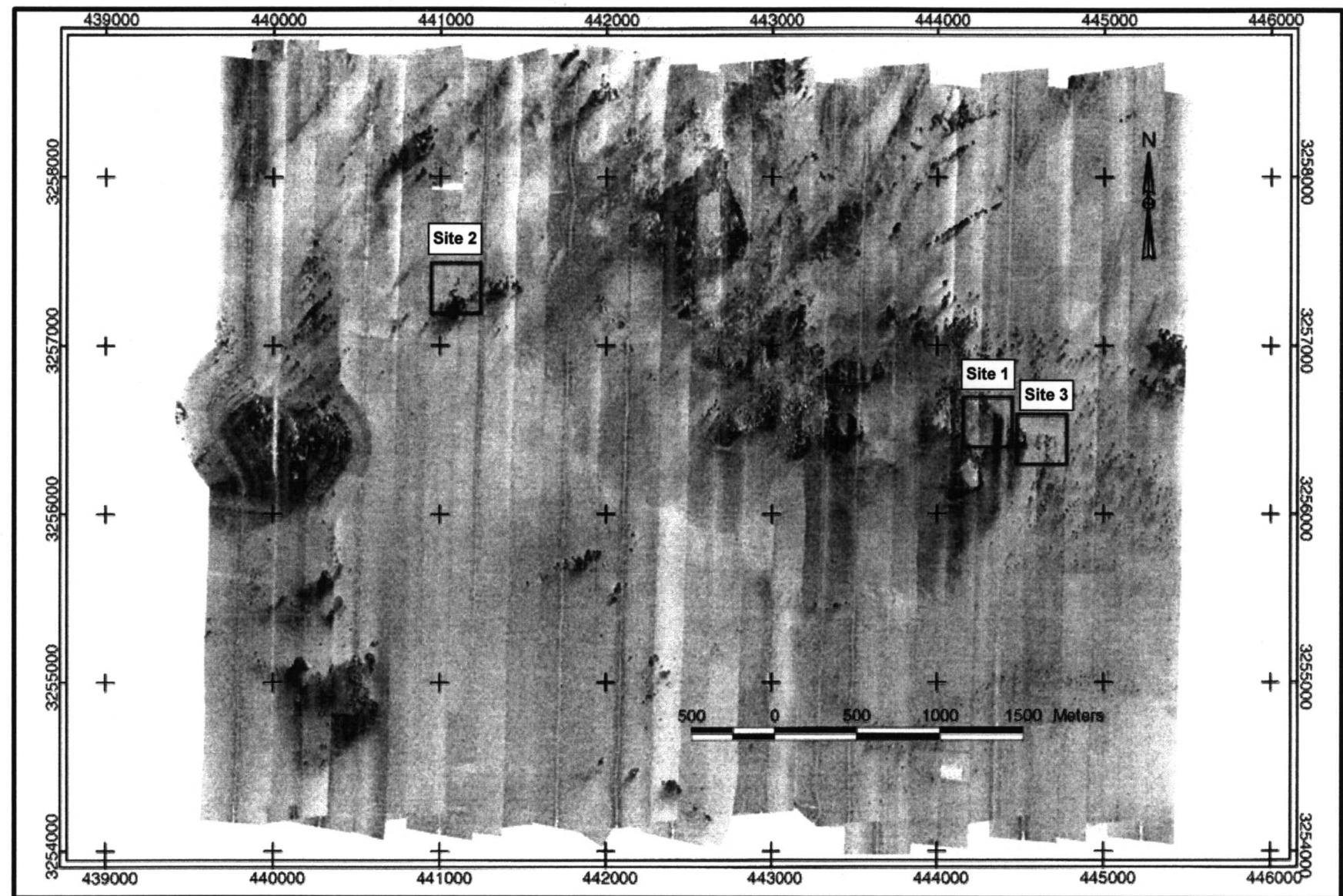
Fig. 4.10. *TAMU²* side-scan sonar mosaic of Megasite 1, showing Monitoring Sites 1-3 (small boxes). Vertical stripes are individual trackline side-scan sonar records pieced together to make the mosaic. Dark areas are high acoustic return (backscatter), whereas light areas are low backscatter. UTM plot with axes labeled in meters.
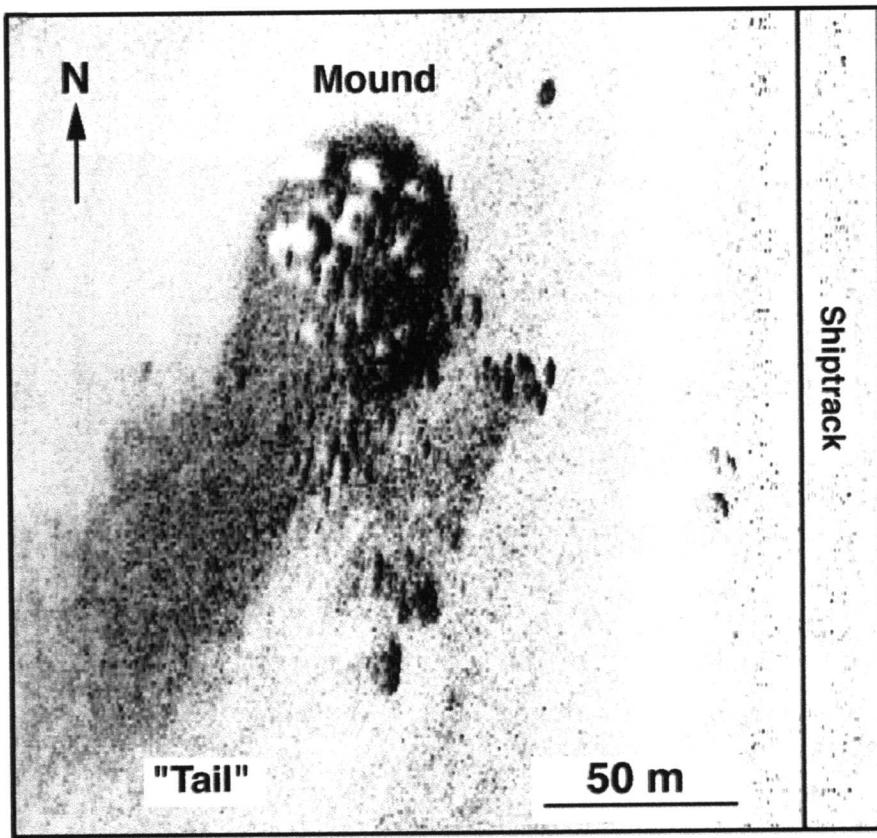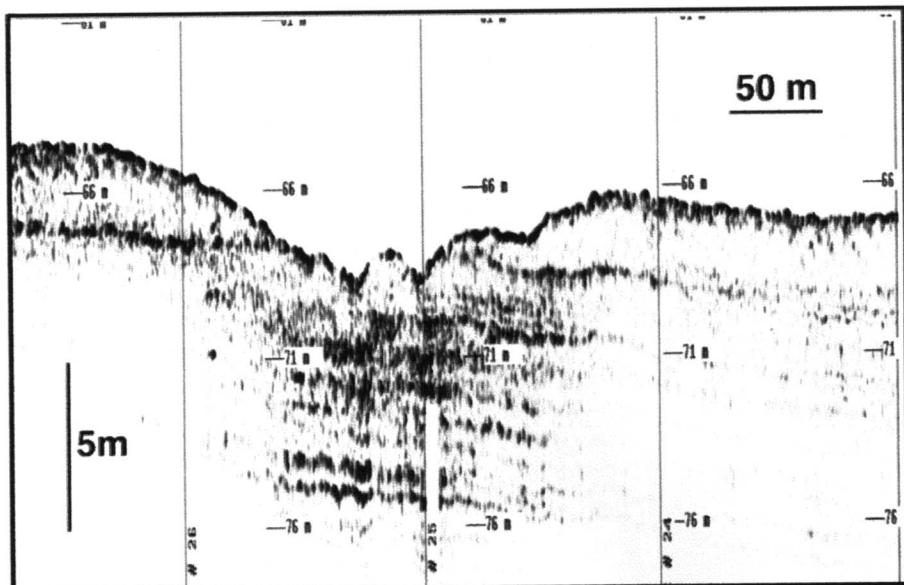
Fig. 4.11. Example of high-backscatter "tail" southwest of a mound in Megasite 1 and associated erosional gully. (Top) Chirp sonar subbottom profile showing gully approximately 3-m deep and 150 m across. (Bottom) High backscatter "tail" to southwest of mound. Dark areas indicate high backscatter and light represents low backscatter. Acoustic illumination is directed away from shiptrack (vertical line at right). Note: The two examples are from different locations because the subbottom profiler must pass directly over the tail feature, but the side-scan sonar does not image well directly beneath the sonar.

53
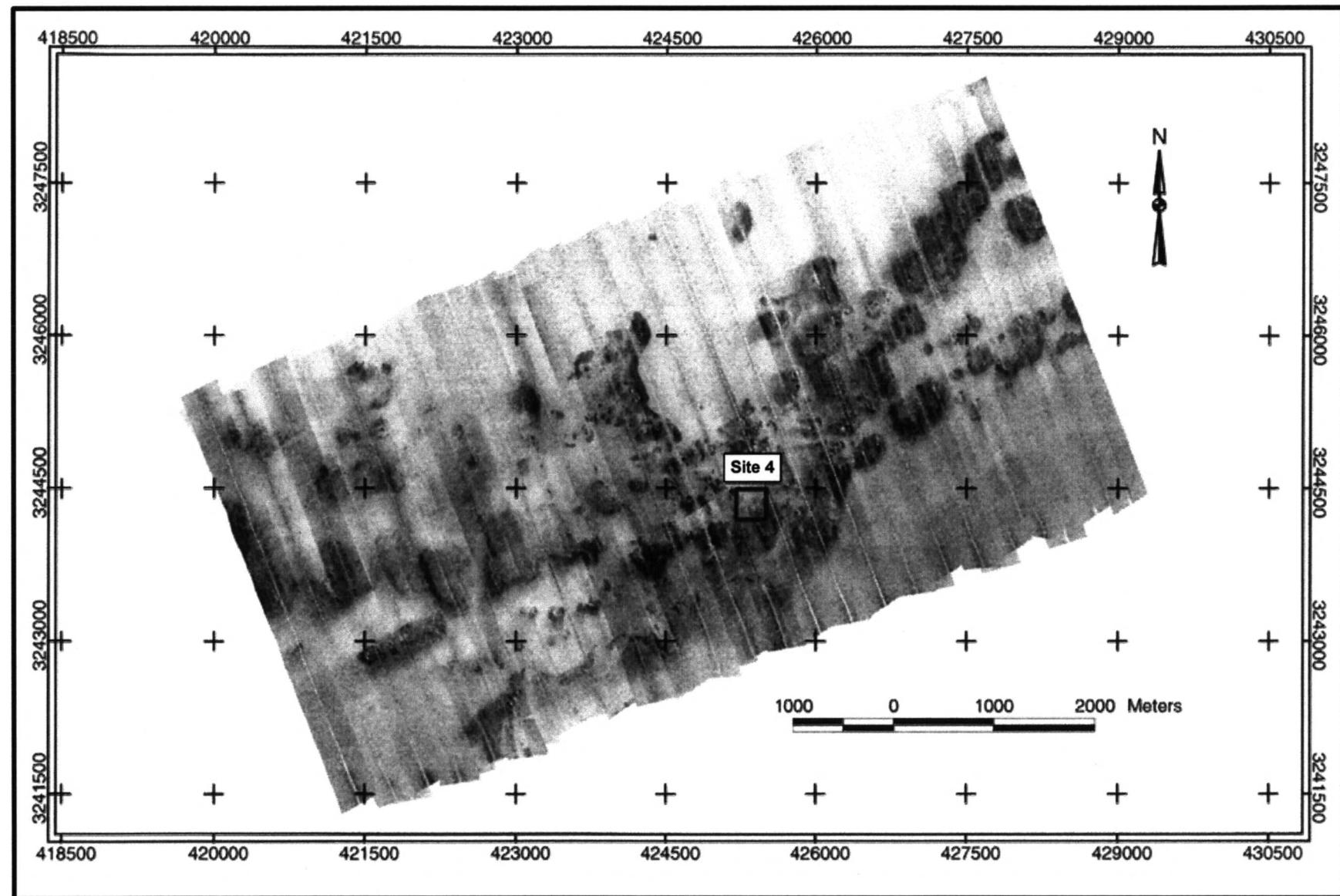
Fig. 4.12. *TAMU²* side-scan sonar mosaic of Megasite 2, showing Monitoring Site 4 (small box). Conventions as in Fig. 4.10.

appear to have a preferred direction or location relative to the mounds. Near the southern edge of the mosaic, a faint, curvilinear higher backscatter feature is the scar of a slump mapped by prior MMS surveys (Laswell et al. 1992).

Megasite 3

The Megasite 3 mosaic shows four main features: mounds, low carbonate hard bottoms, high backscatter areas, and a shoreline ridge (Fig. 4.13). Large mounds are seen clustered in two main areas on the east and west sides of the site. The eastern mounds are mainly subcircular features 50 to 100 m in diameter and many have flat tops. Site 5 is located in the cluster in the eastern central part of the megasite. On the west side of the megasite, large and small mounds are clustered into a linear group that trends to the southeast. Two smaller groups appear to its north and northeast. Two areas of broad carbonate hard bottoms appear in the megasite, one in the center of the survey and another in the northeast corner. These low hard bottoms are similar in appearance to those noted in Megasite 2. Both of these hard bottoms have higher backscatter than the surrounding seafloor, although the northeastern one shows more backscatter contrast. In detail, each hard bottom appears to have many smaller mounds, less than 10 to 15 m across, making up much of its surface. This is also similar in appearance to the Megasite 2 hard bottoms. As at other sites, areas of higher backscatter are associated with the mounds, often on the southwest sides of the topographic features. Also like other sites, many of these high backscatter areas are linear, or have linear edges, with a west-southwest trend. The linear, shoreline ridge feature appears mainly as an extension on the northeast corner of the survey. This extension was added because the ridge was known to be there from previous MMS surveys. The ridge shows high backscatter and is patterned with streaks parallel to its trend. This part of the ridge connects with a larger ridge that extends for over 10 km to the east (Sager et al. 1992).

Megasite 4

The appearance of the Megasite 4 mosaic is unique among all of the sites that were surveyed (Fig. 4.14). Unlike any other site, there are no large mounds. Mounds in this mosaic, if they exist, are seen only as small, subcircular, high backscatter features typically less than 20 m in diameter. Few show any evidence of acoustic shadow, indicating they are also low in height. The most obvious mosaic features are mottled backscatter seafloor in the north and northwest parts of the megasite, and a curvilinear feature that stretches from west to east across the southern part of the megasite. The curvilinear feature coincides with an area of slightly greater slope in the bathymetry (Fig. 4.5) and probably indicates the edge of a delta sediment wedge. The patchy backscatter areas in the northern parts of the survey do not match up with features in the subbottom profiler or bathymetry data. These are probably areas of slightly different sediment texture.

Megasite 5

In the Megasite 5 mosaic, a curvilinear group of hundreds of large to small mounds is the most obvious feature (Fig. 4.15). This group contains most of the mounds in the

Fig. 4.13. *TAMU²* side-scan sonar mosaic of Megasite 3, showing Monitoring Sites 5 and 6 (small boxes). Conventions as in Fig. 4.10.
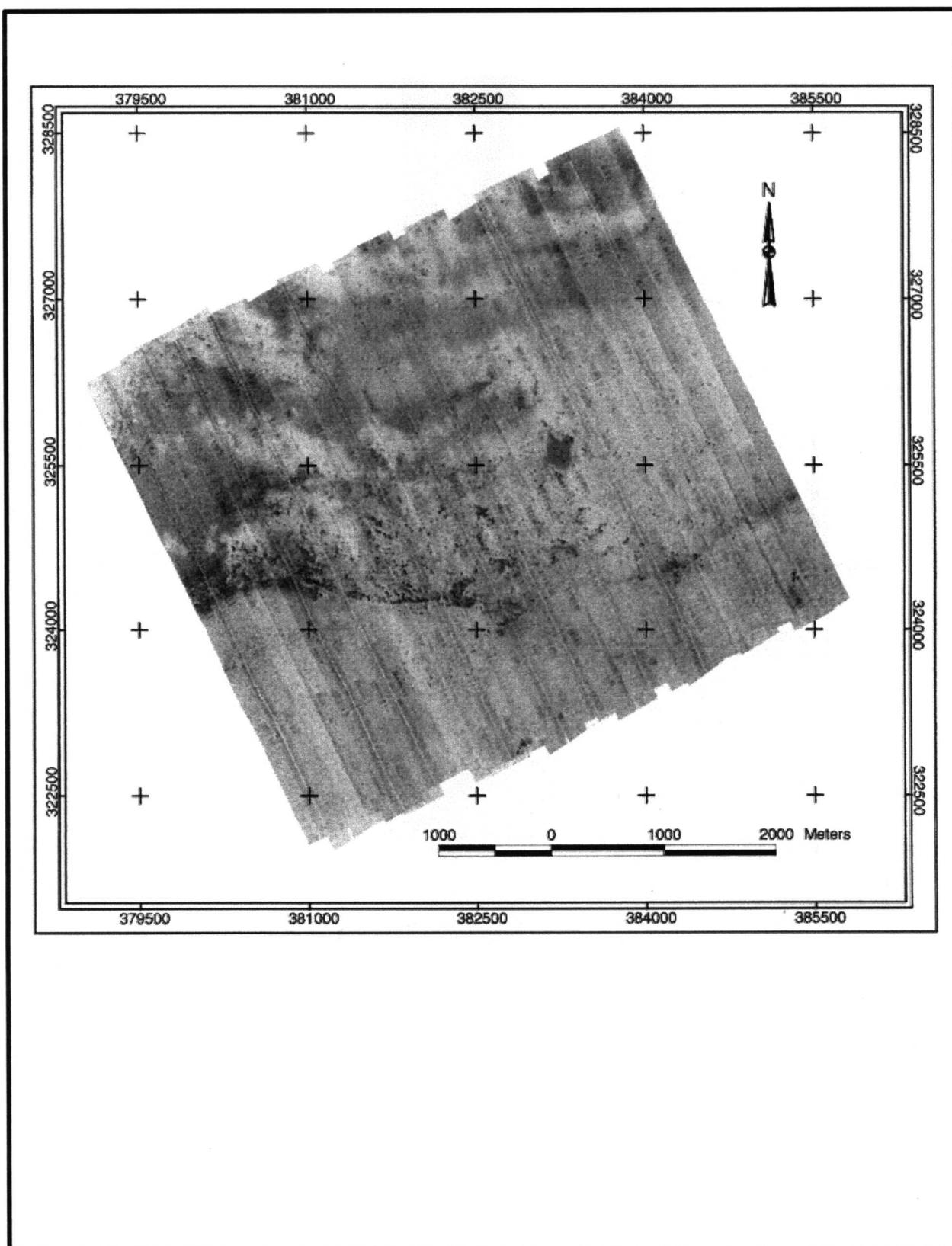
Fig. 4.14. *TAMU²* side-scan sonar mosaic of Megasite 4. Conventions as in Fig. 4.10.
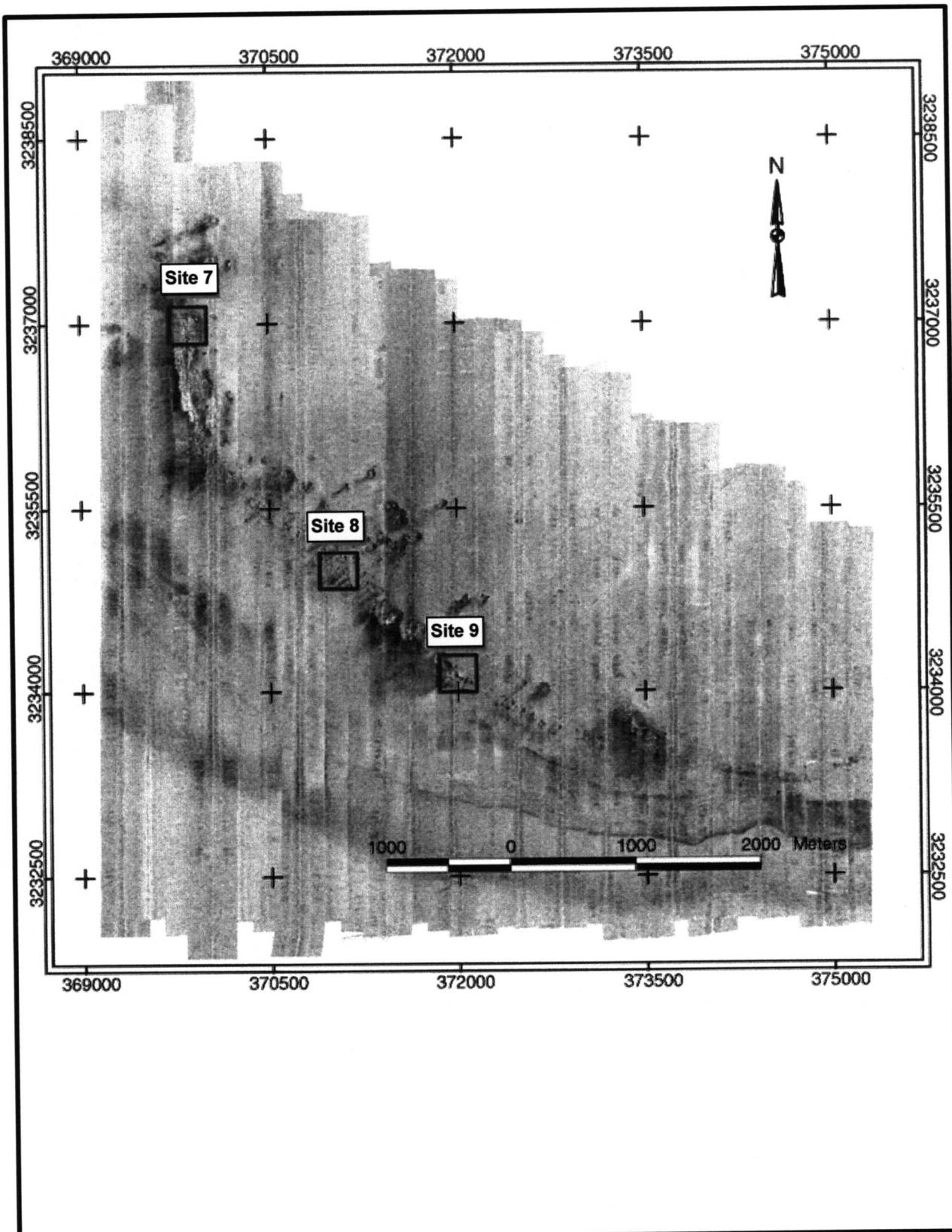
Fig. 4.15. *TAMU²* side-scan sonar mosaic of Megasite 5, showing Monitoring Sites 7-9 (small boxes). Conventions as in Fig. 4.10.

megasite. At its northwest end is a large, rough, linear mound (named "36-Fathom Ridge") whose north-south trend deviates from the overall northwest-southeast trend of the mound group. This mound is about 1,000 m long by about 150 to 300 m wide. Site 7 is at the northeast end of this mound. In the center of the curvilinear mound group are several large mounds, approximately 50 to 100 m across, including two that appear to have flat tops. The number of mounds decreases to the southeast, except for one moderately large group. As at other megasites, high backscatter areas are associated with the mounds. Usually these areas are on the southwest sides of mounds and mound groups and often they are linear with a southwest-northeast trend. A unique feature of Megasite 5 is a curvilinear, high backscatter band that appears seaward of the mound group. This feature is not associated with any mounds nor is it evident in the bathymetry. It appears to be the upper edge of certain sediment layers exposed at the shelf edge.

Mound Morphology and Characteristics

General Observations

Of the five megasites, four of them (1, 2, 3, and 5) contain recognizable carbonate mounds. The size, number, and morphology of mounds at each site vary significantly. Diameters range from 1-2 m to >1 km. Numbers of mounds vary by about two orders of magnitude. At Megasite 1 there are over 1,000 mounds, whereas Megasite 5 contains only about 120. The mounds are generally subcircular in shape with the majority having an aspect ratio of about 1:1 (Fig. 4.16; Note: the aspect ratio is the ratio of the major and minor axes of the ellipse that best fits the mound outline). However, some are elongated with aspect ratios as high as 8:1. Heights are not as well measured by the data as shape and diameter, but it appears the tall mounds in the present study are about 13-23 m tall and the shortest less than 1 m. The largest and tallest mounds are few in number whereas smaller, shorter mounds occur in greater numbers. The previous study (Brooks 1991) suggested that the number of mounds of a given diameter increases exponentially with decreasing diameter.

In general, the mounds can be classified into several different forms: (1) small, "unit" mounds, (2) composite mounds, (3) irregular mounds, (4) smooth-top mounds, and (5) carbonate hard bottoms. These groups are not distinct, i.e., there are no clear boundaries between different groups, but these classifications are useful for the purposes of discussion.

The smallest mounds are subcircular and appear to be about 1 to 15 m in diameter and <1 to 3 m in height. Because they are typically one, subcircular feature, that are called "unit" mounds. They may be isolated or occur in clusters of various densities, although they are commonly found in groups of tens to hundreds in number (Fig. 4.17). Unit mounds occur in all megasites, probably including Megasite 4, in which the complex sea bottom backscatter patterns make it difficult to unequivocally recognize mounds.

Composite mounds are usually several tens of meters in diameter and appear to consist of several to several tens of unit mounds, tightly clustered with sides touching (Fig. 4.17). The height of smaller composite mounds are generally only several meters, but large,
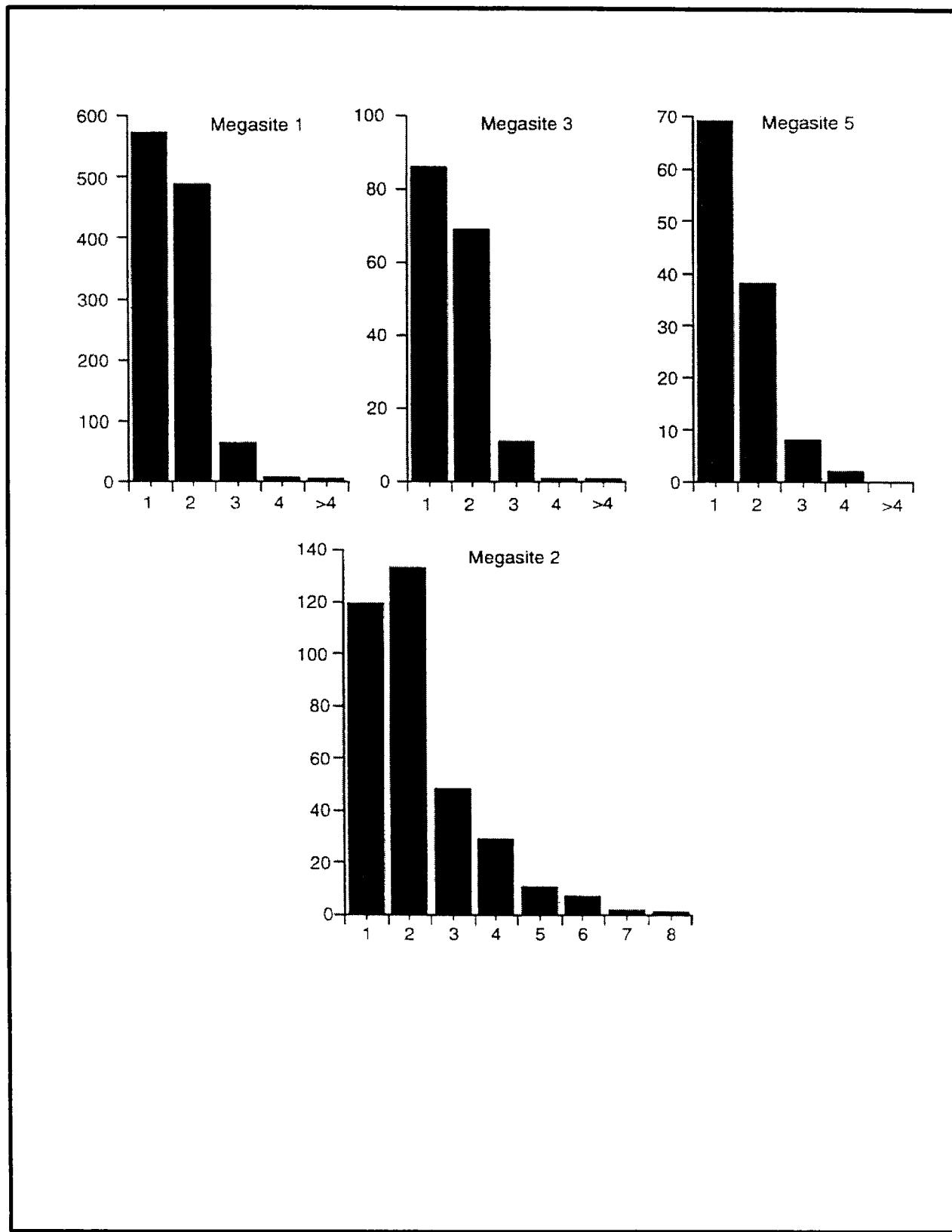
Fig. 4.16. Histograms of aspect ratios from carbonate mounds in Megasites 1-3 and 5. The aspect ratio is the ratio of the maximum and minimum axes of the ellipse that best fits the mound shape.

60
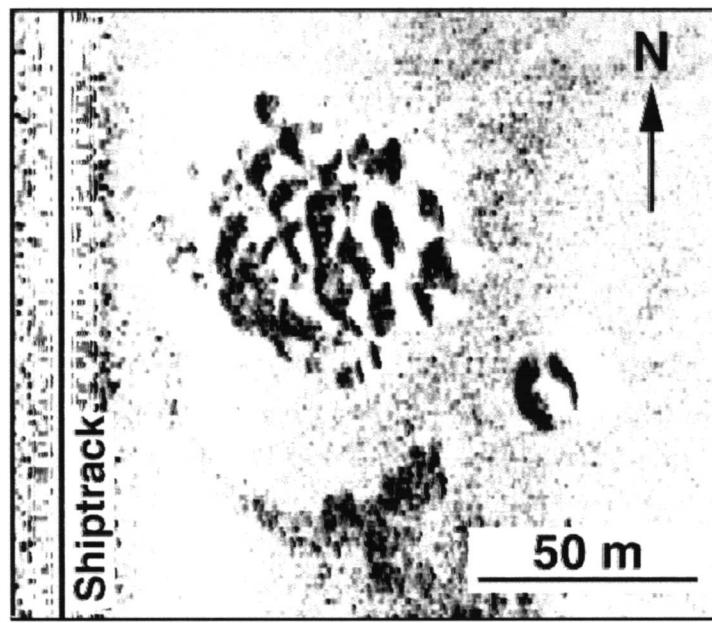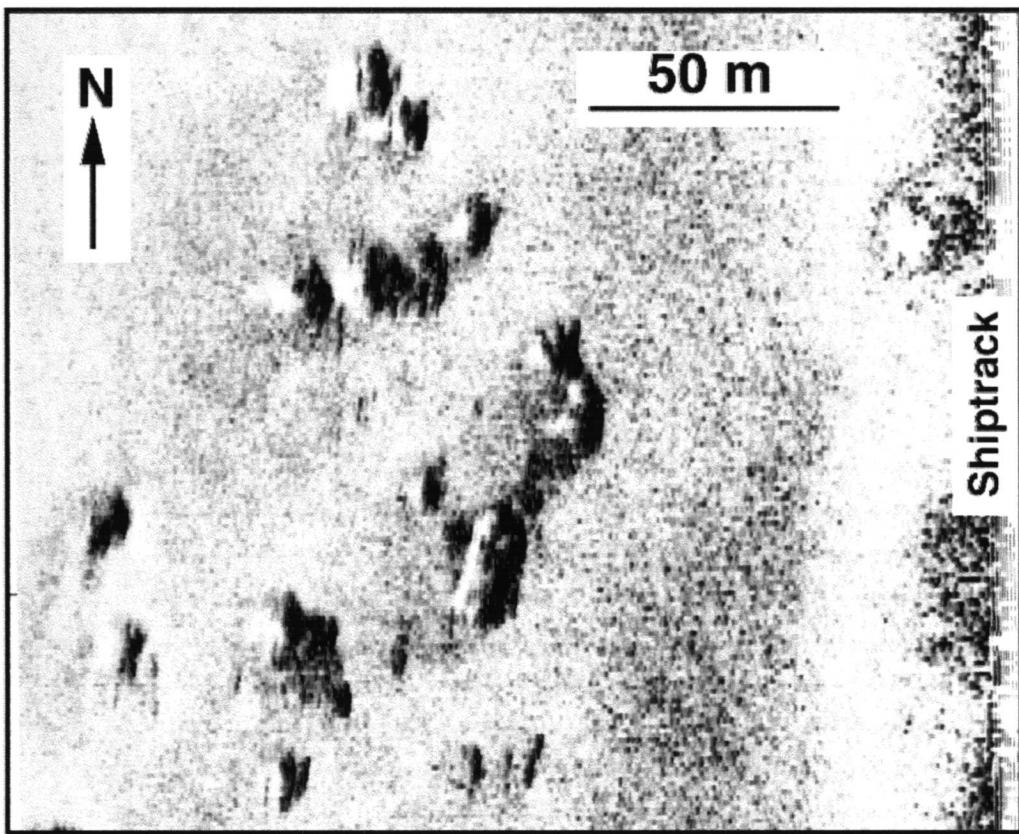
Fig. 4.17. Side-scan sonar images showing individual "unit" mounds (Top) and a composite mound (Bottom). Dark areas represent high-backscatter and light areas are low backscatter. Acoustic illumination is from the shiptrack (vertical line).

smooth-top mounds may also be composite features (see below). Based on appearance, composite mounds are believed to be the result of coalescence of unit mounds. Composite mounds are found in megasites 1-3 and 5.

Irregular mounds are different from composite mounds in that they have jagged, irregular outlines and rough surfaces. Whereas composite mounds seem to be made up of features of similar size and subcircular shape, irregular mounds have surface roughness across a broader size range exhibiting irregular spacing and outline (Fig. 4.18). Irregular mounds rarely occur in Megasites 1, 3, and 5, but are common in Megasite 2.

Many of the largest mounds have smooth tops. Some have flat tops, all at the same level, suggesting sea level control (Sager et al. 1992). However, others are more rounded and not all at the same depth. Typically flat and smooth-top mounds are tall, over 10 m in height. Their sides are typically steep and contain large blocks or monoliths (Fig. 4.19). Smooth-top mounds exhibit edges that range from nearly vertical with few or no blocks to those that contain hundreds of blocks (Fig. 4.19). The blockiness is reminiscent of rubble developed on the edges of carbonate hard bottoms on the U.S. east coast owing to bioerosion of the hard bottom (Riggs et al. 1996). Although bioerosion may be a factor in producing the blocks at the edges of some smooth-top mounds, the blocks rarely form uniform rings around the mounds, as might be expected if bioerosion were isotropically affecting the edges. Furthermore, the blocks sometimes have the appearance of mound clusters and grade from composite mounds into smooth-top mounds. Therefore, the blocky edges of most of the smooth-top mounds are not solely a result of bioerosion. The largest mounds, >500 m in diameter, are smooth-top mounds. At the smallest, these mounds are 40-50 m across. Smooth-top mounds occur in Megasites 1, 3, and 5. The smooth-top mounds tend to be in the shallower sites but not at the deep shelf edge sites (Megasites 2 and 4).

Carbonate hard bottoms are large, extensive carbonate pavements, typically greater than a few hundred meters across. Often these features are buried on their upslope ends with a small drop of a few meters on their seaward ends; this is probably a result of the features being partly buried by sediments being transported seaward. Often these pavements appear to consist of tens or hundreds of unit mounds or a combination of an irregular platform and unit mounds. In Megasite 2, these features are numerous and come in a wide range of heights, some reaching more than 10 m from top to bottom. Many of these are partly buried so that only their tops can be seen on the side-scan sonar records (Fig. 4.18). In Megasite 2, irregular or unit mounds often form lineaments that follow the edges of the carbonate hard bottom (Fig. 4.18). In addition, most of the tall, irregular "pinnacle" mounds of Ludwick and Walton (1957) rest upon such bases. Sager et al. (1992) hypothesized that the low hard bottoms formed during a time when sea level was stable near the shelf edge whereas the irregular pinnacles formed later during rapid sea level rise. Carbonate hard bottoms also occur in Megasites 1 and 3, but are less numerous. Megasite 3 contains two extensive hard bottoms with hundreds of unit mounds. Megasite 1 contains a hard bottom upon which some of the large smooth-top mounds are built.
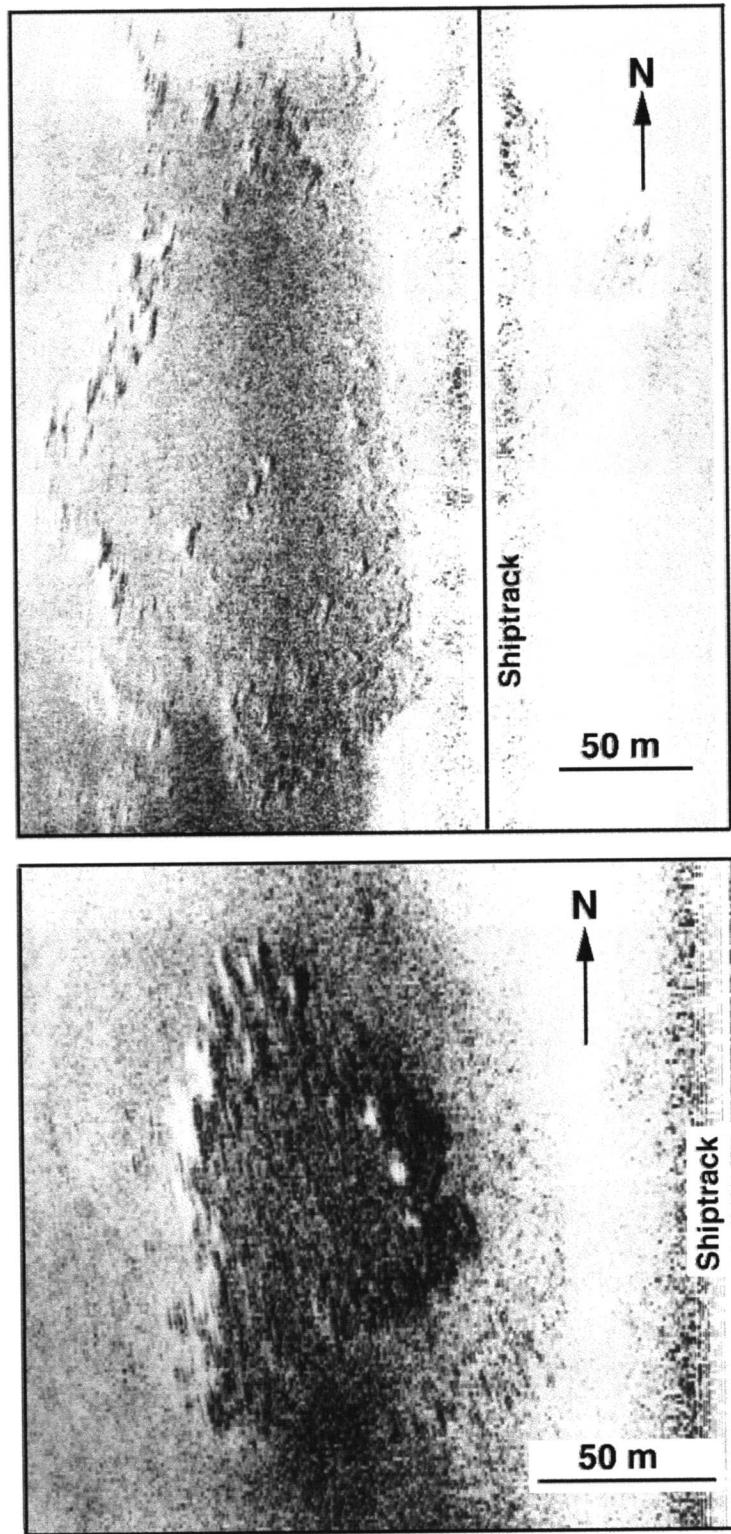
Fig. 4.18. Side-scan sonar images showing complex, irregular mounds from Megasite 2. Conventions as in Fig. 4.17.
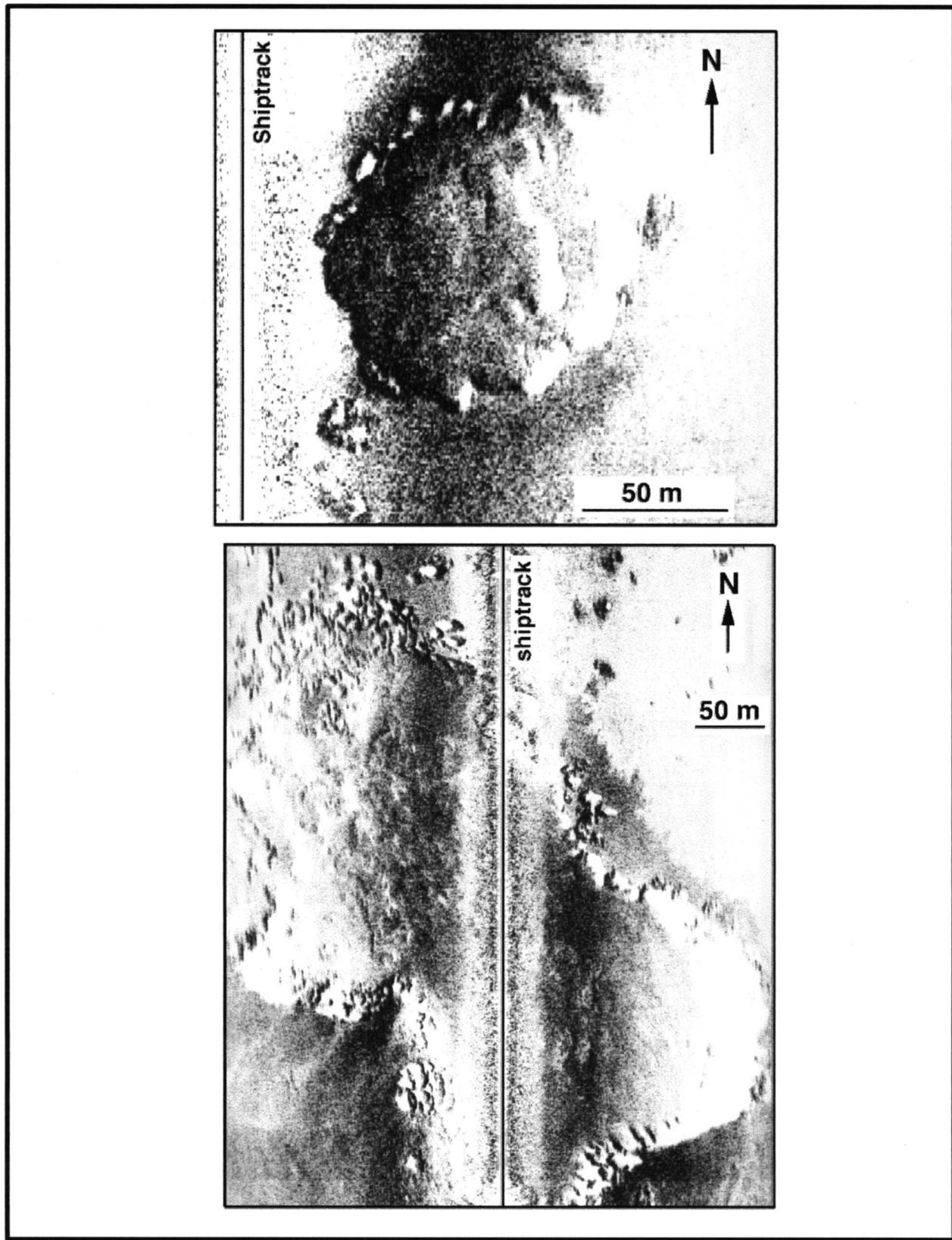
Fig. 4.19. Side-scan sonar images showing smooth-top mounds. (Top) Example from Megasite 3. Note the smooth top shows two levels. (Bottom) Large, flat-topped mound from Megasite 1. Monitoring Site 1 is located on the northeast edge of the top. Conventions as in Fig. 4.17.

Megasite 1

Megasite 1 contains the greatest number of mounds (>1,000). They are dominantly subcircular in shape and the smaller mounds (<10 m) tend to be the most nearly circular. Within Megasite 1, 53% of the mounds have an aspect ratio near 1:1 and 43% have an aspect ratio near 2:1 (Fig. 4.16). The number of mounds with higher aspect ratios falls off dramatically and only 0.05% fall into the 3:1 category or greater.

The majority of small mounds in the surveys are found in this site, especially in the western half. These mounds have both smooth and jagged outlines, with sizes ranging from 2-15 m across. Most are isolated, but some form small clusters. In the southwest corner of the site there is a large raised hard bottom which is marked by an area of very high backscatter and is covered with small mounds. Toward the north and east, medium to large mounds become the dominant features (Fig. 4.10). The larger mounds are typically smooth-topped and have irregular outlines, although some seem to be lower composite mounds. Additionally, in the northeast part of Megasite 1 there are two low hard bottoms which have highly irregular outlines. The first (or more northern) one is the foundation for large mounds that are >50 m across. The second (or more eastern one) is a raised hard bottom characterized by an area of high sonar backscatter which appears to contain many small mounds.

Megasite 2

Unlike other megasites, in which mounds of different sizes cluster in different places, there appears to be little sorting of mounds in Megasite 2, because all sizes of mounds are scattered fairly evenly across the site (Fig. 4.12). This site contains the greatest range of shapes with aspect ratios varying from 1:1 up to 8:1, whereas the other sites only range from 1:1 up to 4:1 (Figs. 4.16, 4.20). The majority of the mounds, however, still fall in the 1:1 and 2:1 categories (34% and 38%, respectively), but unlike other sites, the 2:1 category mounds are more numerous. Mounds at this site are typically elongated and trend in the N-S direction. More so than any other site, many of the mounds in Megasite 2 appear to be composites of smaller ones. Even where true composites are not seen there are often close clusters of small mounds, which may be the antecedents of composite mounds. This gives the edges of many mounds a jagged appearance and causes their surface to appear rough. Another interesting feature of these small mounds is that most appear to be roughly the same size, a few tens of meters across.

The geophysical data reveal a large number of hard bottoms present at this site. They appear on both side-scan and subbottom profile records as areas that have mostly smooth tops and may have 2-12 m of relief. High sonar backscatter is typical, but not universal as some appear to be partially buried with the sediment mantle making the delineation of their true shape more difficult. Smaller, elongate, composite mounds are often arranged in curvilinear arrays on top of the hard bottoms.
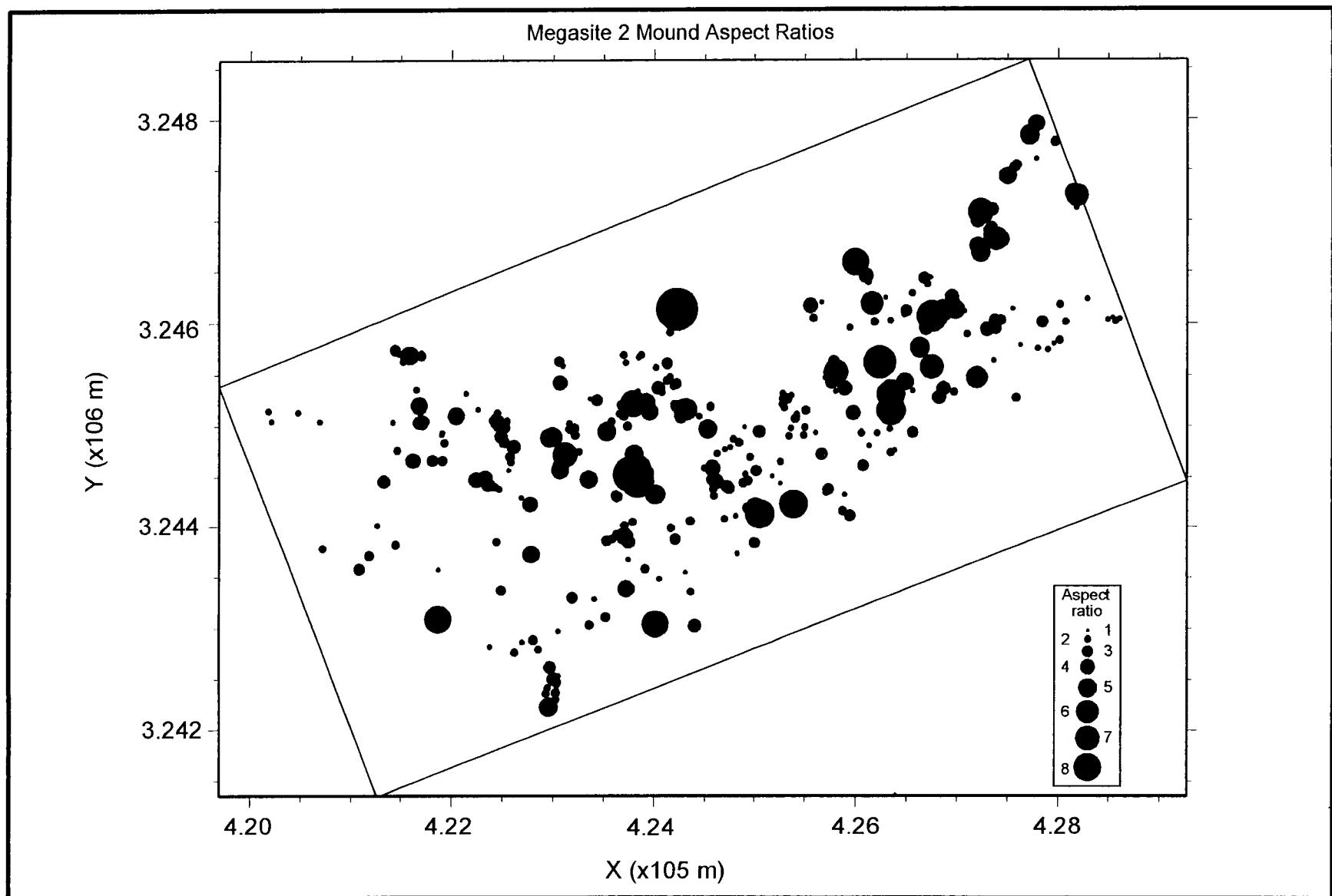
Fig. 4.20. Plot of carbonate mound aspect ratios (see caption to Fig. 4.16) and locations in Megasite 2. Symbols denote mound locations and symbol sizes represent the aspect ratio (see legend). UTM plot with axes labeled in meters.

Megasite 3

Megasite 3 is similar to Megasite 1, in that 51% of the mounds have aspect ratios near 1:1 and 41% are near 2:1 (Figs. 4.16, 4.21). The majority of the mounds lie in the western half of the site and most fall in a NW-SE trending linear array that is composed of small, individual mounds and what appear to be composites of small mounds that have grown together. About a dozen flat top mounds, measuring ~ 60 m across, occur in the eastern part of the megasite (Fig. 4.13). As well as the smaller mounds, two broad, low-relief hard bottoms are present and are characterized by regions of moderate to high backscatter (Fig. 4.13). Both seem to contain a many smaller mounds, although it is not discernable whether the hard bottoms are composites of small mounds or the foundations for a later generation of small mounds.

Megasite 5

The most obvious feature at this site is a curvilinear, nearly isobath-parallel group of hundreds of large to small mounds that contains the majority of the mounds at this site (Fig. 4.14). At the northwest edge of the group there is a large, rough, linear mound which is approximately 1 km in length, 150 to 300 m wide, and 18-24 m tall. It is by far the largest and tallest mound in the study area. In general, the mounds at this site have the following aspect ratio distribution: 59% near 1:1, 32% near 2:1 and 9% at 3:1 or 4:1 (Figs. 4.16, 4.22). Once again, the dominant shape is subcircular. The large mound, mentioned above, has the characteristics of a composite mound which is evidenced by its jagged edges that seem to be made up of small mounds. On the subbottom records, the top surface of the large mound has flat areas at its highest extent, but rough areas of peaks and valleys in between these plateaus. Surrounding this large mound are other small to medium-sized composite mounds as well as a number of singular small mounds that, as with those in Site 1, have a very circular appearance. To the south and east, other composite mounds of various sizes can be identified; however, the number of mounds falls off rapidly toward the eastern edge of the site.

Megasite Subbottom Profiles

Subbottom profiler records acquired with the X-STAR 2-12 kHz chirp sonar show the seafloor and internal acoustic interfaces within the uppermost sub-seafloor sediments. These records were acquired for two purposes: (1) to provide auxiliary data for the interpretation of side-scan sonar records and (2) to examine the distribution of recent sediments. Although the profiles have been useful for the first purpose, preliminary examination suggests that it may not be possible to create isopach (sediment thickness) maps for all of the megasites owing to geologic factors and the limited depth of penetration.

In general, most profiles show a thin, relatively transparent layer of sediments a few meters thick overlying a deeper horizon (Fig. 4.23). In places, this upper drape layer appears to contain more than one unit. The deeper horizon often appears as an angular unconformity where underlying delta foreset beds are truncated. In most of the survey areas, this horizon may represent erosion that occurred during the last glacial lowstand
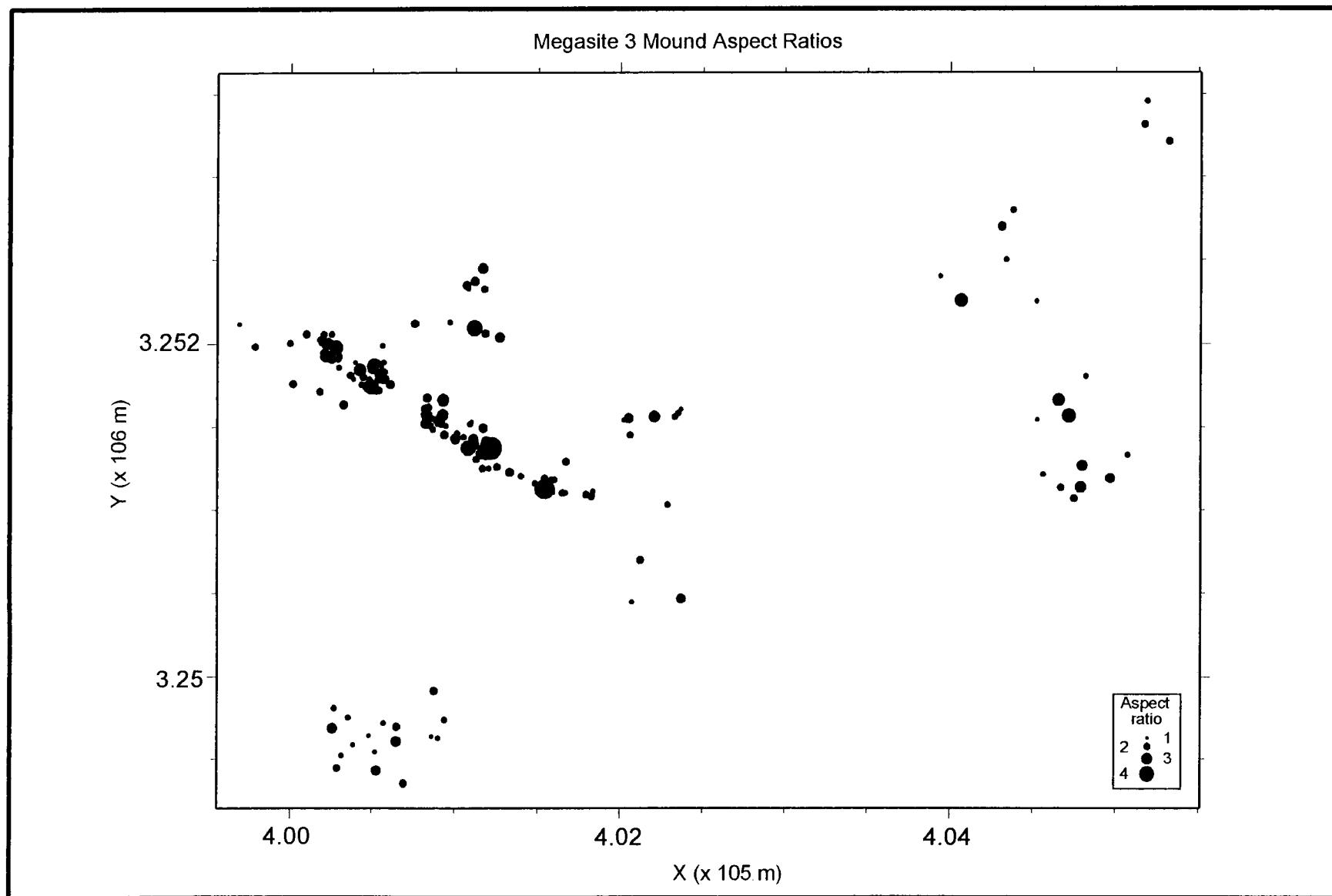
Fig. 4.21. Plot of carbonate mound aspect ratios (see caption to Fig. 4.16) and locations in Megasite 3. Conventions as in Fig. 4.20.
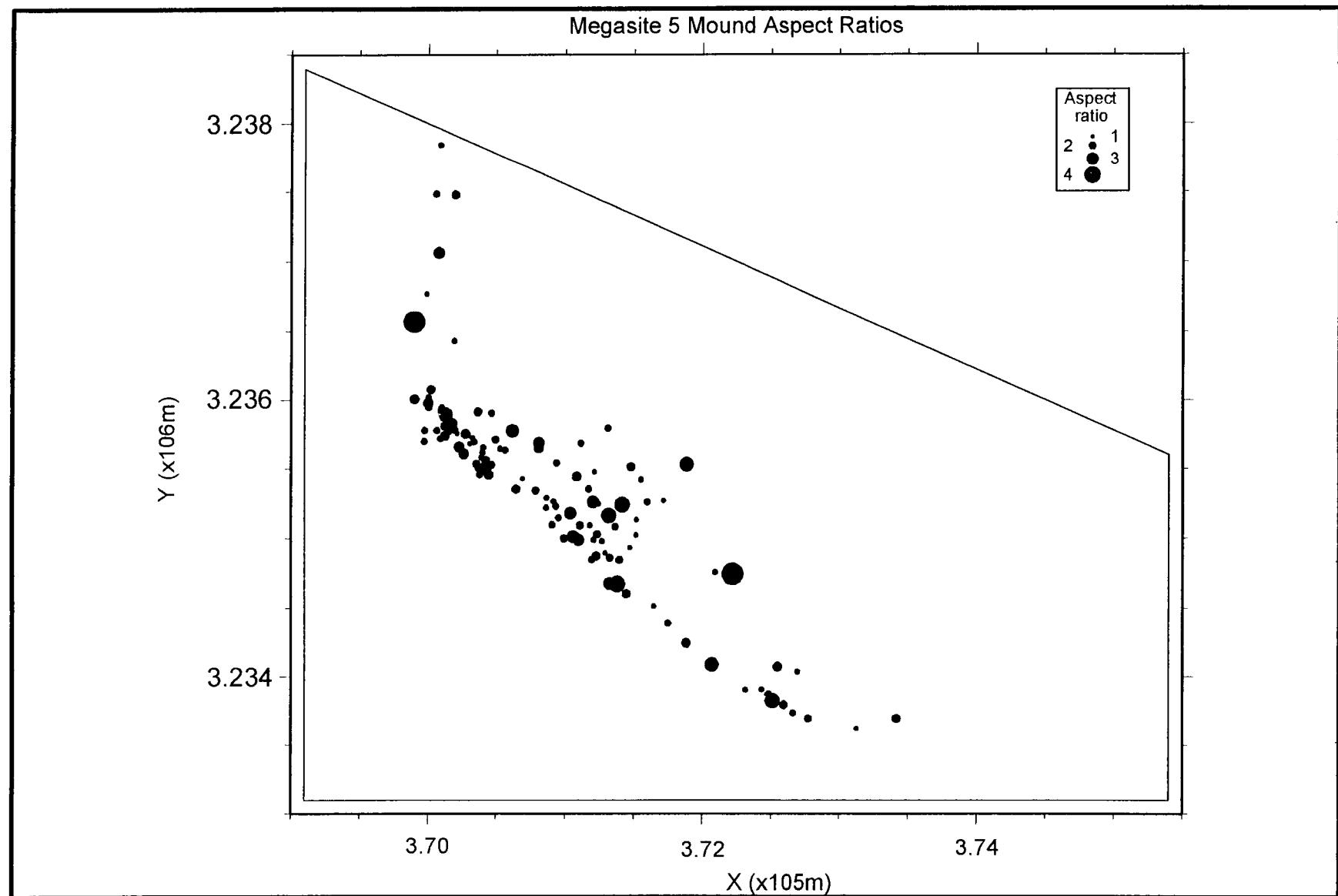
Fig. 4.22. Plot of carbonate mound aspect ratios (see caption to Fig. 4.16) and locations in Megasite 5. Conventions as in Fig. 4.20.
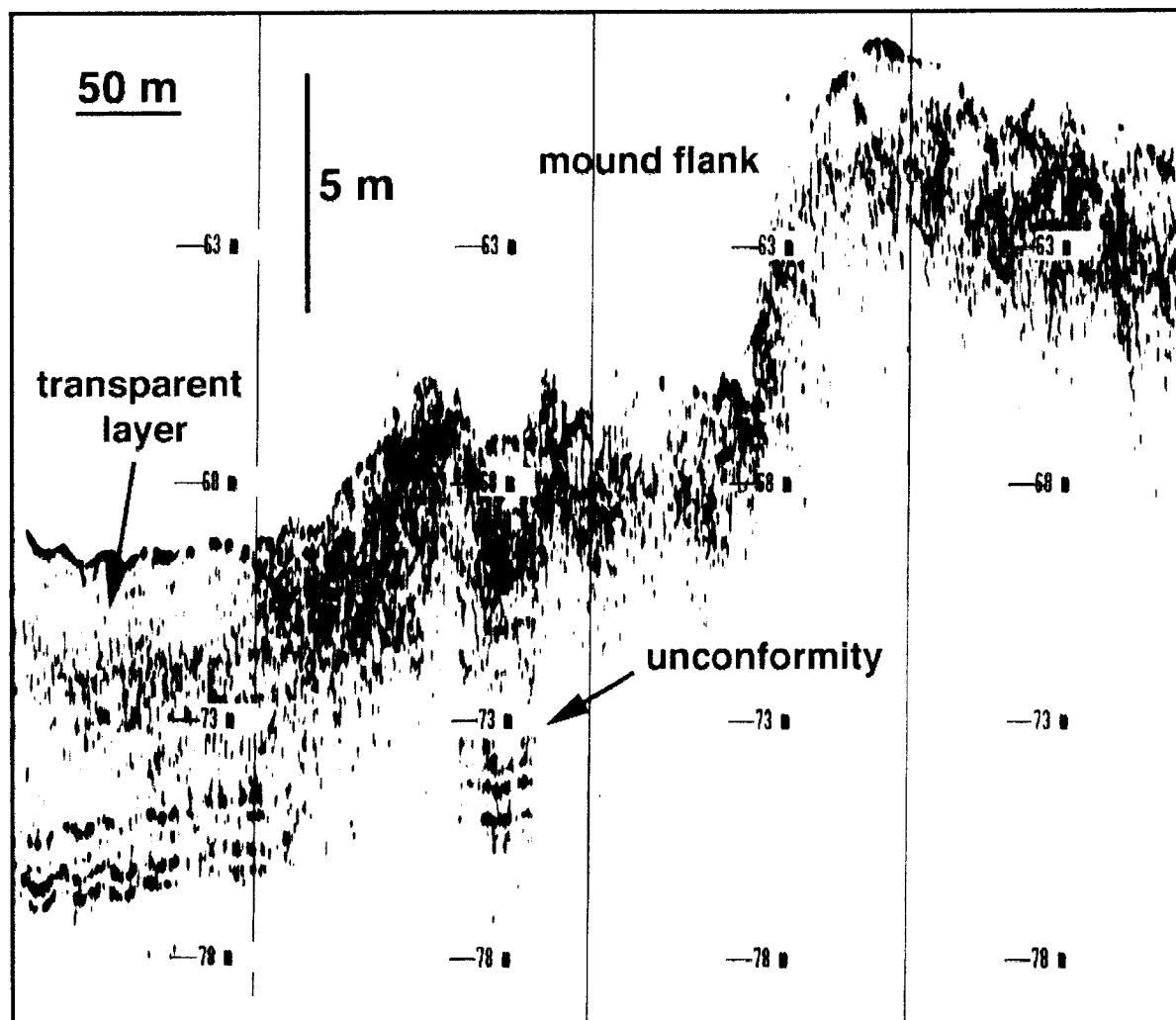
Fig. 4.23. Chirp sonar subbottom profile from Megasite 1 showing rough mound flank and typical sediment layering in the shallow subbottom.

(Kindinger 1989; Sager et al. 1999). However, in Megasite 1, which sits atop the "eastern delta" of the MAMES study, this horizon may be younger (Sager et al. 1999). Thus, the age of the unconformity at a particular site cannot be determined without additional age information.

One goal of the study was to create isopach maps of sediments overlying the erosional unconformity at all sites to better understand the long-term influence of the mounds on sediment distribution. However, there are two impediments to attaining this goal. First, in most records the upper transparent layer appears relatively uniform, i.e., isopach maps show little of interest. Second, it is difficult to discern this horizon or it is difficult to determine reflector continuity in many places. In some spots, it is evident that the sediments overlying the erosional unconformity constitute more than one layer, of which the upper transparent layer is only the latest. Much of the problem is that acoustic penetration has been inadequate to consistently define sediment layer thickness. In part, this may result from unusually impervious seafloor because the X-STAR records show penetration of 15 m or more in Megasite 4, but not in the other areas. The analysis has therefore focused on gleaning clues about the relation of the mounds to the sediments, rather than constructing isopach maps.

Megasite 1

Megasite 1 is an area where the bottom of the transparent layer is relatively easy to map. The upper transparent layer is relatively uniform at 1.0 to 2.5 msec (0.8 to 1.9 m; assuming 1,500 m/sec sound velocity) in thickness, but reaches 5.0 msec (4.0 m) at one location. At this megasite there is a notable correlation between areas where this uppermost layer has been eroded and dark (high backscatter) areas in the side-scan sonar mosaic (Fig. 4.11). The high backscatter areas are preferentially located on the southwest sides of the mounds, so most profiles over larger mounds show an erosional hole on the southwest side. Near the largest mounds, erosion occurs over a broad area several hundred meters across to a depth of 1 to 2 m. Behind one mound at the eastern edge of the megasite, the erosional hole has reached the underlying unconformity, but in most places some of the transparent layer remains. On several profiles, linear high backscatter "tails" trailing southwest from small to medium mounds have been matched with gullies, typically 20 to 200 m wide and 1 to 2 m in depth. The cause of the relationship between erosion and high backscatter is not yet clear. It probably represents a current winnowing effect that coarsens the average sediment texture of the seafloor in those areas.

Subbottom profiles from Megasite 1 also show interesting aspects of mound morphology. Many mounds appear asymmetric in profile with the steepest slopes on the seaward sides. The data show that this is caused by sediment dammed on the landward sides of the topographic features. Furthermore, on some lines there appears to be a 6 to 8 m depth offset across the mounds becoming deeper seaward. Across the large flat-top mound where Site 1 is located, for example, the erosional horizon beneath the transparent layer is at about 70 m depth on the north side of the mound and 76 m on the south side. This observation suggests that some of the mounds may sit atop a scarp.

71

Within Megasite 1 are three small, linear to sub-linear ridges, located in the northern part of the survey area. In the subbottom records, these ridges are asymmetric, with sediment dammed on their north sides and a slight erosional hole on their south sides. Typically the depth offset across these ridges is 1.5 to 2.0 m. The origin of these features is unclear, although previous speculation was that similar ridges are ancient shoreline features (Sager et al. 1992).

Megasite 2

At Megasite 2, the underlying erosional unconformity is not visible in many places. Above this horizon two more-or-less homogeneous layers are visible, the upper one acoustically transparent and the lower acoustically turbid. This configuration is most obvious to the north of the mounds and is often not seen to the south. These layers are typically about 1 to 2 m in thickness, occasionally 5 to 10 m. The surficial sediments lie atop mound flanks in most places. In particular, the linear, high backscatter area in the northeast part of the megasite is a buried ridge with small mounds on the tops of the larger mounds showing through. In many places the upper sediment layers are upturned on the mound flanks and pinch out, leaving the mound top exposed. These sediments typically bury the north sides of low, flat carbonate hard bottoms but leave the south sides exposed.

Megasite 2 profiles show no obvious correlation between high backscatter areas and erosion, in contrast to Megasite 1. This fits the observation from the mosaic that the high backscatter areas have no preferred direction. Because these areas fringe the mounds, it is likely that the high backscatter is caused by textural differences owing to material shed from the mounds.

Megasite 3

In Megasite 3, the surficial sediments also appear as a thin transparent layer, typically 1 to 2 m thick. Similar to those of Megasite 2, the two low, flat carbonate hard bottoms are buried on their north sides and show a 1.5 to 2.0 m scarp on their south sides. The tops appear even with surrounding sediments and there are small, thin, transparent areas that suggest sediment ponds.

The linear mounds in the western part of Megasite 3 show an asymmetric profile with low slopes on their north sides and steep slopes on the south sides. In part this is a result of sediments ponded on the north sides. However, the mounds themselves appear asymmetric and often have a low hump on the north sides and a pinnacle on the south side. Many profiles show a small erosional hole at the base of the south side, with a total height of about 10 m from bottom to pinnacle top.

The profiles show that at least one of the mounds in the eastern part of Megasite 3 has an asymmetric shape, but others have flat tops. In this region the dark high backscatter areas to the southwest of the larger mounds can be seen as an erosional feature on subbottom profiles, as at Megasite 1.

Megasite 4

Like its sonar image data, the subbottom data from Megasite 4 are unique. In this area, seaward-dipping delta foreset beds are regularly seen beneath a thin transparent layer, 1 to 2 m in thickness. Penetration here is greater than at any other megasite and it is possible to see delta beds 10 to 15 m below the seafloor.

The curvilinear high backscatter feature in the southern part of the Megasite 4 mosaic corresponds to a zone of steeper slopes in the subbottom profiles. This is consistent with the bathymetry, which shows closer contours at this location. Interestingly, this zone is at different depths on different profiles. It is deepest on the east side of the megasite and shallows approximately 17 m to the west. This is also consistent with the bathymetry data.

In Megasite 4, it was not possible to match high backscatter areas with mounds or other features of the subbottom profiles, such as erosional areas, because the seafloor in the subbottom profiles usually appears uniform and few mounds are evident. Apparently most of the backscatter features in the side-scan sonar mosaic arise from textural variations at the seafloor.

Megasite 5

As at other sites, the upper transparent layer in Megasite 5 is nearly uniform and 1 to 2 m thick. In some places this layer is seen atop erosionally-truncated delta foreset beds. According to Sydow and Roberts (1994), these beds are part of the Lagniappe Delta. In the subbottom profiler records, this erosional surface is often irregular, a characteristic noted for the Lagniappe Delta top by Sydow and Roberts (1994).

The shelf edge in Megasite 5 has two unusual features. First, the dark band seen in the side-scan sonar mosaic corresponds to a reflection-free zone in the subbottom records. The seaward edge of this zone often appears as dipping reflectors and the landward edge sometimes matches with erosional "notches" in the seafloor. These observations imply this dark band is an exposed delta-front layer. As the dark band widens to the west, the shelf edge develops a large, flat mound of transparent sediments. The origin of this mound is unclear. The other unusual features are asymmetric troughs near the shelf edge with steep landward and shallow seaward walls. Usually just one is seen on a given line, although occasionally two occur. The depth and widths are several meters by 100 to 200 m. The asymmetric shapes suggest this might be a fault caused by an incipient delta-front slump. Sometimes mounds appear associated with the top of the landward wall of this trough.

Like the dark high backscatter "tails" trending southwest from mounds in other megasites, those in Megasite 5 also appear to be erosional gullies. Similarly, high backscatter areas are preferentially located to the southwest of many of the larger mounds, and the subbottom profiles often show slight erosion, especially on the southwest side of the curvilinear mound trend.

ROV Photo Station Geologic Data

Site 1

Most photo stations from Site 1, located on a large, tall flat-topped mound in Megasite 1, are on the top of the mound, so most geologic observations apply to this special environment. Although sediment cover is partial or complete at most stations, outcropping carbonate rock is also common. Nevertheless, meter-scale relief is typically low and the small-scale roughness is low to medium. Sediments are typically coarse and shell hash is common, implying a significant biogenic component.

Site 2

Located atop a medium-sized mound about 35 m in diameter, approximately half of the photo stations show rock outcrop and these are preferentially on the northeast side of the mound. Such a configuration is consistent with current flow from the northeast, which would account for the southwestward trending high backscatter "tail" emanating from this mound group, causing sediments to be eroded off the northeast side of the mound and deposited on the southwest side. Most stations, however, show partial sediment cover and the sediments are generally fine, so any currents are not so energetic as to sweep the mound bare of sediments. Both meter-scale relief and centimeter-scale roughness vary from small to large, and aside from a cluster of stations that show flat seafloor on the southwest side of the mound, these parameters are intermixed. This suggests that the character of the mound varies significantly on a lateral scale of meters.

Site 3

Despite the fact that the sonar mosaic for Site 3 shows a loose cluster of low mounds on an expanse of apparently flat seafloor, many of the photo stations showed outcropping rock and many of these were classified as "reefs," meaning mounds larger than the typical ROV-video view. Roughness and relief both vary from low to high, but low to medium values are more common. Sediment texture is mainly fine and sediment cover is usually partial. These observations make a picture of an environment of flat seafloor with many low mounds from boulder to house-size or larger, surrounded by fine sediments.

Site 4

Although Site 4 is located on the northwest side of a wide, medium-height mound in Megasite 2, photo station observations display considerable lateral variability. Stations at which outcrop is visible or not are about evenly divided and sediment types range from fine to coarse with several stations showing shell hash. Roughness ranges from low to high and relief ranges from flat to medium. Stations nearest the center of the site were mainly classified as "reef." Many peripheral stations were classified as "boulder" and several as "ridge." These observations indicate that geological conditions are highly variable laterally at this site.

Site 5

Site 5 is located on a tall, flat-topped mound in Megasite 3. Stations near the center of the site all show outcrop and are surrounded by stations at which no rock is visible. The no-outcrop stations mainly show no relief ("flat") and have fine sediments. This zonation reflects a sharp change from mound flank to flat seafloor nearby. Roughness is mainly low to medium, but some high values occur atop the mound. Meter-scale relief atop the mound is low to medium, consistent with the flat top observed in the side-scan images.

Site 6

ROV videos from Site 6 show an area that appears blanketed by a cover of fine sediments. Consistent with this observation, most photo stations showed no outcrop, particularly near the center of the site. Stations with outcrops were mostly clustered in the northwest and southeast quadrants. Although many stations are characterized by fine sediments, coarse sediments are common. Relief and roughness are often medium. These observations are consistent with the side-scan images that suggest the site is a low, wide carbonate hard bottom with a rough upper surface. The fine sediment cover is partial and often limited to sediment pockets within the hard bottom, consistent with subbottom profiler records.

Site 7

The initial Site 7 ROV photo analysis described most stations as outcrop, with many stations classified as medium to high relief, and the roughness is often medium. Nevertheless, a number of stations, particularly on top of the mound, are characterized by low roughness. Eleven stations on the west side of the site show flat seafloor or depressions containing shell hash or rubble. These stations are on the seafloor adjacent to and on the west side of the mound that shows high backscatter. These characteristics imply significant input of biogenic material from the mound and the depressions suggest erosion.

The second, more-detailed analysis of Cruises 1C, M2, and M3 gives a picture consistent with the structure of the site interpreted from the side-scan sonar images (Figs. 4.16, 4.24). The center of the site, which corresponds to the top of the mound, consists of a relatively continuous carbonate hard bottom interrupted by occasional cracks and shallow depressions or channels. The surface of this area is blanketed by a layer of silty to sandy sediment ranging from a thin veneer to near complete burial. Although often obscured by sediment cover, the surface texture exhibits small pits and depressions, but lacks large-scale roughness seen in other areas. Surrounding the central region is a ring in which relief becomes more important.

At the edge of the hard bottom, the carbonate surface begins to break up, often in steep, meter scale faces. This transitions outward into an area dominated by high relief monoliths (large, isolated rocks) several meters in relief and extent. These features often have broad bases and steeply slope upward to one or several peaks. The peaks may or may not be flat-topped and some have undercut edges. The surfaces of the monoliths are
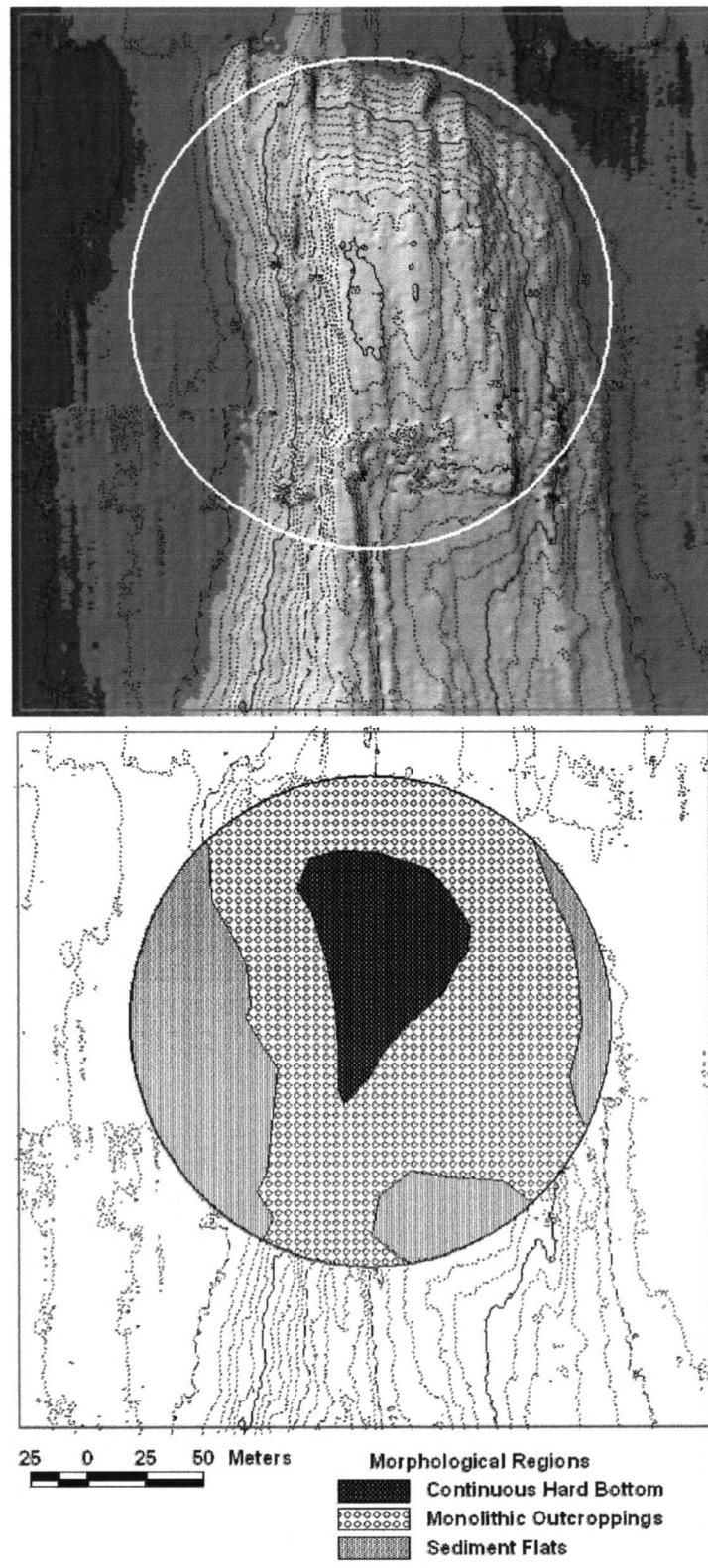
Fig. 4.24. Analysis of sea bottom morphology at Monitoring Site 7 derived from ROV photos and videos. (Top) Shaded relief bathymetry chart (compare to Fig. 4.9 for contour values). White circle denotes area investigated by ROV. (Bottom) Areas of similar seafloor morphology.

76

often mantled by a thin veneer of fine sediment and biogenic material. The monoliths tend to be separated by channels or valleys with sediment flats at their bottoms. General observations suggest the monoliths are more deeply eroded with distance from the center of the mound. The relief and size of these features seems to decrease with distance from the mound center, whereas sediment cover seems to increase.

The region of monoliths changes into a surrounding region in which sediment cover is complete and little or no evidence of outcrop is seen. These areas show a mixture of fine and coarse sediments with loose rocks and shells scattered on the surface. This area appears to begin at roughly equivalent depths on the north, east, and west sides. However, the sediment flats to the south occur at a shallower depth and lack some of the surface rubble seen on other sides.

Site 8

Site 8 is located on a medium mound in Megasite 5 and consequently most stations show outcropping rock and "reef" morphology. Centimeter-scale roughness is mainly low to medium and meter-scale relief is mostly low, except at the mound edges. Sediment textures are mainly fine except at a few stations atop the mound.

Site 9

Consistent with its location on low mounds in the center of Megasite 5, Site 9 is characterized by fine sediments, flat to low relief, low roughness, and fine sediments. One station contains shell hash, one shows medium roughness, and several show medium relief, suggesting scattered small mounds.

Grain Size Data

Grain size data show that sediments recovered in grab samples are typically sands with some gravel and clay. The median mean grain size for the 94 samples from Cruises 1C and M1 is 2.8ϕ (Fig. 4.25), with most samples having mean grain sizes between 1.75ϕ and 4ϕ. Many samples show a bi- or trimodal distribution. Often the size distribution peaks around 1ϕ to 3ϕ (fine sand) with a significant fraction in the smallest size class, $>10\phi$ (fine clay). Few samples contain significant silt. Many samples also have a large amount of the largest size class particles, $<-1.5\phi$ (gravel). These particles are typically shells, shell fragments, and other biologic detritus.

Ternary plots echo these characteristics (Fig. 4.26). On a sand-silt-clay plot, samples show a nearly linear scatter from sand to clay. Only those samples with moderate amounts of clay contain significant silt and even then the greatest silt content is less than 20% (Fig. 4.26). The nearly linear trend implies two sediment sources, one sand and the other clay, that are intermixing. On a gravel-sand-mud ternary plot (Fig. 4.26), samples tend to cluster near the sand apex, but considerably more scatter is apparent owing to variable content of gravel, up to about 50%. The variability of the gravel fractions and their biogenic compositions implies a local source.

77
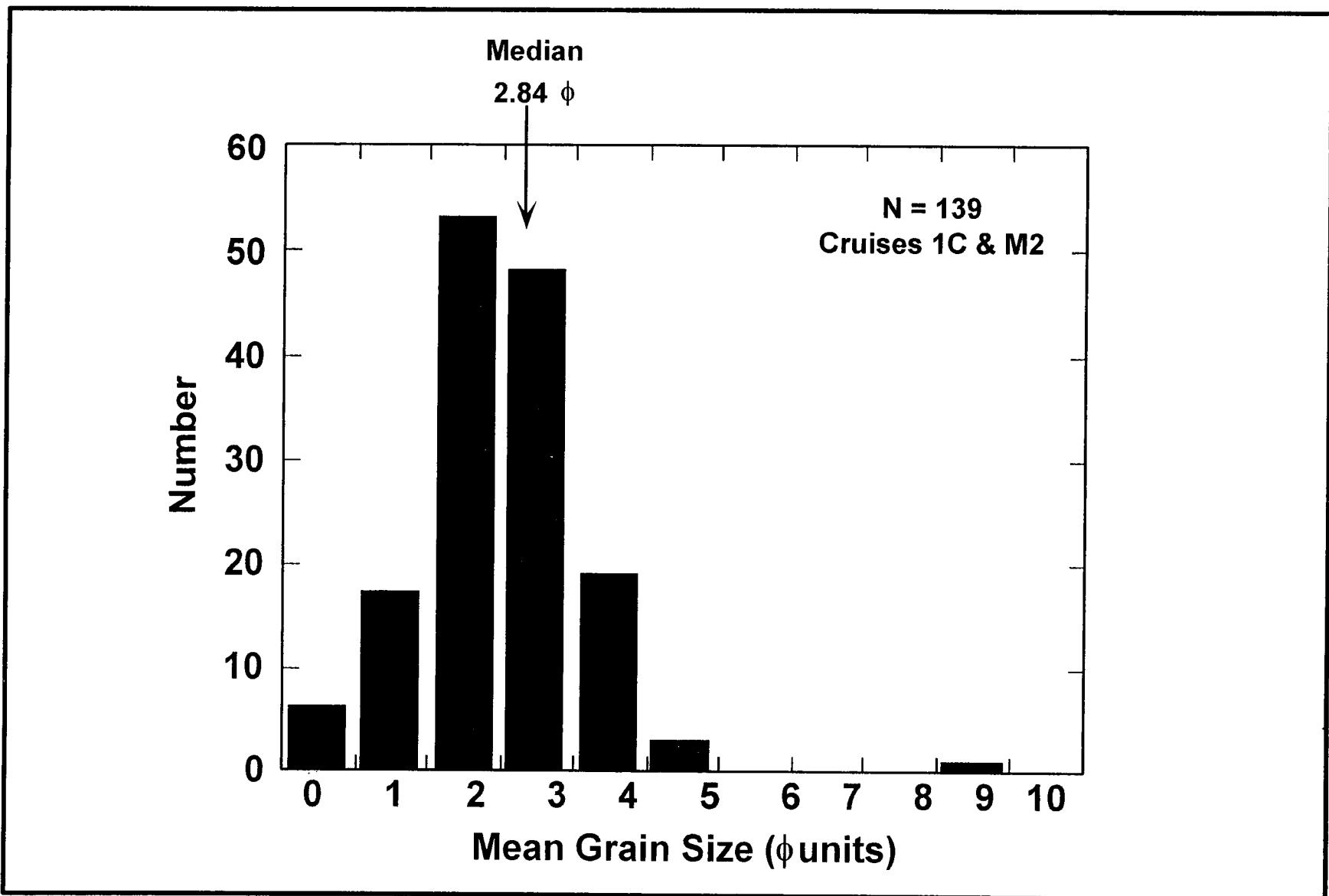
Fig. 4.25. Histogram of mean grain sizes for grab samples from Cruises 1C and M2.
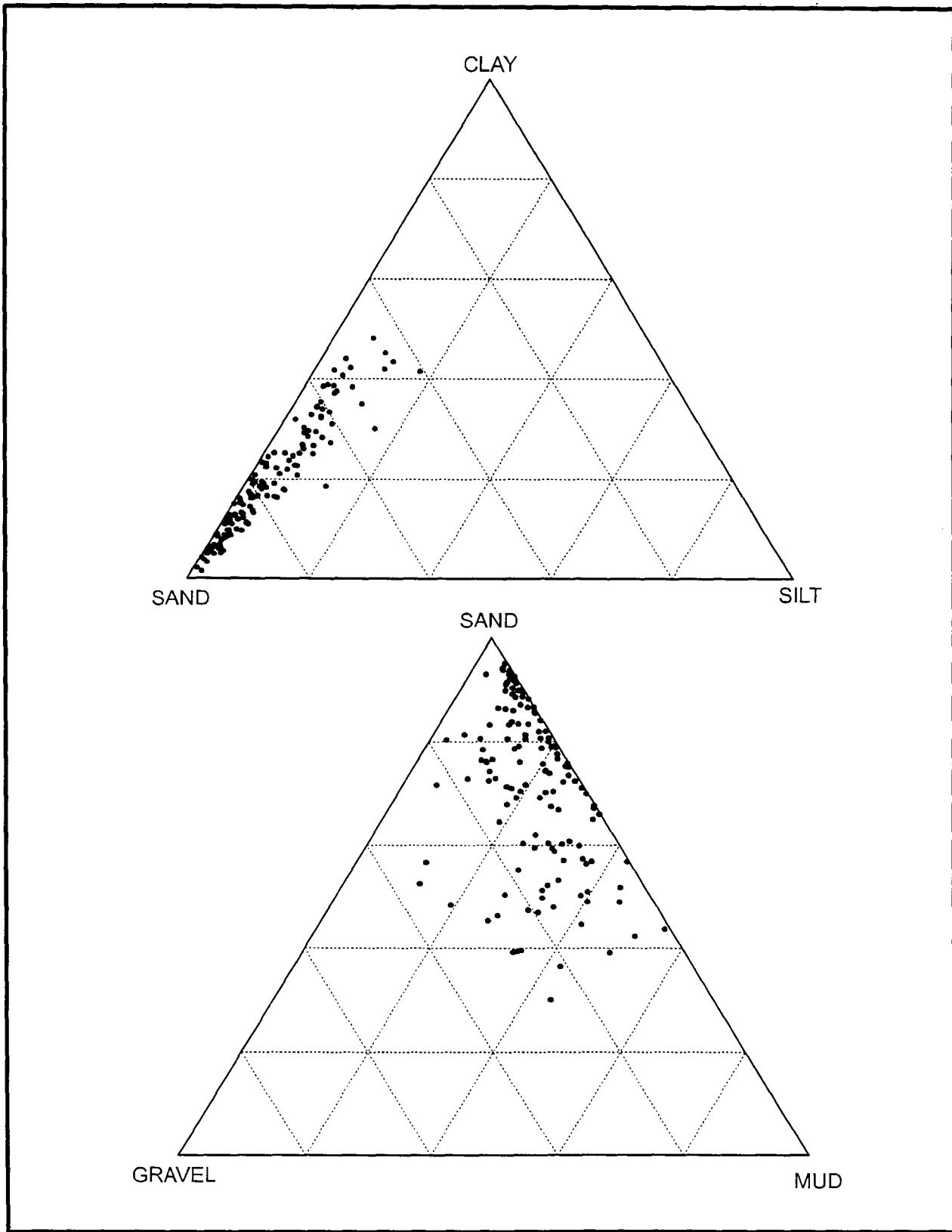
Fig. 4.26. Ternary diagrams showing size classifications of grab samples from Cruises 1C and M2. (Top) Sand-silt-clay ternary diagram. Samples were normalized to 100% after subtracting the gravel fraction. (Bottom) Gravel-mud-sand ternary diagram (Note: mud is combined silt and clay fraction).

79

There appears to be no simple correlation between backscatter and grain size. Samples from higher backscatter seafloor tend to be enriched in both gravel and clay. In addition, the highest gravel-content samples tend to be located near mound edges. For example, around the large mound where Site 7 is located, the grain sizes seem to correlate best with position and backscatter. Backscatter is high on the west and north sides of this mound and lighter to the east. Grabs 2, 6, 7, and 10, all located on the west side of the mound on higher backscatter seafloor, show the greatest concentrations of clay and gravel. In contrast, Grabs 1, 5, 8, and 9, all located on the east side of the mound, show the lowest clay and gravel contents. Furthermore, Grab 7, the sample with the highest gravel content, is located closest to the mound on the western side. At other sites, the correlation is not always as clear. These observations suggest that sediment sorting is a complex process, perhaps involving several mechanisms, and that mound proximity and current direction play major roles.

Discussion

From prior MMS-funded surveys in the Mississippi-Alabama outer shelf region, it was known that carbonate mounds were often clustered with sizes ranging from several meters on a side to hundreds of meters wide and 10 to 18 m high (Brooks 1991; Continental Shelf Associates, Inc. 1992; Sager et al. 1992). It was also known that areas of high acoustic backscatter were associated with many mounds (Brooks 1991; Laswell et al. 1992) and that in some cases these areas were preferentially located to the southwest of the mounds. This new study emphasizes and broadens these findings. In addition, a better understanding of the relationship of backscatter to the mounds and the sediment characteristics is being developed.

Although it was known previously that many of the carbonate mounds are subcircular in plan view, new side-scan sonar data show the details of mound flanks and co-occurrences with far greater resolution than ever before. In prior studies, a difference between mounds at the shelf edge, in water depths of about 105 to 120 m, and those shallower was recognized. The former seemed to have sharper peaks (they were the original Ludwick and Walton [1957] "pinnacles") and the latter sometimes had flat-tops (Sager et al. 1992). The new data show that flat or nearly flat tops are common among large mounds located in the 70 to 90 m water depth band. These data have also extended the observations westward by mapping several such mounds in Megasite 5. The side-scan sonar data also show that the shelf-edge "pinnacle" mounds are unlike the shallower mounds in that the pinnacle mounds are often irregular or linear in plan view whereas the shallower mounds are usually subcircular in plan view and often made up of clusters of smaller subcircular "unit" mounds. What is more, the new data imply a third class of mounds: low, wide, carbonate hard bottoms hundreds of meters in diameter but only a few meters in height. These features are particularly notable near the shelf-edge in Megasite 2, but are also seen in at shallower depths in Megasites 1 and 3. These mounds often have tops with features a few meters or less in height that make them appear to be made up of many smaller "mini-mounds" and in this sense they are similar to many of the other, shallower subcircular mounds.

80

The morphologic differences among mounds suggest differences in development. The low, wide carbonate hard bottoms imply slow upward growth over a large area, perhaps indicating stable sea level or slow sea-level rise. It was previously speculated that such mounds grew at the shelf-edge during the slow sea level rise after the last ice age (Sager et al. 1992), but now they are known to be even more widespread. The tall, steep-sided "pinnacle" mounds suggest rapid growth during faster sea level rise (Sager et al. 1992). Because many of these mounds apparently sit atop the low, wide hard bottoms, this may indicate a switch in mound growth from lateral to vertical aggradation owing to acceleration in sea level rise. The widely-dispersed, shallower mounds, which are highly-variable in size and height, may represent a short period of sea level stabilization in the middle of the deglaciation (Sager et al. 1992).

The new data also provide some insights about the location of carbonate mound formation. Prior data implied the mounds formed atop erosional unconformities on the two deltas in the MAMES survey area (Sager et al. 1992). The new data have supported this observation. Although layers cannot be traced beneath the mounds, owing to the scattering of acoustic energy, in many places delta foreset beds beneath appear continuous when traced from one side to the other of a mound or mound cluster. This would probably not occur if the mound had formed prior to the deposition of the delta beds; instead the beds would be distorted. The new data also imply that in some places, larger mound groups formed on bathymetric scarps, as shown as depth offsets, or atop carbonate hard bottoms. These observations imply that the mounds formed where suitable substrates were available. This is consistent, for example, with organisms requiring hard substrates for attachment.

Subbottom profiles over the mounds frequently show asymmetric profiles, another clue to mound formation. Often large mounds have a peak at the seaward edge and have sediments dammed up on their landward sides. These characteristics suggest that mound growth was most intense on the side facing the sea, where perhaps nutrients are highest and sediments least. This is similar to the formation of coral reefs in shallow water and lends credence to the hypothesis that the mounds were formed by biologic action in shallow water. The damming of sediments indicates that the mounds existed when the surficial sediment layer was deposited. Since it is generally accepted that this layer was formed from reworked sediments when sea level was much lower, this implies that the mounds existed when sea level was lower; in other words, they formed nearer to sea level.

The new findings about sediments give significant insights about sediment distribution and sedimentary processes. The upper acoustically-transparent layer, which apparently represents relict sandy sediments deposited by reworking during lower sea level, is more uniform than expected. This implies that currents and deposition are not highly variable around the mounds. What is more, the patterns in the sediment distribution and sonar backscatter suggest a dominant current direction. The high backscatter regions are located preferentially on the southwest sides of the mounds, except in Megasite 2. Particularly telling are long, thin, high backscatter "tails" that trend southwestward from

many small and medium mounds. These "tails" are erosional gullies clearly caused by flow disturbance owing to the mounds. This implies a general northeast to southwest current regime. This seems consistent with the damming of sediments on the north sides of many large mounds and erosional holes adjacent to their southwest sides. Like a "snow fence" the mounds evidently slow the currents on their "windward" sides, causing deposition and creating turbulence and erosion on the "leeward" sides. Comparison with current meter data suggests that the implied northeast to southwest flow is counter to the normal across-shelf currents. However, current data collected during the passage of a hurricane indicates southwest flow during the storm. Thus, the scouring of surficial sediments may be a storm related phenomenon.

Sediment grain size data imply the surficial sediments are composed of three end-members. Most sediments are mainly sand, with a smaller variable amount of clay added. The linear nature of the size data on the sand-silt-clay ternary diagram implies two end-members, sand and clay, that are intermixed. Since the sediments currently being deposited in the region are fine clays, this could occur owing to resuspension events that mix the clay with the sand near the surface. The third component consists of gravel-sized fragments, usually shells, shell fragments, or other biogenic debris. The gravel content is usually highest near mounds, indicating the mounds as a potential source or suggesting the mound proximity is an important factor for controlling the presence of organisms. Because there is no simple correlation between mound proximity and gravel content (many near-mound stations show no enhancement in gravel-sized fragments), the gravel may be shed from the mounds.

Grabs located in high backscatter areas sometimes, but not always, showed different grain size characteristics. The lack of a simple pattern suggests that several mechanisms contribute to the acoustic backscatter. As mentioned above, Site 7 grab data showed that stations in the high backscatter zone southwest of "36-Fathom Ridge" contain higher concentrations of gravel and clay. The latter is somewhat surprising because it was expected that these areas would be erosional, with preferential removal of fine sediments. Site 7 ROV photo data indicate that this zone is also characterized by meter scale surface relief and the common occurrence of rubble and shell hash. This indicates that the backscatter patterns are partly related to the occurrence of larger fragments and small-scale topography. The intermixing of both gravel and clay with the sand in these erosional areas suggests that the forces causing the erosion also mix the components. The bias towards southwest flanks implies that debris is preferentially swept to this side of the mounds.

Appendix Table 4.A. Grab and box core locations.

	X (m)	Y(m)	Lat.	Lon.	X (m)	Y(m)	Lat.	Lon.	X (m)	Y(m)	Lat.	Lon.
		Cruise 1C				Cruise M2				Cruise M3		
Site 1												
G4	444327	3256626	29.43938	-87.57401								
G5	444340	3256633	29.43944	-87.57388								
G6	444383	3256634	29.43946	-87.57343	444448	3256567	29.43885	-87.57276	444418	3256584	29.43900	-87.57307
G7a	444683	3257043	29.44315	-87.57036	444686	3257071	29.44341	-87.57034	444722	3257115	29.44381	-87.56997
G7b	444665	3257125	29.44390	-87.57055								
G8	444069	3256361	29.43698	-87.57666	444039	3256359	29.43695	-87.57697	443959	3256338	29.43676	-87.57779
G10	443808	3256515	29.43835	-87.57935	443770	3256549	29.43866	-87.57975	443718	3256548	29.43864	-87.58028
G11	443782	3256503	29.43825	-87.57963								
G12	444430	3256347	29.43687	-87.57293								
G13	443909	3256238	29.43586	-87.57830	443867	3256224	29.43573	-87.57873	443794	3256222	29.43571	-87.57949
G14	443866	3255436	29.42861	-87.57870								
G15	444537	3256520	29.43843	-87.57184								
BC1	444499	3256875	29.44163	-87.57225								
BC2	444915	3257109	29.44377	-87.56797								
BC3	445000	3256477	29.43806	-87.56707								
BC4	445417	3257041	29.44318	-87.56279								
BC5	445420	3257057	29.44332	-87.56277								
BC6	445359	3257053	29.44328	-87.56339								
BC7	445112	3256230	29.43584	-87.56589								
BC8	443891	3256184	29.43537	-87.57849								
BC9	444074	3255905	29.43286	-87.57659								
Site 2												
G1	441234	3257219	29.44459	-87.60594	441257	3257180	29.44424	-87.60570	441220	3257182	29.44425	-87.60607
G2	441267	3256983	29.44246	-87.60558	441235	3256944	29.44211	-87.60590	441175	3256957	29.44222	-87.60652
G3	441250	3256661	29.43956	-87.60573								
G4	440981	3257274	29.44508	-87.60854	440988	3257289	29.44521	-87.60848	440945	3257302	29.44532	-87.60892
G5	441068	3257223	29.44462	-87.60764	441009	3257213	29.44453	-87.60825	440962	3257187	29.44429	-87.60873
G6	441083	3257140	29.44387	-87.60748	441089	3257188	29.44430	-87.60743	441005	3257167	29.44411	-87.60829
G7	440686	3257265	29.44498	-87.61159								
G8	440677	3256968	29.44229	-87.61166								
G9	441000	3256953	29.44218	-87.60833								
G10	440690	3256685	29.43975	-87.61151								
G11	440995	3256658	29.43951	-87.60837								

Appendix Table 4.A. (Continued).

X (m)	Y(m)	Lat.	Lon.	X (m)	Y(m)	Lat.	Lon.	X (m)	Y(m)	Lat.	Lon.
		Cruise 1C				Cruise M2				Cruise M3	
Site 2											
BC1 441059	3256957	29.44222	-87.60772								
BC2 440811	3256649	29.43943	-87.61027								
BC3 441244	3254924	29.42388	-87.60571								
BC4 442674	3254665	29.42161	-87.59095								
Site 3											
G1 444786	3256405	29.43740	-87.56927								
G2 444654	3256417	29.43750	-87.57063	444620	3256383	29.43720	-87.57098	444588	3256297.36	29.436425	-87.571305
G3 444581	3256395	29.43731	-87.57138								
G4 444643	3256496	29.43822	-87.57075								
G5 444689	3256309	29.43653	-87.57026								
G6 444677	3256422	29.43755	-87.57039								
G7 444730	3256570	29.43889	-87.56986	444743	3256588	29.43905	-87.56971	444743	3256530	29.43853	-87.56971
G8 444830	3256414	29.43749	-87.56881	444807	3256458	29.43788	-87.56906	444778	3256461	29.43791	-87.56935
G9 444689	3256272	29.43620	-87.57026	444698	3256280	29.43627	-87.57017	444666	3256295	29.43640	-87.57050
G10 444485	3256401	29.43735	-87.57237	444405	3256347	29.43687	-87.57319	444357	3256321	29.43663	-87.57368
Site 4											
G1 425990	3244678	29.33060	-87.76225								
G2 426027	3244584	29.32975	-87.76187								
G3 425969	3244416	29.32823	-87.76246								
G4 425773	3244546	29.32855	-87.76244								
G5 425962	3244308	29.32726	-87.76252	425966	3244300	29.32719	-87.76248	425940	3244313.81	29.32731	-87.762758
G6 425804	3244433	29.32838	-87.76416								
G7 425789	3244524	29.32920	-87.76432								
G8 425666	3244482	29.32881	-87.76559	425660	3244390	29.32798	-87.76563	425700	3244368	29.32778	-87.76522
G9 425462	3244354	29.32765	-87.76768	425440	3244334	29.32747	-87.76791	425443	3244338	29.32750	-87.76787
G10 425785	3244078	29.32517	-87.76433	425791	3244100	29.32537	-87.76427	425832	3244070	29.32511	-87.76384
G11 425488	3243885	29.32341	-87.76737	425510	3243926	29.32379	-87.76715	425545	3243920	29.32374	-87.76679

84

Appendix Table 4.A. (Continued).

	X (m)	Y(m)	Lat.	Lon.	X (m)	Y(m)	Lat.	Lon.	X (m)	Y(m)	Lat.	Lon.
		Cruise 1C				Cruise M2				Cruise M3		
Site 5												
G1	404689	3251639	29.39198	-87.98223								
G2	405037	3251804	29.39350	-87.97865								
G3	404963	3251808	29.39354	-87.97942	404951	3251799	29.39345	-87.97954	404967	3251841	29.39383	-87.97938
G4	404788	3251706	29.39259	-87.98121	404768	3251703	29.39257	-87.98142	404903	3251651	29.39211	-87.98002
G5	404757	3251748	29.39298	-87.98154								
G6	404585	3251757	29.39304	-87.98331	404562	3251810	29.39352	-87.98356	404746	3251837	29.39377	-87.98166
G7	404796	3251527	29.39098	-87.98112	404819	3251506	29.39080	-87.98087	404965	3251513	29.39087	-87.97937
G8	404596	3251406	29.38988	-87.98317								
G9	404759	3251448	29.39027	-87.98149								
G10	404860	3251899	29.39435	-87.98048	404890	3251836	29.39377	-87.98017	404926	3251820	29.39363	-87.97980
Site 6												
G1	405109	3252933	29.40370	-87.97801	405113	3252957	29.40391	-87.97798	405153	3252963	29.40397	-87.97757
G2	405113	3252597	29.40066	-87.97794								
G3	405077	3252473	29.39954	-87.97830	405054	3252489	29.39969	-87.97854	405057	3252519	29.39995	-87.97851
G4	405256	3252407	29.39896	-87.97645								
G5	405068	3252300	29.39798	-87.97838	405026	3252318	29.39814	-87.97881	405037	3252310	29.39807	-87.97870
G6	405169	3252219	29.39726	-87.97733								
G7	405230	3252224	29.39731	-87.97670	405230	3252216	29.39723	-87.97671	405264	3252225	29.39731	-87.97635
G8	405063	3252077	29.39597	-87.97841	405067	3252118	29.39634	-87.97838	405096	3252130	29.39645	-87.97807
G9	405326	3252107	29.39626	-87.97570								
G10	405108	3251999	29.39526	-87.97794								
Site 7												
G1	370017	3237317	29.25964	-88.33779	369884	3237347	29.25990	-88.33916	369914	3237308	29.25955	-88.33885
G2	369571	3236981	29.25656	-88.34233	369550	3236978	29.25653	-88.34255	369552	3236936	29.25615	-88.34253
G3	370183	3236976	29.25658	-88.33604	370199	3237005	29.25685	-88.33587	370166	3237002	29.25681	-88.33622
G4	370116	3236802	29.25500	-88.33670								
G5	370170	3236691	29.25401	-88.33614	370220	3236694	29.25404	-88.33562	370217	3236710	29.25418	-88.33565
G6	369649	3236730	29.25431	-88.34150								
G7	369798	3236370	29.25107	-88.33993	369817	3236352	29.25091	-88.33973	370250	3236107	29.24875	-88.33525
G8	370380	3236388	29.25130	-88.33395								
G9	370156	3236025	29.24799	-88.33620								
G10	369548	3236313	29.25053	-88.34249								

Appendix Table 4.A. (Continued).

	X (m)	Y(m)	Lat.	Lon.	X (m)	Y(m)	Lat.	Lon.	X (m)	Y(m)	Lat.	Lon.
		Cruise 1C				Cruise M2				Cruise M3		
Site 8												
G1	372274	3234519	29.23463	-88.31424	372250	3234496	29.23442	-88.31448	372229	3234520	29.23463	-88.31470
G2	371985	3234253	29.23220	-88.31718	371969	3234226	29.23195	-88.31735	371988	3234221	29.23191	-88.31714
G3	371967	3234026	29.23015	-88.31734								
G4	371920	3233990	29.22982	-88.31782								
G5	371862	3233762	29.22775	-88.31839	371854	3233735	29.22751	-88.31847	371854	3233710	29.22728	-88.31847
G6	371928	3233886	29.22887	-88.31772								
G7	371955	3234012	29.23002	-88.31746	371963	3233984	29.22977	-88.31738	371970	3233980	29.22973	-88.31731
G8	372051	3234150	29.23128	-88.31649								
G9	371904	3234217	29.23186	-88.31801	371887	3234210	29.23180	-88.31818	371907	3234240	29.23207	-88.31798
G10	372222	3234419	29.23371	-88.31477								
G11	374104	3232556	29.21710	-88.29519								
Site 9												
G1	371618	3235244	29.24110	-88.32107	371627	3235249	29.24114	-88.32098	371667	3235220	29.24089	-88.32056
G2	371353	3235110	29.23986	-88.32378								
G3	371180	3234971	29.23859	-88.32555								
G4	371104	3234946	29.23836	-88.32632	371113	3234922	29.23814	-88.32623	371102.	3234893	29.23788	-88.32634
G5	370983	3234785	29.23690	-88.32756								
G6	370787	3234651	29.23567	-88.32955	370752	3234642	29.23558	-88.3299	370806	3234626	29.23544	-88.32936
G7	371171	3235008			371199	3235019	29.23902	-88.32536	371238	3235070	29.23949	-88.32496
G8	371146	3234899	29.23794	-88.32588								
G9	371298	3235066	29.23946	-88.32434								
G10	371273	3234895	29.23792	-88.32458	371202	3234913	29.2380	-88.32531	371184	3234879	29.23776	-88.32549

Chapter 5
Sediment Dynamics

Introduction

The objectives of the sediment dynamics component in collaboration with the geochemistry and geology components are to (1) provide quantitative and qualitative measurements of the extent and occurrence of nepheloid layers; (2) determine sedimentation and resuspension rates; (3) determine how topographic highs affect present-day sedimentation; (4) determine temporal variations in sediment texture; and (5) relate short term sediment dynamics to long term sediment accumulation. To address these goals, sediment traps, OBS instruments, and CTD/DO sensors are used to assess and monitor the extent and variability of nepheloid layers and resuspension events. At the study sites, these processes and their impact on the biological community associated with mounds are being assessed.

The goals, as outlined above, are being met by documenting particle distributions and dynamics with several techniques. Data on the spatial and vertical distribution, intensity, and short time-scale variability of the nepheloid layer were acquired with a transmissometer interfaced to the CTD/DO system. Profiles of beam attenuation were recorded during the cruises. Extended temporal sampling and monitoring of the intensity and temporal variability of nepheloid layers in conjunction with the current regime at the study sites were measured with OBS instruments interfaced with current meters on moorings. Sediment traps were deployed on the moorings to quantify particle flux. Together with surface sediment characterization, these data can be used to delineate the origins of the observed seafloor sediment patterns. Vertically-separated sediment traps were used to sample particulates with nepheloid layers and higher in the water column to estimate short-term sedimentation and resuspension rates. Particles from the traps are compared with sediments from the seafloor to characterize the depositional processes. Grab and sediment trap samples are part of the routine monitoring program to monitor temporal variations as well. The extent and occurrence of nepheloid layer is determined by grids of CTD/DO/transmissometer/OBS casts around the study sites during monitoring cruises along with casts taken at each mooring site during the mooring service cruises. Long-term variations are addressed by OBS instruments deployed on moorings, providing comparisons with current meter records.

Most changes in the optical properties of seawater are caused by particles suspended or settling through the water. Light attenuation as measured with a beam transmissometer is one of the easiest and most versatile optical instruments now in use that measures inherent optical properties in seawater. A Seatech 25-cm pathlength transmissometer was used to provide measurements of optical attenuation coincident with CTD casts. Gross, large-scale measurements can be easily made with this instrument, but to make precise quantitative measurements considerable care must be exercised in cleaning the optical windows, in correcting for the decay of the LED light source, and in calibration with in-situ particle concentration from filtered samples (Bartz et al. 1978; Gardner et al. 1983). Beam attenuation is an inherent property of seawater and is the sum of light

scattering and absorption (Gordon et al. 1984). At the 660 nm wavelength used in the Seatech transmissometer, the scattering function is small. Attenuation is usually considered to be the sum of attenuation of seawater (c_w), yellow matter (c_y), and particles (c_p). In the open ocean c_y is negligible and c_w is constant, so changes in total attenuation result from changes in particle densities (Morel 1974; Jerlov 1976; Pak et al. 1988; Gardner et al. 1995; Walsh et al. 1995). The properties of particles that affect attenuation are their concentration, size distribution, index of refraction, and shape, with concentration and size being most important. If the size distribution, index of refraction and shape of particles are constant, beam attenuation is linearly related to particle concentration (Spinrad et al. 1983; Baker and Lavelle 1984; Moody et al. 1986). Particle characteristics vary between regions, however, so in order to estimate particle mass concentration from attenuation data it is necessary to calibrate the data by filtering water and determining total particle concentrations.

Transmissometers are also effective in locating areas of resuspension of bottom sediments and production of bottom and intermediate nepheloid layers (Walsh 1990; Gardner and Walsh 1990). Because resuspended sediments form the bulk of nepheloid layer particles (Gardner et al. 1983, 1985), monitoring of the nepheloid layer with beam attenuation data can be used to infer spatial and temporal variability of particle concentrations and resuspension events (Walsh 1990; Gardner and Walsh 1990; Walsh et al. 1995).

Field and Laboratory Methods

CTD/DO/Transmissometer/OBS Data Sets

The use of the R/V TOMMY MUNRO for the field work resulted in some changes in data gathering. Because of limited work and bunk space, the filtration work was conducted on the mooring service cruises. This limited the number of filtration samples taken during each cruise, but the total number of cruises from which data are available increases. With this change, the total number of transmissometer casts during the program was increased due to use of the CTD/transmissometer package on monitoring and mooring service cruises.

By using the transmissometer interfaced to the CTD/DO, a minimum of three profiles were collected at each of the monitoring sites on each monitoring cruise. These include profiles at mooring locations when present at a site. The CTD/DO data were compared with the OBS instruments used on the moorings so that a robust correlation could be made between the transmissometer signal and the OBS. On each of the mooring redeployments, CTD/DO/transmissometer casts were made prior to recovery and after redeployment.

Transmissometer data from a Seatech 25-cm pathlength transmissometer were collected with each CTD/DO cast as were data from OBS instruments deployed on the moored current meters. CTD data were plotted graphically in real time on-board ship to determine rosette bottle sampling depths and to monitor the quality of the data. Such data

are especially helpful in defining the thickness of nepheloid and bottom boundary layers and the vertical extent of mixing.

Particle concentration profiles for calibration of the transmissometer beam attenuation data were made at each mooring site by filtration of water from Niskin bottles. One liter water samples were drawn from nine bottles from each cast and vacuum filtered through pre-weighed 47 mm 0.4 μm pore size Poretics filters. The filters were rinsed with distilled water to remove salts and then dried. On shore, the filters were weighed again, and the difference between the pre- and post-weighing yields the particle concentration per liter. Blank filters were used for quality control at all stages of the analysis.

The first calibration data set was produced on the January 1998 mooring service cruise (S2). Six casts were sampled for particles (three at Site 1, one at each of the other three mooring sites). The average blank value was 0.1 mg. The minimum filtration concentration was 0.03 mg/L. The maximum filtration concentration was 1.46 mg/L. A least squares regression of beam attenuation and particle concentration yielded a relationship with a slope of 1.3897 and an r^2 of 0.89 (Fig. 5.1). The slope is within the range reported for the Texas-Louisiana Shelf Circulation and Transport Process (LATEX) Program data sets [1.2 to 1.9 (Zhang 1997)]. Beam attenuation values for the entire data set were adjusted to yield a c_p of zero for a concentration of zero.

Calibration Regression

Fig. 5.1. Calibration plot of Niskin bottle particle concentration from the January 1998 mooring service cruise and the particle beam attenuation data from the transmissometer for the same depths and casts.
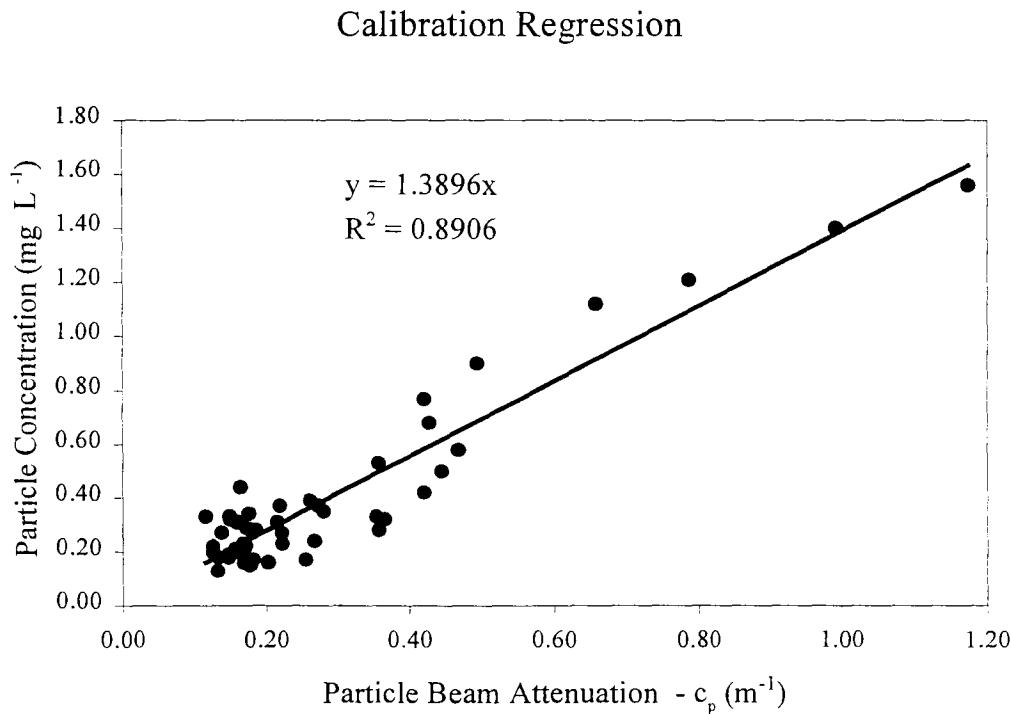
Correlation of the OBS sensor data (a Seatech light scattering sensor [LSS]) on the CTD package with the transmissometer data was completed by cross-correlating the mooring OBS data. Plots of LSS voltage vs. the particle beam attenuation (c_p) as shown for a representative cast in Fig. 5.2 indicate good agreement between the sensors, though the upper and midwater LSS data have considerably more data spiking.

c_p vs. LSS voltage
Cast H1B1, January 1998
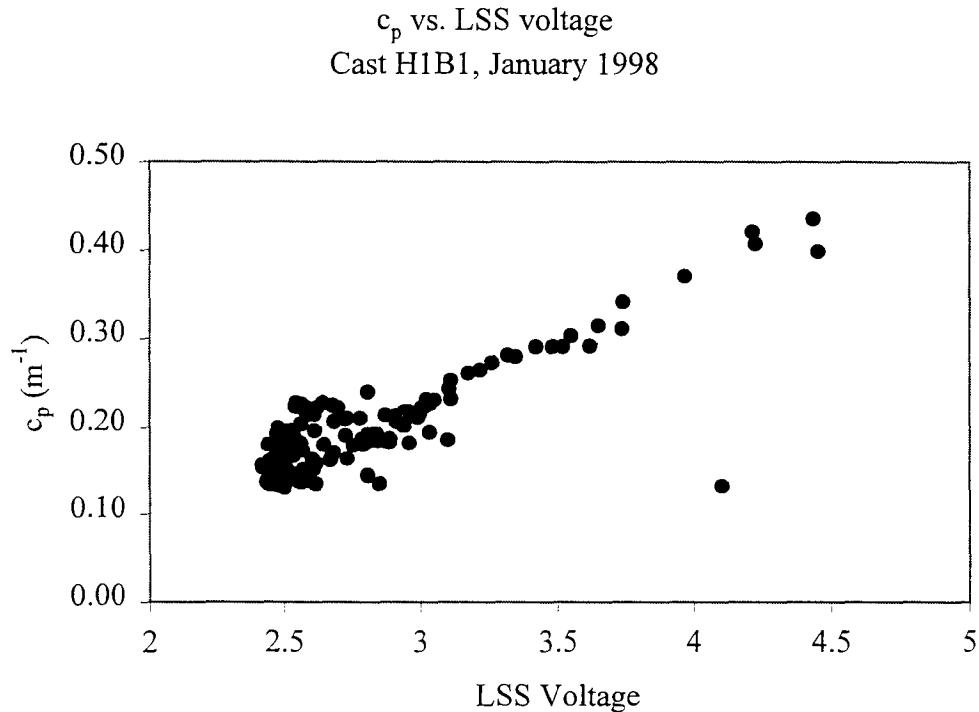
Fig. 5.2. Particle beam attenuation (c_p) plotted against the LSS (Seatech Light Scattering Sensor) data from a representative cast showing the correlation between the two data sets. The high values (i.e., LSS voltage >3) are from nepheloid layers.

Mooring Data Sets

Six moorings were deployed to provide long term data sets and characterize the flow fields, near-bottom oxygen concentrations, and nepheloid layer dynamics with respect to the flow field. A single mooring was placed at four of the sites (1, 4, 5, and 9) for the entire two year study. Two additional moorings were placed at Site 1 during the first year and at Site 5 during the second year. An OBS instrument was located a few meters above the bottom of each mooring and interfaced with a current meter to supply power and record data. The nepheloid layer OBS data characterize the intensity and temporal relationships between the current velocities and the nepheloid layer. Simple particle modeling and observational records are used to determine whether the observed nepheloid layers fluctuate as a result of near-field (active) resuspension or advective

90

processes. Combining the point source records of the current meters and optical instruments with the wider areal coverage and discrete water column profiles from the CTD/DO/transmissometer/OBS yields a robust data set describing the temporal and spatial variability of nepheloid layers over the area and at each of the monitoring sites.

Sediment Traps

Sinking particulate materials were collected using sediment traps. Simple core-tube sediment traps were deployed on each of the moorings to determine particle flux and resuspension rates during the monitoring period. This type of sediment trap has been proven both effective and cost-effective during the LATEX Program on the shelf of the western Gulf of Mexico (Zhang 1997). The traps were placed at 2.5, 7, and 15 meters above bottom (mab). The resuspended component of the bulk sedimentation rate can be derived by partitioning the bulk sediment sample in the 2.5 mab and 7 mab traps using the 15 mab trap and surface sediment samples as end members. Partitioning is based on bulk sedimentation rate, grain size, and data from a suite of chemical analysis made on each sediment sample [e.g., total inorganic carbon (TIC), total organic carbon (TOC), and metals; see Chapter 6]. This partitioning scheme has been effectively used in previous sediment trap studies (Walsh et al. 1988; Walsh and Gardner 1992).

Sediment traps were deployed from May 1997 through April 1999, supplying an estimation of sedimentation rates over two years. Bulk fluxes have been calculated from all recovered samples and processing of the samples has been completed. Chemical analyses (TIC, TOC, and trace metals Ba, Cr, and Fe) have been completed on all samples but the last deployment and discussion will be deferred to the synthesis report. Of the 144 total scheduled samples (3 depths x 6 moorings x 8 cruises = 144 samples), 133 samples were recovered, for a 92% recovery rate (Table 5.1). Five samples were lost due to loss of integrity of sediment trap end caps, spillage at sea, or the loss of the trap. Two moorings failed to release during the project. Mooring C5C7 was not recovered and those samples were lost from the analysis. However, in the case of the first deployment of the mooring at Site 4 (C4A1), the mooring was recovered on the subsequent cruise and the data are reported for periods one and two (Table 5.2). In that case, while samples were lost the complete time series was maintained. In terms of the time series, 136 of 144 sample periods were sampled, for a success rate of 94%.

Sediment trap samples were decanted and refrigerated at sea, with subsequent processing occurring in the laboratory ashore. In the lab, the supernatant was drawn off and the samples were wet sieved through a 1 mm nylon screen. The >1 mm fraction was visually inspected during processing and archived. In all samples to date, the >1 mm fraction is a small portion (<<5%) of the total sample. Two sample splitting procedures were used. For the first four sets of samples the <1 mm fraction was split into six fractions using a forced air, constant stirring splitter. For the rest of the samples a rotating splitter was used to split the sample into 10 fractions. Two splits were combined and archived at this stage (dark refrigeration). Two splits were used for grain size analysis. The remaining splits, in pre-weighed centrifuge tubes, were centrifuged at 15 krpm for 10 minutes. The supernatant was drawn off and samples were resuspended with distilled water to remove salts and centrifuged again. The supernatant was drawn off and the sample tubes

Table 5.1. Matrix of recovered sediment trap samples. Periods are individual deployments. See Table 5.2 for specific deployment and recovery dates. "Lost" indicates that either the trap was not recovered or the sample was lost due to the loss of integrity of the trap's end caps or spillage.

Site	Depth (mab)	Period							
		1	2	3	4	5	6	7	8
1	15	lost	C1A2	C1A3	C1A4	C1A5	C1A6	C1A7	C1A8
	7	C1A1	C1A2	lost	C1A4	C1A5	C1A6	C1A7	C1A8
	2.5	C1A1	C1A2	C1A3	C1A4	C1A5	C1A6	C1A7	C1A8
1	15	C1B1	C1B2	C1B3	lost				
	7	C1B1	C1B2	C1B3	C1B4				
	2.5	C1B1	C1B2	C1B3	C1B4				
1	15	C1C1	C1C2	C1C3	lost				
	7	C1C1	C1C2	C1C3	C1C4				
	2.5	C1C1	C1C2	C1C3	C1C4				
4	15		C4A1	C4A3	C4A4	C4A5	C4A6	C4A7	C4A8
	7		C4A1	C4A3	C4A4	C4A5	C4A6	C4A7	C4A8
	2.5		C4A1	C4A3	C4A4	C4A5	C4A6	C4A7	C4A8
5	15	C5A1	C5A2	C5A3	C5A4	C5A5	C5A6	C5A7	C5A8
	7	C5A1	C5A2	C5A3	C5A4	C5A5	C5A6	C5A7	C5A8
	2.5	C5A1	C5A2	C5A3	C5A4	C5A5	C5A6	C5A7	C5A8
5	15					C5B5	C5B6	C5B7	C5B8
	7					C5B5	C5B6	C5B7	C5B8
	2.5					C5B5	C5B6	C5B7	C5B8
5	15					C5C5	C5C6		lost
	7					C5C5	C5C6		C5C8
	2.5					C5C5	C5C6		C5C8
9	15	C9A1	C9A2	C9A3	C9A4	C9A5	C9A6	C9A7	C9A8
	7	C9A1	C9A2	C9A3	C9A4	C9A5	C9A6	C9A7	C9A8
	2.5	C9A1	C9A2	C9A3	C9A4	C9A5	C9A6	C9A7	C9A8

Abbreviations: mab = meters above bottom

Table 5.2. Matrix of deployment (D) and recovery (R) dates for each trap during the time series. Mooring C4A1 was recovered on a second attempt. Mooring C5C7 was not recovered. Data from C4A1 are reported here over the entire deployment period.

Site	Depth (mab)	Period: Mooring	1 D	1 R	2 D	2 R	3 D	3 R	4 D	4 R	5 D	5 R	6 D	6 R	7 D	7 R	8 D	8 R
1	15	C1A	5/15/97	lost	7/26/97	10/2/97	10/2/97	1/29/98	1/29/98	4/24/98	4/24/98	7/20/98	7/21/98	10/13/98	10/13/98	2/9/99	2/9/99	4/13/99
	7	C1A	5/15/97	7/26/97	7/26/97	10/2/97	10/2/97	lost	1/29/98	4/24/98	4/24/98	7/20/98	7/21/98	10/13/98	10/13/98	2/9/99	2/9/99	4/13/99
	2.5	C1A	5/15/97	7/26/97	7/26/97	10/2/97	10/2/97	1/29/98	1/29/98	4/24/98	4/24/98	7/20/98	7/21/98	10/13/98	10/13/98	2/9/99	2/9/99	4/13/99
1	15	C1B	5/15/97	7/26/97	7/26/97	10/2/97	10/2/97	1/29/98	1/29/98	lost									
	7	C1B	5/15/97	7/26/97	7/26/97	10/2/97	10/2/97	1/29/98	1/29/98	4/24/98									
	2.5	C1B	5/15/97	7/26/97	7/26/97	10/2/97	10/2/97	1/29/98	1/29/98	4/24/98									
1	15	C1C	5/15/97	7/26/97	7/26/97	10/2/97	10/2/97	1/29/98	1/30/98	lost									
	7	C1C	5/15/97	7/26/97	7/26/97	10/2/97	10/2/97	1/29/98	1/30/98	4/24/98									
	2.5	C1C	5/15/97	7/26/97	7/26/97	10/2/97	10/2/97	1/29/98	1/30/98	4/24/98									
4	15	C4A	5/15/97			10/29/97	10/30/97	1/30/98	1/30/98	5/1/98	5/1/98	7/21/98	7/22/98	10/13/98	10/13/98	2/9/99	2/9/99	4/13/99
	7	C4A	5/15/97			10/29/97	10/30/97	1/30/98	1/30/98	5/1/98	5/1/98	7/21/98	7/22/98	10/13/98	10/13/98	2/9/99	2/9/99	4/13/99
	2.5	C4A	5/15/97			10/29/97	10/30/97	1/30/98	1/30/98	5/1/98	5/1/98	7/21/98	7/22/98	10/13/98	10/13/98	2/9/99	2/9/99	4/13/99
5	15	C5A	5/15/97	7/26/97	7/26/97	10/5/97	10/6/97	1/30/98	1/30/98	5/1/98	5/1/98	7/21/98	7/22/98	10/13/98	10/13/98	2/9/99	2/9/99	4/13/99
	7	C5A	5/15/97	7/26/97	7/26/97	10/5/97	10/6/97	1/30/98	1/30/98	5/1/98	5/1/98	7/21/98	7/22/98	10/13/98	10/13/98	2/9/99	2/9/99	4/13/99
	2.5	C5A	5/15/97	7/26/97	7/26/97	10/5/97	10/6/97	1/30/98	1/30/98	5/1/98	5/1/98	7/21/98	7/22/98	10/13/98	10/13/98	2/9/99	2/9/99	4/13/99
5	15	C5B									5/1/98	7/21/98	7/22/98	10/13/98	10/13/98	2/9/99	2/9/99	4/13/99
	7	C5B									5/1/98	7/21/98	7/22/98	10/13/98	10/13/98	2/9/99	2/9/99	4/13/99
	2.5	C5B									5/1/98	7/21/98	7/22/98	10/13/98	10/13/98	2/9/99	2/9/99	4/13/99
5	15	C5C									5/1/98	7/21/98	7/22/98	10/13/98	10/13/98		2/10/99	lost
	7	C5C									5/1/98	7/21/98	7/22/98	10/13/98	10/13/98		2/10/99	4/13/99
	2.5	C5C									5/1/98	7/21/98	7/22/98	10/13/98	10/13/98		2/10/99	4/13/99
9	15	C9A	5/15/97	7/26/97	7/26/97	10/31/97	10/31/97	1/30/98	1/30/98	5/1/98	5/1/98	7/21/98	7/21/98	10/14/98	10/14/98	2/10/99	2/10/99	4/14/99
	7	C9A	5/15/97	7/26/97	7/26/97	10/31/97	10/31/97	1/30/98	1/30/98	5/1/98	5/1/98	7/21/98	7/21/98	10/14/98	10/14/98	2/10/99	2/10/99	4/14/99
	2.5	C9A	5/15/97	7/26/97	7/26/97	10/31/97	10/31/97	1/30/98	1/30/98	5/1/98	5/1/98	7/21/98	7/21/98	10/14/98	10/14/98	2/10/99	2/10/99	4/14/99

Abbreviations: mab = meters above bottom

weighed. The samples were frozen and freeze-dried for 24 to 48 hours depending on the sample volume. After freeze-drying, the tubes were weighed to measure water loss. The samples were removed from the centrifuge tubes and ground to a powder in a mortar. Ground samples were placed into pre-weighed petri dishes and weighed. The empty centrifuge tubes were also weighed to estimate the remaining sample in the tube and as a double check on the petri dish weight. Mass flux was calculated using the dry weight divided by the area of the trap tube and the elapsed time of deployment in days (Table 5.2). Dry splits of the ground samples were provided as subsamples for chemical analysis.

Samples from the first year of sediment trap sampling have been chemically analyzed (methods are described in Chapter 6). Because of the large amount of material collected during sampling period 6 (see below), subsamples for trace metal analysis were provided from both periods 5 and 6; otherwise samples were pooled. TIC and TOC analysis are being conducted on all samples. Results and discussion of the sediment trap chemical analyses will be deferred to the synthesis report.

Results and Discussion

Water Column

The data completed to date indicate that the study site is an area of high spatial and temporal variability in particle flux. Some regional trends are apparent from the data set. The surface layer was characterized by low salinity and a local maximum in the particle concentration reflecting biological activity during both the October 1997 and January 1998 cruises, with lower salinity and higher particle concentrations encountered in a westward direction. A benthic nepheloid layer (BNL) was present at all sites in all casts, though its intensity as measured by the beam attenuation and vertical gradient in attenuation was variable. The BNL increased as bottom water temperatures decreased (Fig. 5.3).

Temporal and spatial variability at Site 1 during the January 1998 mooring service cruise (S2) is illustrated in Fig. 5.4. Two casts were made at Mooring Site B just prior to recovery and immediately after redeployment of the mooring. The two casts, though only a few hours apart, demonstrate that understanding advective processes is important in interpreting the particle distributions.

Below the surface layer the particle concentration reached a minimum in both casts near 40 m. However, a warm saline layer between 20 and 60 m appears in the H1B2 cast but not the H1B1 cast. An intermediate nepheloid layer (INL) is associated with the base of this layer and is separated from the BNL by a layer of lower salinity water. The warm saline layer and its associated INL were found in both of the profiles at mooring C to the southwest of B while the profiles at Mooring Site A to the south of Site B were similar to H1B1.

94

T vs c$_p$ profiles - January 1998
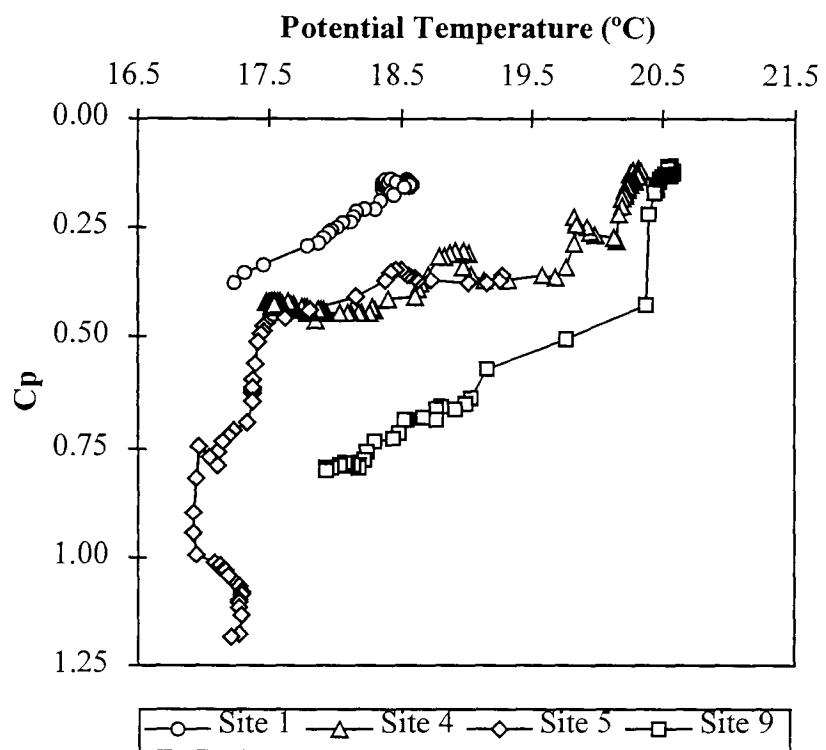
Fig. 5.3. Plot of particle beam attenuation versus potential temperature for selected casts taken during the January 1998 mooring service cruise (S2). Note the increase in beam attenuation with decreasing temperature. [Note: Potential temperature is the temperature that a parcel of water would have if it were moved adiabatically (i.e., with no heat added or removed) to the surface where pressure is assumed to be 1 atmosphere.]
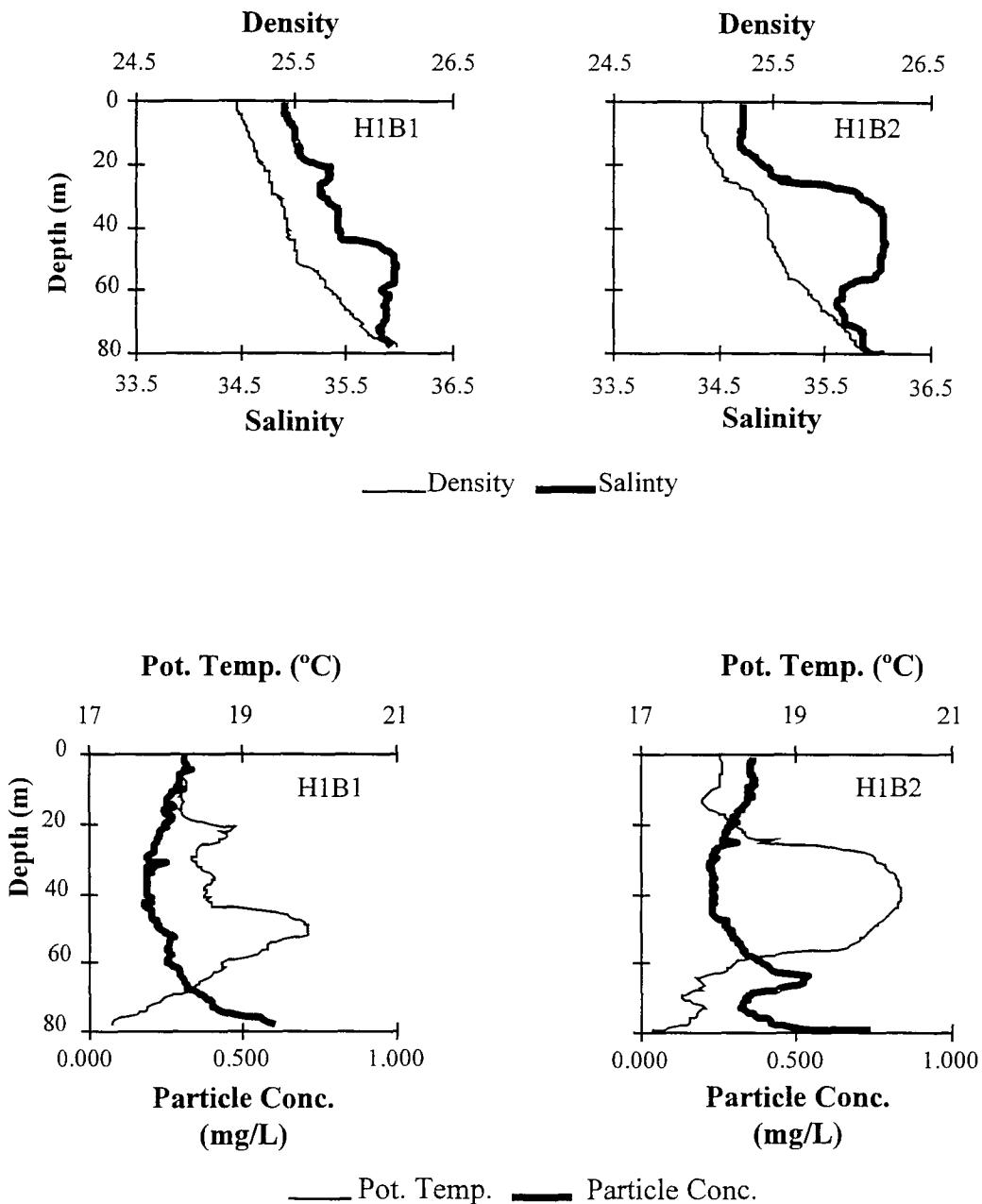
Fig. 5.4. Profiles of density, salinity, potential temperature, and particle concentration from the calibrated beam attenuation data from two casts at Site 1 mooring taken during the January 1998 mooring service cruise (S2). Note the presence of the warm saline intermediate layer in H1B2 and the associated intermediate nepheloid layer.

Sediment Traps

The sediment trap results during the study period reflect the influence of resuspension at the study sites with fluxes increasing toward the bottom for all moorings and time periods (Figs. 5.5 and 5.6). The dominant temporal signal in the data set is the extremely high fluxes recorded during period 6 (7/21-10/13/98; Figs. 5.5 and 5.6). During this period Hurricane Georges passed near the mooring sites and energetic currents were recorded (Chapter 7). Fluxes during this period were the highest recorded for each site and depth during the study, and ranged from 4 to 70 times the average fluxes exclusive of period 6.

Average fluxes during the study, excluding period 6, ranged from 1.5 to 6 g m^{-2} d^{-1} in the traps 15 mab to 6.7 to 29.3 g m^{-2} d^{-1} in the 2.5 mab traps. Comparing between the sites, the study average fluxes increased from Site 1 to Site 4 to Site 5, with Site 9 essentially the same as Site 5 at 15 and 7 mab but with a lower average flux at 2.5 mab. This trend of increasing fluxes towards the west reflects the trend in the water column particle load discussed above. No seasonal trends are apparent over the study period, which may reflect the dominance of storm and event driven resuspension. Integration of the sediment trap results and the complete water column and physical oceanographic data sets should help constrain the relative importance of the physical forcing funtions and seasonality to sedimentation in the study area.

Site 1 Bulk Flux Time Series

Site 4 Bulk Flux Time Series
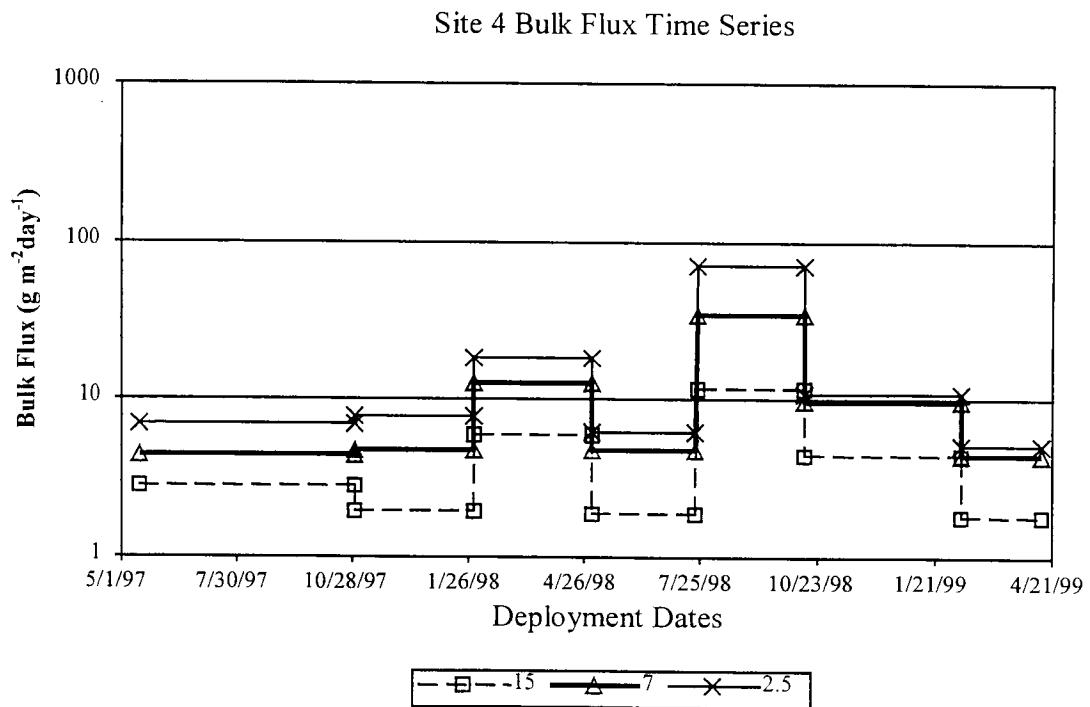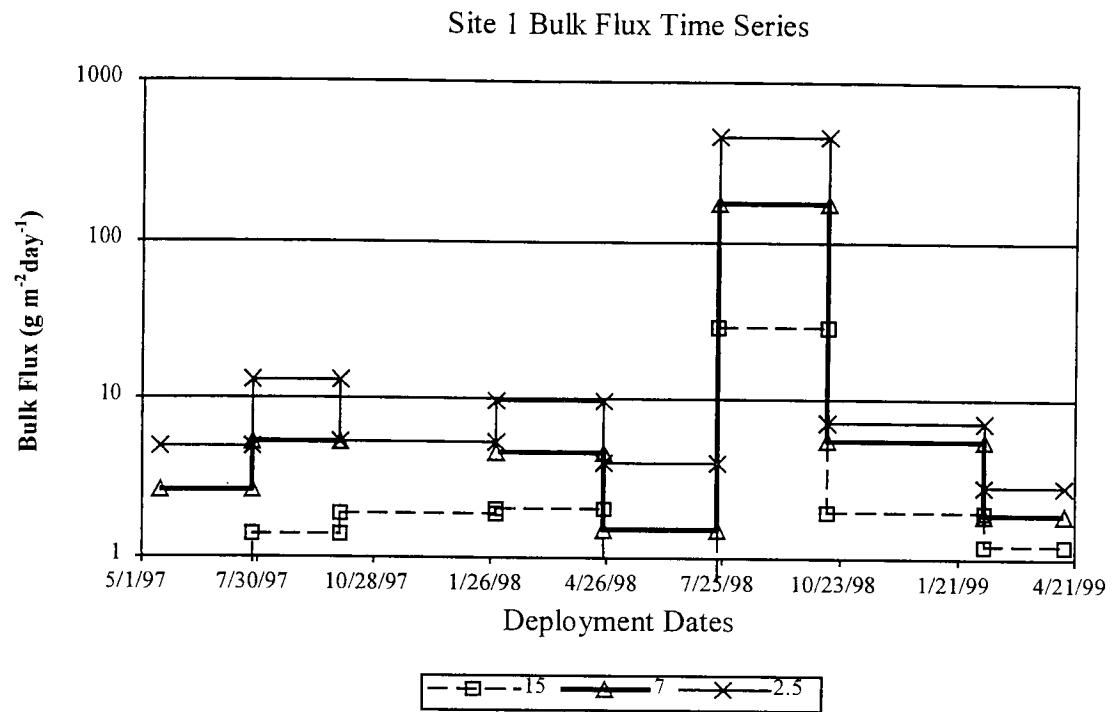
Fig. 5.5. Bulk fluxes recorded during the study at Sites 1 and 4.
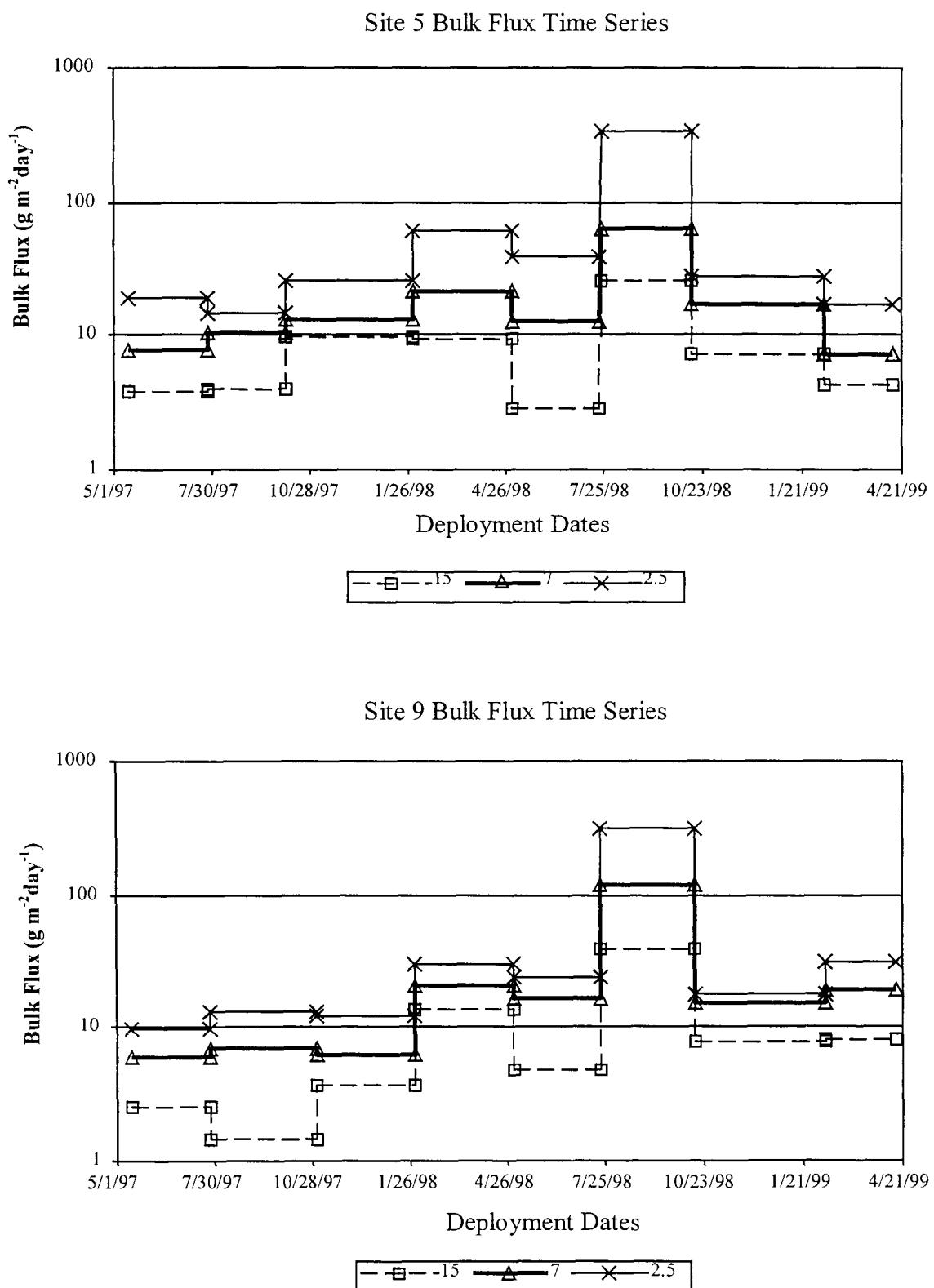
Fig. 5.6. Bulk fluxes recorded during the study at Sites 5 and 9.

Chapter 6
Geochemistry

Introduction

The geochemistry component includes a combination of hydrocarbon, metal, grain size, TOC, and TIC measurements in sediments and sediment trap materials. Contaminant measurements are intended to document the current hydrocarbon and metal concentrations within the study sites. Sediment characteristics (grain size, TOC, TIC) aid in determining the origins of sediment and discerning the relationship between sediment texture and biological patterns at the study sites. Metals, TOC, TIC, mass, and grain size are also measured in sediment trap materials to determine the origins of sediments at the sites and to document whether contaminants are accumulating at the sites during the duration of the study (see Chapter 5).

The two most common contaminants derived from platforms are hydrocarbons and metals (Middleditch 1981; Boesch and Rabalais 1987; Boothe and Presley 1987; Continental Shelf Associates, Inc. 1983, 1985b, 1989). The release of petroleum from a platform to the surrounding environment can occur during drilling and production. Petroleum hydrocarbons are potentially present in a variety of discharges including drilling fluids, cuttings, produced water, spills, deck drainage, and other releases (Kendall 1990). Petroleum hydrocarbons released to the environment can be differentiated from naturally occurring, background biogenic hydrocarbons (Brassell et al. 1978; Philp 1985; Boehm and Requejo 1986; Kennicutt and Comet 1992). Petroleum contains (1) a homologous series of n-alkanes with 1 to more than 30 carbons with odd and even carbon number n-alkanes present in nearly equal amounts; (2) a complex mixture of branched and cycloalkanes; and (3) a suite of polycyclic aromatic hydrocarbons (PAHs). Aliphatic hydrocarbons synthesized by organisms (both planktonic and terrestrial) include a suite of normal alkanes with odd numbers of carbons from 15 to 33. Complex branched and cycloalkanes are rare in organisms. Petroleum PAH mixtures are differentiated from PAHs synthesized by organisms by the structural complexity of the mixture and the presence of substantial amounts of alkyl substituted PAHs. PAHs are the most toxic components of oil and concentrations can indicate potential biological effects. Based on considerations of petroleum chemistry, biological occurrences, and toxicological effects, aliphatic and aromatic hydrocarbons were chosen as tracers of petroleum contamination for this study (Kennicutt 1995).

Metals are also released during offshore drilling and production activities (Lake Buena Vista Symposium 1981; Boesch and Rabalais 1987; Boothe and Presley 1987). Metal contamination can affect both infauna and epifauna in the vicinity of platforms (Southwest Research Institute 1978). Many metals are EPA priority pollutants (antimony, arsenic, cadmium, chromium, copper, lead, mercury, nickel, selenium, silver, and zinc) and are known to be toxic to organisms. These metals are often constituents of drill muds (Houghton et al. 1981; Rubinstein et al. 1981; Tornberg et al. 1981). Tin is known to be toxic and is present in antifouling paints used on platform structures. Barium is used as a tracer of the settable particulate fraction of discharged drilling fluids

and cuttings because it occurs in high concentrations in drilling muds and has a low, natural background in ambient sediments (200 to 500 ppm dry weight; Chow and Snyder 1981; Boothe and James 1985; Boothe and Presley 1987). Barium (as barite, barium sulfate) is the dominant component of drill mud (up to 90% on a dry weight basis). Aluminum and iron are major constituents of alumino-silicate minerals and are used to detect changes in sediment type. Vanadium is of interest because it can occur in significant concentrations in some crude oils.

Methods

The geochemistry portion of this study relied on prior study information and a hierarchical approach to select the analysis to be used. For hydrocarbons, a simple measure of the presence or absence of oil was used. TPHs determined by gas chromatography/flame ionization detection (GC/FID) and a gravimetric measurement of extractable organic matter (EOM) accurately reflect oil contamination (Kennicutt et al. 1996). The origin of hydrocarbons within a site was determined on a single composite of all samples collected at a site. Fingerprinting using PAH compositions was the method of choice to define the origins of any PAH detected at the study sites. Metals (Ba, Cd, Cr, Pb, Hg, and Zn), most closely related to platform discharges, were measured as well. As an indicator of sediment mineralogy, aluminum and iron were also measured. Crustal elements (Fe, Al) were used to normalize the concentration of metals to detect anthropogenic additions.

Collection

Sediments were collected by grab as described in Chapter 4, Geologic Characterization. The top 5 cm of sediment were sampled. Samples for geochemistry were collected concomitantly with geological samples. The collection of sediment trap materials is described in Chapter 5.

Total Inorganic and Organic Carbon

Sediment carbonate content (0.2 to 0.5 g) was determined by treatment with concentrated HCl. Residual organic carbon was converted to CO_2 and analyzed with a non-dispersive infrared spectrophotometer (Leco WR-12 Total Carbon System). Calcium carbonate was determined as the difference between a treated (acidified) and untreated sample. Acidification was carried out in the crucible used for analysis and the residual acid was evaporated in place to avoid the loss of acid soluble organic matter.

Hydrocarbon Analyses

TPHs were determined by GC/FID of sediment extracts. EOM was determined by weighing the extracts.

PAHs were determined by the National Oceanic and Atmospheric Administration National Status and Trends methods (Wade et al. 1988). Briefly, deuterated PAHs were

added before the extraction and were used to calculate analyte concentrations. Sediment samples were mixed with anhydrous sodium sulfate and extracted with methylene chloride/acetone in an Automated Solvent Extractor (ASE). The petroleum hydrocarbons were separated from interfering compounds by silica/alumina columns. The purified extracts were analyzed on an HP 5890/5970 gas chromatograph with a mass selective detector (GC/MS) using a selected ion detection technique. The GC/MS was calibrated with known concentrations of analytes at five different concentration levels and average response factors were used for determination of PAH concentrations. Concentrations of parent and alkylated PAHs were reported as nanogram/gram (ng/g) on a dry weight basis for sediment samples. Each sample batch of 20 samples included a procedural blank, a matrix spike, a matrix spike duplicate, and a standard reference material. Quality assurance samples ensure that the analytical results are valid and of acceptable accuracy and precision.

Trace Metal Analyses

Sediment and sediment trap samples were analyzed for Ba, Cd, Cr, Fe, Hg, Pb, and Zn. Analyses were conducted by National Status and Trends methods. The methods include atomic absorption spectroscopy (AAS), instrumental neutron activation analysis (INAA) and/or inductively coupled plasma spectrometry (ICP), depending on the metal and the concentration (e.g., Taylor and Presley 1998). INAA was used to determine Ba, Cr, and Fe. The precision and accuracy by INAA is excellent regardless of the matrix. A more sensitive method was used when needed for other metals to insure accurate and precise values.

A freeze-dried representative INAA sediment aliquot was ground to a fine powder. No further treatment was needed. For INAA, 0.5 g aliquots of the powdered samples were weighed directly into plastic vials and heat sealed. The samples were irradiated for 12 hours in the 1 megawatt TRIGA reactor. After a 10 day cooling period to allow Na, Cl, and other interfering isotopes to decay to low levels, the samples were counted using a hyper-pure germanium detector coupled to a Nuclear Data Corp. model 9900 multichannel analyzer integrated with a Digital VAX II/GPX graphics workstation. Concentrations were obtained by comparing counts for each sample with those for sediment and rock reference materials of accurately known elemental composition. Details of this method are given in Boothe and James (1985), including information on counting geometry, reference materials, spikes, blanks and other aspects of quality assurance.

National Status and Trends Program methods were used in the AAS/ICP analysis (Lauenstein et al. 1993). The method for Hg included a sulfuric acid-permanganate digestion of the dry powdered sample followed by stannous chloride reduction to Hg metal and detection by cold vapor atomic absorption. For other metals, 200 mg aliquots of the powdered sediment samples were weighed into teflon "bombs" and completely dissolved in a mixture of nitric, hydrofluoric, and boric acids at 130°C. Various dilutions were made of the clear digests to bring them into the working range of the AAS or ICP.

A Perkin-Elmer Corp. model 3300DV (dual view) ICP was used when element concentrations permitted. When concentrations were too low for this instrument, a Perkin-Elmer 3030Z AA equipped with an HGA-600 graphite furnace and an auto sampler were used. Details of furnace programs, matrix modifiers, blanks, spikes, reference materials, and other quality assurance information can be found in the reference given above. The proposed methods ensured that the matrix spike recovery for all elements was greater than 90% and that recoveries of certified values for reference materials from the National Research Council of Canada were 90% or better as well.

Results and Discussion

To survey the monitoring sites for the presence of contaminants, 10 grab samples were collected at each site during the first monitoring cruise (1C). Each grab sample was analyzed for EOM, TOC and TIC content, gas chromatographically resolvable and unresolvable (UCM) hydrocarbons, and metals (Ba, Cd, Cr, Fe, Hg, Pb, and Zn). A composite grab sample at each site was analyzed for total PAHs. The measures of hydrocarbons at the sites were low and relatively uniform. Little or no evidence of petroleum related hydrocarbons was observed at any of the nine study sites (Table 6.1). The slight increase in EOM and PAHs towards the west most likely represents a general fining of sediments. Metals indicative of contamination were at or near background levels at all sites as well (Table 6.1). Barium, a tracer of drill mud discharges, was at background levels and only a few samples might be interpreted as containing slightly elevated barium levels. A slight increase in a few metals (Ba, Cr, Fe, Zn) towards the west most likely represents a general fining of sediments. In conclusion, the sediments collected at the study sites exhibited little or no evidence of significant contamination from drilling or production activities in the area.

TOC in sediments at the study sites during Cruises 1C, M2, and M3 was low and relatively uniform (Table 6.2). In most instances, TOC was less than 0.5%, occasionally reaching 1.0% or more. Sedimentary carbon was primarily in the form of carbonate. TIC content ranged from ~3.5 to more than 8% (pure calcium carbonate would be 12% carbon). Carbonate content decreased from east to west by nearly a factor of two, reflecting proximity to riverine inputs of particulate matter.

Table 6.1. Summary of average sediment characteristics at the study sites during Cruise 1C.

Site	EOM (ppm)	TPH (ppm)	PAH (ppb)	UCM (ppm)	Total Resolved Hydrocarbons (ppm)
1	43.2	11.2	8.2	7.7	9.5
2	35.7	12.0	8.3	9.7	3.2
3	42.1	10.4	10.8	8.6	1.8
4	74.1	20.1	21.5	12.7	7.5
5	59.2	18.4	15.3	13.7	4.7
6	59.2	16.2	15.5	11.3	4.9
7	73.1	21.2	25.7	16.3	4.9
8	33.6	13.2	12.2	10.2	3.0
9	70.9	20.0	20.4	12.7	7.3

Site	Ba (ppm)	Cd (ppm)	Cr (ppm)	Fe (ppm)	Hg (ppm)	Pb (ppm)	Zn (ppm)
1	123.3	0.10	21.0	8858	0.02	7.8	26.2
2	120.1	0.05	21.0	7616	0.02	7.9	22.8
3	111.2	0.07	26.8	8665	0.02	6.7	24.7
4	357.1	0.12	40.0	18,729	0.03	15.0	60.4
5	499.5	0.08	33.8	17,316	0.03	12.3	50.6
6	471.6	0.08	32.0	17,578	0.03	12.5	60.0
7	497.3	0.07	38.0	18,344	0.03	15.3	58.4
8	240.0	0.05	23.5	10,397	0.02	10.6	30.1
9	465.9	0.07	40.6	19,565	0.03	15.3	60.8

Abbreviations: EOM = extractable organic matter; TPH = total petroleum hydrocarbons; PAH = polycyclic aromatic hydrocarbons; UCM = unresolved complex mixture.

Table 6.2. Summary of the average total organic (TOC) and inorganic (TIC) carbon content (%) of sediments at the study sites during Cruises 1C, M2, and M3.

Cruise	Site	n	TOC	TIC	Cruise	Site	n	TOC	TIC	Cruise	Site	n	TOC	TIC
1C	1	8	0.1	8.0	M2	1	5	0.2	6.9	M3	1	6	0.2	7.5
	2	10	0.2	5.1		2	5	0.1	5.7		2	5	0.0	5.0
	3	10	0.2	5.0		3	5	0.1	5.9		3	5	0.0	5.9
	4	9	1.1	7.3		4	5	0.4	8.0		4	11	1.3	7.0
	5	10	1.1	6.1		5	5	0.24	6.16		5	5	0.6	5.3
	6	10	0.2	5.7		6	5	0.4	4.6		6	5	1.2	4.7
	7	10	0.3	5.0		7	5	0.	3.9		7	5	0.2	3.1
	8	10	0.2	3.1		8	5	0.2	3.4		8	5	0.4	3.3
	9	10	0.3	6.1		9	5	0.3	5.1		9	5	0.2	3.8

Chapter 7
Physical Oceanography/Hydrography

Introduction

The purpose of this component of the program is to monitor oceanographic conditions (i.e., DO, turbidity, temperature, salinity, etc.) at the three types of topographic features along the Mississippi-Alabama OCS. Other work elements can then relate observed seasonal and inter-annual changes in community structure and zonation to changes in oceanographic conditions. The specific objectives that focus on the details of this relationship are as follows:

- to characterize the regional and local current dynamics in the study area, which lies on the outer portion (60 to 120 m water depth) of the Mississippi-Alabama continental shelf;

- to determine the dynamics of important oceanographic parameters, including temperature, salinity, DO, and turbidity; and, most important,

- to define the relationship of the current dynamics and oceanographic conditions to the geological and biological process occurring at these hard bottom features.

To address the objectives, the oceanographic-processes effort consists of three elements: instrument moorings, hydrographic stations, and collateral data. Six 18-m high, bottom-mounted instrument moorings were deployed at selected hard bottom sites to continuously measure current velocity, temperature, conductivity/salinity, DO, and turbidity. The moorings also had sediment traps to collect suspended samples of settling suspended particulate matter. Discrete vertical profiles of CTD/DO/transmissivity/light were collected by the same instrument package used during the LATEX study. Collateral data, such as satellite advanced very high resolution radiometer (AVHRR) images, satellite altimetry, river discharge, coastal wind and sea level data, and buoy observations of wind, waves, barometric pressure, air and sea temperature, will be used during the synthesis to describe the primary physical forcing mechanisms. The data collected during the first three deployment periods are described in the Second Annual Report (Continental Shelf Associates, Inc. and Texas A&M University, Geochemical and Environmental Research Group, 1998). In this report, the focus is on data collected by the moored instruments during the fourth through eighth deployment periods and the CTD data collected on the six cruises that deployed and recovered the moorings. At the time of this report, the field work for this component of the program is complete except for the CTD data that were collected during the last monitoring cruise (M4), which was conducted in July-August 1999.

Instrument Moorings

Moored instruments provide information about the temporal scales of physical processes that affect biota associated with benthic habitats in the study area. The variables of greatest interest are current speed and direction, suspended sediments, water temperature, DO, and salinity. The semi-annual monitoring cruises observe the cumulative results of interactions on various time scales among the physical and chemical variables and the biological communities. Time-series data provide information about the time scales, and also capture the details, of events such as the passage of a hurricane or intrusion associated with the Loop Current.

The hard bottom features in the study area include pinnacles that extend up to 15 m above the bottom. Water depth in the region ranges from 60 to 120 m. Six moorings measured currents, conductivity/salinity, temperature, DO, turbidity, and sediment flux. The mooring design is illustrated in Fig. 7.1. Current, temperature, and conductivity/salinity were recorded ~2.5 m above the bottom and at 16 m above the bottom. Sediment traps were attached at three heights above the bottom.

One mooring was placed at each of four of the nine study sites. Three of these (Sites 1, 4, and 5) are medium and high relief features located near the 100 m isobath. The fourth (Site 9) is a low relief site in shallower water near the 60 m isobath (see Chapter 4 for maps of the pinnacle sites.) These four mooring locations were permanent and maintained throughout the two-year field program to providing long-term time series data. The fifth and sixth moorings were re-locatable. During the first year, they were placed at the easternmost high relief site (Site 1) to form, in conjunction with the permanent mooring, a triangular pattern. They were then moved to Site 5 in May 1998 (Cruise M3).

Hydrography

Physical factors that affect the biota in the region include currents, temperature, salinity, DO, turbidity, and light levels. Moored instruments produce time series of all of these variables except light levels. Current, temperature, and salinity were monitored at two depths above the bottom. DO and turbidity were monitored at only one depth above the bottom. Vertical profiles of these variables were taken during the monitoring and servicing cruises to provide valuable information on vertical distributions. Previous studies (Kelly 1991) indicate that water masses in the study area undergo changes both in the near surface and at depth. CTD profiles indicated the presence of near bottom nepheloid layers that vary quite markedly over the area in both space and time.

Vertical variations are induced by Loop Current intrusions, seasonal heating and cooling, wind forcing, fresh water input from the local rivers, and the passage of storms. To assess the effect of these variations at each study site, multiple vertical profiles of conductivity, temperature, PAR, transmissivity, backscattered light, and oxygen concentrations were collected. Vertical profiles were made at three locations around each site to determine if changes in water properties were induced by flow past the topographic features. Water samples were collected for determination of total suspended

5/8" Galv Pear Link
1/2" Galv Shackle
5/8" Galv Thimble

ICEPLAST 11" dia. plastic float
9 kg net buoyancy
750 meter working depth
5/8" Dacron line

5/8" Galv Thimble
1/2" Galv Shackle
5/8" Galv Pear Link
1/2" Galv Shackle
5/8" Galv Thimble

NOT TO SCALE

5/8" Galv Thimble
1/2" Galv Shackle
5/8" Galv Pear Link
1/2" Galv Shackle
Isolator Bar

Altitude (meters)
Above Bottom

Isolator Bar
1/2" Galv Shackle
5/8" Galv Pear Link
1/2" Galv Shackle
5/8" Galv Thimble

Aanderaa RCM7
current meter
W/ Temp., Cond.

— 16 m

Sediment Trap

— 15 m

5/8 Dacron Rope

Sediment Trap

— 7 m

5/8" Galv Thimble
1/2" Galv Shackle
5/8" Galv Pear Link
1/2" Galv Shackle

Oregon Environmental
Current Meter w/ Temp.

— 3.5 m

YSI 6000 w/ D.O.,
Turb., Temp.,Cond.
and sediment trap
on cage

— 2.3 m

1/2" Galv Shackle
5/8" Galv Pear Link
3/8" Galv Shackle

Benthos 866A
Acoustic Release

3/8" SS Droplink
1/2" Galv Thimble
5/8" Galv Shackle

Rope Canister w/ 500 ft 3/8"
 Spectra line
1/2" Galv Shackle
5/8" Galv Shackle
300 kg Anchor

Fig. 7.1. Schematic drawing of the instrument mooring.

109

matter and for calibration of the oxygen sensor. Salinity samples were used to check the sampling depth where the bottle actually closed. Sampling depths focused on depths from the feature height to the regional bottom depth, with fewer samples taken in the overlying water. From these measurements, the depth of the nepheloid layer was inferred and the water masses enveloping the features were characterized. The basic measurements of temperature, salinity, light levels, oxygen, and suspended sediment loads are used as environmental variables in statistical models applied to the biological assemblage data. These data were also used to calibrate and provide quality control for time series measurements made at the moorings.

Methods

Nine cruises have been conducted to collect CTD profiles and to deploy and service the moorings over eight deployment periods. Cruise dates, type of CTD, and number of casts by cruise are summarized in Table 7.1. CTD casts were made at all nine sites during the monitoring cruises (1C, M2, and M3), but only at four sites during moorings servicing cruises. The details of the operations and logistics for each cruise are presented in Chapter 3. The locations, dates, and times of deployment of the instrument moorings are summarized in Table 7.2. CTD casts were made on the final monitoring cruise (M4, Leg 2) during July-August 1999, using a SEACAT with an attached transmissometer.

Table 7.1. Ecosystems monitoring Mississippi/Alabama shelf cruises.

Name	Seq.	Start	End	CTD Casts	Instrument type
1C	c1	5/21/97	5/24/97	29	SBE-911
S1	c2	7/28/97	7/29/97	11	SBE 19 SEACAT
M2	c3	9/30/97	10/31/97	25	SBE-911
S2	c4	1/29/98	1/30/98	12	SBE-911
M3	c5	4/24/98	5/3/98	31	SBE-911
S3	c6	7/20/98	7/22/98	11	SBE-911
S4	c7	10/13/98	10/14/98	12	SBE-911
S5	c8	2/9/99	2/10/99	12	SBE-911
M4 Leg 1	c9	4/14/99	4/15/99	6	SBE-911

The first four cruises (through January 1998) were discussed in the Second Annual Report. The April 1998 cruise was a Monitoring cruise. Generally, three CTD casts were conducted around each pinnacle, and additional casts were made to support the mooring operations. At pinnacles with moorings, CTD locations were chosen to be close to the moorings. A cast was made before a mooring was released, and a CTD cast was made after a new mooring was deployed. The CTD was always lowered as close to the bottom as the sea state would permit, so that the CTD data could be used as a QC check on the data recorded at the beginning and end of the moored records. On mooring service cruises, only the six mooring sites were visited, yielding 12 casts, generally. (One of the 12 on the July 1998 cruise was bad, and the last cruise was a recovery-only cruise.)

Table 7.2. Locations, dates, and times of deployment of the instrument moorings.

ID	Depth	Date In	Time (UTC)	Date Out	Time (UTC)	Easting	Northing	Lat Degree	Lat Min	Lat Sec	Lon Degree	Lon Min	Lon Sec
C1A1	78	05/23/97	0339	07/28/97	1231	444520.7	3256839.9	29	26	28.75	87	34	19.32
C1A2	78	07/28/97	1433	10/03/97	0230	444555.0	3256881.2	29	26	30.09	87	34	18.05
C1A3	80	10/04/97	0826	01/29/98	1656	444532.0	3256877.9	29	26	29.98	87	34	18.91
C1A4		01/29/98	1912	04/04/98	1521	444587.9	3256837.3	29	26	28.67	87	34	16.82
C1A5	77	04/24/98	1925	07/20/98	2332	444704.4	3256821.1	29	26	28.16	87	34	12.50
C1A6	77	07/21/98	0203	10/13/98	1548	444721.0	3256824.0	29	26	28.26	87	34	11.89
C1A7	78	10/13/98	1809	02/09/99	1233	444703.5	3256832.3	29	26	28.53	87	34	12.53
C1A8	75	02/09/99	1454	04/14/99	0348	444700.0	3256831.0	29	26	28.50	87	34	12.65
C1B1	81	05/23/97	0457	07/28/97	1509	444544.5	3256163.9	29	26	6.79	87	34	18.31
C1B2	79	07/28/97	1637	10/03/97	0140	444608.6	3256226.7	29	26	8.84	87	34	15.95
C1B3	83	10/04/97	0717	01/29/98	2104	444581.1	3256249.9	29	26	9.59	87	34	16.97
C1B4		01/29/98	2252	04/24/98	2034	444523.3	3256180.3	29	26	7.31	87	34	19.10
C1C1	82	05/23/97	0109	07/28/97	1739	443761.2	3256406.8	29	26	14.56	87	34	47.43
C1C2	82	07/28/97	1913	10/03/97	0333	443793.8	3256445.8	29	26	15.83	87	34	46.23
C1C3	83	10/03/97	1206	01/30/98	0027	443792.9	3256456.9	29	26	16.18	87	34	46.26
C1C4	81	01/30/98	0205	04/25/98	0035	443879.4	3256453.1	29	26	16.07	87	34	43.06
C4A1	115	05/21/97	2121	10/29/97	1730	426583.3	3244597.2	29	19	47.66	87	45	22.15
C4A2	na	na	na	na	na								
C4A3	112	10/30/97	0643	01/30/98	0540	426551.2	3244767.9	29	19	53.20	87	45	23.38
C4A4		01/30/98	0906	05/01/98	1800	426721.2	3244688.8	29	19	50.66	87	45	17.06
C4A5	113	05/01/98	1957	07/21/98	0512	426675.8	3244722.9	29	19	51.76	87	45	18.75
C4A6	113	07/21/98	2157	10/13/98	2032	426681.0	3244824.0	29	19	55.05	87	45	18.58
C4A7	111	10/13/98	2229	02/09/99	1649	426657.8	3244812.6	29	19	54.67	87	45	19.44
C4A8	112	02/09/99	1927	04/14/99	0709	426651.0	3244816.0	29	19	55.09	87	45	19.69

Table 7.2. (continued).

ID	Depth	Date In	Time (UTC)	Date Out	Time (UTC)	Easting	Northing	Lat Degree	Lat Min	Lat Sec	Lon Degree	Lon Min	Lon Sec
C5A1	81	05/23/97	1303	07/29/87	0206	405132.8	3251628.7	29	23	30.94	87	58	39.59
C5A2	82	07/29/97	0340	10/06/97	0426	405132.8	3251592.8	29	23	29.77	87	58	39.58
C5A3	82	10/06/97	0717	01/30/98	1221	405119.8	3251578.2	29	23	29.29	87	58	40.06
C5A4		01/30/98	1403	05/01/98	1348	405088.9	3251517.0	29	23	27.29	87	58	41.18
C5A5	79	05/01/98	1618	07/21/98	1724	405074.4	3251623.1	29	23	30.74	87	58	41.75
C5A6	79	07/22/98	0659	10/14/98	0315	405129.3	3251625.0	29	23	30.82	87	58	39.71
C5A7	78	10/14/98	0515	02/10/99	0037	405134.1	3251632.0	29	23	34.28	87	58	39.54
C5A8	78	02/10/99	0322	04/14/99	1220	405134.0	3251637.0	29	23	31.20	87	58	39.50
C5B5	82	05/01/98	1137	07/21/98	1551	404551.0	3251700.6	29	23	33.11	87	59	1.19
C5B6	78	07/22/98	0737	10/14/98	0235	404473.1	3251710.2	29	23	33.40	87	59	4.09
C5B7	78	10/14/98	0558	02/09/99	2358	404451.3	3251715.9	29	23	33.58	87	59	4.90
C5B8	78	02/10/99	0454	04/14/99	1142	404462.0	3251703.0	29	23	33.18	87	59	4.50
C5C5	79	05/01/98	1250	07/21/98	1456	404864.7	3252078.8	29	23	43.33	87	58	49.67
C5C6	78	07/22/98	0823	10/14/98	0205	404862.0	3252075.7	29	23	45.38	87	58	49.78
C5C7	79	10/14/98	0650	na	na	404878.5	3252069.8	29	23	45.20	87	58	49.16
C5C8	78	02/10/99	1405	04/14/99	1115	405010.0	3252201.0	29	23	49.50	87	58	44.33
C9A1	91	05/23/97	2030	07/29/97	0718	371417.2	3235151.9	29	14	24.89	88	19	23.29
C9A2	93	07/29/97	0900	10/31/97	0600	371400.2	3235151.4	29	14	24.78	88	18	23.92
C9A3	94	10/31/98	0858	01/30/98	1818	371134.1	3235538.5	29	14	37.35	88	19	33.94
C9A4	93	01/30/98	1957	05/02/98	0000	371053.6	3235704.3	29	14	42.70	88	19	36.98
C9A5	92	05/02/98	0158	07/22/98	0224	371252.9	3235236.2	29	14	27.57	88	19	29.41
C9A6	88	07/22/98	0339	10/14/98	1144	371226.2	3235241.2	29	14	27.73	88	19	30.40
C9A7	91	10/14/98	1254	02/10/99	0824	371197.2	3235253.4	29	14	28.11	88	19	31.48
C9A8	90	02/10/99	1033	04/14/99	1530	371190.0	3235250.0	29	14	28.00	88	19	31.73

Abbreviations: UTC = Coordinated Universal Time.

During the February 1999 cruise, Mooring 5C would not surface, although the acoustic release appeared to function properly. Passes were made over the site while ranging acoustically on the release. The results indicated that the release was still on the bottom. A fishing boat off Destin, Florida found the mooring's flotation and top (RCM7) current meter in May. The data appear good through about the beginning of February 1999. During the final monitoring cruise, the ROV attempted to locate the bottom instruments, but they were not found. A spare mooring with an upper and lower RCM7 current meter (but no YSI oxygen/turbidity meter) was deployed at Site 5C during the February 1999 cruise.

Equipment

Moorings

Six multi-parameter physical oceanography moorings were deployed. Their principal components are shown in Fig. 7.1.

A mooring was constructed using 5/8" Dacron rope. The linkage between the acoustic release and the anchor was also rope, rather than chain, so that it could be cut by an ROV should the release fail. The rope canister contained 152 m of 3/8" Spectra line, a length that permitted the mooring to rise to the surface and be recovered before pulling up the anchor. Strings of ICEPLAST Model 1102 plastic floats (9 kg of net buoyancy each) provided flotation. Static mooring analysis was computed for the mooring using the program BUOY2.41 developed by Specialty Devices Inc. The amount of flotation was selected to assure that mooring "blow-over" was less than 1.0 m for current profiles up to 40 cm/s. However, peak current speed at the upper current meter exceeded this value at times and was more than double it during Hurricane Georges. An assessment of the amount of vertical excursion during such strong current events is underway.

Acoustic Releases

A Benthos Model 866A Continental Shelf Release was used on each current mooring.

Current Meters

The bottom current meter on each mooring was an Oregon Environmental, Inc. (OEI) Model 9407 with temperature sensor. The top current meter on each mooring was an Aanderaa Model RCM7 with conductivity and temperature sensors. On occasion, a spare RCM7 replaced the OEI current meter. Both types vector-averaged currents, recorded into battery-backed solid-state memory, and downloaded directly to PC-type computers. Each instrument was serviced according to the manufacturers' instructions before and after deployment.

The OEI current meter suffered from firmware bugs and a fragile compass. The former caused no data to be recorded sometimes. The latter has resulted in some uncertainty in the quality of the direction values in some of the OEI meters during the second field year. Unfortunately, OEI went out of business in February 1999. GERG is conducting a

careful calibration of the OEI meters and a review of all the data collected by these instruments.

Dissolved Oxygen and Turbidity Recorders

A YSI Model 6000 recording system with oxygen, turbidity, temperature, and conductivity sensors was immediately below the OEI current meter. The YSI 6000 also recorded internally. An external battery pack extended the instrument's total battery life to at least four months.

To reduce biofouling, the standard sensor-guard of the YSI 6000 (conceptually, a cup with holes in it) was replaced with an "anti-fouling sensor-guard" custom manufactured by Oceanographic Industries of Miami Beach, FL. The inside of the guard was covered with an antifouling gel. Freshly coated guards were installed during each servicing cruise. Used guards were returned to the manufacturer for re-coating.

The DO sensor was calibrated to 100% saturation, following the manufacturer's instructions, just prior to deployment. The turbidity sensor was calibrated using distilled water and a solution of standard turbidity provided by the manufacturer. The standard was a 100 nephelometric turbidity unit (NTU) ± 2% solution made with Styreen/DVB Copolymer. The turbidity sensor was quite linear between 0 and 100 NTU, but the turbidity in the study region was low, usually less than 10 NTU. Therefore, a 10 NTU substandard was created by precision dilution.

CTD/DO/Transmissivity/Light-Profiling Instruments

The primary system for continuous measurements was a Seabird Electronics, Inc. SBE-911 CTD system with a SBE-11 deck unit. The Seabird SBE-911 CTD is a research grade CTD system which offers high quality profiles of oceanic temperature, salinity, and density at all ocean depths. The SBE-911 uses ultra-stable time-response matched sensors and fast, high-resolution parallel sampling for data acquisition.

In addition to providing precise measurements of temperature and salinity with depth, the TAMU/GERG Seabird CTD system has other sensors integrated into its data acquisition unit. DO is measured with a "Beckman" polarographic type *in situ* DO sensor. Downwelling irradiance is measured with a Biospherical Instruments, Inc. Model QSP-200L irradiance profiling sensor. Particle scattering is measured with a Seatech light scattering sensor. In addition to the light scattering sensor, the CTD is equipped with a Seatech, Inc. 25-cm transmissometer. Samples for discrete measurements of suspended particulate concentration (Chapter 5) were drawn from the 10-liter PVC Niskin bottles mounted on the General Oceanics Rosette sampler, which is part of the CTD profiling system.

A SBE-19 SEACAT CTD was used on the July 1997 mooring service cruise.

114

Results

Time-Series Data

Each mooring nominally had three different instruments recording time series data. The upper one, at 16 meters above bottom (mab), was always an Aanderaa RCM7 current meter with temperature and conductivity sensors (one vector and two scalar series). The current meter at 4 mab was usually an OEI 9407 current meter with a temperature sensor (one vector and one scalar series). On occasion, it was replaced with a RCM7. Just below it was a YSI 6000 Monitor with temperature, conductivity, DO, and turbidity sensors (four scalar series). For record keeping and graphical display purposes, a naming convention was devised that identifies instrument type, site, position at site, deployment period, and for current meters, the height above bottom, e.g., C1B2 16 mab. The coding is as follows:

Instrument type: C = current meter, O = oxygen/turbidity system
Site: 1, 4, 5, or 9
Position at site: A, B, or C; generally, A is NNE of pinnacle, B is SSE, C is W
Deployment: 1, 2, 3, ...
Height: 16 mab, or 4 mab (for instrument type C)

Each instrument's time series data are plotted and reported as a group by deployment. A joining of the records by parameter for seasonal analysis will be discussed in the synthesis report. Three types of graphical displays illustrate the results. A summary page (e.g., Fig. 7.2) for a current velocity record displays basic statistics, a scatter plot, and a table of joint frequency for speed and direction, which is the tabular version of a current rose. The start and stop times at the top of the summary page include all times for which the instrument's sensors produced good records. The number of points refers specifically to the velocity record, which may be shorter than the instrument's deployment period. Current velocity data are then plotted in time series format, together with scalar data collected at the same time by the current meter (e.g., Fig. 7.3). The scale is one month per page to visually resolve the tidal and inertial fluctuations in speed and direction. The four parameters measured by the YSI 6000 are also plotted as a time series group, but at a scale of one deployment period per page. With this latter format, the variability in DO and turbidity during the deployment can be seen (e.g., Fig. 7.4).

Only selected examples of the graphical records are used in this report to illustrate the principal features of the time-series records. A complete set of the data is maintained on an Internet Website in both graphical postscript and ASCII tabular formats. The Website address is http://www.gerg.tamu.edu/mames. The site will be maintained for the duration of the project. Upon completion of the project, it is planned to publish a CD-ROM containing all project data. Note that until the completion of the project, all data made available on the Internet Site are considered preliminary and subject to change.

The time-series data returned by the instruments are summarized in Table 7.3, sorted by deployment period and instrument location. Note that the period of a time-series record is usually shorter than the total period of deployment (Table 7.2) because of instrument

```
                          C1A7 - 16 mab
START TIME: 10/13/1998 18:30        STOP TIME: 02/09/1999 12:00 GMT

            Num pts.      Mean    Std Dev   Minimum   Maximum
   SPEED:      5700       9.80      6.56      1.10      34.50
 U COMP:       5700       0.41      9.96    -29.99      31.65
 V COMP:       5700       0.23      6.30    -26.99      24.73
        MEAN CURRENT VECTOR:     0.47 cm s⁻¹  @  60.7° True
```
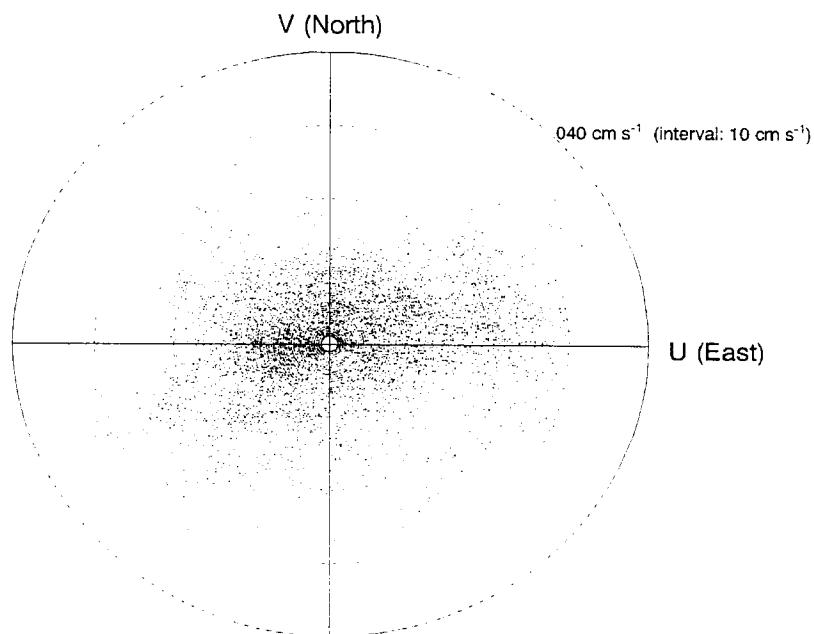
	N	NE	E	SE	S	SW	W	NW	TOTAL
< 5	3.58	2.51	3.05	1.60	2.93	4.47	4.98	2.37	25.48
5 - 10	3.91	4.61	4.31	2.68	1.72	4.77	7.73	3.58	33.32
10 - 15	1.68	3.44	3.89	1.05	1.49	3.14	4.16	2.63	21.48
15 - 20	0.16	1.17	3.00	0.40	0.77	1.95	1.75	1.02	10.22
20 - 25	0.02	1.30	2.98	0.42	0.07	1.10	0.53	0.37	6.79
25 - 30	0.00	0.23	1.37	0.11	0.07	0.40	0.09	0.11	2.37
30 - 35	0.00	0.09	0.05	0.02	0.02	0.09	0.07	0.02	0.35
> 35	0.00	0.00	0.00	0.00	0.00	0.00	0.00	0.00	0.00
TOTAL	9.35	13.34	18.66	6.28	7.07	15.92	19.31	10.08	

Speed (cm/s)

Fig. 7.2. Example of a Summary Page (C1A7) for a current velocity time series.

116
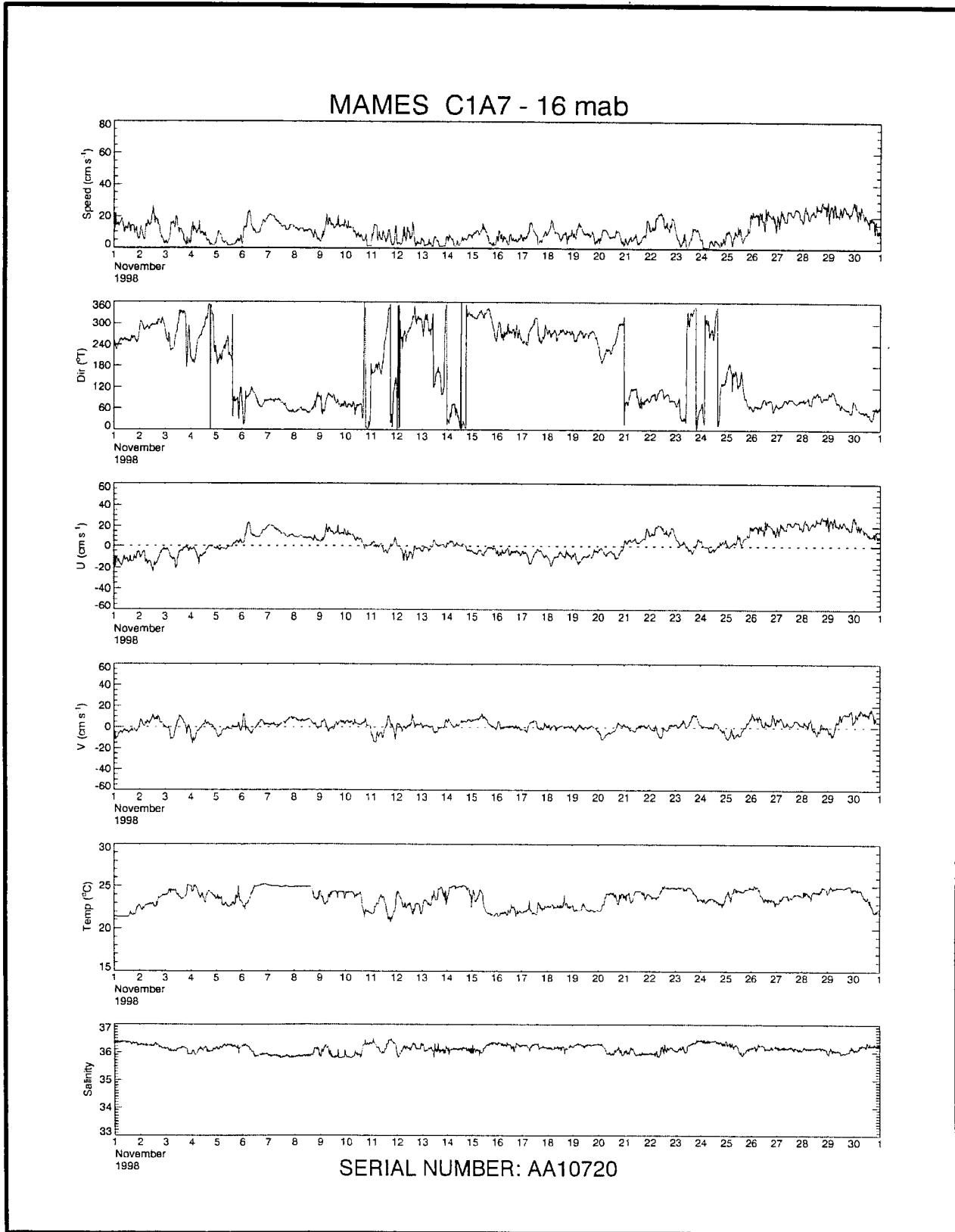
Fig. 7.3. Example of a monthly time-series plot (C1A7) for data recorded by a current meter.
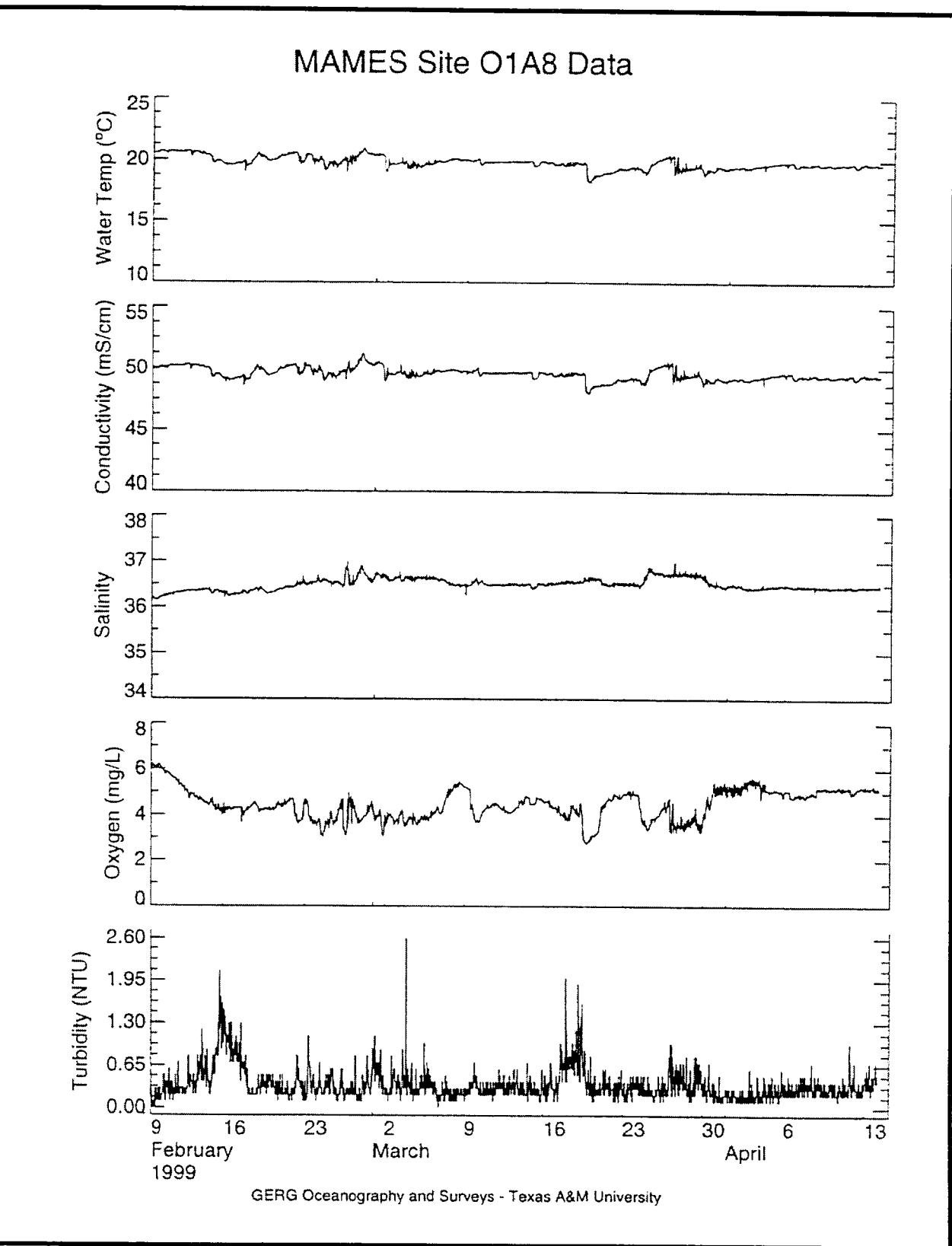
Fig. 7.4. Example of a plot of data (O1A8) collected by the YSI 6000 Monitor.

Table 7.3. Summary of the time-series data return, sorted by deployment period and instrument locations.

ID	Start	UTC	Stop	UTC	Sensors	Comments
SITE 1A						
C1A1 16 mab	05/23/97	4:30	07/28/97	12:00	V,T,C	
C1A2 16 mab	07/28/97	16:00	10/03/97	1:30	V,T,C	Data gap 8/4 - 9/3
C1A3 16 mab	10/04/97	9:00	01/29/98	16:30	V,T,C	
C1A4 16 mab	1/29/98	19:30	4/24/98	15:00	V,T,C	
C1A5 16 mab	4/24/98	20:00	7/20/98	23:00	V,T,C	
C1A6 16 mab	7/21/98	2:30	10/13/98	15:30	V,T,C	
C1A7 16 mab	10/13/98	18:30	2/9/99	12:00	V,T,C	
C1A8 16 mab	2/9/99	15:30	4/14/99	3:30	V,T,C	
C1A1 4 mab	05/23/97	4:00	07/28/97	12:00	V,T	
C1A2 4 mab	07/28/97	15:00	10/03/97	2:00	V,T	
C1A3 4 mab	10/04/97	9:00	01/29/98	15:30	V,T	
C1A4 4 mab	na	na	na	na	na	No data
C1A5 4 mab	4/24/98	20:00	7/20/98	12:00	V,T	
C1A6 4 mab	7/21/98	2:30	10/13/98	15:30	V,T	Direction questionable, speed ok
C1A7 4 mab	na	na	na	na	na	No data
C1A8 4 mab	2/9/99	15:30	4/14/99	3:30	V,T	Direction bad; speed ok
O1A1	05/23/97	4:00	07/28/97	12:00	O2,Turb,T,C	
O1A2	7/28/97	16:00	10/3/97	1:30	O2,Turb,T,C	Oxygen bad; turbidity ends 9/13/97
O1A3	na	na	na	na	na	Connector leaked - no data
O1A4	1/29/98	19:30	4/24/98	15:00	O2,Turb,T,C	
O1A5	4/24/98	19:30	7/20/98	23:30	O2,Turb,T,C	Oxygen bad
O1A6	7/21/98	2:52	10/13/98	15:22	O2,Turb,T,C	
O1A7	na	na	na	na	na	Connector leaked - no data
O1A8	2/9/99	15:30	4/14/99	3:30	O2,Turb,T,C	
SITE 1B						
C1B1 16 mab	05/23/97	4:00	07/28/97	13:00	V,T,C	
C1B2 16 mab	07/28/97	17:30	10/03/97	0:30	V,T,C	No cond. data

Table 7.3. (Continued).

ID	Start	UTC	Stop	UTC	Sensors	Comments
C1B3 16 mab	10/04/97	8:00	01/29/98	20:30	V,T,C	
C1B4 16 mab	1/29/98	23:00	4/24/98	21:00	V,T,C	
C1B1 4 mab	05/23/97	5:30	07/28/97	15:00	V,T	
C1B2 4 mab	07/28/97	17:00	10/03/97	0:00	V,T	Velocity ends 9/18/97 due to fouling
C1B3 4 mab	10/04/97	8:00	01/29/98	20:00	V,T	Velocity ends 1/17/98 due to fouling
C1B4 4 mab	na	na	na	na	na	No data
O1B1	05/23/97	5:30	07/28/97	15:00	O2,Turb,T,C	Turbidity data bad after 7/16/97
O1B2	7/28/97	17:30	10/3/97	0:30	O2,Turb,T,C	Turbidity bad
O1B3	10/04/97	8:00	01/29/98	20:30	O2,Turb,T,C	Turbidity bad
O1B4	1/29/98	23:00	4/24/98	20:00	O2,Turb,T,C	
SITE 1C						
C1C1 16 mab	05/23/97	7:00	07/28/97	17:30	V,T,C	
C1C2 16 mab	07/28/97	19:30	10/03/97	3:00	V,T,C	
C1C3 16 mab	10/03/97	12:30	01/30/98	0:00	V,T,C	
C1C4 16 mab	01/30/98	2:30	04/25/98	0:00	V,T,C	
C1C1 4 mab	na	na	na	na	na	No data recorded by OEI 9407
C1C2 4 mab	na	na	na	na	na	No data recorded by OEI 9407
C1C3 4 mab	10/03/97	12:30	01/30/98	0:00	V,T,C	RCM7 instead of 9407; velocity ends 10/29/97 - fouling
C1C4 4 mab	1/30/98	2:30	4/25/98	0:30	V,T,C	RCM7 instead of 9407
O1C1	05/23/97	7:00	07/28/97	17:00	O2,Turb,T,C	
O1C2	07/28/97	17:00	10/03/97	3:00	O2,Turb,T,C	
O1C3	10/03/97	12:00	01/30/98	0:00	O2,Turb,T,C	Oxygen questionable
O1C4	1/29/98	23:00	4/24/98	20:00	O2,Turb,T,C	
SITE 4A						
C4A1 16 mab	05/22/97	3:00	08/04/97	12:30	V,T,C	Recording stopped by low battery; cond. sensor failed
C4A2 16 mab	na	na	na	na	na	Mooring not rotated during July 97 cruise
C4A3 16 mab	10/30/97	7:00	01/30/98	5:00	V,T,C	

Table 7.3. (Continued).

ID	Start	UTC	Stop	UTC	Sensors	Comments
C4A4 16 mab	na	na	na	na	na	Bad Data Storage Unit
C4A5 16 mab	05/01/98	19:59	05/03/98	6:34	V,T,C	1-minute sample interval
C4A6 16 mab	7/21/98	22:30	10/13/98	19:30	V,T,C	
C4A7 16 mab	10/13/98	23:00	2/9/99	16:30	V,T,C	
C4A8 16 mab	2/9/99	20:00	4/14/99	6:30	V,T,C	
C4A1 4 mab	na	na	na	na	na	No data recorded by OEI 9407
C4A2 4 mab	na	na	na	na	na	Mooring not rotated during July 97 cruise
C4A3 4 mab	10/30/97	7:00	01/30/98	5:00	V,T	
C4A4 4 mab	1/30/98	9:30	5/1/98	18:00	V,T	
C4A5 4 mab	na	na	na	na	na	No data
C4A6 4 mab	7/21/98	22:30	10/13/98	22:00	V,T	Direction bad; speed ok
C4A7 4 mab	10/13/98	23:00	2/9/99	11:30	V,T	Fouled after 12/1/98
C4A8 4 mab	2/9/99	20:00	4/14/99	6:30	V,T	
O4A1	05/22/97	3:00	09/19/97	12:00	O2,Turb,T,C	Turbidity bad beginning 8/1/97
O4A2	na	na	na	na	na	Mooring not rotated during July 97 cruise
O4A3	na	na	na	na	na	Connector leaked - no data
O4A4	1/29/98	23:00	4/24/98	20:00	O2,Turb,T,C	Turbidity bad; oxygen bad after 2/15/98
O4A5	na	na	na	na	na	No data
O4A6	7/21/98	22:30	10/13/98	19:30	O2,Turb,T,C	
O4A7	10/13/98	23:00	2/9/99	16:30	O2,Turb,T,C	
O4A8	2/9/99	20:00	4/14/99	6:30	O2,Turb,T,C	
SITE 5A						
C5A1 16 mab	05/23/97	18:30	07/29/97	2:00	V,T,C	
C5A2 16 mab	07/29/97	4:30	10/06/97	4:00	V,T,C	
C5A3 16 mab	10/06/97	7:00	01/30/98	11:00	V,T,C	
C5A4 16 mab	na	na	na	na	na	No data
C5A5 16 mab	05/01/98	16:19	05/03/98	6:35	V,T,C	1-minute sample interval
C5A6 16 mab	7/22/98	7:30	10/14/98	2:30	V,T,C	

Table 7.3. (Continued).

ID	Start	UTC	Stop	UTC	Sensors	Comments
C5A7 16 mab	10/14/98	6:00	2/10/99	0:00	V,T,C	
C5A8 16 mab	2/10/99	4:00	4/14/99	12:00	V,T,C	
C5A1 4 mab	05/23/97	18:00	07/29/97	1:30	V,T	
C5A2 4 mab	07/29/97	4:00	10/06/97	4:00	V,T	
C5A3 4 mab	10/06/97	7:30	01/30/98	11:00	V,T	Velocity ends 12/1/97 due to fouling
C5A4 4 mab	1/30/98	15:00	5/1/98	13:30	V,T,C	RCM7
C5A5 4 mab	05/01/98	16:19	05/03/98	6:35	V,T,C	RCM7; 1-minute sample interval
C5A6 4 mab	7/22/98	7:30	10/14/98	3:00	V,T	Fouling problems
C5A7 4 mab	10/14/98	6:00	2/10/99	0:00	V,T	Fouling problems
C5A8 4 mab	2/10/99	4:00	4/13/99	12:00	V,T	
O5A1	05/23/97	18:00	07/29/97	1:30	O2,Turb,T,C	
O5A2	07/29/97	4:00	10/06/97	4:00	O2,Turb,T,C	Turbidity bad
O5A3	10/06/97	7:30	01/30/98	11:00	O2,Turb,T,C	
O5A4	na	na	na	na	na	Not deployed
O5A5	5/1/98	13:00	7/21/98	14:30	O2,Turb,T,C	T, C, Oxy. end 6/11/98
O5A6	7/22/98	8:00	10/14/98	2:30	O2,Turb,T,C	
O5A7	na	na	na	na	na	No data
O5A8	2/10/99	4:00	4/14/99	12:00	O2,Turb,T,C	Oxygen bad
SITE 5B						
C5B5 16 mab	05/01/98	11:39	05/03/98	6:35	V,T,C	1-minute sample interval
C5B6 16 mab	7/22/98	8:00	10/14/98	2:00	V,T,C	
C5B7 16 mab	10/14/98	6:30	2/9/99	23:30	V,T,C	
C5B8 16 mab	2/10/99	5:30	4/14/99	11:00	V,T,C	
C5B5 4 mab	5/1/98	12:00	7/21/98	15:30	V,T	
C5B6 4 mab	7/22/98	8:00	10/14/98	2:00	V,T	Direction questionable
C5B7 4 mab	10/14/98	6:30	2/10/99	0:00	V,T	Direction, temperature bad; speed ok
C5B8 4 mab	2/10/99	5:30	4/14/99	11:00	V,T	Direction questionable; speed ok
O5B5	5/1/98	12:30	6/28/98	8:00	O2,Turb,T,C	

Table 7.3. (Continued).

ID	Start	UTC	Stop	UTC	Sensors	Comments
O5B6	7/22/98	8:00	9/5/98	5:30	O2,Turb,T,C	
O5B7	na	na	na	na	na	
O5B8	na	na	na	na	na	
SITE 5C						
C5C5 16 mab	5/1/98	13:30	7/21/98	14:30	V,T,C	
C5C6 16 mab	7/22/98	9:00	10/14/98	1:30	V,T,C	
C5C7 16 mab	10/14/98	7:30	2/10/99	0:00	V,T,C	
C5C8 16 mab	2/10/99	14:30	4/14/99	10:30	V,T,C	
C5C5 4 mab	na	na	na	na	na	No data
C5C6 4 mab	7/22/98	8:30	10/14/98	2:00	V,T	Direction questionable; speed ok
C5C7 4 mab	na	na	na	na	na	Instrument lost
C5C8 4 mab	2/10/99	14:30	4/14/99	10:30	V,T,C	RCM7
O5C5	5/1/98	16:55	7/21/98	16:55	O2,Turb,T,C	
O5C6	7/22/98	9:00	8/10/98	15:30	O2,Turb,T,C	
O5C7	na	na	na	na	na	Instrument lost
O5C8	na	na	na	na	na	Instrument not deployed
SITE 9A						
C9A1 16 mab	05/24/97	2:00	07/29/97	7:00	V,T,C	
C9A2 16 mab	07/28/97	10:00	10/02/97	2:30	V,T,C	
C9A3 16 mab	10/31/97	9:30	01/30/98	18:00	V,T,C	
C9A4 16 mab	1/30/98	20:30	5/2/98	14:30	V,T,C	
C9A5 16 mab	5/2/98	2:30	5/24/98	21:00	V,T,C	
C9A6 16 mab	7/22/98	4:00	10/14/98	11:00	V,T,C	
C9A7 16 mab	10/14/98	13:30	2/10/99	8:00	V,T,C	
C9A8 16 mab	2/10/99	11:00	4/14/99	15:00	V,T,C	
C9A1 4 mab	05/24/97	2:00	07/29/97	7:00	V,T	
C9A2 4 mab	na	na	na	na	na	No data recorded by OEI 9407
C9A3 4 mab	10/31/97	9:30	01/30/98	18:00	V,T	

Table 7.3. (Continued).

ID	Start	UTC	Stop	UTC	Sensors	Comments
C9A4 4 mab	1/30/98	20:30	3/11/98	4:00	V,T	
C9A5 4 mab	5/2/98	2:30	7/22/98	2:00	V,T	
C9A6 4 mab	7/22/98	4:00	10/14/98	11:30	V,T	Direction questionable; speed ok
C9A7 4 mab	na	na	na	na	na	No data
C9A8 4 mab	2/10/99	11:00	4/14/99	15:00	V,T,C	RCM7
O9A1	05/24/97	2:00	07/29/97	7:00	O2,Turb,T,C	Turbidity questionable
O9A2	07/28/97	10:00	10/02/97	2:30	O2,Turb,T,C	
O9A3	10/31/97	9:30	01/30/98	18:00	O2,Turb,T,C	
O9A4	1/30/98	21:00	5/1/98	23:30	O2,Turb,T,C	
O9A5	5/2/98	2:30	7/22/98	2:00	O2,Turb,T,C	Turbidity bad
O9A6	na	na	na	na	na	No data
O9A7	10/14/98	14:00	11/29/98	13:30	O2,Turb,T,C	
O9A8	2/10/99	11:00	4/14/99	15:00	O2,Turb,T,C	Oxygen bad

Abbreviations: mab = meters above bottom; na = not applicable; V = velocity; T = temperature; C = conductivity; UTC = Coordinated Universal Time.

124

equilibration at the beginning or other editing. The time between recovery and redeployment of instruments was usually a few hours. It was up to several days in duration during multidisciplinary monitoring cruises because of the logistical demands. Fouling, individual sensor failure, or total instrument failure also caused data gaps in the records. Fouling can bias the speed and/or direction sensors by causing drag or complete lock-up of the rotors and/or vanes. Fouling can bias the inductive-type conductivity sensors on the RCM7 by changing the effective cell constant. Each instrument was inspected upon recovery, and observations about the degree and effects of fouling were noted on the mooring log sheet. Several velocity records have been manually truncated after initial processing, based on these recovery notes and a subjective inspection of the time series plot.

Some of the OEI 9407 and YSI 6000 meters suffered total instrument failure. In the case of the OEI 9407, firmware bugs caused no data to be recorded at times. The YSI 6000 had some problems with waterproof connectors and fittings. Saltwater leakage caused some individual sensors to fail or the main logger to lose all data.

Vertical Profiles

CTD casts collected during the first four cruises were discussed in the Second Annual Report. Seventy-two CTD stations were completed during the remaining five cruises covered by this reporting period (Table 7.1). The data have been processed using the Seabird standard software. Plots of temperature, salinity, and sigma-theta have been prepared for all casts and are available on the Website. An example of a composite plot of temperature and salinity for a cruise and a representative vertical profile are shown in Figs. 7.5 and 7.6, respectively. A vertical profile for each cast and a composite plot for each site by cruise are available on the Web site. A discussion of the optical properties measured by the CTD is found in Chapter 5.

Discussion

Time-Series Data

Flow at 16 mab

The current meters at 16 mab measure the mesoscale flow just above the pinnacles. This height is above the bottom Ekman layer. The larger pinnacles may slightly perturb the flow, a possibility that will be examined during the synthesis phase. Across the entire pinnacle study region there is substantial similarity in the observed flow fields. For example, Figs. 7.7 and 7.8 show summary pages for Sites 1 and 9 for the first year. The most frequent direction octant and the direction of the vector mean current are northeast. The most frequent speed range is 5-10 cm/s, reflecting the normal tidal influence. Strong currents, i.e., greater than 35 cm/s, are most frequently directed to the southwest. The maximum currents at 16 mab approached 50 cm/s during the first year. To further condense the information content of the velocity series, six statistics have been extracted from the individual summary pages and placed in Table 7.4. Note that the vector mean
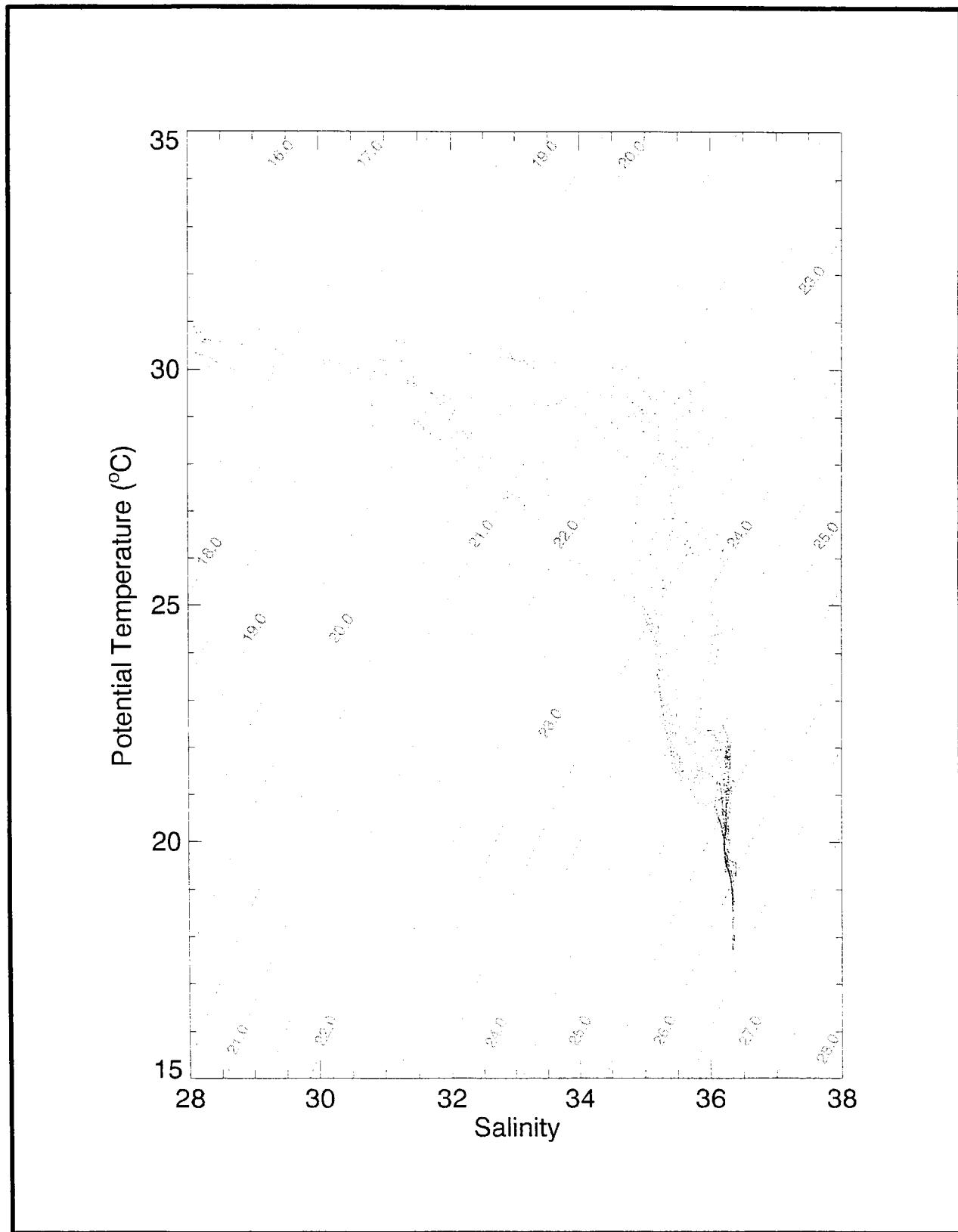
Fig. 7.5. Example of a composite temperature versus salinity plot (for Cruise C6, 20-22 July, 1998).
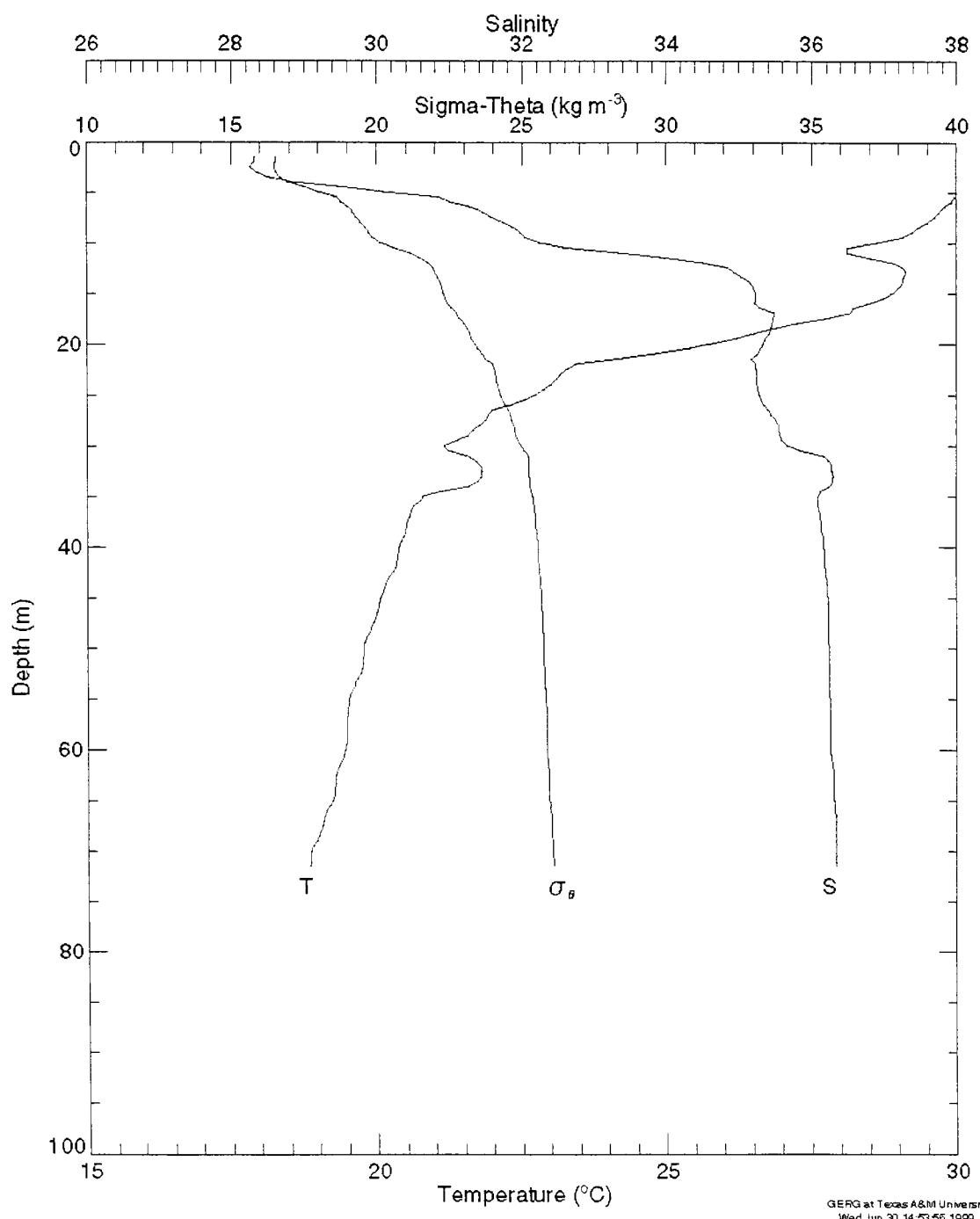
Fig. 7.6. Example of a vertical profile of temperature, salinity, and sigma-theta for a CTD cast (Station H5A2 during Cruise C6).

127

```
                        C1A1  -  16 mab
START TIME: 05/23/1997 04:30        STOP TIME: 04/24/1998 15:00 GMT

            Num pts.      Mean    Std Dev    Minimum    Maximum
  SPEED:     14105       11.12      7.91       1.10       49.60
  U COMP:    14105        2.80     11.24     -45.07       40.02
  V COMP:    14105        0.60      7.19     -36.36       29.87
        MEAN CURRENT VECTOR:     2.86 cm s⁻¹  @   77.9° True
```

V (North)

040 cm s⁻¹ (interval: 10 cm s⁻¹)

U (East)

Speed (cm/s)	N	NE	E	SE	S	SW	W	NW	TOTAL
< 5	1.73	3.02	4.49	2.55	2.59	3.88	4.91	2.58	25.74
5 - 10	1.84	4.30	5.13	2.53	2.85	4.25	4.63	2.67	28.18
10 - 15	0.91	2.77	3.74	1.09	1.66	2.13	2.55	1.13	15.98
15 - 20	0.50	3.65	4.59	0.65	0.69	1.87	1.81	0.69	14.45
20 - 25	0.29	2.81	4.29	0.30	0.16	0.89	1.30	0.24	10.28
25 - 30	0.11	0.67	1.33	0.04	0.02	0.64	0.51	0.15	3.46
30 - 35	0.03	0.22	0.64	0.01	0.02	0.31	0.13	0.03	1.38
> 35	0.00	0.07	0.12	0.01	0.02	0.26	0.04	0.01	0.52
TOTAL	5.41	17.50	24.31	7.17	8.01	14.23	15.88	7.50	

Fig. 7.7. Summary of current meter observations at Site 1A at 16 meters above the bottom (mab) for the period 23 May 1997 through 24 April 1998: basic statistics (top), scatter plot (middle), and percent joint occurrence of speed and direction (bottom).

128

C9A1 - 16 mab

START TIME: 05/24/1997 02:00   STOP TIME: 05/02/1998 14:30 GMT

	Num pts.	Mean	Std Dev	Minimum	Maximum
SPEED:	14758	11.47	7.75	1.10	36.80
U COMP:	14758	3.18	11.57	-35.35	35.20
V COMP:	14758	-0.06	6.89	-28.67	28.36

MEAN CURRENT VECTOR: 3.18 cm s^{-1} @   91.0° True

V (North)

040 cm s^{-1} (interval: 10 cm s^{-1})

U (East)

Speed (cm/s)	N	NE	E	SE	S	SW	W	NW	TOTAL
< 5	1.53	3.65	4.19	3.12	2.66	2.47	2.61	2.20	23.42
5 - 10	2.70	5.35	4.98	3.26	3.20	3.64	3.73	2.17	29.03
10 - 15	0.89	3.64	3.85	1.61	1.52	2.69	2.18	0.78	17.15
15 - 20	0.20	2.49	4.62	1.12	0.56	2.08	1.52	0.20	12.79
20 - 25	0.14	2.11	5.14	0.41	0.26	1.77	1.15	0.19	11.17
25 - 30	0.05	0.94	2.72	0.03	0.01	0.89	0.64	0.01	5.31
30 - 35	0.00	0.22	0.52	0.01	0.01	0.11	0.14	0.01	1.01
> 35	0.00	0.03	0.03	0.01	0.01	0.01	0.01	0.01	0.12
TOTAL	6.51	18.44	26.05	9.56	8.21	13.66	12.00	5.57	

Fig. 7.8. Summary of current meter observations at Site 9A at 16 meters above the bottom (mab) for the period 24 May 1997 through 2 May 1998: basic statistics (top), scatter plot (middle), and percent joint occurrence of speed and direction (bottom).

Table 7.4. Statistics for the velocity time series at 16 mab.

Station	Scalar Avg. Speed (cm/s)	Scalar Max Speed (cm/s)	Scalar Std. Dev. (cm/s)	Vector Mean Speed (cm/s)	Vector Mean Dir. (Deg. T)	Most Frequent Octant	%
C1A1	14.7	37.1	7.9	13.1	68.6	E	47.1
C1B1	13.3	41.1	7.7	12.0	69.8	E	48.8
C1C1	12.7	37.1	6.9	11.4	65.7	E	44.6
C4A1	11.9	34.8	6.3	8.3	81.2	E	54.0
C5A1	10.1	30.7	5.6	7.1	65.3	NE	33.5
C9A1	10.4	33.4	7.1	6.8	80.9	E	39.5
C1A2	5.0	23.8	4.7	1.5	129.2	E	24.8
C1B2	6.9	27.5	4.8	2.3	103.4	E	20.8
C1C2	6.1	25.2	4.5	1.6	73.4	NE	16.6
C4A2	--	--	--	--	--	--	--
C5A2	8.1	32.8	5.8	3.4	76.6	E	29.0
C9A2	7.3	30.7	5.5	1.2	52.2	NE	21.5
C1A3	10.2	40.6	6.9	1.6	99.1	E	19.9
C1B3	9.1	36.8	6.9	1.7	110.1	SW	19.6
C1C3	8.2	34.2	6.1	1.5	81.2	NE	18.6
C4A3	11.2	41.7	7.4	2.1	170.6	E	26.0
C5A3	11.0	42.7	7.2	1.2	66.1	E	22.3
C9A3	14.2	36.8	7.9	8.6	75.2	E	33.0
C1A4	12.5	49.6	8.6	3.1	250.0	W	33.5
C1B4	9.5	47.9	8.6	4.7	242.3	SW	28.0
C1C4	8.5	47.6	8.1	3.0	257.7	W	29.3
C4A4	--	--	--	--	--	--	--
C5A4	--	--	--	--	--	--	--
C9A4	12.6	36.6	8.0	5.3	220.6	SW	24.9
C1A5	9.0	34.2	6.3	2.3	82.4	NE	22.5
C4A5	--	--	--	--	--	--	--
C5A5	--	--	--	--	--	--	--
C5B5	--	--	--	--	--	--	--
C5C5	7.2	23.5	4.5	1.4	78.2	E	24.6
C9A5	9.0	29.6	6.7	4.9	261.3	W	28.6
C1A6	11.9	96.7	10.5	5.3	228.7	SW	27.4
C4A6	10.5	65.9	8.3	4.8	237.8	SW	31.6
C5A6	11.5	95.3	8.5	0.6	115.5	E	22.1
C5B6	13.2	82.2	9.9	1.4	113.9	E	25.3
C5C6	12.3	98.5	9.6	1.4	134.1	E	25.6
C9A6	13.6	91.7	10.5	1.6	95.2	E	28.1
C1A7	9.8	34.5	6.6	0.5	60.7	W	19.3
C4A7	10.3	36.3	6.2	4.0	227.4	SW	35.9

130

Table 7.4. (Continued).

Station	Scalar Avg. Speed (cm/s)	Scalar Max Speed (cm/s)	Scalar Std. Dev. (cm/s)	Vector Mean Speed (cm/s)	Vector Mean Dir. (Deg. T)	Most Frequent Octant	%
C5A7	8.6	32.8	6.4	0.6	110.8	W	23.1
C5B7	10.4	36.3	7.3	1.4	85.5	E	23.3
C5C7	10.3	37.7	6.9	0.4	250.0	W	28.3
C9A7	12.7	44.4	10.0	3.5	88.3	E	28.3
C1A8	7.2	34.2	5.5	1.9	274.9	W	19.1
C4A8	10.1	36.6	5.9	3.8	243.6	SW	26.9
C5A8	9.0	29.6	6.2	0.7	275.6	W	24.6
C5B8	8.7	27.0	5.9	1.0	273.2	W	25.0
C5C8	8.0	26.1	5.5	1.1	264.3	W	27.2
C9A8	11.4	34.5	7.3	4.2	242.7	W	25.3

Abbreviations: mab = meters above bottom.

speed and the scalar average speed can be quite different, which indicates the amount of directional variability in the flow.

Flow at 4 mab

Information about the near bottom flow is summarized in Table 7.5. Compared with the flow at 16 mab, the near-bottom flow was more site specific. Bottom friction and the local topography influenced flow. The most frequent direction octants were those with a southerly component (Table 7.5). Average scalar speeds were comparable at times to those at 16 mab, and mean vector speeds sometimes exceeded the overlying flow because of greater directionality.

Dissolved Oxygen and Turbidity

Time series of DO and turbidity were collected at a height of ~2.3 mab at each mooring. Data return is good for DO, but not for turbidity. Sensor or instrument malfunction rather than fouling are responsible for data loss. DO values were generally near or above 4 mg/L (e.g., Fig. 7.4), except at Site 5 during the second deployment period. In this record, values were below 3.0 mg/L much of the time and fell below 2.0 mg/L during 18 to 28 August and 5 to 13 September, 1997. Turbidity values were generally quite low, i.e., 0 to 2 NTU, with brief periods during which turbidity rose to the 2 to 10 NTU range.

Temperature and Conductivity/Salinity

The moored instruments collected time series temperature and conductivity, which together yield a time series of calculated salinity. The basic statistics for each deployment-length record of temperature and salinity are detailed in Tables 7.6 and 7.7, respectively. These statistics are preliminary because a QC comparison with the CTD collected by this study and other studies is still underway. Temperature from the instrument moorings followed a small seasonal cycle with superposed variability caused by advective changes from tidal and inertial currents and possible intrusions by mesoscale water mass motion. Salinity ranged from about 34.9 to 36.8 but generally was in the 36.2 to 36.4 range. Values above 36.5 suggest possible intrusion of Loop Current related water.

September 1998

September 1998 was the most unusual month of the study because of several events. Hurricane Earl's path (Fig. 7.9) crossed the eastern side of the study area on 3 September and the eye of Hurricane Georges (Fig. 7.10) passed directly over Site 5 on 29 September. The resulting currents at 16 mab are shown in stick vector form in Fig. 7.11.

Currents were strongest during Hurricane Georges. At Site 1, speed reached 96.7 cm/s at the 16 mab level. The direction of the hurricane driven currents was mainly southwest at Sites 1 and 4, and shifted between southwest and northwest at Sites 5 and 9. Hurricane Earl, which moved more quickly across the shelf, forced a response of about half the

Table 7.5. Statistics for the velocity time series at 4 mab.

Station	Scalar Avg. Speed (cm/s)	Scalar Max Speed (cm/s)	Scalar Std. Dev. (cm/s)	Vector Mean Speed (cm/s)	Vector Mean Dir. (Deg. T)	Most Frequent Octant	%
C1A1	5.7	30.8	4.1	2.3	96.5	SE	19.5
C1B1	11.6	34.1	6.8	6.9	63.4	NE	45.9
C1C1	--	--	--	--	--	--	--
C4A1	--	--	--	--	--	--	--
C5A1	10.4	30.6	5.9	1.1	176.9	SW	23.6
C9A1	10.6	35.0	6.5	6.9	125.3	SE	33.3
C1A2	4.6	19.5	3.5	2.3	162.2	S	24.2
C1B2	8.0	22.5	5.6	3.9	191.8	S	28.6
C1C2	--	--	--	--	--	--	--
C4A2	--	--	--	--	--	--	--
C5A2	7.1	29.7	5.6	1.2	183.3	SW	23.5
C9A2	--	--	--	--	--	--	--
C1A3	5.3	28.5	4.4	2.1	176.4	S	26.7
C1B3	10.0	30.2	6.1	3.6	184.4	S	26.5
C1C3	7.9	29.9	7.0	6.1	201.7	S	36.9
C4A3	7.3	41.8	6.1	2.3	181.2	SW	27.5
C5A3	8.9	25.8	6.0	2.6	240.4	SW	23.2
C9A3	10.9	49.6	7.3	7.7	140.9	S	27.6
C1A4	--	--	--	--	--	--	--
C1B4	--	--	--	--	--	--	--
C1C4	6.9	51.4	7.9	5.0	207.7	S	31.8
C4A4	7.0	30.0	8.0	10.4	222.8	SW	51.1
C5A4	7.3	40.2	5.9	0.9	187.0	SW	27.2
C9A4	13.0	35.7	6.6	2.9	188.8	SW	33.4
C1A5	7.5	28.0	5.5	2.7	155.8	N	25.6
C4A5	--	--	--	--	--	--	--
C5A5	--	--	--	--	--	--	--
C5B5	7.9	19.5	4.5	1.2	245.9	SW	25.7
C5C5	--	--	--	--	--	--	--
C9A5	5.5	19.7	4.7	3.3	258.0	W	36.6
C1A6	9.4	49.1	6.4	QC	QC	QC	QC
C4A6	8.4	56.1	8.0	QC	QC	QC	QC
C5A6	8.5	60.0	7.2	QC	QC	QC	QC
C5B6	4.8	39.7	5.7	QC	QC	QC	QC
C5C6	2.9	45.1	5.0	QC	QC	QC	QC
C9A6	10.4	60.0	7.3	.06	7.6	NE	30.2
C1A7	--	--	--	--	--	--	
C4A7	11.3	35.0	7.1	7.5	229.0	SW	33.0

133

Table 7.5. (Continued).

Station	Scalar Avg. Speed (cm/s)	Scalar Max Speed (cm/s)	Scalar Std. Dev. (cm/s)	Vector Mean Speed (cm/s)	Vector Mean Dir. (Deg. T)	Most Frequent Octant	%
C5A7	6.7	24.0	4.2	3.5	351.6	N	30.0
C5B7	6.2	33.7	4.8	QC	QC	QC	QC
C5C7	--	--	--	--	--	--	--
C9A7	--	--	--	--	--	--	--
C1A8	6.3	24.5	4.7	QC	QC	QC	QC
C4A8	9.9	56.9	5.9	4.7	243.8	SW	28.6
C5A8	4.7	28.2	5.6	1.3	237.8	E	54.1
C5B8	5.5	29.8	6.2	QC	QC	QC	QC
C5C8	6.7	21.7	4.0	1.8	237.6	SW	26.4
C9A8	6.1	27.7	5.7	3.4	239.4	SW	34.2

Abbreviations: -- = no data; mab = meters above bottom; QC = Quality Control review of direction in progress.

Table 7.6. Statistics for the temperature time-series data collected by a) the current meters at 16 m above bottom (mab), b) the current meters at 4 mab, and c) the YSI 6000 Monitor at 2.5 mab.

Station	Start Date	Time (UTC)	Stop Date	Time (UTC)	No. Obs.	No. Bad	Mean	Std. Dev.	Min.	Max.
C1A1	5/23/1997	4:30	7/28/1997	12:00	3184	0	21.48	0.45	20.30	23.40
C1B1	5/23/1997	4:00	7/28/1997	13:00	3187	0	21.25	0.43	19.71	22.82
C1C1	5/23/1997	7:00	7/28/1997	17:30	3190	0	21.19	0.45	19.68	23.05
C5A1	5/23/1997	18:30	7/29/1997	2:00	3184	0	20.70	0.85	18.36	22.24
C9A1	5/24/1997	2:00	7/29/1997	7:00	3179	0	20.36	0.92	17.10	21.87
C1B2	7/28/1997	17:30	10/3/1997	0:30	3183	0	20.51	0.58	18.77	22.34
C1C2	7/28/1997	19:30	10/3/1997	3:00	3184	0	20.56	0.56	18.96	22.49
C4A2	5/22/1997	3:00	8/4/1997	12:30	3572	0	19.16	1.22	15.85	21.44
C5A2	7/29/1997	4:30	10/6/1997	4:00	3312	0	20.73	0.40	18.99	21.91
C9A2	7/28/1997	10:00	10/2/1997	2:30	3154	0	20.32	0.45	18.08	21.50
C1A3	10/4/1997	9:00	1/29/1998	16:30	5632	0	20.40	1.56	15.61	23.35
C1B3	10/4/1997	8:00	1/29/1998	20:30	5642	0	20.13	1.56	15.34	23.24
C1C3	10/3/1997	12:30	1/30/1998	0:00	5688	0	20.18	1.54	15.62	23.29
C4A3	10/30/1997	7:00	1/30/1998	5:00	4413	0	17.90	1.92	10.93	21.05
C5A3	10/6/1997	7:00	1/30/1998	11:00	5577	0	20.20	1.50	13.76	22.77
C9A3	10/31/1997	9:30	1/30/1998	18:00	4386	0	19.69	1.43	15.38	22.57
C1A4	1/29/1998	19:30	4/24/1998	15:00	4072	0	18.53	0.73	15.44	20.42
C1B4	1/29/1998	23:00	4/24/1998	21:00	4077	0	18.45	0.77	15.11	20.14
C9A4	1/30/1998	20:30	5/2/1998	14:30	4405	0	18.40	1.02	14.72	23.54
C1A5	4/24/1998	20:00	7/20/1998	23:00	4183	0	20.35	0.68	18.77	22.15
C5C5	5/1/1998	13:30	7/21/1998	14:30	3891	0	19.92	0.64	18.72	21.84
C9A5	5/2/1998	2:30	5/24/1998	21:00	1094	0	19.31	0.28	18.41	20.11
C1A6	7/21/1998	2:30	10/13/1998	15:30	4059	0	20.81	1.87	18.41	27.45
C4A6	7/21/1998	22:30	10/13/1998	19:30	4027	0	18.81	0.94	15.88	22.65
C5A6	7/22/1998	7:30	10/14/1998	2:30	4023	0	21.19	1.93	18.02	27.21
C5B6	7/22/1998	8:00	10/14/1998	2:00	4021	0	21.17	1.94	17.88	27.19

Table 7.6. (Continued).

Station	Start Date	Time (UTC)	Stop Date	Time (UTC)	No. Obs.	No. Bad	Mean	Std. Dev.	Min.	Max.
C5C6	7/22/1998	9:00	10/14/1998	1:30	4018	0	21.14	1.90	17.99	27.29
C9A6	7/22/1998	4:00	10/14/1998	11:00	4047	0	20.65	1.50	17.88	26.90
C1A7	10/13/1998	18:30	2/9/1999	12:00	5700	0	21.85	1.49	18.53	25.21
C4A7	10/13/1998	23:00	2/9/1999	16:30	5700	0	19.61	0.70	15.99	21.45
C5A7	10/14/1998	6:00	2/10/1999	0:00	5701	0	21.90	1.26	18.19	25.19
C5B7	10/14/1998	6:30	2/9/1999	23:30	5699	0	22.72	2.95	18.16	32.08
C5C7	10/14/1998	7:30	2/10/1999	0:00	5698	0	21.68	1.21	18.12	25.15
C1A8	2/9/1999	15:30	4/14/1999	3:30	3049	0	20.13	0.44	18.87	21.30
C4A8	2/9/1999	20:00	4/14/1999	6:30	3046	0	19.18	0.65	16.75	21.06
C5A8	2/10/1999	4:00	4/14/1999	12:00	3041	0	19.84	0.32	18.75	20.75
C5B8	2/10/1999	5:30	4/14/1999	11:00	3036	0	19.77	0.32	18.70	21.06
C5C8	2/10/1999	14:30	4/14/1999	10:30	3017	0	19.77	0.31	18.71	20.68
C9A8	2/10/1999	11:00	4/14/1999	15:00	3033	0	19.97	0.52	18.80	21.95
C1A1	5/23/1997	4:00	7/28/1997	12:00	3185	0	20.38	0.67	17.48	21.69
C1B1	5/23/1997	5:30	7/28/1997	15:00	3188	0	20.08	0.76	16.93	21.66
C5A1	5/23/1997	18:30	7/29/1997	1:30	3183	0	18.90	0.88	16.84	21.25
C9A1	5/24/1997	2:00	7/29/1997	7:00	3179	0	18.87	1.09	16.60	21.20
C1A2	7/28/1997	15:00	10/3/1997	2:00	3191	0	19.91	0.77	17.73	21.15
C1B2	7/28/1997	17:00	10/3/1997	0:00	3183	0	19.78	0.81	17.42	21.14
C5A2	7/29/1997	4:00	10/6/1997	4:00	3313	0	19.67	0.78	17.71	21.06
C1C3	10/3/1997	12:30	1/30/1998	0:00	5688	0	18.88	1.97	12.33	21.71
C1A3	10/4/1997	9:00	1/29/1998	15:30	5632	0	19.12	2.05	12.49	21.94
C1B3	10/4/1997	8:00	1/29/1998	20:00	5643	0	19.03	1.97	12.32	21.81
C4A3	10/30/1997	7:00	1/30/1998	5:00	4413	0	17.00	2.15	10.78	20.23
C5A3	10/6/1997	7:30	1/30/1998	11:00	5578	0	18.92	1.77	13.42	21.73
C9A3	10/31/1997	9:30	1/30/1998	18:00	4386	0	18.34	1.38	13.77	21.33
C1C4	1/30/1998	2:30	4/25/1998	0:30	4077	0	17.97	1.11	14.26	21.78

136

Table 7.6. (Continued).

Station	Start Date	Time (UTC)	Stop Date	Time (UTC)	No. Obs.	No. Bad	Mean	Std. Dev.	Min.	Max.
C5A4	1/30/1998	15:00	5/1/1998	13:30	4366	0	17.89	0.94	14.74	19.25
C4A4	1/30/1998	9:30	5/1/1998	18:00	4384	0	16.52	1.27	12.40	19.08
C9A4	1/30/1998	20:30	3/11/1998	4:00	1888	0	17.12	1.26	13.11	20.10
C1A5	4/24/1998	20:00	7/20/1998	12:00	4161	0	19.69	0.66	17.29	21.08
C5B5	5/1/1998	12:00	7/21/1998	15:30	3896	0	19.54	0.63	18.21	20.53
C9A5	5/2/1998	2:30	7/22/1998	2:00	3888	0	19.13	0.45	17.95	20.38
C1A6	7/21/1998	2:30	10/13/1998	15:30	4059	0	20.43	1.36	17.68	27.71
C4A6	7/21/1998	22:30	10/13/1998	22:00	4015	0	30.40	4.55	17.79	34.11
C5A6	7/22/1998	7:30	10/14/1998	3:00	4024	0	20.28	1.41	15.29	27.45
C5B6	7/22/1998	8:00	10/14/1998	2:00	4021	0	12.89	1.17	7.99	19.35
C5C6	7/22/1998	8:30	10/14/1998	2:00	4020	0	18.12	3.21	14.06	27.17
C9A6	7/22/1998	4:00	10/14/1998	11:30	4048	0	19.72	1.03	16.83	25.98
C4A7	10/13/1998	23:00	2/9/1999	11:30	5691	0	19.37	0.87	15.33	21.10
C5A7	10/14/1998	6:00	2/10/1999	0:00	5701	0	21.12	0.77	19.20	23.07
C5B7	10/14/1998	6:30	2/10/1999	0:00	5700	5700				
C9A7	10/14/1998	13:00	2/10/1999	8:00	5705	0	19.89	0.52	18.19	21.46
C5C8	2/10/1999	14:30	4/14/1999	10:30	3017	0	19.50	0.32	18.53	20.12
C9A8	2/10/1999	11:00	4/14/1999	15:00	3033	0	19.20	0.46	17.63	20.53
C1A8	2/9/1999	15:30	4/14/1999	3:30	3049	0	12.15	1.29	8.30	15.14
C4A8	2/9/1999	20:00	4/14/1999	6:30	3046	0	18.80	0.95	15.93	20.08
C5A8	2/10/1999	4:00	4/13/1999	12:00	2993	0	20.04	0.32	18.97	20.67
C5B8	2/10/1999	5:30	4/14/1999	11:00	3034	0	19.43	1.15	14.15	20.30
O1A1	5/23/1997	1:30	7/28/1997	10:00	3186	0	20.07	0.76	17.20	21.49
O1B1	5/23/1997	1:30	7/28/1997	11:30	3189	0	19.78	0.84	16.54	21.54
O1C1	5/23/1997	1:30	7/28/1997	12:30	3191	0	19.83	0.70	17.43	21.39
O5A1	5/23/1997	1:30	7/28/1997	9:00	3184	0	18.77	0.86	16.70	21.14
O9A1	5/23/1997	2:00	7/28/1997	7:00	3179	0	18.60	1.07	16.51	20.91

Table 7.6. (Continued).

Station	Start Date	Time (UTC)	Stop Date	Time (UTC)	No. Obs.	No. Bad	Mean	Std. Dev.	Min.	Max.
O1A2	7/28/1997	16:00	10/3/1997	1:30	3188	0	19.70	0.78	17.55	20.83
O1B2	7/28/1997	17:30	10/3/1997	0:30	3183	0	19.55	0.81	17.30	20.82
O1C2	7/28/1997	19:30	10/3/1997	3:00	3184	0	19.68	0.78	17.54	21.11
O4A2	5/22/1997	3:00	9/18/1997	22:00	5751	0	17.54	1.55	14.50	20.54
O5A2	7/28/1997	4:30	10/5/1997	4:00	3312	0	19.56	0.82	17.39	21.01
O9A2	7/28/1997	10:00	10/30/1997	5:00	4503	0	19.25	0.74	16.65	20.84
O1B3	10/4/1997	8:00	1/20/1998	23:30	5216	0	18.92	2.02	12.32	21.60
O1C3	10/3/1997	12:30	1/30/1998	0:00	5688	0	18.79	2.00	12.37	21.69
O5A3	10/6/1997	7:00	1/30/1998	10:00	5575	0	18.76	1.75	13.13	21.60
O9A3	10/31/1997	9:30	1/30/1998	18:00	4386	0	18.08	1.37	13.61	20.99
O1A4	1/29/1998	19:30	4/24/1998	15:00	4072	0	17.93	1.10	14.45	19.56
O1B4	1/29/1998	23:00	4/24/1998	20:00	4075	0	17.88	1.11	14.29	19.51
O1C4	1/30/1998	2:00	4/25/1998	0:00	4077	0	17.89	1.12	14.20	19.64
O4A4	1/30/1998	9:30	4/27/1998	11:30	4181	0	16.52	1.29	12.49	19.06
O9A4	1/30/1998	21:00	5/1/1998	23:30	4374	0	17.56	1.09	13.18	20.05
O1A5	4/24/1998	19:30	7/20/1998	23:30	4185	0	19.48	0.66	17.21	20.92
O5A5	5/1/1998	13:00	7/21/1998	14:30	3892	1943	19.20	0.55	18.30	20.27
O5B5	5/1/1998	12:30	6/28/1998	8:00	2776	0	19.47	0.60	18.37	20.35
O5C5	5/1/1998	16:55	7/21/1998	16:55	3889	0	19.35	0.63	18.03	20.37
O9A5	5/2/1998	2:30	7/22/1998	2:00	3888	0	19.05	0.44	17.90	20.21
O1A6	7/21/1998	2:52	10/13/1998	15:22	4058	0	19.61	1.35	17.01	27.30
O4A6	7/21/1998	22:30	10/13/1998	19:30	4027	0	18.08	0.97	15.53	21.39
O5A6	7/22/1998	8:00	10/14/1998	2:30	4022	0	19.66	1.40	17.59	27.17
O5B6	7/22/1998	8:00	9/5/1998	5:30	2153	0	19.22	0.75	17.72	22.45
O5C6	7/22/1998	9:00	8/10/1998	15:30	926	0	19.31	0.30	18.73	20.09
O9A6	7/22/1998	4:30	7/25/1998	12:05	57	0	19.35	0.13	19.14	19.61

Table 7.6. (Continued).

Station	Start Date	Time (UTC)	Stop Date	Time (UTC)	No. Obs.	No. Bad	Mean	Std. Dev.	Min.	Max.
O4A7	10/13/1998	23:00	2/9/1999	16:30	5700	0	19.18	0.90	15.26	20.95
O9A7	10/14/1998	14:00	11/29/1998	13:30	2204	0	20.13	0.39	18.84	21.17
O1A8	2/9/1999	15:30	4/14/1999	3:30	3049	0	19.80	0.43	18.23	20.92
O4A8	2/9/1999	20:00	4/14/1999	6:30	3046	0	18.54	0.98	15.76	19.86
O5A8	2/10/1999	4:00	4/14/1999	12:00	3041	0	19.57	0.34	18.46	20.30
O9A8	2/10/1999	11:00	4/14/1999	15:00	3033	0	19.20	0.47	17.65	20.47

Abbreviations: UTC = Coordinated Universal Time.

Table 7.7. Statistics for the salinity time-series data collected by a) the current meters at 16 m above bottom (mab), and b) the YSI 6000 Monitor at 2.5 mab.

Station	Start Date	Time (UTC)	Stop Date	Time (UTC)	No. Obs.	No. Bad	Mean	Std. Dev.	Min.	Max.
C1A1	5/23/1997	4:30	7/28/1997	12:00	3184	0	36.29	0.11	35.92	36.79
C1B1	5/23/1997	4:00	7/28/1997	13:00	3187	0	35.86	0.58	34.83	36.52
C1C1	5/23/1997	7:00	7/28/1997	17:30	3190	0	36.29	0.10	35.92	36.74
C5A1	5/23/1997	18:30	7/29/1997	2:00	3184	0	36.27	0.05	36.01	36.47
C9A1	5/24/1997	2:00	7/29/1997	7:00	3179	0	36.42	0.05	36.26	36.64
C1B2	7/28/1997	17:30	10/3/1997	0:30	3183	3183	-999.00	0.00	-999.00	-999.00
C1C2	7/28/1997	19:30	10/3/1997	3:00	3184	0	36.45	0.10	36.27	36.81
C4A2	5/22/1997	3:00	8/4/1997	12:30	3572	3572	-999.00	0.00	-999.00	-999.00
C5A2	7/29/1997	4:30	10/6/1997	4:00	3312	0	36.46	0.09	36.29	36.76
C9A2	7/28/1997	10:00	10/2/1997	2:30	3154	0	36.47	0.07	36.32	36.76
C1A3	10/4/1997	9:00	1/29/1998	16:30	5632	0	36.42	0.49	35.04	36.99
C1B3	10/4/1997	8:00	1/29/1998	20:30	5642	0	36.26	0.30	35.29	36.59
C1C3	10/3/1997	12:30	1/30/1998	0:00	5688	0	36.14	0.46	34.56	36.65
C4A3	10/30/1997	7:00	1/30/1998	5:00	4413	0	36.35	0.25	35.54	36.79
C5A3	10/6/1997	7:00	1/30/1998	11:00	5577	0	36.26	0.34	35.21	36.66
C9A3	10/31/1997	9:30	1/30/1998	18:00	4386	0	36.33	0.16	35.91	36.71
C1A4	1/29/1998	19:30	4/24/1998	15:00	4072	0	36.02	0.15	35.52	36.38
C1B4	1/29/1998	23:00	4/24/1998	21:00	4077	0	35.76	0.32	34.38	36.47
C9A4	1/30/1998	20:30	5/2/1998	14:30	4405	0	35.68	2.95	0.04	36.47
C1A5	4/24/1998	20:00	7/20/1998	23:00	4183	0	36.24	0.06	35.93	36.49
C5C5	5/1/1998	13:44	7/21/1998	14:42	3891	0	36.19	0.05	35.93	36.35
C9A5	5/2/1998	2:30	5/24/1998	21:00	1094	1094	-999.00	0.00	-999.00	-999.00
C1A6	7/21/1998	2:30	10/13/1998	15:30	4059	0	36.31	0.19	35.42	36.93
C4A6	7/21/1998	22:30	10/13/1998	19:30	4027	0	36.43	0.10	36.14	36.84
C5A6	7/22/1998	7:30	10/14/1998	2:30	4023	0	36.20	0.25	34.93	36.56
C5B6	7/22/1998	8:00	10/14/1998	2:00	4021	0	36.23	0.26	34.95	36.64
C5C6	7/22/1998	9:00	10/14/1998	1:30	4018	0	36.08	0.24	34.85	36.43

140

Table 7.7. (Continued).

Station	Start Date	Time (UTC)	Stop Date	Time (UTC)	No. Obs.	No. Bad	Mean	Std. Dev.	Min.	Max.
C9A6	7/22/1998	4:00	10/14/1998	11:00	4047	0	36.45	0.16	35.53	36.82
C1A7	10/13/1998	18:30	2/9/1999	12:00	5700	0	36.09	0.26	35.27	36.55
C4A7	10/13/1998	23:00	2/9/1999	16:30	5700	0	36.31	0.26	35.42	36.67
C5A7	10/14/1998	6:00	2/10/1999	0:00	5701	0	36.80	0.31	35.53	37.33
C5B7	10/14/1998	6:30	2/9/1999	23:30	5699	0	35.52	1.53	29.12	36.51
C5C7	10/14/1998	7:30	2/10/1999	0:00	5698	0	35.95	0.35	34.79	36.68
C9A7	10/14/1998	13:30	2/10/1999	8:00	5702	0	36.11	0.37	34.79	36.57
C1A8	2/9/1999	15:30	4/14/1999	3:30	3049	0	36.07	0.14	35.60	36.54
C4A8	2/9/1999	20:00	4/14/1999	6:30	3046	0	36.35	0.14	35.97	36.75
C5A8	2/10/1999	4:00	4/14/1999	12:00	3041	0	35.83	0.19	35.35	36.44
C5B8	2/10/1999	5:30	4/14/1999	11:00	3036	0	36.07	0.16	35.60	36.64
C5C8	2/10/1999	14:30	4/14/1999	10:30	3017	0	36.21	0.15	35.69	36.77
C9A8	2/10/1999	11:00	4/14/1999	15:00	3033	0	36.09	0.17	35.68	36.85
C1C3	10/3/1997	12:30	1/30/1998	0:00	5688	0	36.15	0.4	35.04	36.55
C1C4	1/30/1998	2:30	4/25/1998	0:30	4077	0	35.85	0.19	33.79	36.31
C5A4	1/30/1998	15:00	5/1/1998	13:30	4366	0	35.64	0.42	34.65	36.44
C5C8	2/10/1999	14:30	4/14/1999	10:30	3017	0	36.19	0.22	35.42	36.68
C9A8	2/10/1999	11:00	4/14/1999	15:00	3033	0	36.19	0.19	35.78	36.64
O1A1	5/23/1997	1:30	7/28/1997	10:00	3186	0	36.06	0.10	35.76	36.35
O1B1	5/23/1997	1:30	7/28/1997	11:30	3189	0	35.22	0.11	34.78	35.83
O1C1	5/23/1997	1:30	7/28/1997	12:30	3191	0	35.55	0.10	35.18	36.11
O5A1	5/23/1997	1:30	7/28/1997	9:00	3184	0	36.19	0.19	35.76	36.45
O9A1	5/23/1997	2:00	7/28/1997	7:00	3179	0	36.25	0.08	35.93	36.43
O1A2	7/28/1997	16:00	10/3/1997	1:30	3188	0	36.54	0.06	36.20	36.70
O1B2	7/28/1997	17:30	10/3/1997	0:30	3183	0	36.24	0.11	35.90	36.70
O1C2	7/28/1997	19:30	10/3/1997	3:00	3184	0	35.54	0.19	35.30	36.50
O4A2	5/22/1997	3:00	9/18/1997	22:00	5751	0	35.67	0.17	35.30	36.60
O5A2	7/28/1997	4:30	10/5/1997	4:00	3312	0	36.32	0.08	36.20	36.60

Table 7.7. (Continued).

Station	Start Date	Time (UTC)	Stop Date	Time (UTC)	No. Obs.	No. Bad	Mean	Std. Dev.	Min.	Max.
O9A2	7/28/1997	10:00	10/30/1997	5:00	4503	0	37.67	0.13	37.35	37.90
O1B3	10/4/1997	8:00	1/20/1998	23:30	5216	0	36.03	0.22	35.30	36.40
O1C3	10/3/1997	12:30	1/30/1998	0:00	5688	0	36.66	0.31	35.70	37.05
O5A3	10/6/1997	7:00	1/30/1998	10:00	5575	0	36.99	0.32	36.30	37.50
O9A3	10/31/1997	9:30	1/30/1998	18:00	4386	0	36.60	0.20	36.00	37.10
O1A4	1/29/1998	19:30	4/24/1998	15:00	4072	0	35.39	0.17	34.90	35.80
O1B4	1/29/1998	23:00	4/24/1998	20:00	4075	0	35.86	0.11	35.50	36.20
O1C4	1/30/1998	2:00	4/25/1998	0:00	4077	0	36.65	0.40	35.40	37.20
O4A4	1/30/1998	9:30	4/27/1998	11:30	4181	0	36.31	0.37	35.20	37.30
O9A4	1/30/1998	21:00	5/1/1998	23:30	4374	0	35.60	0.15	34.90	35.90
O1A5	4/24/1998	19:30	7/20/1998	23:30	4185	0	35.71	0.09	35.54	36.33
O5A5	5/1/1998	13:00	7/21/1998	14:30	3892	1943	35.64	0.13	34.85	36.40
O5B5	5/1/1998	12:30	6/28/1998	8:00	2776	0	35.67	0.12	35.31	36.29
O5C5	5/1/1998	16:55	7/21/1998	16:55	3889	0	36.28	0.08	36.06	36.47
O9A5	5/2/1998	2:30	7/22/1998	2:00	3888	0	36.24	0.12	35.91	36.50
O1A6	7/21/1998	2:52	10/13/1998	15:22	4058	0	36.85	0.27	35.88	37.29
O4A6	7/21/1998	22:30	10/13/1998	19:30	4027	0	36.09	0.11	35.26	36.39
O5A6	7/22/1998	8:00	10/14/1998	2:30	4022	0	35.90	0.27	34.46	36.36
O5B6	7/22/1998	8:00	9/5/1998	5:30	2153	0	36.01	0.12	35.49	36.49
O5C6	7/22/1998	9:00	8/10/1998	15:30	926	0	36.38	0.08	36.19	36.53
O9A6	7/22/1998	4:30	7/25/1998	12:05	57	0	36.60	0.08	36.42	36.73
O4A7	10/13/1998	23:00	2/9/1999	16:30	5700	0	36.43	0.16	35.93	37.00
O9A7	10/14/1998	14:00	11/29/1998	13:30	2204	0	35.58	0.12	35.06	36.12
O1A8	2/9/1999	15:30	4/14/1999	3:30	3049	0	36.50	0.13	36.14	36.99
O4A8	2/9/1999	20:00	4/14/1999	6:30	3046	0	36.09	0.13	35.70	36.45
O5A8	2/10/1999	4:00	4/14/1999	12:00	3041	0	36.85	0.35	35.78	37.37
O9A8	2/10/1999	11:00	4/14/1999	15:00	3033	0	35.57	0.12	35.32	36.09

Abbreviations: UTC = Coordinated Universal Time.
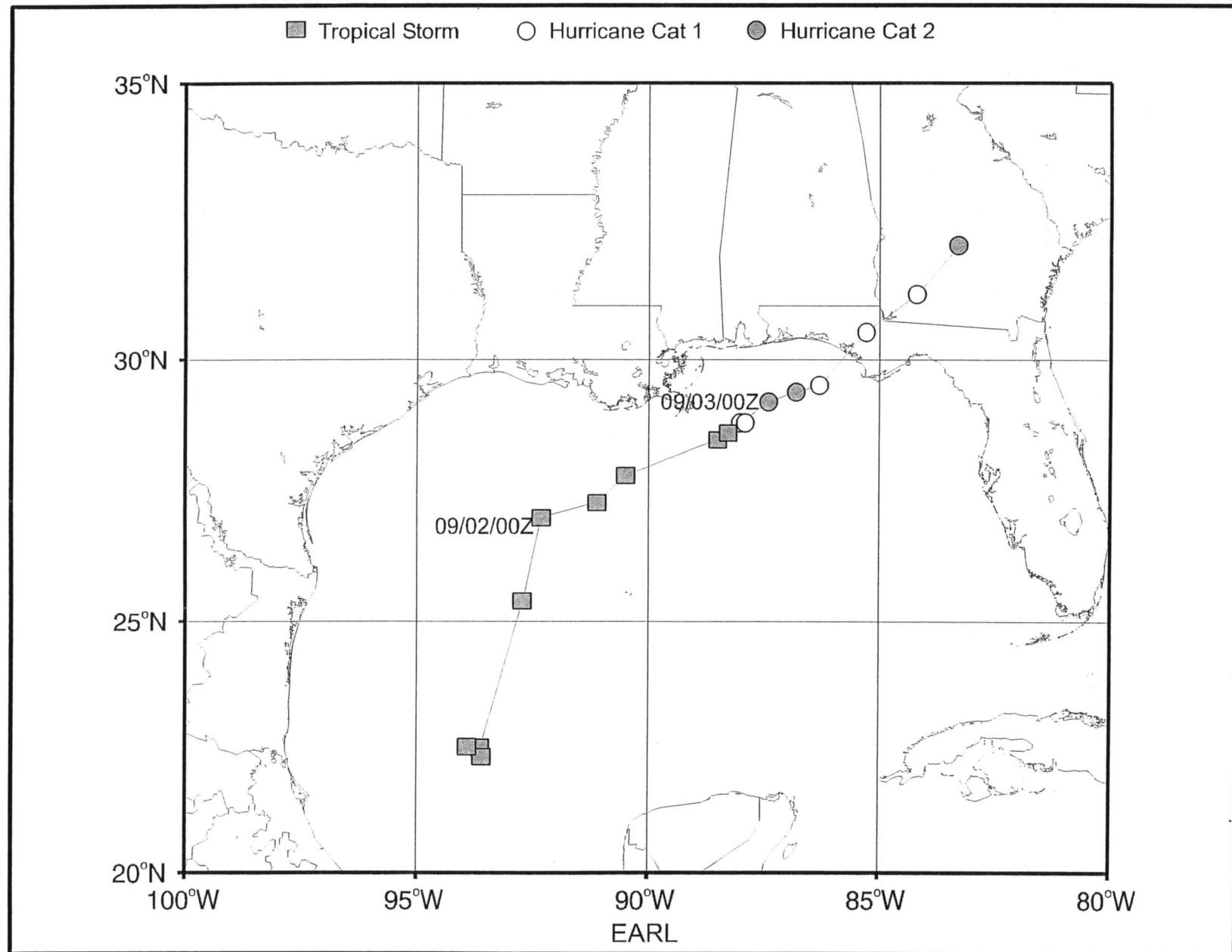
Fig. 7.9. Map showing the path of Hurricane Earl.
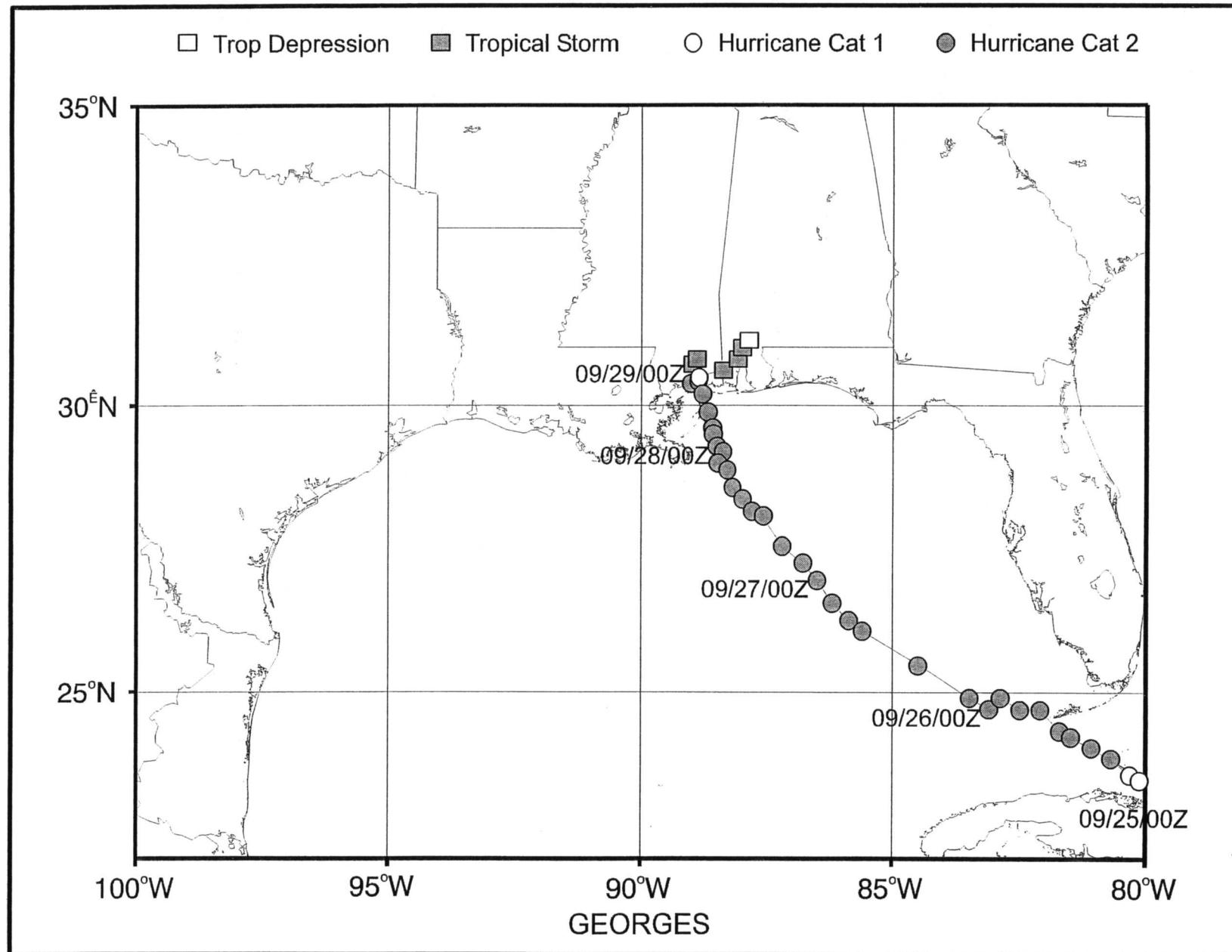
Fig. 7.10. Map showing the path of Hurricane Georges.
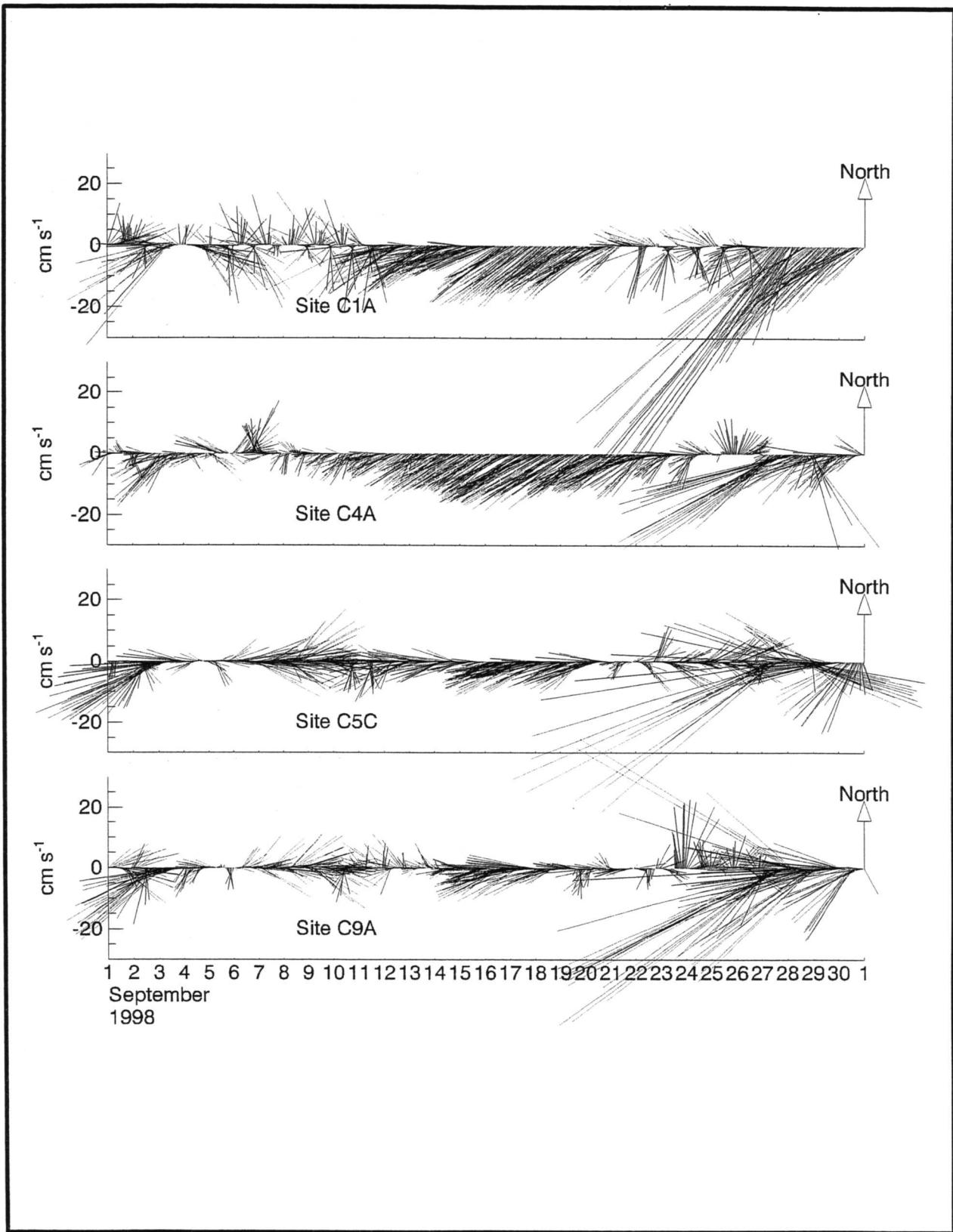
Fig. 7.11. September 1998 stick vector plot of currents recorded at 16 meters above the bottom (mab) at Sites 1, 4, 5, and 9. North is vertically upward, and a scale for the magnitude is in the left side of each panel.

145

intensity forced by Hurricane Georges. Between the two events, an oceanic circulation feature may have intruded onto the shelf. Currents were persistently southwestward during 11-21 September at Sites 1 and 4, with speeds of 15-20 cm/s. This signature was also observed at Site 5 and Site 9 for briefer periods.

The speeds recorded at 4 mab during September 1998 are shown in Fig. 7.12. The response to Hurricane Earl at this depth was strongest at Site 1, reaching about 50 cm/s, and almost nonexistent at Site 4. During Hurricane Georges, the response was strongest at Site 4, reaching 60 cm/s. Since the eye of Georges passed directly over Site 5, a barotropic response to sea level fluctuations is exhibited by the near bottom current. The intrusion event between the hurricanes is most evident at Site 4, where current speed exceeded 20 cm/s for eight days. The effect of the strong bottom currents on sediment during the hurricanes at Site 5 is shown in Fig. 7.13. Only during these events do turbidity values exceed normal background ranges.

Vertical Profiles

CTD casts were taken during each of the monitoring and servicing cruises to assess the vertical profiles of salinity, temperature, PAR, transmissivity, backscattered light, and oxygen concentrations. During the monitoring cruises three profiles were generally taken around each site to assess variability at each site. In general profiles at each site differed very little from one another. Fig. 7.14 summarizes the temperature-salinity relationships for the nine cruises. A composite T-S plot is given for each cruise (Fig. 7.14a-i), and for all casts of all cruises (Fig. 7.14j).

In May 1997 (Fig. 7.14a) salinity reached a maximum of about 36.5, which is typical of the upper waters of much of the Gulf of Mexico. In the upper part of the water column, the profiles at the shallower Sites 5 and 6 exhibited the coolest and freshest water, while the profiles at Sites 7, 8, and 9, which are closest to the Mississippi Delta, showed warmer fresh water. In July 1997 (Fig. 7.14b), all sites show little influence from fresh water. Fresher waters were again present in October 1997 (Fig. 7.14c), and all sites showed evidence of cooling. Colder waters in the upper layers were found at Sites 7, 8, and 9 and, interestingly, at Site 4. Warmer fresher waters were found at the other sites.

By January 1998 (Fig. 7.14d) all water temperatures were below 21C, and maximum salinities also decreased. Bottom salinities at many stations were below 36.0. This correlates well with the lower salinities recorded by the current meters during the third deployment period. In April 1998 (Fig. 7.14e), the upper waters were slightly warmer and much fresher. The freshest water was found at Sites 4, 5, and 6 (lower cluster of points in Fig. 7.14e). Sites 7, 8, and 9 forming the middle cluster on this diagram with lower temperatures and salinities than at Sites 1, 2, and 3.

The annual pattern was repeated during the second year, except in the near surface waters, where salinity variability is large because of the influence of river discharge.

146
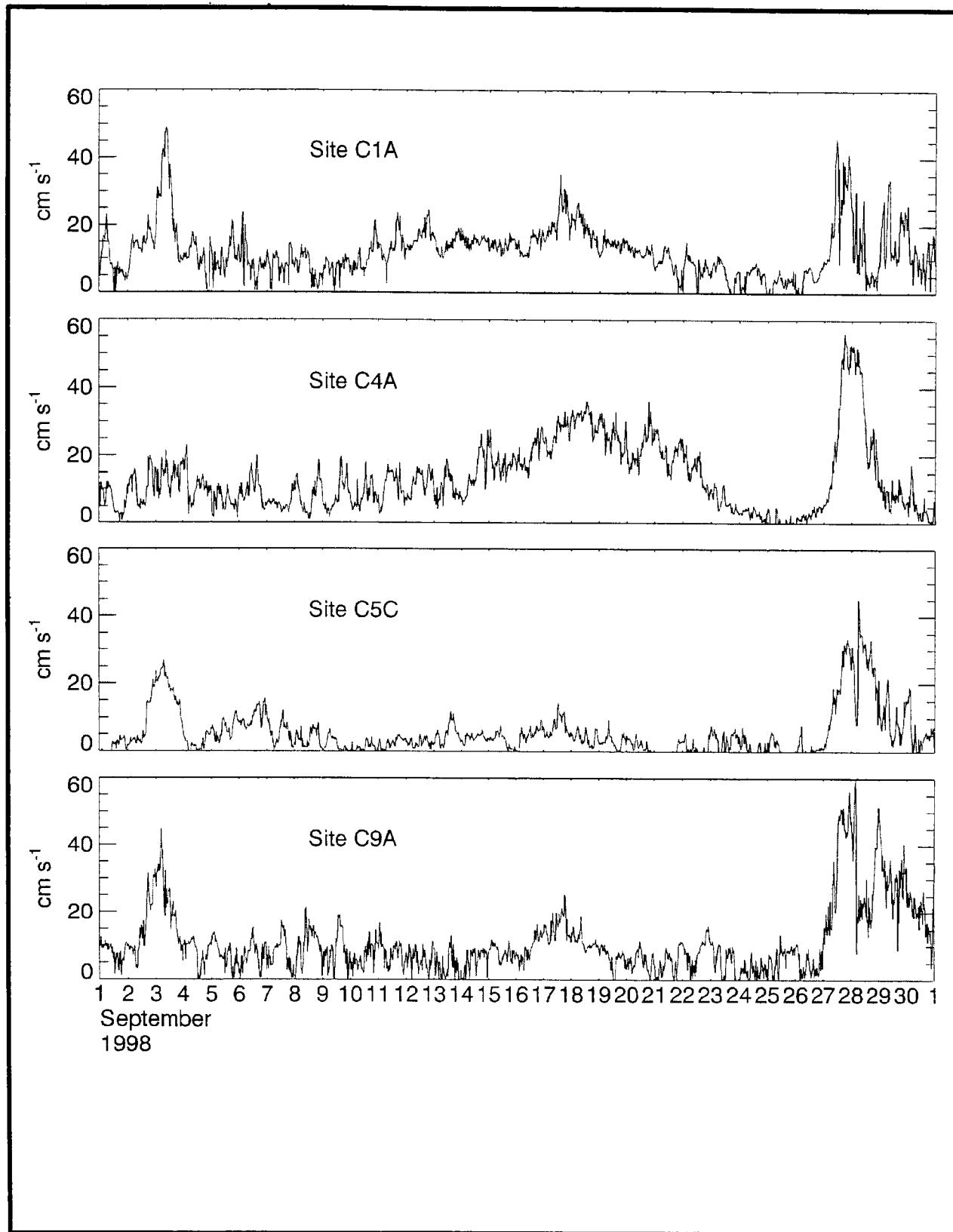
Fig. 7.12. September 1998 current speeds recorded at 4 meters above the bottom (mab) at Sites 1, 4, 5, and 9.

147
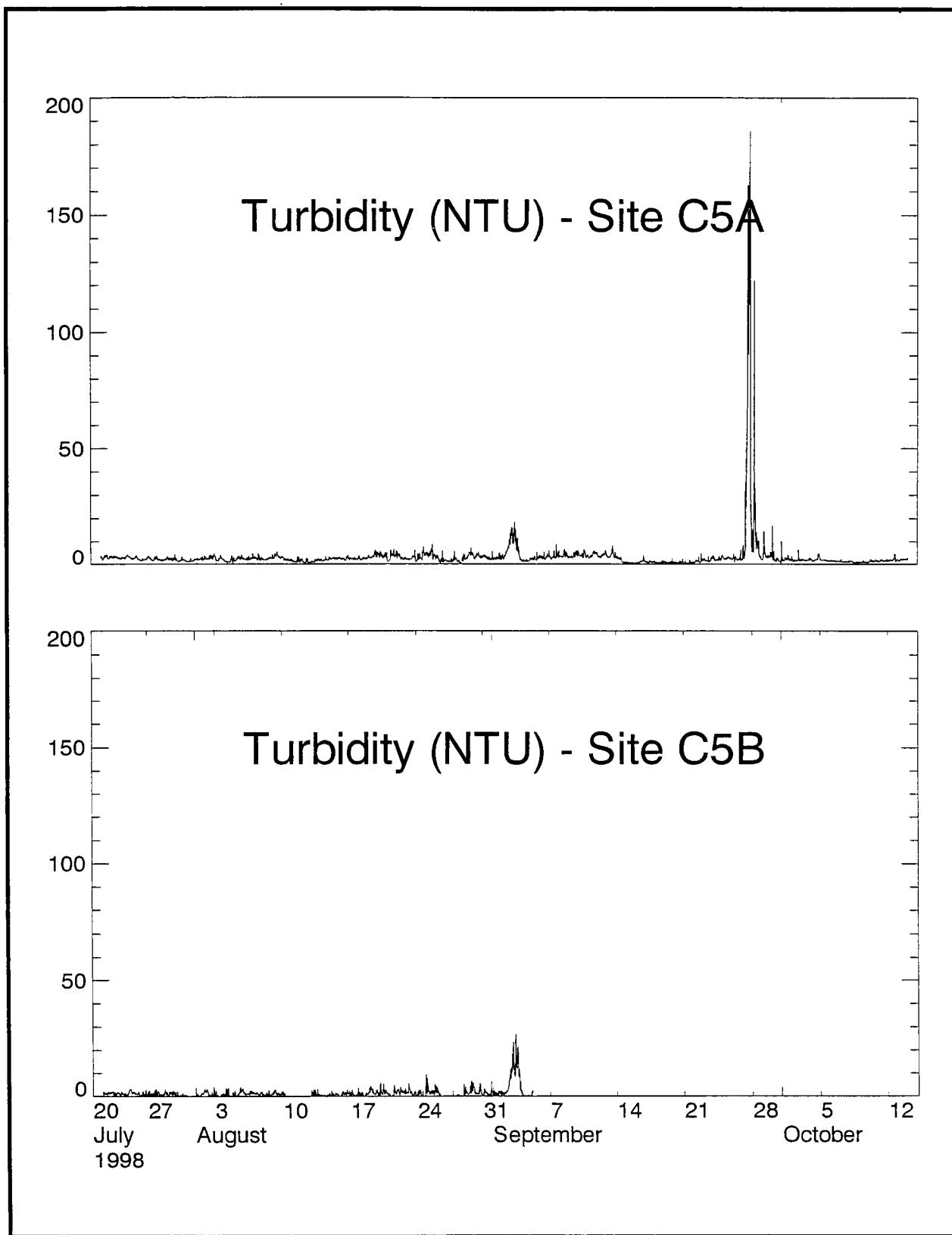
Fig. 7.13. Turbidity (NTU) recorded at Sites 5A and 5B at 2.3 meters above the bottom during 20 July through 14 October 1998.

148
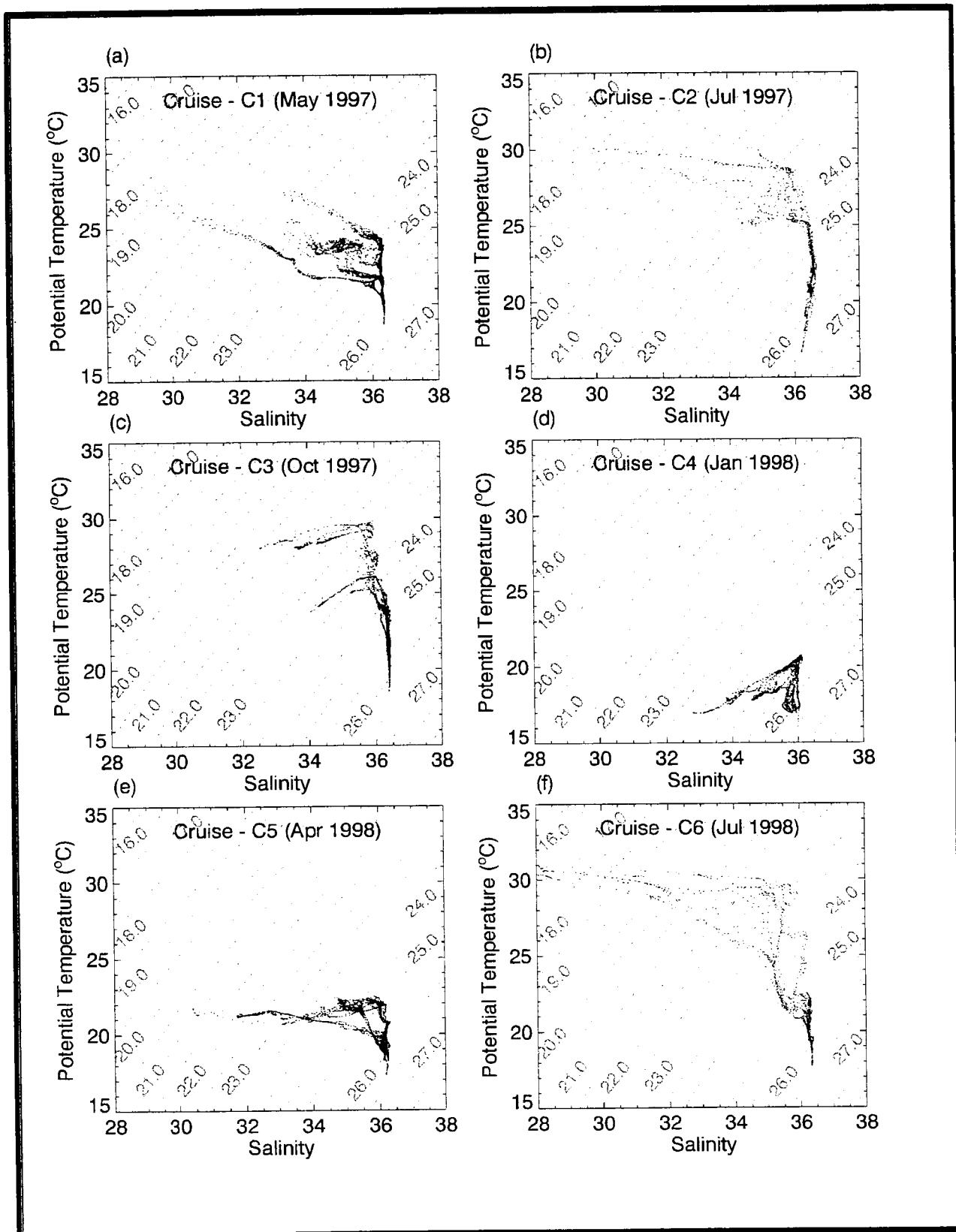
Fig. 7.14. Temperature-salinity (T-S) relationships for the nine cruises thus far in the program. A composite T-S plot is given for each cruise (a-i), and for all casts of all cruises (j).

149
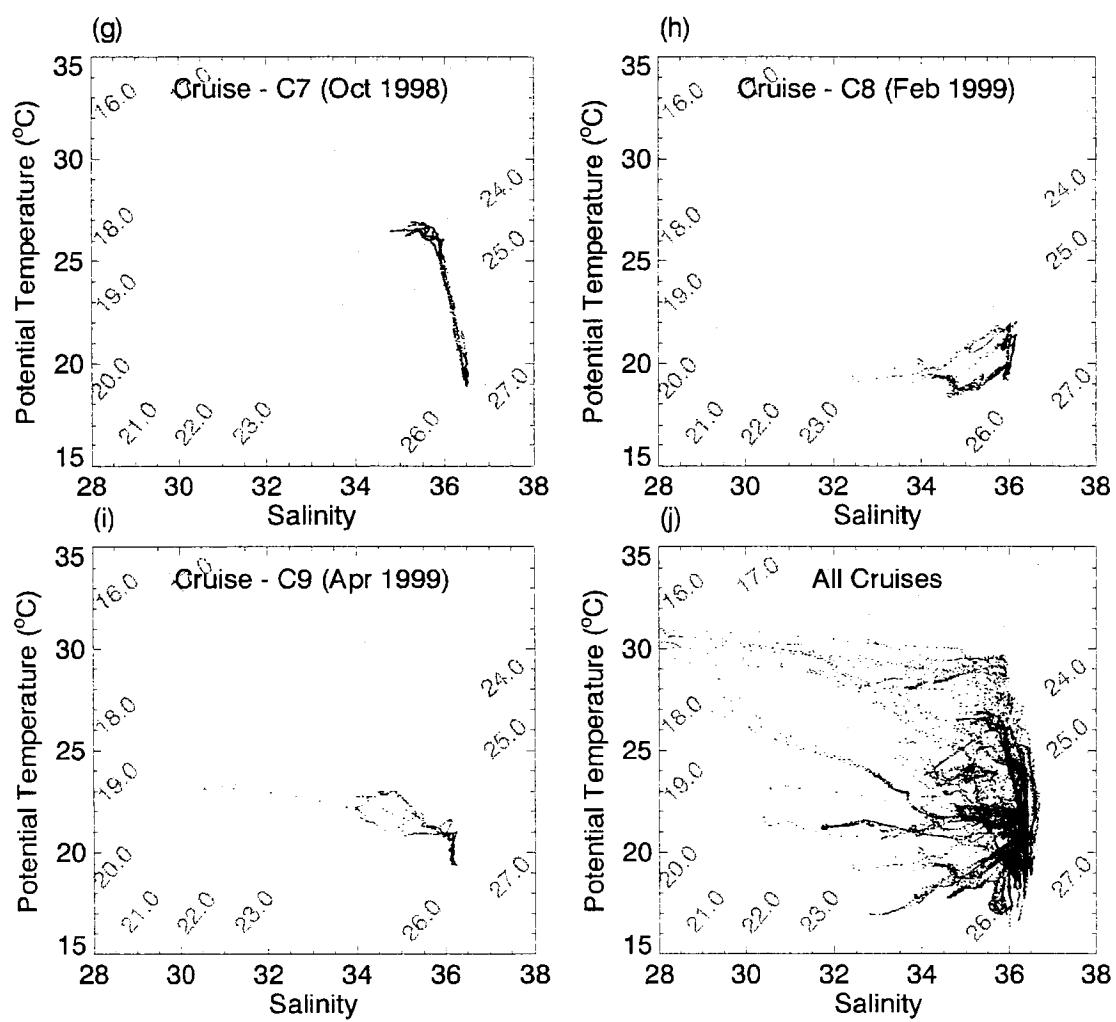
Fig. 7.14. (Continued).

Chapter 8
Hard Bottom Communities

Introduction

Hard bottom communities at greater than 50 m water depth include organisms that are slow growing (Carricart-Ganivet et al. 1994; Mortensen and Rapp 1998; Parker et al. 1997), are long lived (Gili et al. 1989; Parker et al. 1997), and are sensitive to physical disturbance (Hardin et al. 1993). Studies near several offshore petroleum platforms off Point Conception in California (Hyland et al. 1994) measured decreased abundances of some epifaunal species associated with fluxes of drilling muds near the seabed. Observations within the current study region by Gittings et al. (1992) indicated variation in epibiota associated with longitude (proximity to the Mississippi River), vertical relief of hard bottom, and position on hard bottom features possibly related to current exposure and near-bottom fluxes of suspended sediments. Hardin et al. (1994) also found variation in the distribution and abundance of epibiota related to depth, vertical relief of hard bottom features, position on hard bottom features, and flux of suspended sediments. The slow growth and possible sensitivity of hard bottom epibiota to drilling muds and/or suspended sediments suggest the importance of investigating the factors that may control these communities in areas affected by petroleum development, such as the Gulf of Mexico.

Hard bottom communities are being sampled at nine sites by remotely operated vehicle (ROV). Sampling sites were chosen to fall within three categories of relief (i.e., low, medium, and high; see Chapter 2) in three regions from east to west. Site selection was based on data from geophysical surveys and ROV reconnaissance surveys. At each site, random photographs are taken and random video transects are being surveyed during each monitoring cruise. The random photographs are used to estimate the abundances of sessile and motile epibiota, whereas video images are used to quantify larger and more widely dispersed organisms and to broadly characterize substrates and species composition. In addition, fixed video/photoquadrats have been established that are resampled on subsequent cruises to describe temporal changes related to growth, recruitment, competition, and mortality. Voucher specimens are also being collected to aid in species identification. Geological and oceanographic data collected during this program are also used to help interpret and describe hard bottom community dynamics, variation within and among sites, and relationships between the biota and physical variables. This chapter reports preliminary results based on analysis of random photographic samples from Cruise 1C (May 1997) and Cruise M2 (October 1997). Results from the other two monitoring cruises, including fixed photoquadrats, will be presented in the synthesis report.

Field Methods

Field sampling includes qualitative data collection, random photographic stations and video transects, fixed video/photographic stations, and voucher specimen collection. The

ROV being used for field sampling is a Benthos Openframe SeaROVER with a Python multifunction manipulator arm. Video, photographic, and ancillary equipment include a Sony high-resolution video camera, DeepSea Power & Light Micro-SeaCam 2000 color video camera, Photosea 1000 35-mm still camera and strobe, DeepSea Power & Light lasers, and a Simrad MS900 color imaging sonar. The location and track of the ROV on the seabed is determined with a precision acoustic navigation system.

Both qualitative and quantitative video and still photographic data are collected at each site. The ROV is equipped with two independent video camera systems and one still camera system that are used to collect video and still photograph data. One of the video cameras is aimed forward to help maneuver the ROV and collect qualitative video images for identifying substrates, epibiota, and fish. The second video camera and the still camera are used to collect either qualitative or quantitative video and still photographs. These two cameras are aligned to have the same field of view and can be remotely positioned to be perpendicular to the targeted substrate or subject. The second video camera and still camera also allow the scientific observer and ROV pilot to observe the four lasers which are used to determine distance above the bottom and scale within the video and still photographs. Video and photographic data, ROV position, and observations concerning specific features of interest are correlated using the Mission Manager software system (C-Map Systems, Inc.) and written logs.

Due to the small sizes of many of the more abundant species, the camera-to-subject distance for still photographs is set at 60 cm. This is the closest distance from which an in-focus photograph can be taken. This provides the highest resolution possible with the Photosea camera for discerning small biota.

Random Photographic Stations and Video Transects

At each of the nine monitoring sites, the ROV collects video footage and still photographs at pre-selected random locations and along transects between these locations. Prior to the monitoring cruise, 100 locations were randomly selected for each of the nine monitoring sites. These random locations were selected using the digital elevation models for each of the sites that were created from the detailed bathymetric data collected during Cruise 1A.

The results of an analysis of the digital elevation data were considered in determining the size of the nine sites. In this analysis, the standard deviation of the slope magnitude, slope direction, and depth were iteratively calculated for progressively larger areas of each feature, starting at the center of the study site. Plots of these calculated standard deviations versus area were examined to ascertain the areas around the study site central locations over which the standard deviations stabilized. This insured that the variability in elevation that the feature added to the surrounding background elevation was appropriately considered in the site boundary evaluation process.

Each of the nine monitoring sites is defined as a circular area with a site-specific diameter. Each circular site is divided into eight sectors (Fig. 8.1), with 16 points randomly positioned in each sector. The ROV maneuvers between each of the random
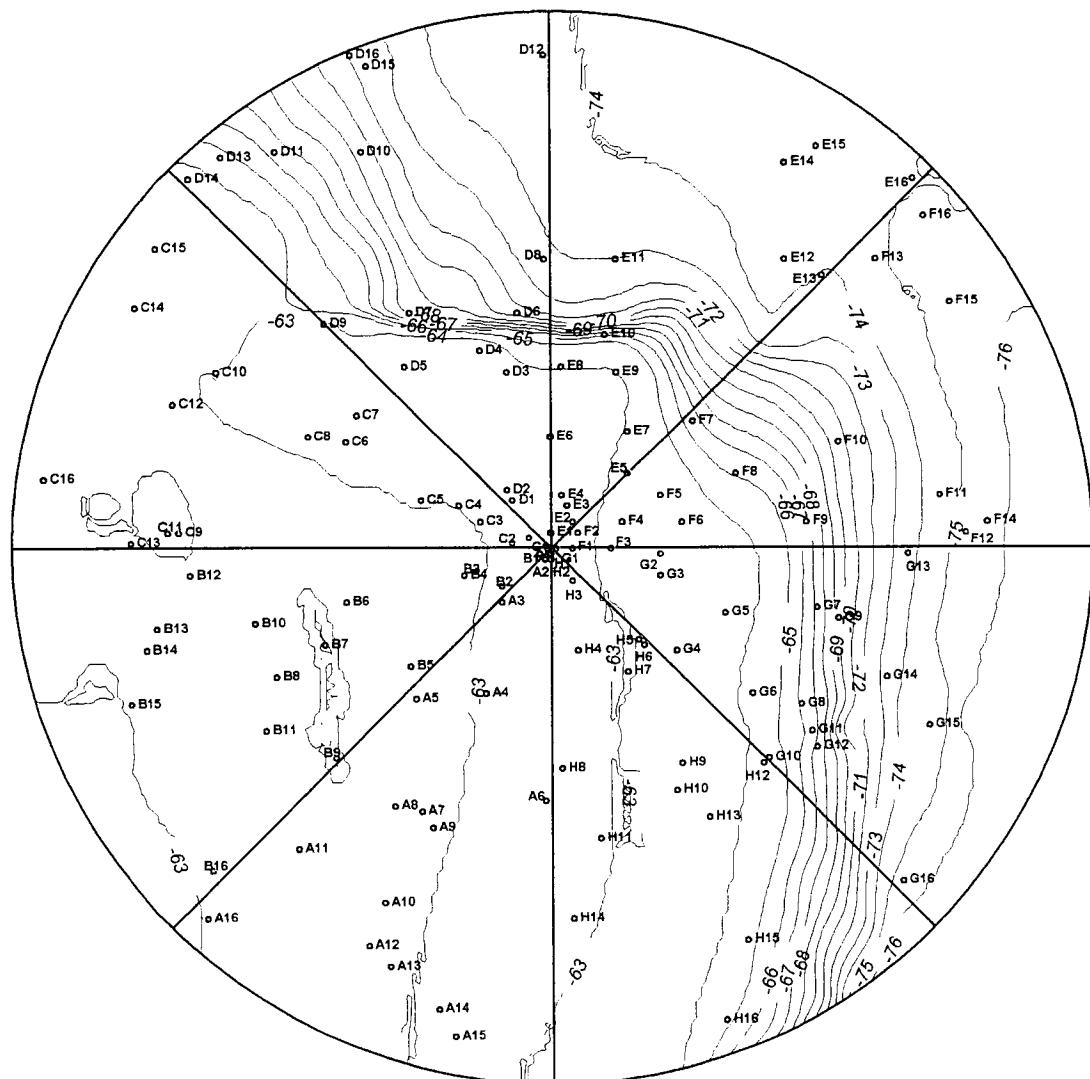
Fig. 8.1. Example of random point allocation within eight sectors of a site. A quantitative photograph was taken at each random point. Qualitative and quantitative video and additional photographs were collected along transects between random points.

153

locations in a sector, collecting a quantitative still photograph with a camera orientation perpendicular to the substrate at each random location. If the random point does not fall on hard substrate, additional random points are sampled until the required number is obtained. Both qualitative and quantitative video data are collected along the transects between each of the random still photo locations, with one video camera (qualitative) aimed ahead for navigating the ROV and the second video camera (quantitative) oriented perpendicular to the substrate. Upon the completion of a sector, the ROV moves to the next adjacent sector and continues collecting video and still photo data until each of the eight sectors are covered. Additional photographs are taken of specific features or biota along the transects to aid in bottom characterization or individual species identifications.

The quantitative video and still cameras are maintained at a specific distance from the bottom by the use of four lasers mounted on the ROV. This laser system consists of three lasers mounted around the video and still cameras with their beams parallel and aimed to fall within the cameras' fields of view. The three lasers are oriented in the shape of an equilateral triangle with the resultant beam pattern providing a constant scale in all video and still photo data. The fourth laser was mounted at a convergent angle to coincide with one of the three parallel lasers when the quantitative video camera and still camera lenses are 60 cm from the bottom. All four lasers are visible to the ROV pilot in the quantitative video camera field of view, enabling him to maneuver the ROV at a constant height above the bottom along the transects.

Voucher Specimen Collection

Epibiota and rock samples are collected when feasible to provide a specimen inventory to aid in the identification of species appearing on video and in photographs and to provide information to help characterize the substrates. Selected specimens are picked up with the ROV's manipulator arm, placed in the sample basket that is lowered to the seabed, and the basket is returned to the surface by the ROV. At the surface the specimens are assigned a unique identification number, photographed, and then labeled and preserved.

Laboratory Methods

Random Photographic Stations and Video Transects

For analysis purposes a replicate video transect consists of a standardized time increment of visually acceptable video data. Time is counted only when the ROV is in motion and remains at the proper distance from the bottom, and when visibility is acceptable. Video images recorded along each replicate transect are reviewed to characterize substrates and determine species composition. Video data are reviewed using an S-VHS videocassette recorder interfaced with a 20-inch color monitor and Mission Manager software system. All recognizable substrate features and epibiota are listed as either present or absent. Biota is identified to the lowest practical taxonomic grouping. Substrate types are separated into the following categories:

- soft bottom;
- hard bottom with a sediment veneer;
- low relief hard bottom;
- medium relief hard bottom (vertical to irregular topography);
- high relief hard bottom (flat-topped); and
- high relief hard bottom (vertical to irregular topography).

Areal coverage of substrate and epibiota within the random quantitative photographs is estimated using the quantitative analysis method developed by Bohnsack (1976, 1979). Each photograph (slide or photo CD image) is analyzed in one of two ways. If using the original slide film, the image is projected onto the 30 cm by 40-cm screen of a slide viewer and a clear acetate overlay containing 50 randomly located points is superimposed on the screen. If using photo CDs made from the original slide film, the stored image is viewed on a high-resolution monitor and a set of 50 randomly generated points is added to the display.

For each analysis method the number of points that covers each taxon and/or substrate type is recorded for each frame or image. The percent coverage of each taxon and substrate type is the percentage of the total points that contact each taxon and substrate type. Since some points may fall on deep shadows and be unreadable, the denominator in the percent cover calculations is reduced by the number of points overlaying shadowed areas. These percentages are combined for all frames from each site to obtain the average percent coverage for each taxon and substrate type. The numbers of individuals of solitary species are also counted and all species that are present in the photographic frame are recorded. The data for point contacts, numbers of individuals, and species presence are directly entered into a computer database for subsequent calculation of percent cover, density, and diversity.

Epifauna such as sponges, hydroids, octocorals, and antipatharians may be attached at a single point and their morphologies are commonly branched above the point of attachment. This morphology creates a canopy effect when viewed from above during quantitative photography. Therefore, the coverage measured for these groups in quantitative photographs is probably more correctly termed "areal cover" rather than percent cover of substrate inhabited by the taxon.

Due to difficulties in taxonomic identification, certain epifauna observed in the photographs are given descriptive names only, which are assigned to specific morphological forms that can be consistently distinguished. Groupings based on specific morphology can result in either overestimation or underestimation of the abundance of the correct species. Conversely, because some descriptive groupings may contain several species that cannot be distinguished from one another, an underestimation of the species richness may result. These uncertainties are unavoidable, and are being minimized by the careful collection and identification of voucher specimens and the construction of the voucher photographic image catalogue.

155

Statistical Analyses

Statistical analyses were performed to expand on the initial broadscale evaluation of the distribution and abundance of epibiota described in the Second Annual Interim Report (Continental Shelf Associates, Inc. and Texas A&M University, Geochemical and Environmental Research Group 1998). These results will help guide future analytical approaches.

Because most of the hard bottom taxa in the study area are colonial, percent cover was usually used as the measure of importance in the statistical analyses. Although colonies were counted, the sizes of colonies may vary from sample to sample and the most accurate indicator of abundance for most colonial organisms is percent cover (i.e., areal cover). Organisms that occur as individuals (e.g., ahermatypic corals) were also counted and analyses of abundances were based on densities (number per m^2) for these organisms.

Statistical procedures included graphical and parametric approaches. Similarities among sites were determined using the Bray Curtis similarity index (Bray and Curtis 1957) calculated from the mean percent cover for a list of taxa composed of the 10 most abundant at each site. The similarities were clustered using an unweighted pair-group method (Swartz 1978). Because habitat relief is an important variable affecting the distributions and abundances of hard bottom organisms, a list was made of the 10 most abundant taxa in each category of habitat relief for both density and percent cover. Those taxa that occurred in the top 10 within a relief category for both measures of importance were then tested with a two-way analysis of variance (ANOVA) (Statview 4.5.1, SAS Institute) to determine the effects of region and relief. The mean percent cover or density from each of the two sampling periods provided the replicate values for estimates of variance within each region x relief cell.

Results

A total of 1,675 random photoquadrats have been analyzed from Cruises 1C and M2 (Table 8.1). All sites had at least 85 random photoquadrats for analysis from each cruise, except for Site 9 in Cruise 1C, where high turbidity resulted in all but six samples being rejected due to poor image quality.

A total of 42 taxa comprise the 10 taxa with the highest mean density at each site (Table 8.2). Cnidaria was the most-represented phylum with 10 taxa of octocorals, five taxa of ahermatypic corals, four taxa of antipatharians, and single taxa of hermatypic corals and actinarians (anemones). Porifera was the next most-represented phylum with seven taxa, followed by Ectoprocta with five taxa. The phylum Echinodermata was represented by three taxa (two crinoids and one echinoid). Algae were represented by two taxa of rhodophyta. The phyla Urochordata and Arthropoda and were represented by single taxa of ascidians, galatheids, respectively.

Hard bottom community composition revealed by the percent cover data was slightly different from that revealed by the density data. There were 40 taxa comprising the 10

Table 8.1. Physical characteristics and number of random photographs analyzed for each hard bottom site.

	Site 1	Site 2	Site 3	Site 4	Site 5	Site 6	Site 7	Site 8	Site 9
Depth Range (m)	63-76	69-81	76-80	95-107	62-78	75-78	69-88	88-96	89-95
Depth – Midpoint of Depth Range (m)	69	75	78	101	70	77	79	92	92
Region	East	East	East	Central	Central	Central	West	West	West
Relief Category	High	Medium	Low	Medium	High	Low	High	Medium	Low
Approx. Distance from Miss. Delta (km)	145	142	145	126	105	105	70	72	71
Mean Flux of Susp. Sediment $(g/m^2/day)^a$	4.02	--	--	5.70	12.97	--	--	--	14.10
Number of Photographs Analyzed:									
Cruise 1C	98	99	85	102	102	99	101	98	6
Cruise M2	100	100	96	100	89	100	100	100	100

[a] The average flux among the sediment traps occurring within the depth range for the four sites at which traps were deployed (see Chapter 5). The averages of all three sediment trap depths (i.e., 2.5, 7, and 15 meters above bottom [mab]) were used for Sites 1, 4, and 5, and the averages of sediment traps from 2.5 and 7 mab were used for Site 9. Sediment trap data for the period affected by Hurricane Georges were not included in the calculations.

Table 8.2. Dominant epibiota at hard bottom sites, as measured by mean density (number/m^2) over two sampling cruises (1C and M2), ordered according to overall mean density. Taxa that were marked present but not counted for either of the two cruises were given a default density of 0.01/m^2 for calculating these means.

Taxa	Group[a]	Site 1	Site 2	Site 3	Site 4	Site 5	Site 6	Site 7	Site 8	Site 9	Overall
Rhizopsammia manuelensis	Aherm.	2.05	197.55	14.79	178.83	448.83	47.45	510.54	635.39	309.26	261.68
Scleractinia (solitary)	Aherm.	0.63	10.41	6.06	2.30	45.18	22.29	6.09	30.89	10.30	14.72
Stenogorgiinae	Octo.	5.99	5.03	4.65	1.26	3.01	2.41	0.87	6.25	2.95	3.94
Nicella sp. A	Octo.	8.94	2.42	1.98	5.34	0.03	0	1.06	6.20	1.94	3.05
Ellisella spp.	Octo.	5.57	0.94	1.99	4.33	0.14	0.67	0.51	3.15	2.73	2.27
Bryozoa	Ecto.	2.44	1.69	0.96	0.74	2.09	3.42	3.55	0.28	0.36	1.79
Antipathes ?furcata	Antipath.	0.11	0.45	0.89	13.08	0.18	0.15	0.21	0.75	0.70	1.77
Crinoidea -10 arm	Crinoid	0	0.11	0.98	5.52	0.39	0	5.18	0.26	0	1.43
?Paracyathus pulchellus	Aherm.	0.26	0.56	0.33	0	7.30	1.18	0	2.91	0	1.41
Galatheidae	Galath.	0.05	6.23	0.62	0.02	0.02	4.45	0.19	0.31	0.64	1.34
Bebryce cinerea/grandis	Octo.	1.79	0.81	0.64	0.88	0.04	3.15	1.34	0.74	1.91	1.30
Thesea sp. (white)	Octo.	0.94	0.05	0.10	0.15	0.31	8.31	0.07	0.24	0.09	1.15
Porifera (yellow encrusting)	Porif.	0.01	0.01	0.12	0.93	0.01	0.01	4.53	0.01	4.62	1.13
?Didemnidea	Ascid.	0.09	0.22	1.07	1.53	0.03	0.57	1.44	0.05	4.97	1.01
Madrepora carolina	Herm.	0	0.86	1.04	2.00	0.85	0.11	0	0.97	0.70	0.82
Scleractinia (large solitary)	Aherm.	0	0	0.17	4.21	0.24	0.24	0.19	0.58	1.71	0.81
?Idmidronea sp.	Ecto.	0.70	0.32	0.27	0	0.84	5.29	0	0	0	0.81
Hydroida	Hydroid	0.25	0.38	0.83	0.80	1.22	0.31	2.62	0.66	0.36	0.77
Thesea sp. (red)	Octo.	0	0.60	1.12	0.13	0.23	0.54	0.28	1.64	2.19	0.76
Madracis myriaster	Aherm.	0.02	0.71	0.66	0.63	2.19	0.07	0.64	0.76	0.43	0.71
Stylocidaris affinis	Echinoid	0.15	0.15	0.18	0.20	1.52	0.07	1.14	2.33	0.43	0.70
Stylopoma spongites	Ecto.	0.34	2.83	0.01	0.01	0.13	1.58	0.01	0.77	0.01	0.63
Porifera (orange - encrusting)	Porif.	0.01	0.01	0.17	0.01	0.01	0.01	3.42	0.33	1.78	0.62
Antipathes spp.	Antipath.	0.02	1.20	0.17	1.09	0.79	0.17	0.66	0.41	0.58	0.58
Porifera (yellow - boring)	Porif.	0	0.01	0.17	0.32	0	0	4.64	0	0	0.55
Placogorgia/Paramuricea sp.	Octo.	0	0.43	0.30	0.92	0.19	0.71	0.26	1.49	0.26	0.51

Table 8.2. (continued).

Taxa	Group[a]	Site 1	Site 2	Site 3	Site 4	Site 5	Site 6	Site 7	Site 8	Site 9	Overall
Antipathes atlantica/gracilis	Antipath.	0	0.64	0.13	0	0.96	0.20	1.35	0.13	0.02	0.40
Dysidea sp.	Porif.	3.23	0.05	0	0	0	0	0	0	0.01	0.36
Peyssonnelia spp.	Rhodo.	0.01	0.01	0.63	0	0	0	3.15	0	0	0.35
Crinoidea	Crinoid	1.31	0.49	0.97	0	0	0	0	0	0	0.34
Swiftia exserta	Octo.	0.13	0.02	0.79	0.26	0.51	0	0.76	0.05	0.41	0.31
Stichopathes ?lutkeni	Antipath.	0.07	0.88	0.55	0.02	0.18	0.09	0.45	0.15	0.05	0.31
?Ciolcalapata gibbsi	Porif.	2.44	0	0.40	0	0	0	0	0	0	0.29
?Cellaria sp.	Ecto.	0.91	0.20	0.32	0	0.13	0.67	0	0	0	0.28
Porifera (amorphous - indistinct)	Porif.	0.53	0.84	0.10	0.02	0.17	0.39	0.07	0.42	0	0.27
Thesea/Scleracis sp.	Octo.	0	0.02	0.18	0.68	0	0.02	0.44	0	0.64	0.22
Zoantharia	Actin.	0.07	0.02	0.11	0.07	0.03	0.05	0.15	1.30	0	0.21
Rhodophyta	Rhodo.	1.17	0.01	0.01	0	0	0.00	0	0	0	0.13
Homotrema rubrum	Foram.	0.01	0.01	0.04	0.19	0.01	0.01	0	0.01	0.71	0.11
Porifera (yellow - amorphous)	Porif.	0.26	0.60	0.17	0	0	0.02	0	0	0.01	0.10
?Reteporellina evelinae	Ecto.	0.03	0.02	0.23	0	0	0.59	0	0	0	0.10
Thesea sp. (violet)	Octo.	0.02	0.22	0.20	0	0.03	0.34	0	0	0.02	0.09
Total density for dominant taxa	All	40.46	237.93	44.40	226.40	517.70	105.45	555.73	699.38	350.71	310.14
Total density for dominant ahermatypic corals	Aherm.	2.95	209.22	23.43	185.96	503.72	71.22	517.45	670.53	321.69	279.33
Total density for dominant octocorals	Octo.	23.37	10.52	8.72	13.93	4.46	16.14	5.56	19.74	13.11	13.60
Total density for dominant antipatharians	Antipath.	0.20	3.17	1.08	14.19	2.11	0.60	2.67	1.44	1.34	3.06
Total density for dominant poriferans	Porif.	6.46	1.50	1.48	1.27	0.19	0.43	12.65	0.76	6.41	3.33
Total density for dominant ectoprocts	Ecto.	4.41	5.05	5.29	0.74	3.18	11.53	3.56	1.05	0.37	3.61

[a] = Aherm. = ahermatypic coral, Octo. = octocoral, Ecto. = ectoproct, Antipath. = antipatharian, Galath. = galatheid, Porif. = poriferan, Ascid. = ascidian, Herm. = hermatypic coral, Rhodo. = rhodophyta.

taxa with the highest mean percent cover at each site (Table 8.3). Cnidaria was again the most-represented phylum with 10 taxa of octocorals, four taxa of antipatharians, three taxa of ahermatypic corals, and a single taxon of hermatypic corals. Porifera was again the second most-represented phylum with six taxa, followed by Echinodermata with four. Ectoprocta and Rhodophyta each had three taxa and the phyla Urochordata and Arthropoda were again represented by single taxa of ascidians, and galatheids, respectively. There was a single vertebrate taxon recorded in the percent cover data.

Although octocorals were represented by the most taxa in both density and percent cover data, ahermatypic corals had the highest mean abundances with 279.33 organisms per m^2 and 5.62 percent cover over all sites, due to the dominance of *Rhizopsammia manuelensis* (Table 8.2 and Table 8.3). Octocorals had the second highest mean density and percent cover over all sites with 13.60 per m^2 and 3.00 percent cover. The relative ranking of antipatharians, poriferans, and ectoprocts varied between density and percent cover data.

The aggregate percent cover data for major groups represented by the 40 most abundant taxa suggest substantial variation among sites (Table 8.3). Mean percent cover for ahermatypic corals ranged from 0.03 at Site 1 to 10.96 at Site 7. Mean percent cover for antipatharians were also quite variable among sites, ranging from 0.04 at Site 1 to 16.18 at Site 4. High coverage by antipatharians at Site 4 led to high overall percent cover at that site. Octocorals, poriferans, and ectoprocts displayed relatively less variation among sites.

Despite the high variation among sites, there was little difference between sampling times (Fig. 8.2). Only at Site 6 was there a noticeable difference between Cruises 1C and M2, with an apparent large reduction in the coverage of ectoprocts between Cruise 1C and Cruise M2. Abundances at high relief site (Sites 1, 5, and 7) were neither obviously greater nor more diverse than at sites with lower relief.

The high variation among sites resulted in generally low similarities (Fig. 8.3). One cluster was composed of all the sites from the west region (Sites 7, 8, and 9) plus the high-relief site from the central region (Site 5). These sites shared high abundances of ahermatypic corals, principally *Rhizopsammia manuelensis* (Table 8.3 and Fig. 8.2). Although the medium and low relief sites from the east region (Sites 2 and 3) clustered weakly with each other and the first cluster, the similarity was probably due to the moderate abundances of octocorals at all six sites.. The medium and low relief sites from the central region (Sites 4 and 6) and the high relief site from the east region (Site 1) were not very similar to any other sites. Site 4 was notable for its high abundances of antipatharians, Site 6 had relatively high abundances of ectoprocts, and Site 1 had very low abundances of *R. manuelensis*.

Little of the biological variation among sites is apparently due to consistent effects of habitat relief. Some taxa occurred in high abundances in all relief categories and others varied inconsistently among relief categories (Table 8.4). *Rhizopsammia manuelensis* dominated all relief categories for both percent cover and density, although it was more abundant in medium and high relief than in low relief. The solitary scleractinian had

160

Table 8.3. Dominant epibiota at hard bottom sites, as measured by mean percent cover over two sampling cruises (1C and M2), ordered according to overall mean percent cover.

Taxa	Group[a]	Site 1	Site 2	Site 3	Site 4	Site 5	Site 6	Site 7	Site 8	Site 9	Overall
Rhizopsammia manuelensis	Aherm.	0.03	3.43	0.59	4.55	9.51	1.16	10.83	9.92	9.15	5.46
Antipathes ?furcata	Antipath.	0	0.52	0.38	15.71	0.08	0.02	0.50	0.59	1.45	2.14
Stenogorgiinae	Octo.	1.34	0.49	1.28	0.40	1.03	0.67	0.39	1.59	0.79	0.88
Nicella sp. A	Octo.	2.21	0.49	0.26	1.02	0.01	0	0.39	2.32	1.05	0.86
Porifera	Porif.	3.54	0.45	0.46	0.10	0.23	0.09	0.82	0.17	0.50	0.70
Crinoidea	Crinoid	1.01	0.38	0.29	2.23	0.04	0	2.18	0.10	0	0.69
Antipathes atlantica/gracilis	Antipath.	0	0.63	0.31	0	1.23	0.17	1.31	0.24	0.01	0.43
Bebryce cinerea/grandis	Octo.	0.33	0.20	0.22	0.23	0	1.34	0.34	0.18	1.06	0.43
Crinoidea - 10 arm	Crinoid	0	0.03	0.62	2.07	0	0	0.89	0.17	0	0.42
Bryozoa	Ecto.	0.76	0.28	0.22	0.08	0.45	1.35	0.42	0.01	0.04	0.40
Hydroida	Hydroid	0.32	0.05	0.15	0.12	0.80	1.36	0.50	0.22	0.09	0.40
Ellisella spp.	Octo.	0.53	0.40	0.38	0.71	0.02	0.13	0.07	0.86	0.46	0.39
?Idmidronea sp.	Ecto.	0.02	0.08	0.28	0.01	0.09	2.69	0	0.01	0	0.35
Antipathes spp.	Antipath.	0.04	0.34	0.33	0.47	0.55	0.18	0.11	0.22	0.18	0.27
Corallinaceae	Rhodo.	1.01	0.96	0.06	0	0.02	0	0.32	0	0	0.26
Swiftia exserta	Octo.	0.25	0	0.32	0.20	0.71	0	0.22	0.05	0.23	0.22
Rhodophyta	Rhodo.	1.49	0	0.30	0	0	0	0	0	0	0.20
?Astrocyclus caecilia	Ophiuroid	0.01	0.08	0.30	0.42	0.02	0	0.03	0.23	0.68	0.19
Peyssonnelia spp.	Rhodo.	1.21	0.03	0	0	0	0	0.16	0	0	0.16
Madracis myriaster	Aherm.	0	0.13	0.22	0.15	0.46	0	0.12	0.03	0.11	0.13
Porifera (yellow - encrusting)	Porif.	0	0.21	0.42	0.04	0.10	0.03	0	0	0.16	0.11
Osteichthyes	Vert.	0.23	0.07	0.06	0	0.10	0.10	0.07	0.13	0	0.08
Stylopoma spongites	Ecto.	0	0.14	0.31	0.01	0.02	0.18	0.05	0	0.01	0.08
Madrepora carolina	Herm.	0	0.10	0.19	0.10	0.13	0.03	0	0.07	0.08	0.08
Diadema antillarum	Echinoid	0	0.07	0.34	0.03	0	0	0.11	0.01	0.09	0.07
Thesea/Scleracis sp.	Octo.	0	0.04	0.26	0.17	0	0	0	0	0.16	0.07

161

Table 8.3. (continued).

Taxa	Group	Site 1	Site 2	Site 3	Site 4	Site 5	Site 6	Site 7	Site 8	Site 9	Overall
Stylocidaris affinis	Echinoid	0.01	0	0.02	0.03	0.17	0	0.10	0.24	0.05	0.07
Ulosa sp.	Porif.	0.61	0	0	0	0	0	0	0	0	0.07
Porifera (white - encrusting)	Porif.	0	0	0.26	0.06	0.22	0.05	0	0	0	0.07
?Didemnidae	Ascid.	0	0	0.09	0.11	0.01	0.07	0.12	0.01	0.17	0.06
Stichopathes ?lutkeni	Antipath.	0	0.10	0.29	0	0.01	0.03	0.09	0.02	0	0.06
Pseudoceratina crassa	Porif.	0.16	0	0	0	0	0	0.30	0	0	0.05
Hypnogorgia pendula	Octo.	0	0.03	0	0	0.02	0	0	0.18	0.22	0.05
Porifera (orange - encrusting)	Porif.	0	0.11	0.14	0.02	0.02	0.06	0	0	0	0.04
Placogorgia/Paramuricea sp.	Octo.	0	0.07	0.03	0.09	0	0.05	0	0	0.10	0.04
Siphonogorgia agassizii	Octo.	0	0.01	0	0.01	0	0	0	0.02	0.24	0.03
Scleractina (solitary)	Aherm.	0	0.01	0.01	0.06	0	0.06	0.02	0.03	0.06	0.03
Thesea sp. (violet)	Octo.	0	0	0	0	0.01	0.18	0	0	0.01	0.02
Galatheidae	Galath.	0	0.05	0	0	0	0.09	0	0.01	0	0.02
Crinoidea - 20 arm	Crinoid	0	0.04	0	0.03	0	0	0	0.06	0	0.01
Total percent cover of dominant taxa	All	15.09	9.95	9.31	29.17	16.02	10.06	20.43	17.64	17.12	16.09
Total percent cover of dominant ahermatypic corals	Aherm.	0.03	3.57	0.82	4.75	9.97	1.22	10.96	9.98	9.32	5.62
Total percent cover of dominant octocorals	Octo.	4.66	1.71	2.74	2.81	1.80	2.37	1.41	5.19	4.31	3.00
Total percent cover of dominant anthpatharians	Antipath.	0.04	1.59	1.30	16.18	1.87	0.40	2.01	1.06	1.64	2.90
Total percent cover of dominant poriferans	Porif.	4.31	0.76	1.27	0.22	0.56	0.23	1.11	0.17	0.66	1.03
Total percent cover of dominant ectoprocts	Ecto.	0.78	0.50	0.80	0.10	0.56	4.21	0.47	0.02	0.05	0.83

[a] = Aherm. = ahermatypic coral, Antipath. = antipatharian, Octo. = octocoral, Porif. = poriferan, Ecto. = ectoproct, Rhodo. = rhodophyta, Vert. = vertebrate, Herm. = hermatypic coral, Ascid. = ascidian, Galath. = galatheid.

162
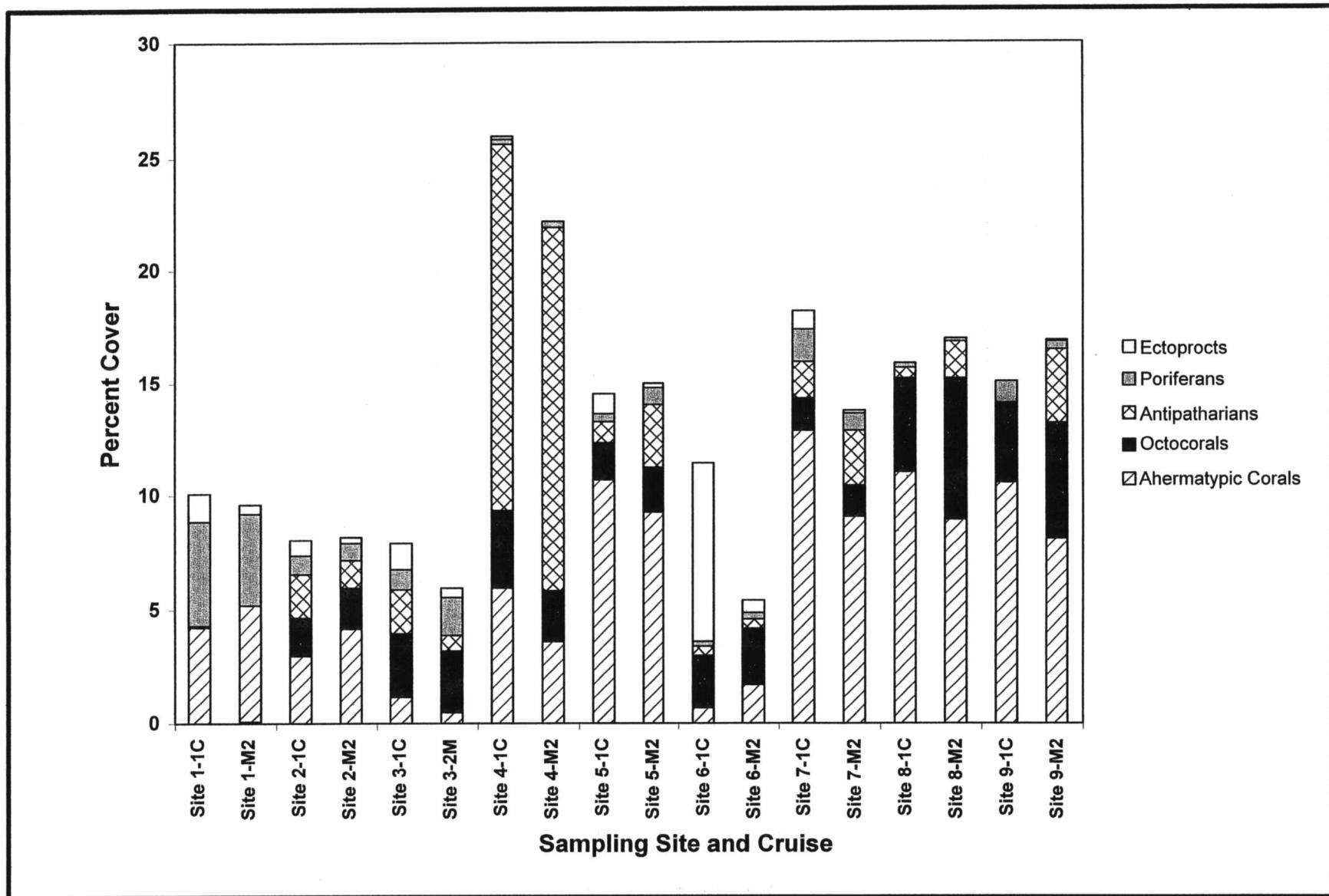
Fig. 8.2. Mean percent cover of the most abundant hard bottom taxa in five major taxonomic groups for sampling each site and cruise.
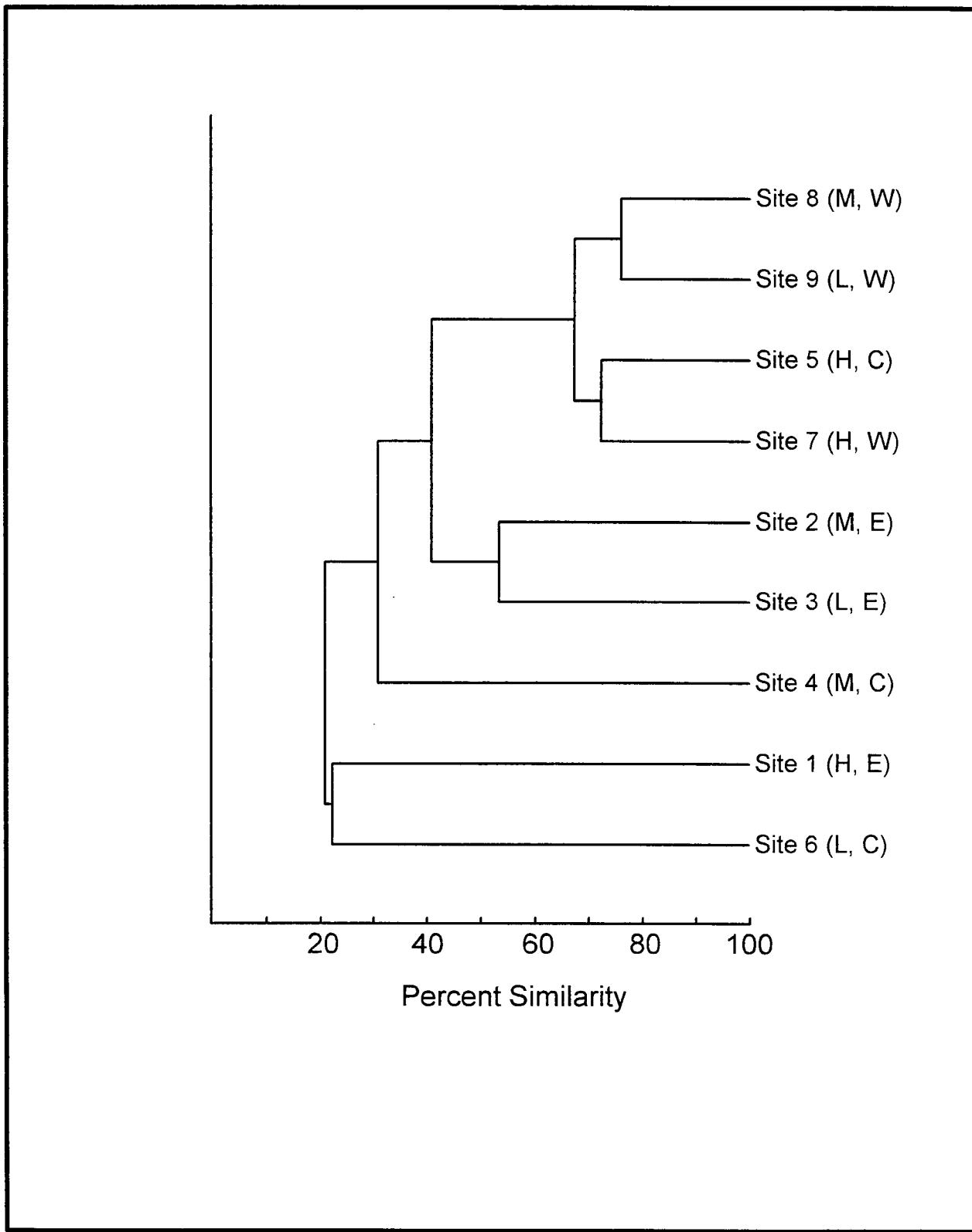
Fig. 8.3. Clusters of similarities among hard bottom sampling sites calculated from mean percent cover data for the 40 most abundant taxa using the Bray Curtis similarity index and the unweighted pair-group clustering method. Site qualifiers refer to habitat relief and region, as follows: L = low relief, M = medium relief, H = high relief, W = west, C = central, E = east.

Table 8.4. Dominant taxa in each category of hard bottom habitat relief, as measured by mean percent cover and mean density (number/m^2).

Taxa	Group[a]	Low Relief Mean	Taxa	Group[a]	Medium Relief Mean	Taxa	Group[a]	High Relief Mean
Percent Cover								
Rhizopsammia manuelensis	Aherm.	3.63	*Rhizopsammia manuelensis*	Aherm.	5.96	*Rhizopsammia manuelensis*	Aherm.	6.79
?Idmidronea sp.	Ecto.	0.99	*Antipathes ?furcata*	Antipath.	5.60	Porifera	Porif.	1.53
Stenogorgiinae	Octo.	0.91	*Nicella* sp. A	Octo.	1.27	Crinoidea	Crinoid	1.08
Bebryce cinerea/grandis	Octo.	0.87	Crinoidea	Crinoid	0.90	Stenogorgiinae	Octo.	0.92
Antipathes ?furcata	Antipath.	0.62	Stenogorgiinae	Octo.	0.82	*Nicella* sp. A	Octo.	0.87
Bryozoa	Ecto.	0.54	Crinoidea - 10 arm	Crinoid	0.76	*Antipathes atlantica/gracilis*	Antipath.	0.85
Hydroida	Hydroid	0.53	*Ellisella* spp.	Octo.	0.65	Bryozoa	Ecto.	0.54
Nicella sp. A	Octo.	0.43	*Antipathes* spp.	Antipath.	0.34	Hydroida	Hydroid	0.54
Porifera	Porif.	0.35	Corallinaceae	Rhodo.	0.32	Rhodophyta	Rhodo.	0.50
?Astrocyclus caecilia	Ophiuroid	0.32	*Antipathes atlantica/gracilis*	Antipath.	0.29	*Peyssonnelia* spp.	Rhodo.	0.46
Density								
Rhizopsammia manuelensis	Aherm.	123.83	*Rhizopsammia manuelensis*	Aherm.	337.26	*Rhizopsammia manuelensis*	Aherm.	320.47
Scleractinia (solitary)	Aherm.	12.88	Scleractinia (solitary)	Aherm.	14.53	Scleractinia (solitary)	Aherm.	17.30
Stenogorgiinae	Octo.	3.33	*Antipathes ?furcata*	Antipath.	4.76	*Nicella* sp. A	Octo.	3.34
Thesea sp. (white)	Octo.	2.83	*Nicella* sp. A	Octo.	4.65	Stenogorgiinae	Octo.	3.29
?Didemnidea	Ascid.	2.20	Stenogorgiinae	Octo.	4.18	Bryozoa	Ecto.	2.69
Bebryce cinerea/grandis	Octo.	1.90	*Ellisella* spp.	Octo.	2.80	*?Paracyathus pulchellus*	Aherm.	2.52
Galatheidae	Galath.	1.90	Galatheidae	Galath.	2.19	*Ellisella* spp.	Octo.	2.07
?Idmidronea sp.	Ecto.	1.85	Crinoidea -10 arm	Crinoid	1.96	Crinoidea -10 arm	Crinoid	1.86
Ellisella spp.	Octo.	1.80	Scleractinia (large solitary)	Aherm.	1.60	Porifera (yellow - boring)	Porif.	1.55
Bryozoa	Ecto.	1.58	*Madrepora carolina*	Herm.	1.28	Porifera (yellow encrusting)	Porif.	1.52

[a] = Aherm. = ahermatypic coral, Ecto. = ectoproct, Octo. = octocoral, Antipath. = antipatharian, Porif. = poriferan, Galath. = galatheid, Rhodo. = rhodophyta, Ascid. = ascidian, Herm. = hermatypic coral

165

second highest densities in each relief category and did not differ appreciably among categories. None of the other dominant taxa in any of the relief categories varied among categories consistent with an effect of relief.

ANOVAs for the effects of relief and region revealed numerous significant effects of each factor, but very few were absent significant interactions (Table 8.5), indicating that the effects of relief differed among regions. Moreover, only the significant relief effects on the cover of all taxa suggested a possible gradient of percent cover from high relief to low relief. Only the effect of region on the densities of *Rhizopsammia manuelensis* and all ahermatypic corals combined suggested a gradient from west to east. The significant relief x region interaction for densities of the 10-armed crinoid revealed highest abundances occurred on progressively higher relief moving from east to west (Fig. 8.4), suggesting a possible response to higher near-bottom sediment fluxes in the west region (see Table 8.1).

Discussion

The paucity of significant effects of habitat relief substantiates preliminary results reported in the Second Annual Interim Report (Continental Shelf Associates and Texas A&M University, Geochemical and Environmental Research Group 1998). These results contradict those of Pequegnat (1964), Genin et al. (1986), Messing et al. (1990), Gittings et al. (1992), and Hardin et al. (1994), all of which indicated higher organism abundances with increasing habitat relief. The analytical approach that was taken for this report could obscure such relationships by incorporating substantial physical variation into each site due to the large size, complex topography, and vertical relief of the hard bottom features. Large ranges of potentially important physical variables such as distance above unconsolidated seabed, exposure to currents, slope, and topographic variation affecting sedimentation exist within each site; the physical and biological variations within sites may be nearly as large as those between sites. Therefore, an important objective in future analyses will be to account for this within-site variation. Nevertheless, while it is likely that physical variables affect the distribution and abundances of hard bottom biota on scales smaller than the defined sampling sites, it is puzzling that the data reveal so few possible effects on broader scales.

Future analyses will utilize the expanding database to address these unanswered questions. For instance, inverse similarity calculations using station means will help describe assemblages of taxa that may provide more fruitful groupings for discerning possible effects of habitat relief, sediment flux, current speed, current direction, and distance from the Mississippi River on the distribution and abundances of organisms. Ordination and classification analyses may also be used to explore patterns and structure in the biological data and to identify species groupings for further analysis. Strong relationships between biological groupings and physical variables also may be identified through discriminant analysis and canonical correlation analysis.

166

Table 8.5. ANOVA results for the effects of habitat relief and region on the abundances of nine hard bottom taxa, the aggregate abundances for five groups, and the total aggregate abundance for the 40 most abundant hard bottom taxa.

Taxa/measure of importance	Relief		Region		Relief x Region Interaction
	p^a	a posteriori^b	p^a	a posteriori^b	p^a
Rhizopsammia manuelensis/density	0.0168*	M = H > L	0.0004**	W > C > E	0.0668
Antipathes ?furcata/cover	<0.0001**	M > L > H	<0.0001**	C > W > E	<0.0001**
Stenogorgiinae/cover	0.9237	H = M = L	0.4783	E = W = C	0.0731
Nicella sp. A/cover	0.0600	M = H = L	0.0374*	W = E = C W > C	0.0074**
Bebryce cinerea/grandis/cover	0.0655	L = M = H	0.5397	W = C = E	0.3384
Bryozoa/cover	0.5455	H = L = M	0.5609	C = E = W	0.5965
Ellisella spp./cover	0.1901	M = L = H	0.7247	E = W = C	0.5273
?Idmidronea sp./cover	0.2421	L = M = H	0.2966	C = E = W	0.3353
Crinoid – 10 arm/density	0.1952	M = H = L	0.2141	C = W = E	0.0050**
Ahermatypic Corals/density	0.0239*	M = H > L	0.0007**	W > C > E	0.0585
Octocorals/cover	0.3380	M = H = L	0.0368*	W = E = C	0.0014**
Antipatharians/cover	<0.0001**	M > H = L	<0.0001**	C > W = E	<0.0001**
Poriferans/cover	<0.0001**	H > L = M	<0.001**	E > W = C	0.0003**
Ectoprocts/cover	0.3621	L = H = M	0.3931	C = E = W	0.4144
All Taxa/cover	0.0014**	H = M > L	0.0005**	C = W > E	0.0006**

^{a} = * = Significant at the 0.05 level, ** = significant at the 0.01 level.
^{b} = values are arranged with the highest mean on the left and the lowest mean on the right.
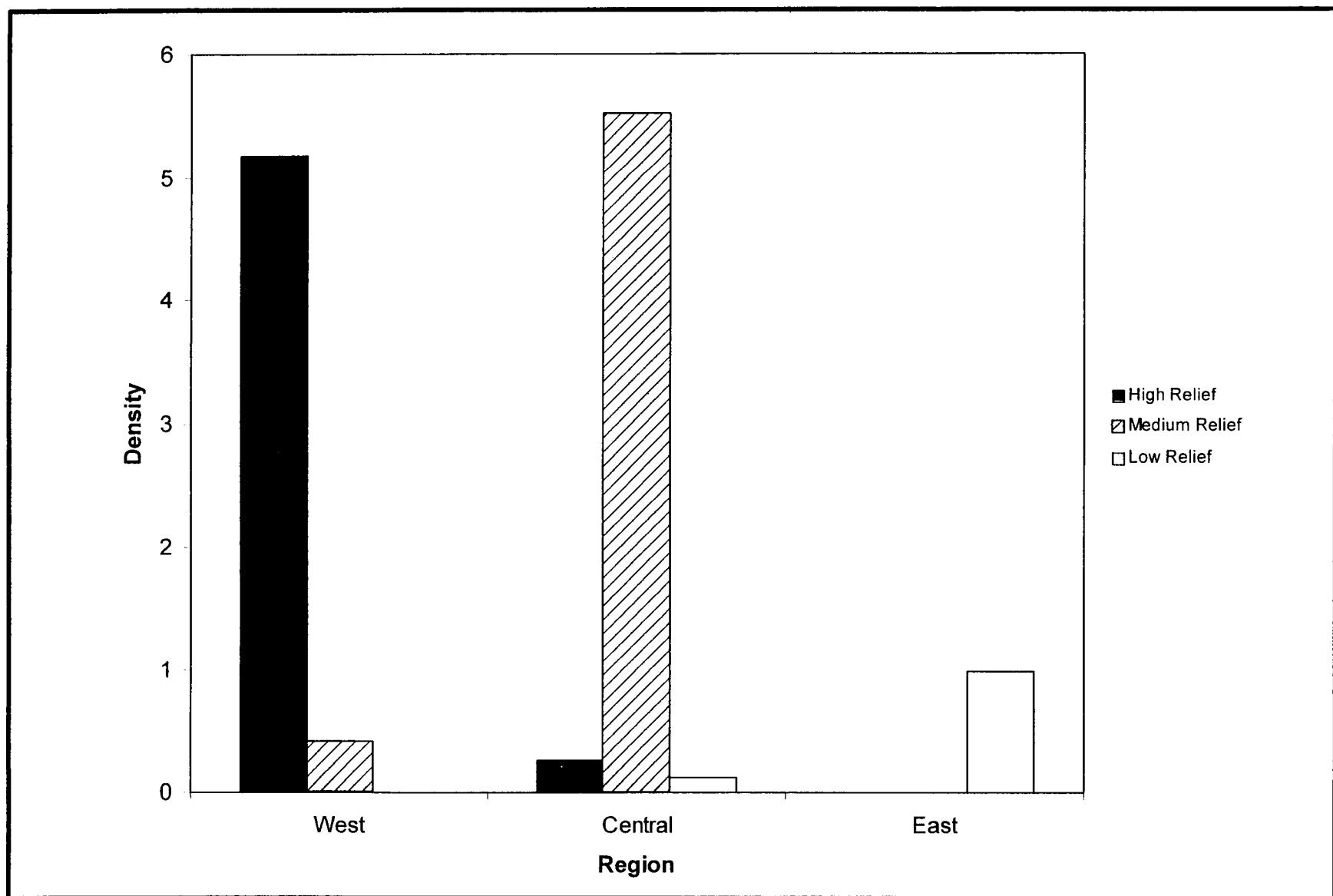
Fig. 8.4. Mean densities (number/m^2) of 10-armed crinoids in each relief category and region.

Chapter 9
Fish Communities

Introduction

The objectives of this program component are to (1) describe fish community composition, taxonomic richness, and temporal dynamics at each monitoring site; (2) identify differences in fish community composition among sites differing in relief and location; (3) identify relationships between fish communities and environmental parameters such as small-scale habitat variability, rock type, sediment cover, etc.; and (4) identify trophic relationships among fishes, as well as between fishes and the epibenthic community.

The first three objectives are being addressed by analyzing photographs and videotapes recorded by the ROV during routine hard bottom monitoring (see Chapter 8). The program does not include any "dedicated" fish censusing or sampling. Nevertheless, the photographs and video collected while performing other tasks provide images suitable for qualitative analysis of fish assemblages. The data consist of species occurrences that can be partitioned by site, time (cruise), and habitat (substrate). Trophic interrelationships are being studied by reviewing literature from the Gulf of Mexico and South Atlantic Bight and will be discussed in the synthesis report. The current report covers the first three monitoring cruises (1C, M2, and M3).

Methods

Field Methods

Because qualitative data are being extracted opportunistically from video transects not specifically made for fishes (i.e., epibiota), the field methods are identical to those described for hard bottom community assessment in Chapter 8. Only the aspects of these methods most important to fish assessment need to be restated. Two videocameras simultaneously record the path taken by the ROV during its operations; one is forward-viewing for piloting the ROV, while the other is downward-viewing perpendicular to the substrate for recording quantitative benthic data. A 35 mm Benthos camera equipped with a Nikkor 28 mm lens and a 200 watt-second electronic strobe is being used to collect the photographs. The camera is aligned perpendicular to the substrate for all quantitative photographs, and aligned parallel with the downward-viewing videocamera. A coordinate laser system mounted on the ROV is being used to estimate proper distance. Still photographs have the high resolution needed for accurate identifications of fishes, particularly small ones, and the video provides redundant images should the still camera fail during a dive.

The most important field task pertaining to the fish data is the collection of random photographs (Chapter 8). Random photographs are collected within eight sectors of a circular plot located within each site. The paths recorded on video by the ROV as it

169

moves from photograph to photograph provide the best data available for characterizing the fish taxa present at each site.

Laboratory Analysis

In the laboratory, videos from both videocameras (forward-viewing and downward-viewing) were examined simultaneously for the presence of fishes. Videotapes from both of these cameras are useful because they produce complementary observations. The forward-viewing camera will often record larger fishes such as amberjacks, snappers, groupers, or sharks that are not seen by the downward camera. On the other hand, the downward-viewing camera records small reef associated species (streamer basses, damselfishes, squirrelfishes) not discernable by the forward-viewing camera.

Fish species occurrences were recorded for each random path taken within a sector of a site. Also, within each sector, the time spent by the ROV over soft bottom and hard bottom was recorded. The photographs (35 mm transparencies) were viewed on a large screen film viewer. All fish in the quantitative photographs were identified to the lowest practical taxon and added to the species list for a particular site or sector from which the photograph was taken. Identifications were confirmed for some species by hook and line sampling for specimens. All photographic data (including still photographs) collected during ROV operations were reviewed for new species to add to the master species list for the hard bottom features. The final data include frequency of occurrence at all features by area and cruise.

Data Analysis

All data analyzed for this report, with the exception of the overall species list (Table 9.1) that included taxa observed in still photographs, are from videotape analyses. These data consist of presence-absence and frequency of occurrence of fish taxa by transect within the nine study sites. Frequency of occurrence was examined for each cruise separately and for the three cruises combined. The total number of taxa recorded for each site within each cruise was used as an estimate of taxonomic richness. Relationships between richness and two variables (average water depth and sample area) were examined for each site with Pearson's product-moment correlation. Patterns of co-occurrence among taxa and similarity of species composition among samples were analyzed by the multivariate ordination method of Correspondence Analysis (CA). Observed patterns were analyzed with respect to pre-defined location (east, central, and west) and relief (high, medium, and low) categories. CA ordination was performed on a taxa-by-samples data matrix. For CA, the matrix consisted of species frequencies (summed across the eight transects for each site) by station-time (=site-cruise). Pelagic species such as amberjacks, sharks, and mackerels and taxa not identified below the family level were not included in the matrix. This produced a matrix of 25 samples by 54 taxa. The number of station-times was 25 (instead of 27) because Sites 5 and 6 were not sampled during Cruise M3. Relationships between CA axis 1 scores with distance from the Mississippi River mouth and water depth were examined by linear regression.

Table 9.1. Preliminary list of fish taxa observed in still photographs and videotapes from each site during Cruises 1C, M2, and M3.

Taxa	Site 1	2	3	4	5	6	7	8	9
Relief Category:	H	M	L	M	H	L	H	M	L
CARCHARHINIDAE									
Mustelus sp.	--	--	--	●	●	--	●	--	--
Rhizoprionodon terranovae	--	--	--	--	--	--	●	--	--
RAJIIDAE									
Raja olseni	--	--	--	--	--	--	--	--	●
MURAENIDAE									
Gymnothorax kolpos	--	--	--	●	--	--	--	--	--
Muraena retifera	--	●	●	--	--	--	--	--	--
Muraenid sp.	--	●	--	--	--	--	--	--	--
SYNODONTIDAE									
Saurida sp.	--	●	●	--	●	---	--	--	●
Synodus intermedius	--	●	●	--	--	--	--	--	--
Synodus sp.	--	--	●	--	--	●	--	--	--
BATRACHOIDIDAE									
Opsanus pardus	●	--	●	--	--	--	--	●	--
ANTENNARIIDAE									
Antennarius ocellatus	--	--	--	--	--	--	●	--	--
OGCOCEPHALIDAE									
Ogcocephalus corniger	●	●	●	--	--	--	●	●	●
Ogcocephalus sp.	●	●	--	●	--	--	●	●	●
GADIDAE									
Urophycis sp.	●	--	--	●	--	--	--	●	--
OPHIDIIDAE									
Brotula barbata	--	--	--	●	--	--	--	●	●
HOLOCENTRIDAE									
Corniger spinosus	●	●	--	●	--	--	●	--	●
Holocentrus adscensionis	●	--	--	--	--	--	--	--	--
Holocentrus bullisi	●	--	--	--	--	--	--	--	--
Holocentrus sp.	--	--	--	●	--	--	--	--	--
FISTULARIIDAE									
Fistularia petimba	●	--	●	--	--	--	●	--	--
SCORPAENIDAE									
Scorpaena dispar	●	●	●	●	●	●	●	●	●
Scorpaena sp. B	--	●	--	●	--	--	●	--	--

Table 9.1. (continued).

Taxa	Site								
	1	2	3	4	5	6	7	8	9
Relief Category:	H	M	L	M	H	L	H	M	L
SERRANIDAE									
Centropristis ocyurus	--	--	●	--	●	●	--	--	--
Centropristis striata	--	--	--	--	●	--	--	--	--
Epinephelus niveatus	--	--	●	●	--	●	--	●	●
Epinephelus adscensionis	--	--	--	--	●	--	--	--	--
Gonioplectrus hispanus	--	●	●	●	--	--	●	●	●
Hemanthias vivanus	●	●	●	●	●	●	●	●	●
Holanthias martinicensis	●	●	●	●	●	●	●	●	●
Liopropoma eukrines	●	●	--	●	●	●	●	●	●
Mycteroperca phenax	●	●	●	●	--	●	●	●	●
Mycteroperca microlepis	--	●	--	--	--	--	--	--	--
Paranthias furcifer	●	--	--	--	--	--	●	--	--
Rypticus saponaceous	--	--	--	--	--	●	--	--	--
Rypticus sp.	--	--	--	--	--	●	--	--	--
Serranus atrobrancus	●	●	●	●	●	--	●	●	●
Serranus phoebe	●	●	●	●	●	●	●	--	--
PRIACANTHIDAE									
Priacanthus arenatus	●	--	--	●	●	●	●	--	--
Pristigenys alta	●	●	●	●	●	●	●	●	●
APOGONIDAE									
Apogon pseudomaculatus	●	●	●	●	--	●	--	--	--
MALACANTHIDAE									
Caulolatilus sp.	--	--	--	●	--	--	--	--	--
Malacanthus plumieri	●	--	--	--	--	--	--	--	--
CARANGIDAE									
Seriola dumerili	●	●	●	●	●	●	●	●	--
Seriola rivoliana	●	●	--	--	●	--	●	--	--
Trachurus lathami	●	--	●	●	--	--	--	--	--
LUTJANIDAE									
Lutjanus campechanus	--	●	●	●	●	●	●	●	●
Rhomboplites aurorubens	●	●	--	●	●	●	●	●	●
SPARIDAE									
Calamus sp.	--	●	--	--	●	--	●	--	--
SCIAENIDAE									
Equetus iwamotoi	●	●	●	●	●	●	--	●	●
Equetus umbrosus	●	--	--	●	--	●	●	●	●

172

Table 9.1. (continued).

Taxa	Site								
	1	2	3	4	5	6	7	8	9
Relief Category:	H	M	L	M	H	L	H	M	L
CHAETODONTIDAE									
Chaetodon aya	●	●	●	●	●	●	●	●	●
Chaetodon ocellatus	--	●	--	--	--	--	--	--	--
Chaetodon sedentarius	●	●	●	--	●	--	●	--	--
POMACANTHIDAE									
Holacanthus bermudensis	●	●	--	●	●	●	●	●	--
Holacanthus tricolor	●	--	--	--	--	--	--	--	--
POMACENTRIDAE									
Chromis enchrysurus	●	--	●	--	●	●	●	●	--
LABRIDAE									
Bodianus pulchellus	●	●	--	--	--	--	●	--	--
Decodon puellaris	●	--	●	●	--	--	●	--	●
Halichoeres sp.	●	--	●	--	--	--	--	--	--
GOBIIDAE									
Gobiids	●	--	--	--	--	--	●	--	--
GEMPYLIDAE									
Trichiurus lepturus	●	--	●	--	--	--	--	--	--
SCOMBRIDAE									
Scomberomorus cavalla	--	--	--	--	--	--	●	--	--
BOTHIDAE									
Bothid sp.	--	--	●	●	--	--	--	--	--
Cyclopsetta sp.?	--	●	--	--	--	--	--	--	--
Syacium sp.	--	--	--	--	--	--	●	--	--
BALISTIDAE									
Balistes capriscus	--	--	●	--	--	--	--	--	--
Monacanthus sp.	●	--	--	--	--	--	--	--	--
OSTRACIIDAE									
Lactophrys polygonia	●	--	--	--	--	--	--	--	--
Lactophrys quadricornis	--	--	--	●	--	--	--	--	--
TETRAODONTIDAE									
Canthigaster rostrata	●	--	--	--	--	--	●	--	--
Sphoeroides spengleri	●	--	--	--	--	--	--	--	--
DIODONTIDAE									
Chilomycterus sp.	--	--	--	●	--	--	--	--	--
Diodon holocanthus	--	--	--	●	--	--	●	●	●
TOTAL TAXA	40	31	30	34	23	23	36	23	22

173

Results

Analysis of videotapes and still photographs from the first three monitoring cruises (1C, M2, and M3) revealed a total of 73 fish taxa from 32 families (Table 9.1). The most speciose families were sea basses (Serranidae), squirrelfishes (Holocentridae), lizardfishes (Synodontidae), jacks (Carangidae), wrasses (Labridae), and butterflyfishes (Chaetodontidae). The most frequently occurring taxa in video transects for the combined cruises were roughtongue bass (*Pronotogrammus martinicensis*), short bigeye (*Pristigenys alta*), bank butterflyfish (*Chaetodon aya*), and red barbier (*Hemanthias vivanus*) (Table 9.2). Video transects from Cruise 1C yielded 44 taxa, those taken during Cruise M2 produced 67 taxa, and Cruise M3 transects produced 63 taxa. Rank order of the most frequently occurring taxa at each site is shown in Table 9.3.

Taxonomic richness recorded from videotapes for each cruise differed across all sites (Fig. 9.1). During Cruise 1C, the number of taxa observed ranged from 5 at Site 9 to 22 at Site 7 and averaged 15.3 taxa per site. Cruise M2 yielded an average of 20.7 taxa per site, ranging from 13 taxa at Site 6 to 30 taxa at Site 1. Cruise M3 yielded an average of 28.1 taxa per transect, ranging from 37 taxa at Site 1 to 19 taxa at Site 8. The number of taxa was weakly correlated with sample area for the nine sites during both Cruise 1C ($r = 0.38$) and M2 ($r = 0.51$). The correlation between sample area and number of taxa was higher ($r = 0.82$) for the seven sites sampled during Cruise M3. The correlation between the average water depth at each site and number of taxa was higher, but still relatively weak for Cruise 1C ($r = 0.55$), M2 ($r = 0.69$), and M3 ($r = 0.58$).

The influence of relief category (high, medium, and low relief), location (east, central, west), water depth, and distance from the Mississippi River mouth on fish assemblage composition in videotapes was examined by CA. CA ordination axes 1 and 2 accounted for 14.3% and 10.5% of the variation in the data matrix. The separation of samples along CA axis 1 reflected to some extent relief and location (Fig. 9.2). Three samples from high-relief eastern (H-E) Site 1 had the highest scores on CA axis 1. Samples representing most of the other location and relief categories clustered together near the origin of the ordination indicating their similarity in species composition. CA axis 2 did not reveal any specific patterns with respect to relief or location; however, one medium relief-central (M-C) sample separated from the cluster of other samples with the highest score on CA axis 2. Regression of CA axis 1 scores on water depth accounted for 38% of the variation in that relationship, whereas, the regression of CA axis 1 scores and distance from the Mississippi River mouth explained only 18% of the variation for that relationship (Fig. 9.3).

Taxa responsible for these patterns observed in the site scores are shown in the ordination of taxon scores for CA axes 1 and 2 (Fig. 9.4). Taxa with high scores on CA axis 1 were sand tilefish (*Malacanthus plumieri*), deepwater squirrelfish (*Sargocentron bullisi*), honeycomb cowfish (*Lactophrys polygonia*), rock beauty (*Holacanthus tricolor*), squirrelfish (*Holocentrus adscensionis*), and sharpnose puffer (*Canthigaster rostrata*). Those exhibiting low CA axis 1 scores included snowy grouper (*Epinephelus niveatus*), bearded brotula (*Brotula barbata*), red snapper (*Lutjanus campechanus*), burrfish

174

Table 9.2. Top 20 fish taxa observed in video transects at all nine sites combined during Cruise 1C, M2, and M3 ranked by frequency of occurrence.

| Taxa	Cruise 1C		Cruise M2		Cruise M3		Total	
	No. of Transects	% of Transects	No. of Transects	% of Transects	No. of Transects	% of Transects	No. of Transects	% of Transects
Total Transects Available	72	100	72	100	56	100	200	100
Pronotogrammus martinicensis	39	54.2	56	77.8	49	87.5	144	72.0
Pristigenys alta	36	50.0	44	61.1	52	92.9	132	66.0
Chaetodon aya	23	31.9	35	48.6	40	71.4	98	49.0
Hemanthias vivanus	17	23.6	29	40.3	39	69.6	85	42.5
Scorpaena dispar?	5	6.9	34	47.2	20	35.7	69	34.5
Mycteroperca phenax	9	12.5	16	22.2	29	51.8	54	27.0
Serranus phoebe	16	22.2	17	23.6	15	26.8	48	24.0
Holacanthus bermudensis	19	26.4	10	13.9	10	17.9	39	19.5
Liopropoma eukrines	12	16.7	14	19.4	11	19.6	37	18.5
Seriola dumerili	15	20.8	8	11.1	13	23.2	36	18.0
Chromis enchrysurus	13	18.1	11	15.3	10	17.9	34	17.0
Equetus iwamotoi	12	16.7	12	16.7	10	17.9	34	17.0
Chaetodon sedentarius	8	11.1	10	13.9	16	28.6	34	17.0
Corniger spinosus	3	4.2	14	19.4	10	17.9	27	13.5
Lutjanus campechanus	17	23.6	1	1.4	9	16.1	27	13.5
Equetus umbrosus	3	4.2	16	22.2	5	8.9	24	12.0
Serranus atrobranchus	3	4.2	7	9.7	12	21.4	22	11.0
Priacanthus arenatus	5	6.9	9	12.5	5	8.9	19	9.5
Ogcocephalus corniger			9	12.5	10	17.9	19	9.5
Gonioplectrus hispanus	6	8.3	5	6.9	7	12.5	18	9.0

Table 9.3. Top 20 fish taxa observed in video transects during Cruises 1C, M2, and M3 combined at Sites 1 through 9, ranked by frequency of occurrence.

| Species	Site 1 No. Transects	Site 1 %	Site 2 No. Transects	Site 2 %	Site 3 No. Transects	Site 3 %	Site 4 No. Transects	Site 4 %	Site 5 No. Transects	Site 5 %	Site 6 No. Transects	Site 6 %	Site 7 No. Transects	Site 7 %	Site 8 No. Transects	Site 8 %	Site 9 No. Transects	Site 9 %	Total No. Transects	Total %
Total Transects Available	24	100	24	100	24	100	24	100	16	100	16	100	24	100	24	100	24	100	200	100
Pronotogrammus martinicensis	18	75.0	24	100.0	15	62.5	18	75.0	11	68.8	8	50.0	24	100.0	9	37.5	17	70.8	144	72.0
Pristigenys alta	19	79.2	12	50.0	21	87.5	17	70.8	10	62.5	2	12.5	23	95.8	12	50.0	16	66.7	132	66.0
Chaetodon aya	16	66.7	11	45.8	14	58.3	8	33.3	6	37.5	5	31.2	24	100.0	8	33.3	6	25.0	98	49.0
Hemanthias vivanus	14	58.3	7	29.2	8	33.3	9	37.5	8	50.0	5	31.2	10	41.7	13	54.2	11	45.8	85	42.5
Scorpaena dispar?	9	7.5	9	37.5	7	29.2	16	66.7	2	12.5	5	1.2	12	50	3	12.5	6	25	69	34.5
Mycteroperca phenax	4	16.7	9	37.5	3	12.5	13	54.2	3	18.8	2	12.5	9	37.5	5	20.8	6	25.0	54	27.0
Serranus phoebe	8	33.3	9	37.5	4	16.7	3	12.5	12	75.0	4	25.0	8	33.3	--	--	--	--	48	24.0
Holacanthus bermudensis	9	37.5	3	12.5	--	--	2	8.3	7	43.8	2	12.5	14	58.3	2	8.3	--	--	39	19.5
Liopropoma eukrines	3	12.5	6	25.0	2	8.3	1	4.2	5	31.2	2	12.5	10	41.7	4	16.7	4	16.7	37	18.5
Seriola dumerili	2	8.3	5	20.8	4	16.7	3	12.5	6	37.5	1	6.2	14	58.3	1	4.2	--	--	36	18.0
Chromis enchrysurus	15	62.5	1	4.2	3	12.5	--	--	8	50.0	2	12.5	4	16.7	1	4.2	--	--	34	17.0
Equetus iwamotoi	1	4.2	5	20.8	5	20.8	8	3.3	6	37.5	5	31.2	--	--	1	4.2	3	12.5	34	17.0
Chaetodon sedentarius	12	50.0	3	12.5	1	4.2	--	--	1	6.2	--	--	15	2.5	1	4.2	1	4.2	34	17.0
Corniger spinosus	3	12.5	5	20.8	--	--	4	6.7	1	6.2	--	--	10	1.7	2	8.3	2	8.3	27	13.5
Lutjanus campechanus	--	--	2	8.3	3	12.5	--	--	4	25.0	8	50.0	2	8.3	4	16.7	4	16.7	27	13.5
Equetus umbrosus	3	12.5	--	--	--	--	3	2.5	--	--	7	43.8	4	16.7	4	16.7	3	12.5	24	12.0
Serranus atrobranchus	2	8.3	6	25.0	9	37.5	2	8.3	1	6.2	--	--	1	4.2	--	--	1	4.2	22	11.0
Priacanthus arenatus	2	8.3	--	--	--	--	1	4.2	5	31.2	2	12.	9	37.5	--	--	--	--	19	9.5
Ogcocephalus corniger	4	16.7	1	4.2	1	4.2	1	4.2	--	--	--	--	2	8.3	5	20.8	5	20.8	19	9.5
Gonioplectrus hispanus	--	--	3	12.5	3	12.5	3	12.5	--	--	--	--	1	4.2	5	20.8	3	12.5	18	9.0
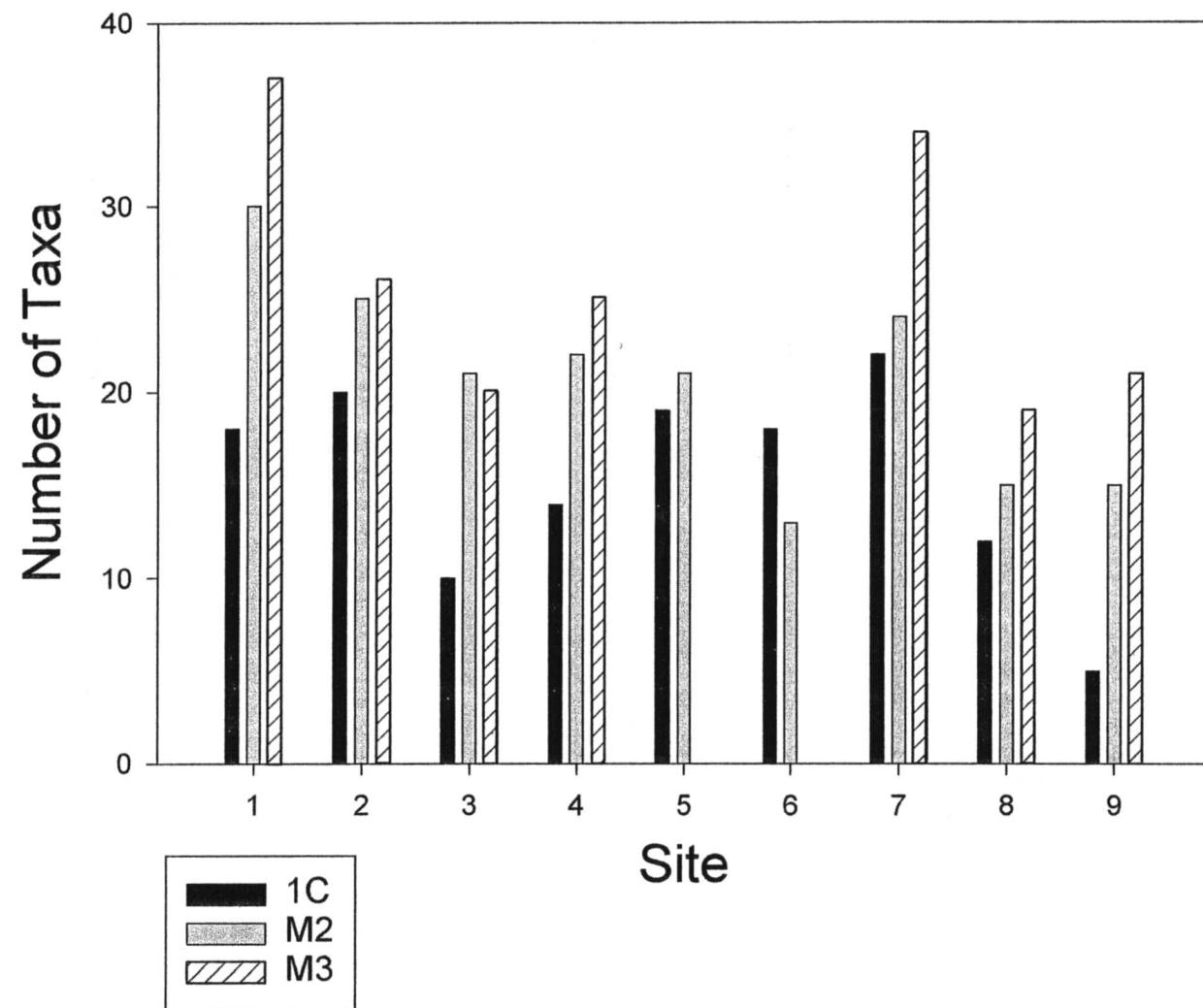
Fig. 9.1. Total fish taxa observed in video transects across study Sites 1 through 9 for Cruises 1C, M2, and M3.

6 ┤

M-C

4 ┤

Axis 2

2 ┤

M-E M-E H-W
M-E H-C H-E
M-C L-E H-E
L-W
M-C H-W
L-C L-E L-C H-W
L-W M-W
M-W L-W

0 ┤

-2 ┤   M-W

H-E

-4 ┤
   -3   -2   -1   0   1   2   3

Axis 1
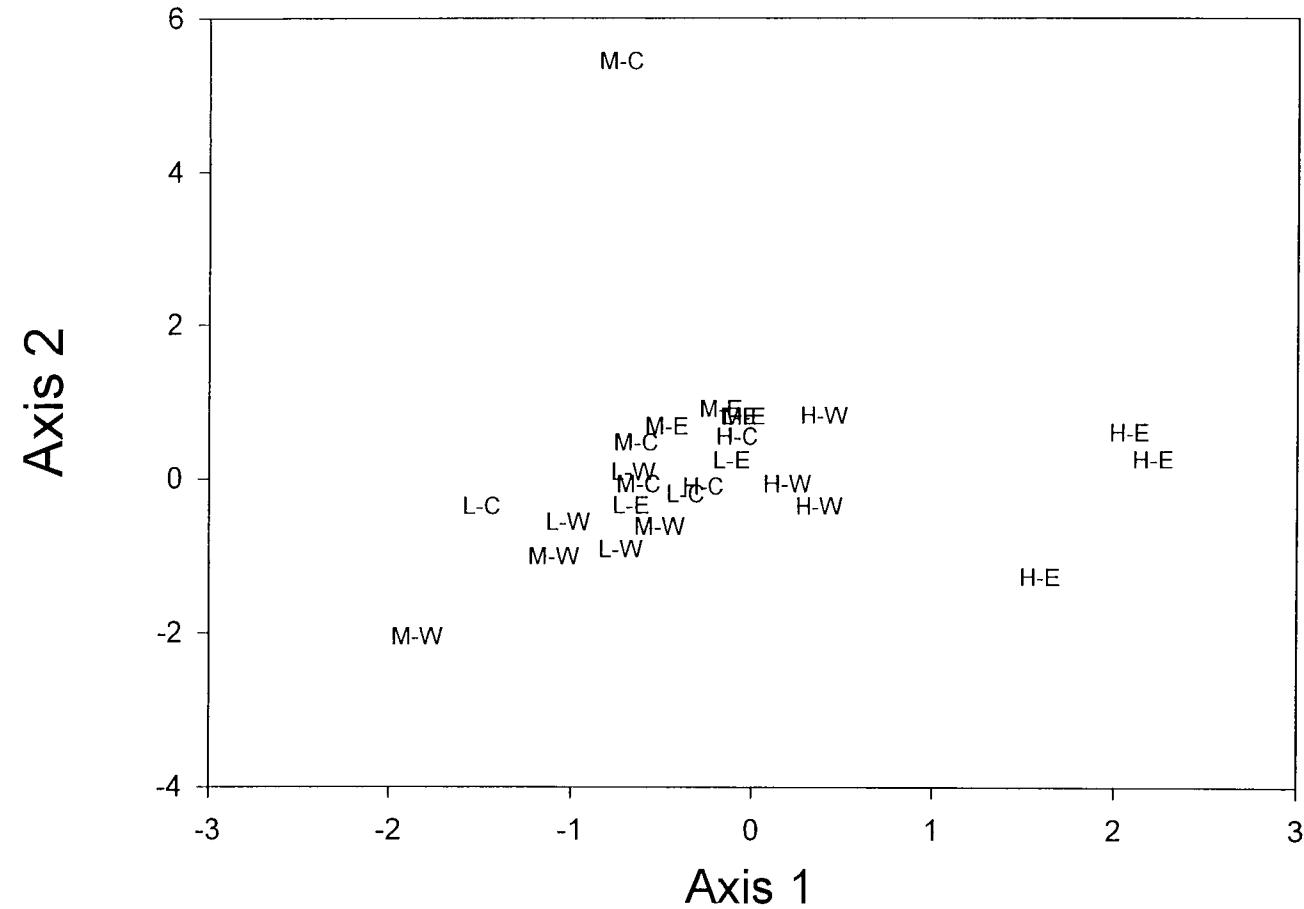
Fig. 9.2. Sample scores from correspondence analysis of a taxa-by-samples matrix based on video transects plotted on Axes 1 and 2. Scores are labeled by relief category [high (H), medium (M) and low (L)] and location [east (E), central (C), and west (W)].
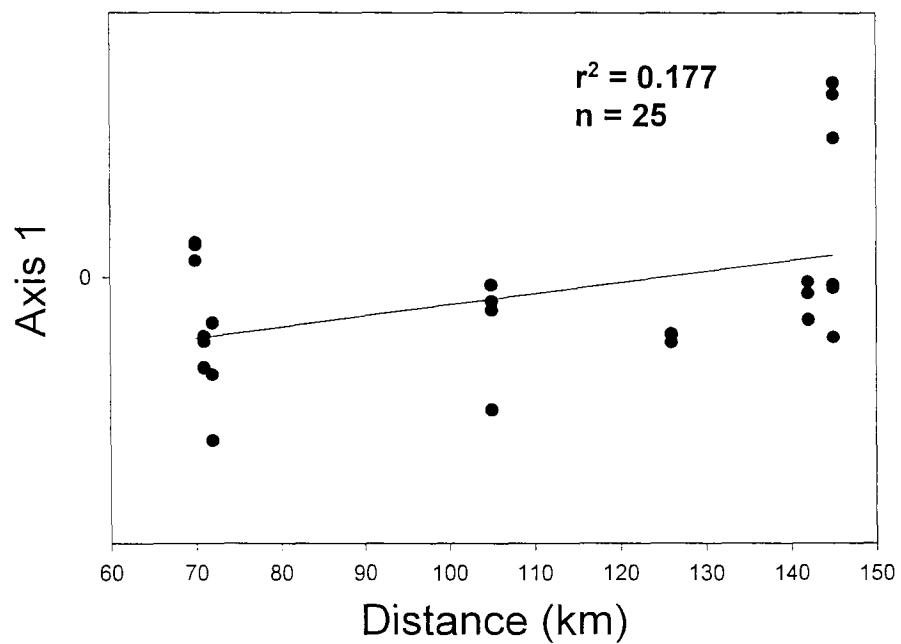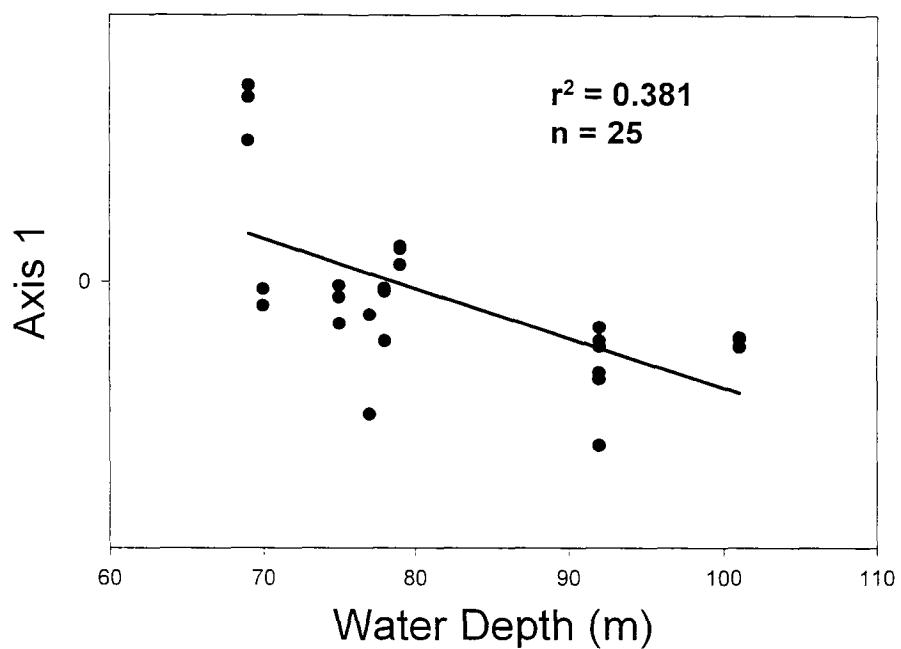
Fig. 9.3. Plots of Axis 1 scores from correspondence analysis against (a) water depth and (b) distance from the Mississippi River mouth. Lines determined by least squares linear regression.

179
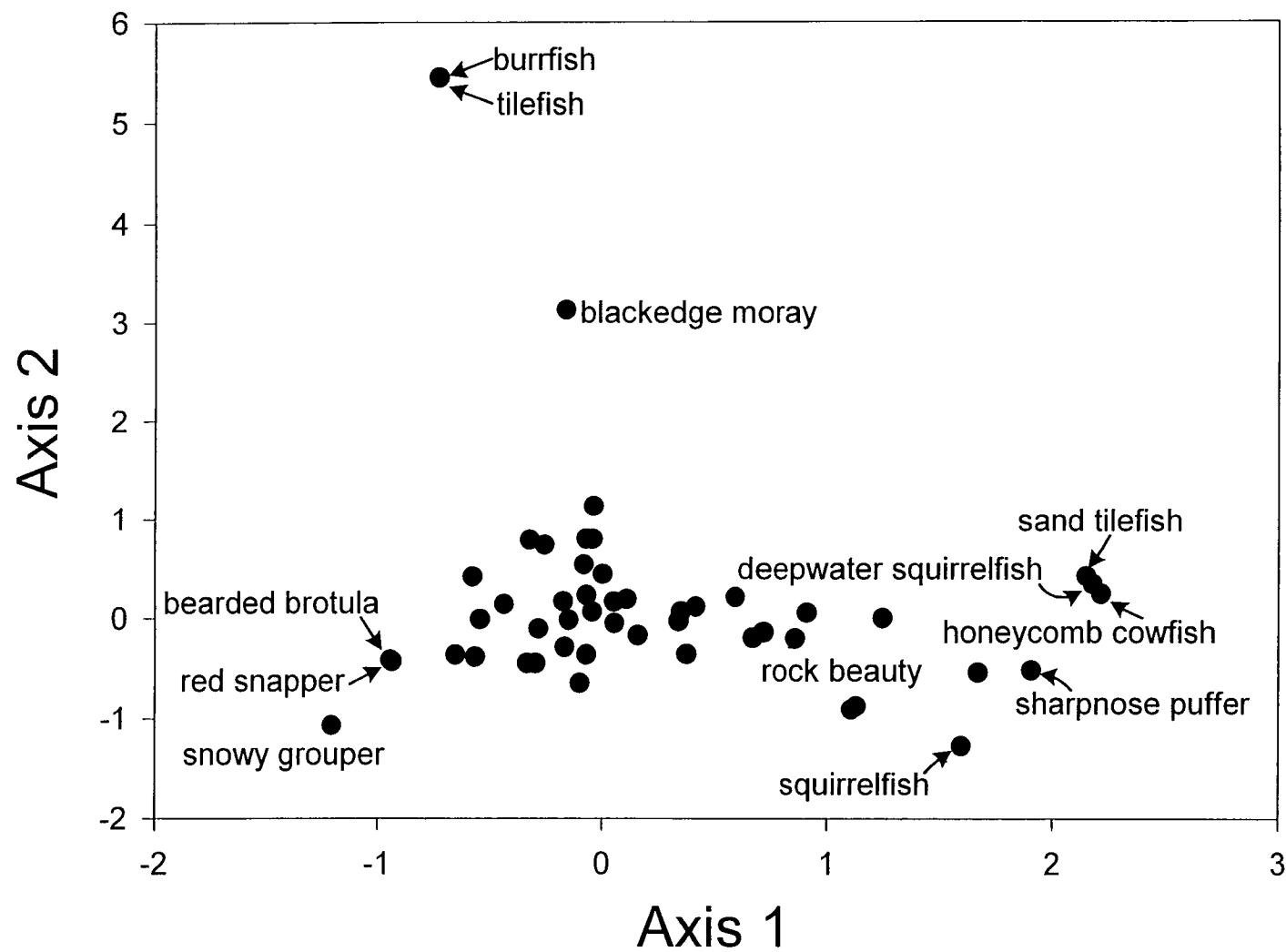
Fig. 9.4. Taxa scores from correspondence analysis of a taxa-by-samples matrix based on video transects plotted on Axes 1 and 2.

(*Chilomycterus* sp.), tilefish (*Caulolatilus* sp.), Spanish flag (*Gonioplectrus hispanus*), and blackbar drum (*Equetus iwomotoi*). On CA axis 2, taxa with the highest scores were blackedge moray (*Gymnothorax nigromarginatus*), tilefish, and burrfish. Taxa with low CA axis 2 scores were creole-fish (*Paranthias furcifer*), bandtail puffer (*Sphoeroides spengleri*), longspine squirrelfish (*Holocentrus rufus*), and snowy grouper.

Discussion

Qualitative video data collected during the three monitoring cruises show that the ichthyofauna inhabiting the pinnacle features consists primarily of reef fishes. Pelagic (e.g., sharks, jacks, bluefish, and king mackerel) and demersal (flounders) fishes also were observed, but infrequently when compared with reef species. The most commonly occurring reef fish species observed in video and photographs were members of the deep reef fish assemblage reported for water depths of 50 to over 200 m in the western Atlantic (e.g., Colin 1974, 1976; Parker and Mays 1998). This assemblage is much less diverse than the reef fish assemblages reported for water depths less than 50 m. The deep reef assemblage is somewhat distinctive in its species composition and is characterized by the presence of roughtongue bass, tattler (*Serranus phoebe*), short bigeye, yellowtail reeffish (*Chromis enchrysurus*), bank butterflyfish, red barbier, and various scorpionfishes (*Scorpaena* spp.). Similar species were reported by previous investigations of the pinnacle features (e.g., Continental Shelf Associates, Inc. 1985a; Darnell 1991). Similar deep reef fish assemblages have been documented off the southeastern U.S. (Miller and Richards 1980; Parker and Ross 1986; Gilmore et al. 1987), within the lower portion of the Algal-Sponge Zone of the west Flower Garden Banks in the northwestern Gulf of Mexico (Bright and Pequegnat 1974; Boland et al. 1983; Dennis and Bright 1988a), and near the head of De Soto Canyon (Shipp and Hopkins 1978; Continental Shelf Associates, Inc. 1987). The total of 73 taxa represents about half of the fish fauna known from the hard banks and reefs of the northern Gulf of Mexico (Cashman 1973; Bright and Pequegnat 1974; Smith et al. 1975; Smith 1976; Sonnier et al. 1976; Boland et al. 1983; Dennis and Bright 1988a,b).

One obvious spatial pattern in the species composition observed in video transects from the study sites during the three cruises was that all three samples from Site 1 separated from all other samples along CA axis 1. This site also supports the highest richness of reef species among all sites. Several factors could explain these observations. Site 1 is the farthest from the Mississippi River mouth (and easternmost), and therefore farthest from potential effects of riverine discharge on the water quality of the site. However, the relationships between distance from the river mouth and CA axis 1 scores and total number of taxa were not particularly strong in the regression analyses. Site 1 is in the high relief category, and more importantly, the shallowest of all the study sites. Many of the fishes observed here, but not at other sites, are those that commonly occur in shallow waters. These include species with high scores on CA axis 1 such as honeycomb cowfish, sand tilefish, sharpnose puffer, rock beauty, and squirrelfish. The shallow water species add to both the richness and uniqueness of Site 1. Thus, the different species composition and richness observed at Site 1 may be due simply to shallow water depth or

other unmeasured correlates of shallow water depth rather than distance from the Mississippi River mouth, or relief category.

The remaining samples from the other eight study sites were composed generally of deep reef species. The sea bass family (Serranidae) contributed the most species observed at the study sites. The streamer basses (*Pronotogrammus martinicensis*; *Hemanthias vivanus*) were the most frequently occurring serranids and they probably numerically dominate the pinnacle habitats. These species feed upon plankton and were commonly observed hovering above the substrate picking plankton from the water column. Streamer basses provide forage for a number of piscivorous species (e.g., amberjacks, groupers, sharks, and mackerels). Other serranids frequently observed in the videotapes were tattler, blackear bass (*Serranus atrobranchus*), Spanish flag, and wrasse bass (*Liopropoma eukrines*). Few larger groupers were seen, with the gag (*Mycteroperca microlepis*), scamp (*M. phenax*), and snowy groupers (*Epinephelus niveatus*) represented by some large individuals. These species have probably endured heavy fishing pressure along the pinnacle trends. Other frequently occurring species such as short bigeye (*Pristigenys alta*), bank butterflyfish (*Chaetodon aya*), and yellowtail reeffish (*Chromis enchrysurus*) were more closely associated with the substrate.

Chapter 10
Companion Study: GIS and Micro-Habitat Studies

Introduction

The GIS (geographic information system) and microhabitats study focuses on relationships between the physical environment and the composition, abundance, and health of a marine, hard bottom ecosystem. The general goal of this portion of the program is to provide uniform mapping products and geographic tools in support of the overall program. Application of ArcView GIS software makes it possible to combine geographic data layers in a single map. Random photo locations and bathymetry, for example, can be overlain upon a side-scan sonar image. Maps have been produced for reporting and to assist individual principal investigators. The maps, many of which were published in the previous interim report, have included georectified mosaics and bathymetry from the $TAMU^2$ side-scan sonar imagery. Mooring locations and grab samples also were plotted. The specific goal of this study is to perform a detailed analysis of physical and geological attributes at representative sites and to evaluate the influence of these attributes on the abundance and distribution of selected species or groups of species.

Present reporting is concerned with results obtained during the 1998-1999 program year. The approach and rationale for this study have been previously described and will be only briefly described here. This section summarizes the GIS map layers available for use by the program and as deliverables at the conclusion of the program. Where new GIS data utilities have been developed during 1998-1999, examples are provided to illustrate their uses. Analysis of microhabitat attributes was completed at a selected site (Site 7). Results have been obtained for two species of soft coral (*Bebryce* sp. and *Antipathes atlantica*).

Methods

GIS Layers and Integration

The data available from the different program elements are either raster type, such as side-scan sonar images or bathymetric grids, or point type data such as locations where samples were collected. To compile a complete GIS, the raster data were first processed to a common Universal Transverse Mercator (UTM) projection at meter scale. The north-UTM zone was 16 and the spheroid was Clark 1866. The side-scan sonar images were geo-rectified with ER Mapper software by applying the registration points provided by the side-scan subcontractor (C&C Technologies, Inc.). The rectified images were imported into a series of ARCView 3.1a projects projected as backdrops over which point-type data from mooring locations, grab samples, or random photo stations can be overlain.

Subsets of all bathymetric data were compiled in 300 by 300 m areas centered on the pinnacle or pinnacles at the study sites. These data, which contained unavoidable gaps because of the limits of swath side-scan bathymetry methodology, were fitted to a 1 m grid by ArcView routines. These 300 by 300 m grids were then contoured to provide base

maps for use during ROV operations and analyzed to objectively determine the boundaries of the sites. This procedure has been described in detail in previous reports. For the GIS, depth contours were calculated and saved as separate GIS layers.

Following each monitoring cruise, random photo-stations occupied at each site were plotted as points in separate layers. Digitized versions of the photos were compiled on photo CD ROM disks, generally two per site per cruise. Video records from the main science camera were archived on 2-hour tapes. Additional information about the photo-stations, such as the time, photo CD number, etc. were listed for each point. An investigator can access this information by clicking a point of interest. Video and ROV navigation records were reviewed to determine the direction taken between stations. The track followed by the ROV was represented as a straight line between stations. In practice, the ROV might have deviated significantly from a straight line, but the navigation records were not adequate to resolve this variation. A hotlink layer was compiled to facilitate viewing of the digitized photographs. To use a hotlink, the investigator could display the photo-stations for a given cruise, determine which CD contained images of interest, and then display successive images by clicking on individual stations in the GIS display. Table 10.1 shows the ArcView GIS layers currently available for all program areas.

Table 10.1. Layers of GIS Database

Available for All Sites

- Detailed side-scan imagery
- Megasite side-scan overview
- Bathymetric contours (1 m)
- Two-dimensional shaded bathymetric surface
- Three-dimensional bathymetric surface
- Random photo locations for first three monitoring cruises with hotlinks to photo CDs
- Approximate ROV paths between random photo points for 1C and M3 monitoring cruises (categorized by videotape)
- Bottom classifications based on Cruise M2 photos and video records
- Layout maps of all detail and megasite side-scan views with graticule, scale bars, site boundaries, and grab and mooring locations.
- 300 meter square site boundaries
- Overview map with Gulf of Mexico coastline, megasite locations, and all side-scan imagery

Available for Site 7 only

- Random photo geological characterizations for first three monitoring cruises
- Boundaries of morphological regions defined from videotape analysis
- Locations of distinctive geological features identified in video analysis
- Sea fan locations categorized by species and colony numbers per photograph

Selection of Microhabitat and Classification of Substrata

The microhabitat study will focus on two of the nine monitoring sites, Site 7 (medium relief) and Site 9 (low relief). These sites were principally selected to allow comparison of the effects of relief. Additionally, the side-scan and bathymetric data available for these sites was largely free of artifacts. Finally, the current meter mooring near Site 9 can be

used to determine environmental conditions for both sites. At present, microhabitat classifications have been completed for Site 7. Classification of Site 9 is in progress and will not be presented in this report.

During the previous reporting period, the bottom type for each random photo-station at all sites from Cruise 1C was classified following the scheme developed during previous studies of pinnacle fauna (Gittings et al. 1991). These results were described in the previous report and are available as GIS layers. This effort was not repeated for subsequent monitoring cruises.

For the microhabitat characterization, the Gittings et al. (1991) classifications were adapted and simplified for the specific conditions at Site 7 and used to classify each random photo. Classification of substratum was carried out by first determining the major category, i.e., whether the station contained an **outcrop** (i.e., evident rocky substratum), or was a **flat** region (generally the areas away from the base of pinnacles). Subsequent classification of subcategories used a controlled vocabulary to describe specific attributes of outcrops or flats. A detailed description of the classifications and terms is given below. Examples of classified random photos are shown in Figs. 10.1 through 10.3 following the classification descriptions.

Major Category: Flat

Subcategory criterion: Location on flat - Standard term in open means that it occurred at least several meters away from any high relief feature. In channel means that it was found on a sediment flat at the bottom of a deep channel or crevasse between two high relief features. On terrace means that the flat was bordered by a high relief feature on only one side. There may be a certain amount of inaccuracy in these definitions, as the video can never completely reveal all features in the area.

Subcategory criterion: Sediment Components - Standard term fine means silty sediments, Coarse means sand and shell-hash. Rubble indicates small rocks and debris.

Major Category: Outcrop

Subcategory criterion: Morphology - Three common morphological features were described in Site 7 and are defined as follows:

Mound - Sediment flats are common throughout Site 7, in which sediment accumulation in cracks, channels, or flat terraces has completely buried any underlying structure. Within these flats are often found small "tip-of-the-iceberg" outcroppings less than a meter in extent and relief. Mounds occur frequently in the photographic sampling and are likely over represented because of the inclination of ROV pilots to avoid areas of sediment devoid of structure or biology.
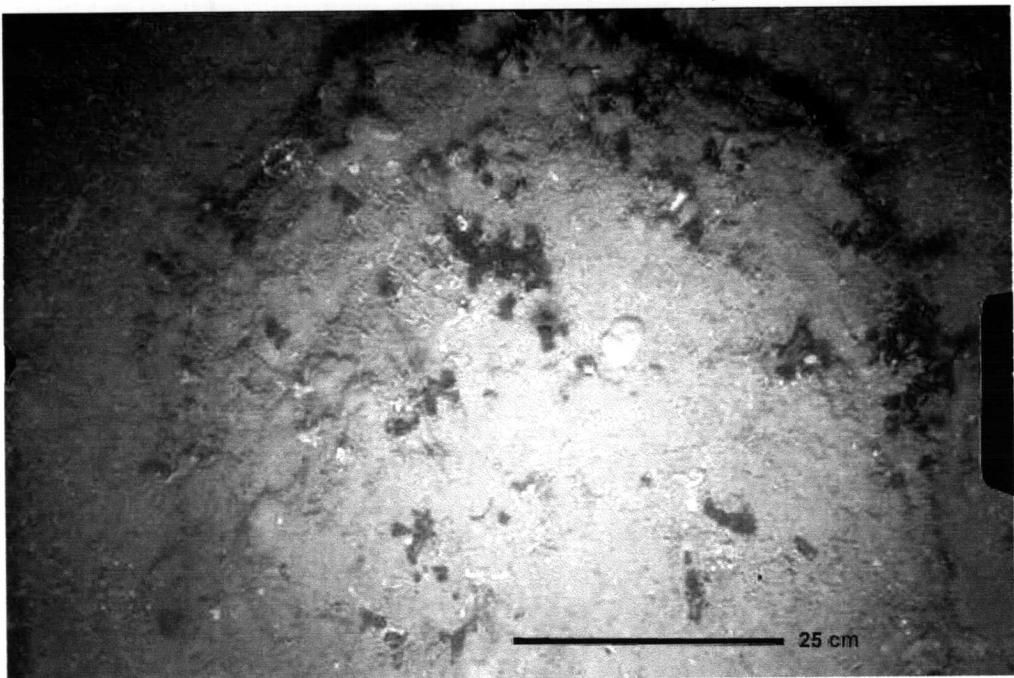
Figure 10.1. Examples of substrate classifications. A. Vertical outcrop, no sediment cover and large-scale perforation with medium surface roughness. B. Mounded outcrop, moderate silty veneer and no sand-fill.
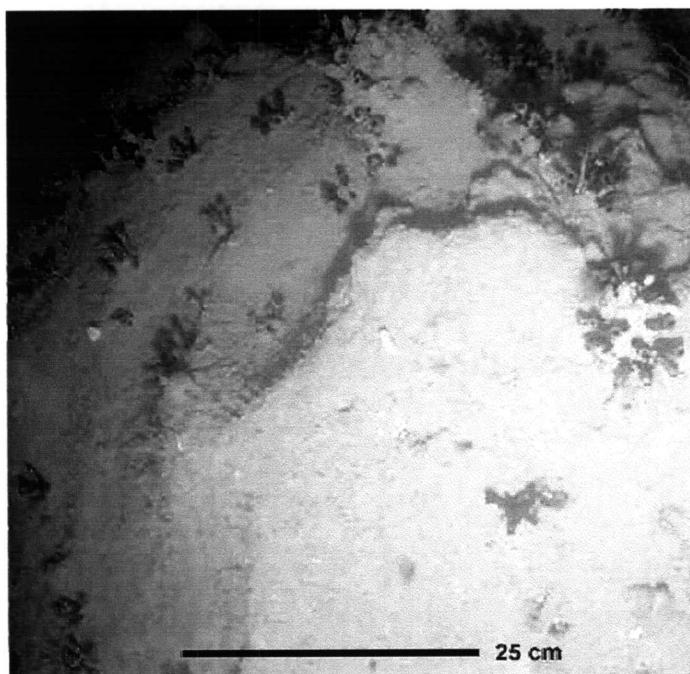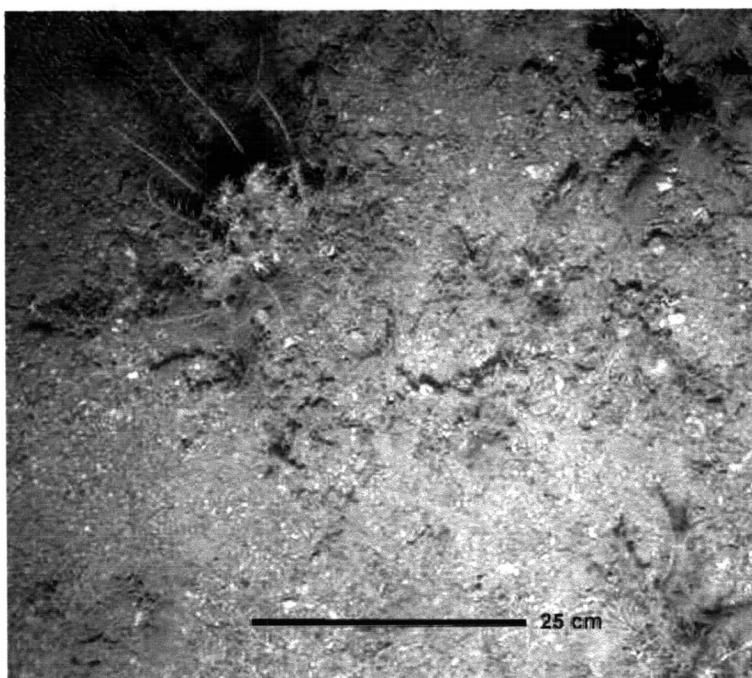
Figure 10.2. Additional examples of substrate classifications. A. Fine sediment as thick, silty veneer on outcropped surface. B. Coarse sediment as sandy fill with near-complete burial of outcropped surface.

187
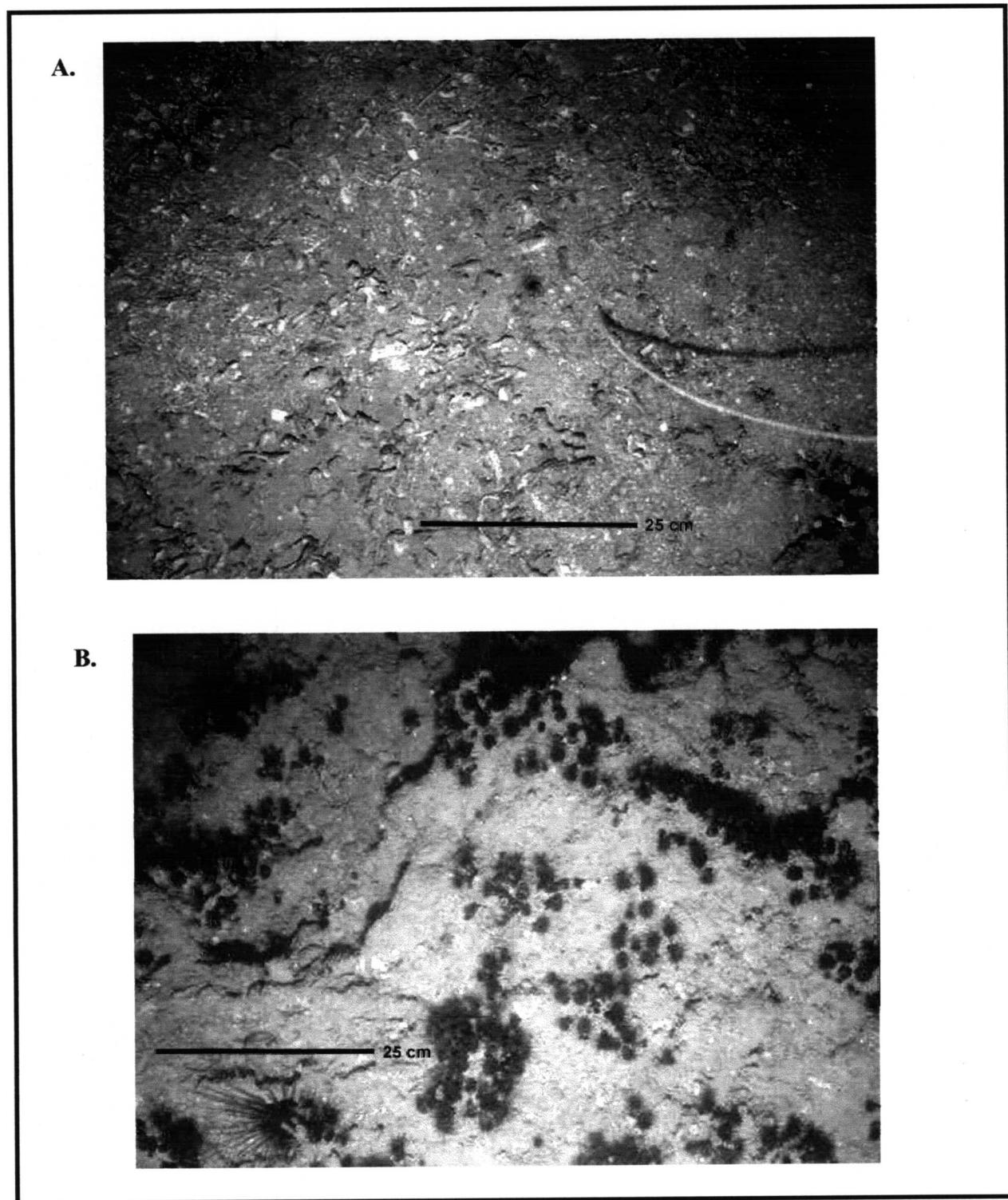
Figure 10.3. Further examples of substrate classifications. A. Combination of fine, coarse, and rubble sediment in an area of no outcropping. B. Outcropping with high surface roughness and moderate silty veneer.

188

Monolith - The most typical feature of Site 7, a monolith is a large (several meters in relief and extent) isolated feature. Monoliths often have very high relief and even sheer faces. They are distinguished as "isolated" because of their separation from other features by deep channels or wide cracks. The size of these features often makes it difficult to determine their overall extent so it is possible that they may occur as part of an elongated ridge; however in at least one direction their peaks become valleys within a distance of several meters.

Continuous hard bottom - The central area of Site 7 consists of a large expanse (tens of meters) of relatively consolidated, flat or consistently sloping outcrop. When the ROV is on a feature where no dramatic changes in relief or depth occur within a large area, the feature is defined as a reef. Cracks or narrow channels are frequently visible; however they lack the width and depth that distinguishes monoliths as separate features. The size of the feature (i.e., reef vs. monolith) is often not immediately evident so definitions are sometimes applied only after the ROV has continued some distance beyond the site.

Subcategory criterion: Height Above Bottom - Where a site was on a feature that rose out of an area of unconsolidated sediment, the height above this sediment surface was estimated whenever possible.

Subcategory criterion: Sediment Cover - Silt veneer conformed with uniform thickness to the surface morphology of the outcrop. Sandy fill/burial, tended to fill in depressions but did not necessarily stick to the surface. Areas of outcrop almost always displayed some degree of sediment coverage. Although sediment determination from visual records was not always conclusive, these two types of sediment cover were generally found on hard outcrop.

Subcategory criterion: Roughness - This describes the surface texture of the outcrop features visible in the photographs at a centimeter scale. It is classified as low, medium, or high, where the latter indicates narrow irregular pits and tunnels deep enough for small fish to use as shelter.

Subcategory criterion: Perforation - This was characterized by dramatic indentations and tunnels which gave structures a very irregular "swiss cheese" appearance on a scale visible from a wider angle perspective than that of the random photographs. Also subjectively classified as small, medium, or large.

Data Reduction and Statistical Comparisons

The goal of microhabitat analyses in the present phase of the study is to evaluate various GIS data reduction techniques and to make preliminary comparisons regarding the distribution of key species. The approach selected was to examine species counts within random photo with use of dispersion indices (Ludwig and Reynolds 1988). The standard indices that were applied are the index of dispersion (ID), Green's Index (GI), and Ludwig and Reynold's *d*. ID is calculated by

189

$$ID = \frac{s^2}{\bar{x}}$$

where s^2 and x are the mean standard deviation, respectively, of the number of coral colonies per random photo. GI is calculated by

$$GI = \frac{(s^2 / \bar{x}) - 1}{n - 1}$$

where n is the total number of colonies observed. The d index is calculated by

$$d = \sqrt{2\chi^2} - \sqrt{2(N - 1) - 1}$$

where χ^2 is the *chi-square* statistic for species counts per photo, and N is the number of photos. These indices were calculated for the total area of Site 7 and for large subregions of the total area defined by substratum type. Because the sample size was large (N>30) a *chi-square* statistic tends to a normal distribution. A t-test for significance of the d index was employed at P ≤ 0.05.

Results and Discussion

GIS Layers and Map Products

The layers shown in Table 10.1 have been periodically distributed to principal investigators on CD ROM. It is anticipated that numerous additional layers will be added to the GIS during the remainder of the program. These will include the random photo stations locations and hotlink layers from Cruise M4, grab and mooring locations, and ongoing analytical results of substratum classification, species counts and identification, etc. As the number and variety of layers increases, the utility of the GIS tool expands. The database can be used to access information regarding samples and observations or to make a diverse array of maps. Fig. 10.4 shows a schematic of the integration of a typical series of GIS layers, including an active hotlink. A more advanced use of the GIS is to generate new variables by combining or intersecting layers. For example, each random photo station at Site 7 presently includes substrate classification and limited collection information. To add a depth variable to photo record, an investigator can intersect the depth layer with the photo station layer. The GIS and Microhabitat Study Group is actively working with principal investigators to facilitate use of the ArcView toolkit.

190
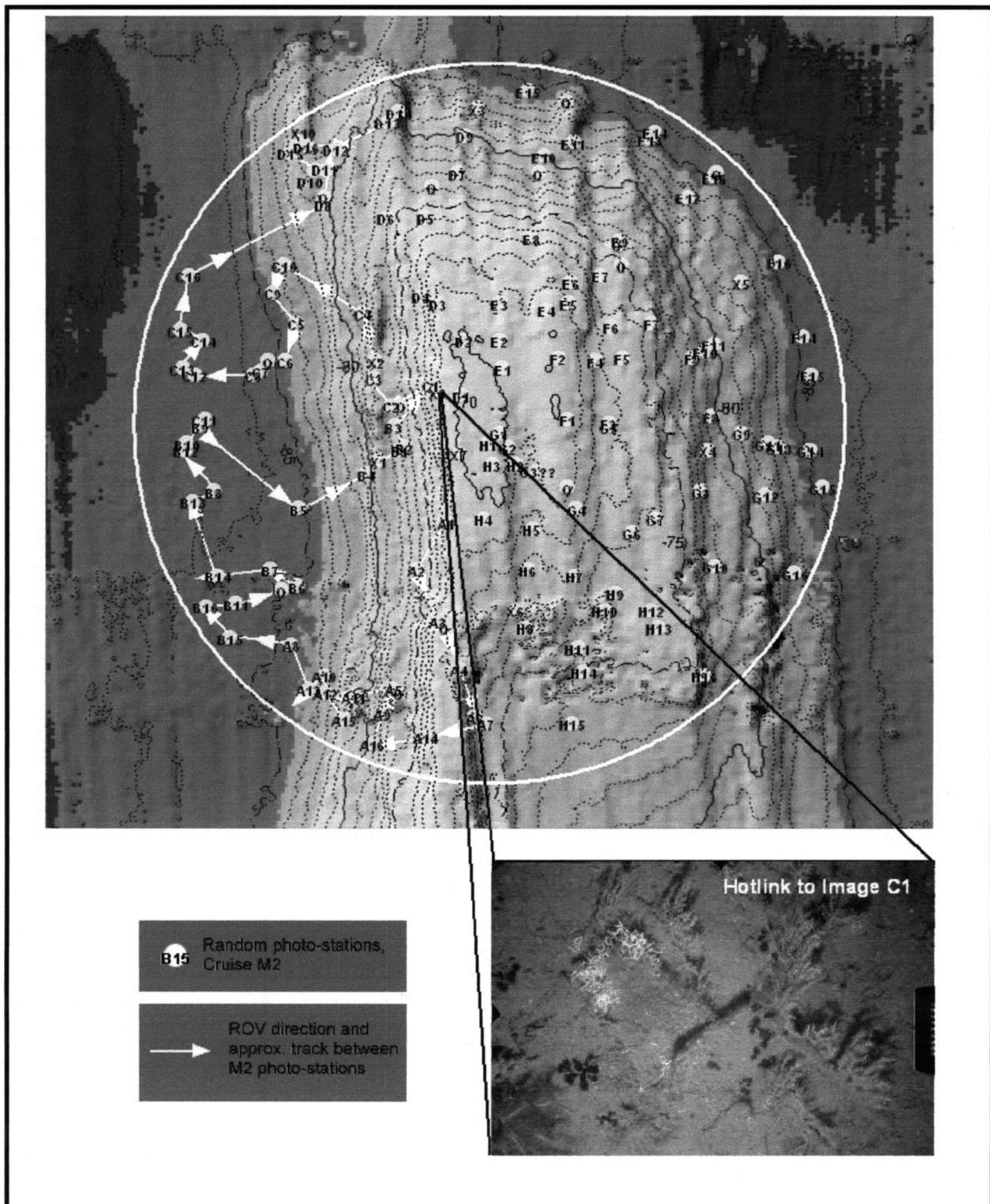
Figure 10.4. GIS layers showing the integration of different observation types. The large circle shows limits of the Site 7 photo-survey area. Mouse-clicks can access information on photo-stations and ROV track. Hotlinks provide dynamic access to photos on CD ROM.

191

Classification of Substrata

The classification scheme described above was applied to all photographs taken during the 1C, M2, and M3 surveys of Site 7. The objective was to develop a method that adequately and repeatably described processes that potentially influenced faunal distributions and associations within microhabitats. Operator judgement and extraneous categories were to be avoided. Upon careful review of the results, this objective was largely met. A few terms were more difficult to apply uniformly and may not be robust descriptions. Thickness of sediment cover was difficult to determine in the video and photos and may be re-evaluated as a descriptor. Likewise, determination of sediment texture often depended on lighting, view-angle, and similar uncontrolled aspects. Further evaluation of the classification will be carried out and unreliable classifications will be deleted. Additional refinements of the classification scheme may be required at Site 9 due to its low-relief setting.

## Influence of Microhabitat on Faunal Distribution

Two octocoral species were chosen for preliminary analysis: *Bebryce* sp., a fan-shaped gorgonian with sparse, stiff arms, and *Antipathes atlantica*, an alcyonarian with a brush-like array of flexible, many-branched arms. These colonial animals were common at Site 7, were readily identifiable in the photos, and--due their different growth form--they might be expected to occupy different microhabitats within the pinnacle area. The colony numbers of *Bebryce* sp. in random photo stations at Site 7 are shown in Fig. 10.5. Bathymetric contours at 1-m intervals are overlain with regions of contiguous substrata. A similar display for *A. atlantica* is shown in Fig. 10.6. A number of differences and similarities in the distribution of the two animals are apparent by comparison of these figures. The numbers of *Bebryce* sp. colonies are higher per photo and higher overall than the numbers of *A. atlantica*. Both species are almost entirely absent from the sedimented flat region surrounding the Site 7 pinnacle and have the greatest density in the continuous hard bottom region on the pinnacle top. It appears that *A. atlantica* is more broadly dispersed than *Bebryce*, but this interpretation requires objective testing.

The objective of testing during this phase of the study is to distinguish microhabitat regions in which the two species had clumped versus random distributions. The hypothesis is that if individuals of a species have a clumped distribution within a region, then there are some environmental factors causing them to prefer one part of the region over the rest. To discover what factor or factors is contributing to this preference, one progressively subdivides the region into homogeneous areas through the use of objective criteria and reexamines the distribution of individuals. When a subarea is generated in which the individuals have a random distribution, then the attributes of that subarea describe the species preferred microhabitat.

Indices that distinguish clumped from random distribution (described above) were calculated for the two species; first for the total area of Site 7, then for the photos from the combined areas of continuous hard bottom and monolithic outcrops, then separately for the areas of continuous hard bottom and monolithic outcrops (see Figs. 10.5 and 10.6). These tests are summarized in Table 10.2. The indices give similar results, but are not truly
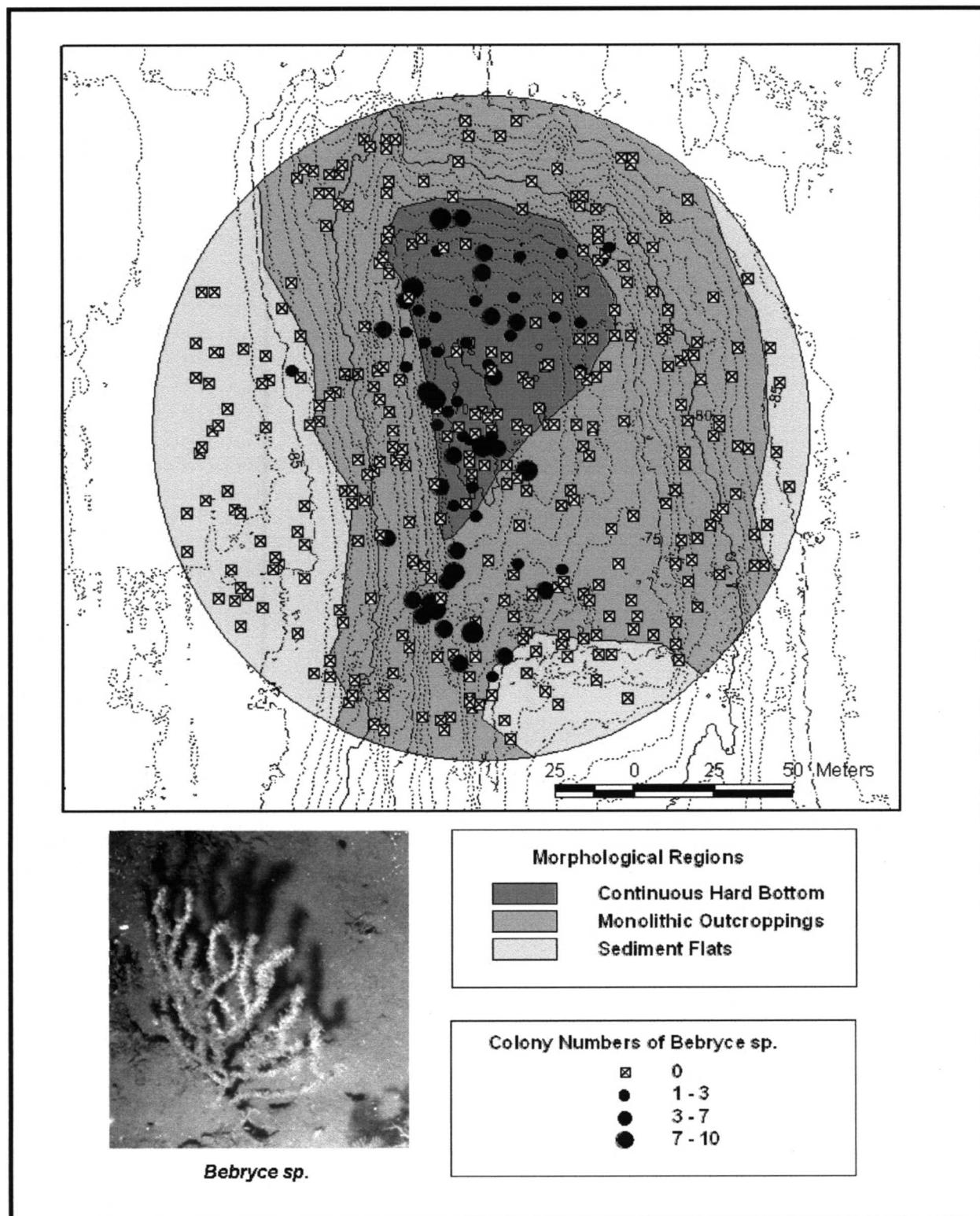
Figure 10.5. Numbers of *Bebryce* sp. in random photo stations from Site 7. Contiguous morphological regions were derived from a combination of video and photo analysis, but correspond to attributes in the photos.

193
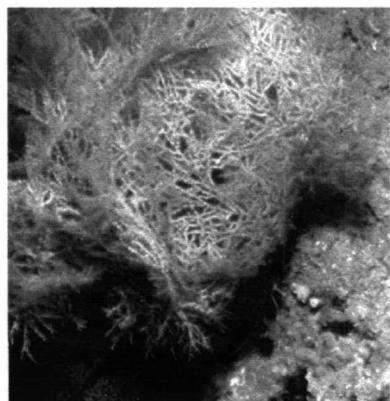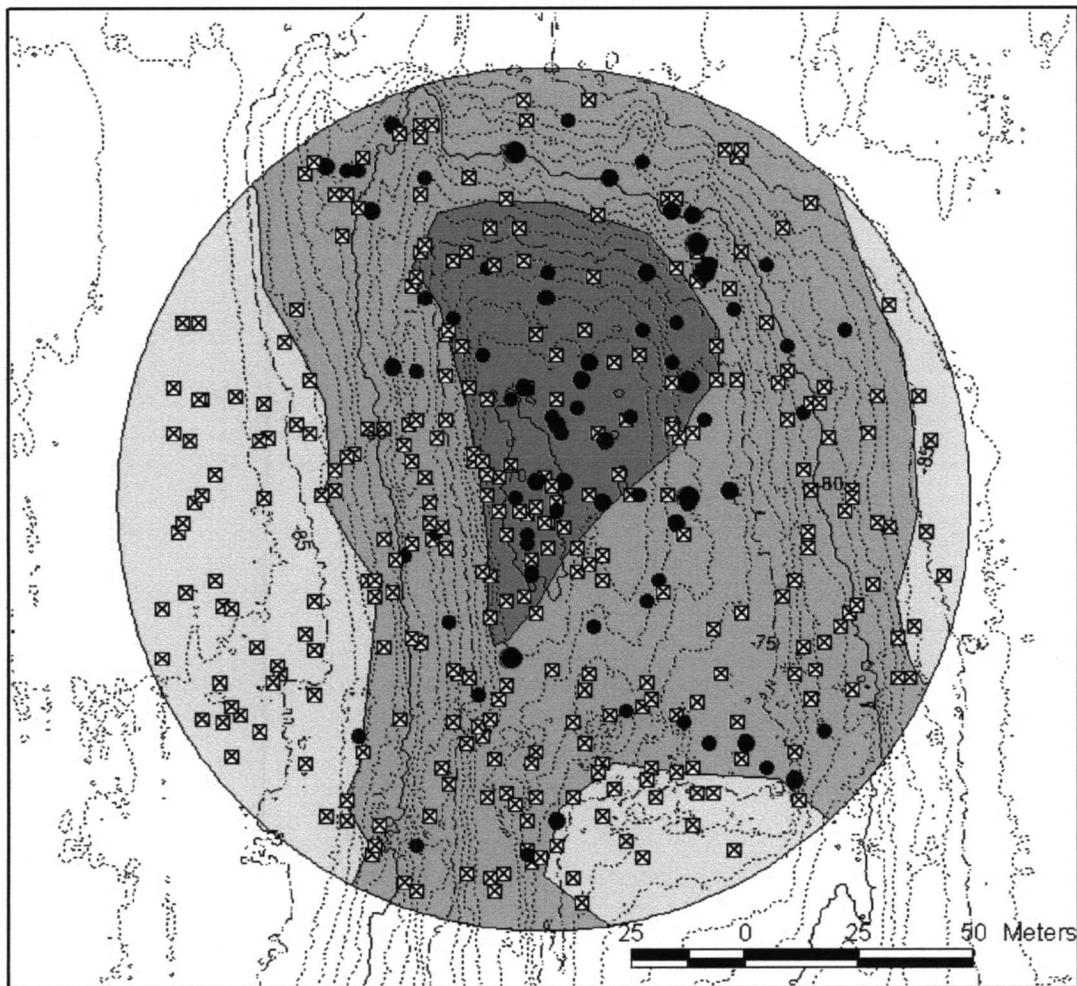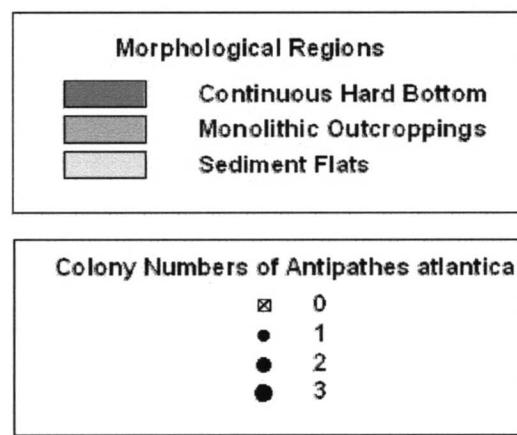
Figure 10.6. Numbers of *Antipathes atlantica* in random photo stations from Site 7. Contiguous morphological regions were derived from a combination of video and photo analysis, but correspond to attributes in the photos.

194

Table 10.2. Indices of dispersion for two octocoral species at Site 7, where ID = index of dispersion, GI = Green's index, and d from Ludwig and Reynolds. Microhabitat regions are described in the text.

Microhabitat Region	*Bebryce* sp.			*Antipathes atlantica*		
	ID	GI	d	ID	GI	d
Total Sampled Area	5.5	0.45	37.7	1.39	0.13	5.00
Combined Areas of Outcropping (monolithic and continuous)	5.4	0.44	32.4	1.30	0.10	3.53
Monolithic Outcropping Region	6.1	0.51	30.5	1.33	0.11	3.18
Continuous Hard Bottom Region	4.0	0.30	12.8	1.17	0.06	1.07

independent because they were computed from the same samples. According to Ludwig and Reynolds (1988) the index of dispersion (ID) indicate uniformity at values near 0, randomness near 1, and maximum clumping approaching the total number of individuals. All values for ID indicates some degree of clumping; *Bebryce* seems to show greater clumping than *A. atlantica*; neither species is shown to approach a random distribution of individuals. ID is not particularly effective for distinguishing the degree of clumping. Green's index (GI), which is often used to compare samples that vary in the number of individuals, sample means, and the number of samples, has a similar range of responses for the two species. There is a marked drop in the GI value for *A. atlantica* within the continuous hard bottom region. Individuals of *Bebryce* are clumped in all subareas. The d index suggests that *A. atlantica* has a random distribution within the region of continuous hard bottom at Site 7, which approximates the pinnacle top. Distribution of *Bebryce* colonies does appear less clumped within the continuous hard-bottom subarea, but a random distribution cannot be accepted at $P<0.05$.

Conclusions and Future Work

The interpretation of these findings is that the continuous hard bottom designation adequately describes the microhabitat for *A. atlantica*. *Bebryce*, in contrast appears to have some preference which is not captured by the classification of substratum. Several cautions should be noted. *Bebryce* sometimes occurred as a large number of small individuals (up to 10 per photo), elsewhere as one or two large individuals. *A. atlantica* is a more solitary species and was never photographed with more than two individuals per station. *Bebryce* would probably never show a random distribution if individual numbers are used as the sampling criterion. A possible alternative would be to use an estimate of colony size--fan width squared for example--as an alternative abundance value. Even with this adjustment, the distribution of points in Fig. 10.5 suggests a greater degree of clumping than that shown by *A. atlantica*. There are probably additional factors that influence their distribution at Site 7. Work in upcoming phases of the study will consider how a combination of substratum and physical factors such as current direction and the effect of topography on local current strength might create additional microhabitats within program study sites. Additional statistical analyses will examine the interaction of species. The distributions of very abundant species, such as *Rhizopsammia manuelensis*, will be examined within individual photos as well.

195

Chapter 11
Companion Study: Epibiont Recruitment

Introduction

The goal of this companion study is to support the descriptive and monitoring portions of the program with experiments (based on testable hypotheses) that define ecological mechanisms responsible for spatial and temporal changes in hard bottom epifauna. Development of an epibiont community is the net result of the interactions between biotic and abiotic processes. Spatial and temporal variation of hard bottom communities are therefore functional responses to biotic and abiotic processes.

There are primarily three biological processes: recruitment, competition, and predation. Recruitment rates involve substrate selection, settlement, and growth of invertebrate larvae onto hard bottom habitats. The most important factor regulating recruitment and recruitment rates in hard bottom habitats is the availability of open space for colonization and competition for that space. Abiotic processes affecting spatial and temporal variability in deep water include abrasion, turbidity and turbulence.

The major elements of the settling plate experiment studies were as follows:

1. Spatial study at four stations to last for one year;
2. Replication of the spatial study during the second year;
3. Two settling surface treatments: hard and soft;
4. Three settling plate treatments: uncaged, caged, and partially-caged;
5. Three heights, or distances from the bottom (0, 2, and 13 m); and
6. Time series study at one station, cruise every year for retrieval.

The temporal experiments (Site 4) were designed to test for differences in recruitment and growth over time. The spatial experiments (Sites 1, 5, and 9) were designed to test for differences among habitats (Table 11.1).

Table 11.1. Time line and sampling schedule for experimental studies. For each cruise, the table gives the study, number of stations being sampled, and the duration of the deployment over the entire study period, where D = deployed, --- = submerged, and R = retrieved.

Study and Locations	Cruise (No., Date, and Months Exposed)									
	1C May 97 0	S1 Jul 97 3	M2 Oct 97 6	S2 Jan 98 9	M3 Apr 98 12	M3 Aug 98 16	S4 Oct 98 18	S5 Jan 99 21	M4 Apr 99 24	M4 Jul-Aug 99 27
Time Series (Site 4)	D	-------	R (B4E)							
	D	-------	-------	-------	-------	R (B4B)				
	D	-------	-------	-------	-------	R (B4G)				
	D	-------	-------	-------	-------	R (B4H)				
	D	-------	-------	-------	-------	R[a]				
	D	-------	-------	-------	-------	-------	------	-------	-------	R
	D	-------	-------	-------	-------	-------	-------	-------	-------	R
	D	-------	-------	-------	-------	-------	-------	-------	-------	R
				D	-------	-------	-------	-------	-------	R
Spatial (Site 1)	D	-------	-------	-------	-------	R				
				D	-------	-------	-------	-------	-------	R
Spatial (Site 5)	D	-------	-------	-------	-------	------[b]	-------	-------	-------	R[b]
				D	-------	-------	-------	-------	-------	R
Spatial (Site 9)	D	-------	-------	-------	-------	R				
				D	-------	-------	-------	-------	-------	R
Total Deployed	11	0	0	4	0	0	0	0	0	0
Total Retrieved	0	0	1	0	0	5	0	0	0	8

[a] Biomooring B4F had no triads attached upon retrieval.

[b] Turbidity prevented retrieval of the Site 5 biomooring on Cruise M3. It was retrieved on Cruise M4.

Methods

Settling plates are arranged in three experimental treatments: an uncaged treatment (U), a caged treatment (C), and a partially caged control treatment (P). The acronyms U, C, and P refer to experimental treatments, which are used to measure ecological processes. The uncaged (U) settling plate measures net recruitment with biotic and abiotic interactions. This includes gross larval settlement, recruitment, growth, and community development (S) and predation and disturbance (D):

$$U = S + D$$

The caged (C) settling plate is the experimental treatment to exclude predators. A common problem with enclosures is that water flow (W) at the settling plate surface is disrupted:

$$C = S + W$$

Therefore, we must add a cage-control treatment to subtract effects due to the enclosure. The control is a partial cage (P) that would have the same effects on water flow, but would allow predators access to the experimental treatment. Thus, the control treatment includes net recruitment (S + D) in addition to water flow interactions (W):

$$P = S + D + W$$

Mathematical combinations of the experimental treatments calculate the effects on rates of recruitment by ecological process; predation (D), water flow (W), and net recruitment (S):

$$W = P - U$$

$$D = P - C$$

$$S = U + C - P$$

The three experimental treatments (U = uncaged, C = caged, and P = partially caged control) are attached to one another forming a "Y"-shaped triad. Each treatment consists of four settling plates, or replicates, that have been attached to the triad (see Continental Shelf Associates, Inc. and Texas A & M University, Geochemical and Environmental Research Group 1998). Three of the replicate settling plates are hard surfaces made of ceramic tiles and the other is a soft surface made of outdoor carpet. Due to shackle failure, all of the biomoorings retrieved to date have been recovered from the sea floor (0 m). In addition, the final orientation of the triads was unknown. Therefore, there is no analysis based on orientation for this report.

Settling plates are preserved in 2% formalin for transport. Once in the lab, each is then put into 50% ethanol solution for storage until analysis. Settling plates are scored for abundance as percent cover by taxa or predetermined category (e.g. 'uncolonized') to the lowest taxonomic level possible. Comparing organisms on the settling plates with organisms found in the video/photographic transects ensures taxonomic validation. A transparent scoring card with 841 cells is placed on the plate. The outside 0.75 cm of

each side of the plate is ignored due to possible shifting of the plates during exposure and retrieval. Presence of a species in any part of a cell counts for the entire cell. The size of non-colonial organisms is also measured. Densities of all solitary organisms were calculated for the first year. Comparisons between treatments within a site are analyzed via ANOVA.

The sum of mean coverages may be much greater than 100% due to overgrowth of polychaetes, bivalves, and bryozoans by other organisms. The top valve of a mollusk, for example, may be covered with part of a zoanthid colony, stolons, hydroid zooids, and cheilostomatous bryozoans while still being able to live and feed. In this case, each organism is counted as covering that particular 14.7 mm^2 area. In another case, hydroids may be living adjacent to a bryozoan colony which is next to a foram. They may all be small enough to fit within a single cell and, therefore, each are counted for that area. As both of these cases occur often over the entire plate, most coverages will add up to over 100%.

The first, preliminary analyses of temporal and spatial differences have been completed. Due to misidentification of a hydroid as a bryozoan, many of the samples will have to be reanalyzed and have not been included in this report. All samples from Site 9 (Biomooring B9A1) and several from Site 4 (Biomooring B4B) have been completed and are reported here, although no firm statistics have been performed for the second year due to an insufficient number of total samples.

The category 'unknown' is comprised of 14 subcategories, 13 of which have been described and are consistently catalogued together. The unknown categories, however, are still unidentified at this time.

The taxa/categories for the second year have been increased to due the ease in identifying the organisms to lower taxonomic categories as they grow. Hydroids and bryozoans, in particular, have been identified to Order but are grouped together here for simplicity.

Results

The results of the first 6-month exposure at Site 4 are reported again here due to reanalysis of the samples (Fig. 11.1). There were no significant differences in coverage between treatments except for Mollusca ($\alpha=0.05$). Note that the category 'uncolonized' still accounts for much of the total coverage of the plates after 6 months. Densities were also analyzed for several solitary organisms. None were significantly affected by the different ecological processes (Table 11.2).

Table 11.2. Average densities (per 92 cm^2) of solitary organisms by treatment (6-month exposure at Site 4).

Taxa	Treatment		
	Caged	Uncaged	Partial Cage
Bivalvia	1.33	0.33	1.22
Polychaeta	6.22	2.22	7.44
Cirripedia	0.00	0.00	0.00
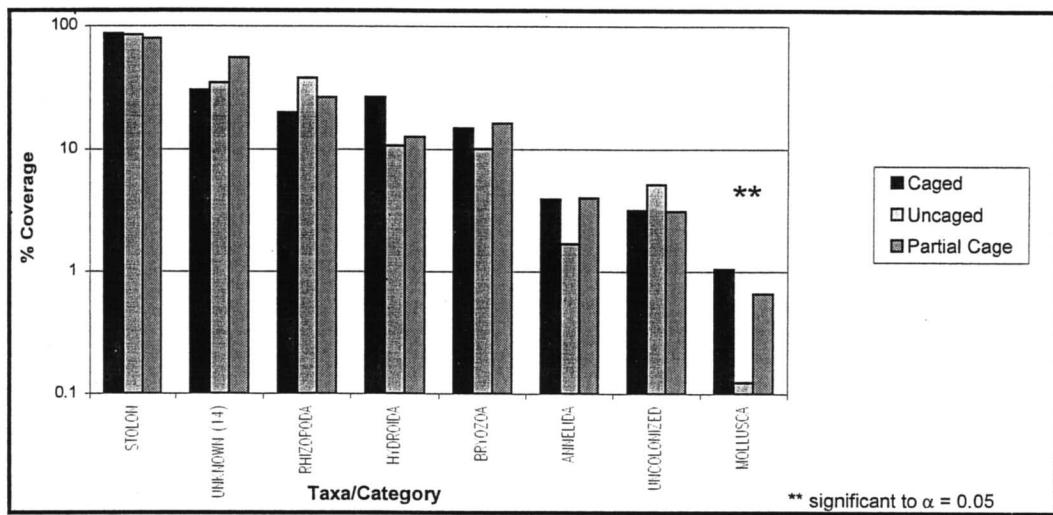
Fig. 11.1. Relative contribution of taxa/category to total coverage of organisms after 6 months at Site 4.

Comparisons of 6-month and 16-month data display the changes that took place in mean coverages over the course of a year (Fig. 11.2). All organisms occupied more space by the second year, except for the stolons of the colonial organisms. There was no uncolonized space free for recruitment by the second year (Fig. 11.2).
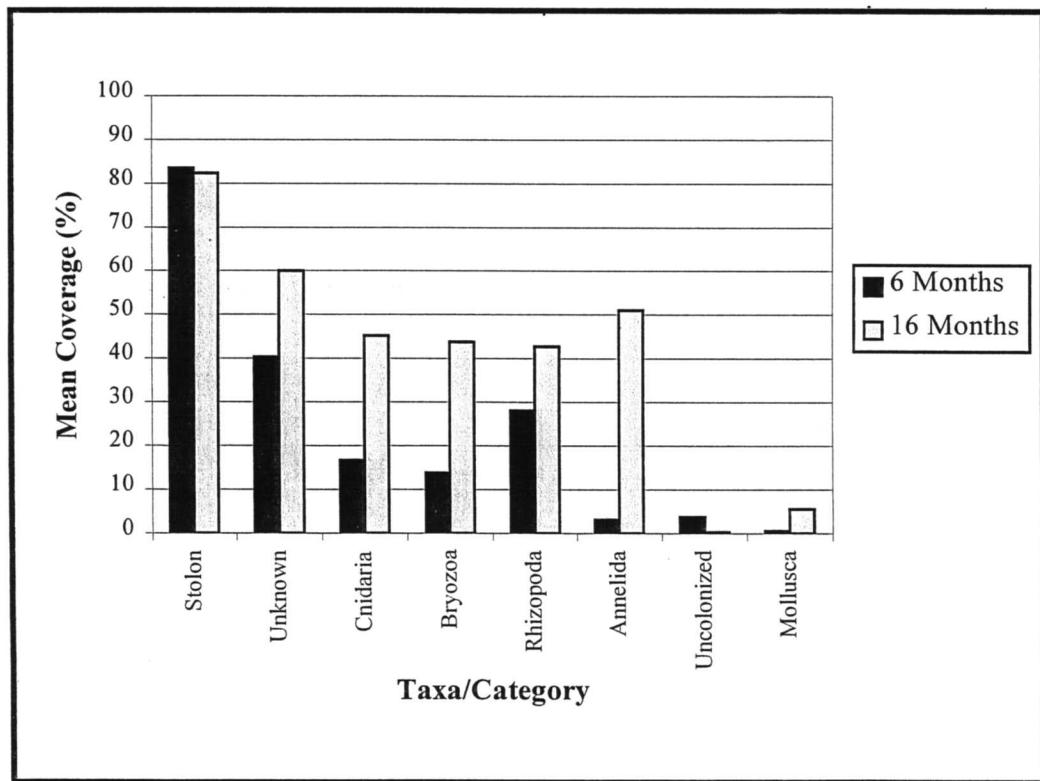
Fig. 11.2. Comparison of temporal differences in mean coverage by taxa/category at Site 4.

201

The biomoorings at both Site 4 and Site 9 were exposed for 16 months and represent the spatial differences that are present within the Pinnacle Habitat (Fig. 11.3). The only striking differences are between Annelida, which are four times greater at Site 4, and Mollusca, which are almost 10 times greater at Site 9. Anthozoa was only consistently present at Site 9, making it the seventh most abundant organism for Site 9.

Tables 11.3 and 11.4 compare the influences that the targeted ecological processes have on each taxa/category by exposure and by site. Both present calculated rates of change in coverage due to each process. Temporal changes are clearly evident under the gross recruitment process, although this may only be relevant to the solitary organisms (Table 11.3). Some organisms, which were suppressed by a given process in the first 6 months, show enhancement by that same ecological process during the second year. The converse also occurs. Ecological processes do not seem to have very similar effects among sites, but final statistical analysis of all the corrected samples are necessary to determine final conclusions.

Total coverage of each taxa/category changed due to ecological processes by site (Table 11.4). Large differences between the rates of all ecological processes at Sites 4 and 9 exist. For example, both annelids and hydroids are negatively affected at both sites by water flow disruption. However, annelids are inhibited by several orders of magnitude more at Site 4, while at Site 9 hydroids are more severely affected. The same is true for disturbance. Bryozoans are positively affected at both sites, but are enhanced 18 times more at Site 9 than at Site 4. In general, colonial organisms are favored at Site 9 while the solitary organisms are favored at Site 4.
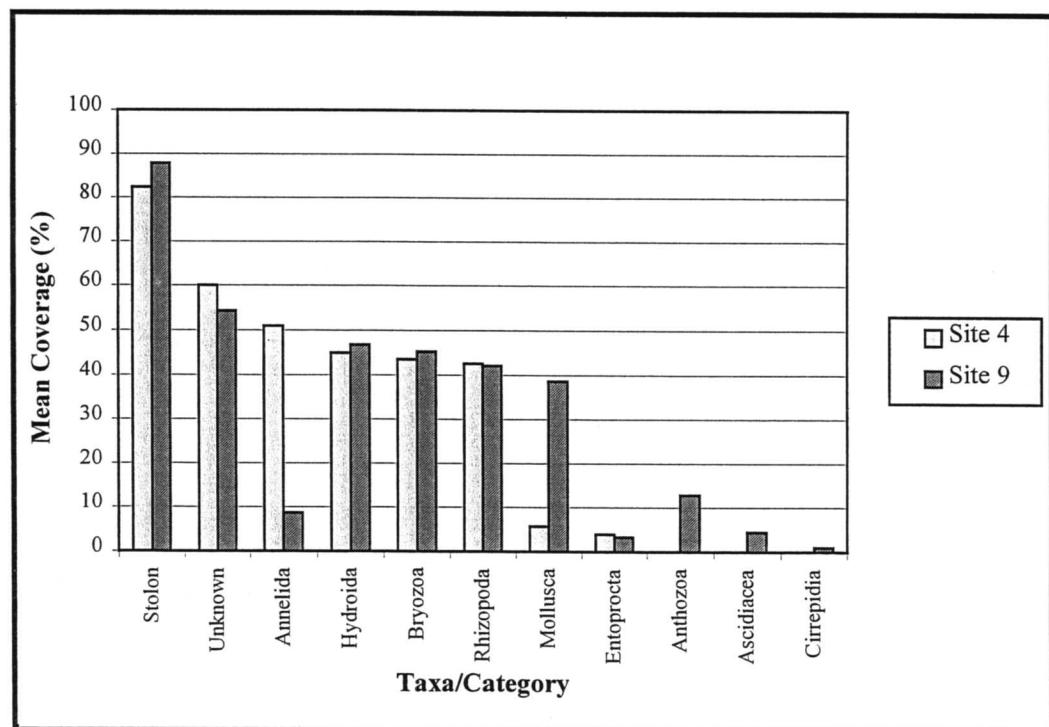

Fig. 11.3. Comparison of spatial differences in mean coverage by taxa/category.

Table 11.3. Temporal comparison (exposure in months) of change in coverage (Δ cm^2) due to ecological processes within Site 4.

Taxa/Category	Ecological Process By Exposure					
	Flow Disruption		Disturbance		Gross Recruitment	
	6 mo.	16 mo.	6 mo.	16 mo.	6 mo.	16 mo.
Stolon	-4.64	12.79	-6.50	25.14	80.53	50.20
Unknown	18.09	15.88	22.00	31.16	8.49	23.59
Cnidaria	1.68	22.64	-12.23	53.43	21.61	48.44
Bryozoa	5.44	-19.11	1.18	2.21	7.62	51.45
Rhizopoda	-10.30	59.24	5.71	18.30	27.69	-12.35
Annelida	2.05	-40.72	0.08	-14.04	1.38	83.42
Uncolonized	-1.80	0.00	-0.05	-1.03	4.57	1.03
Mollusca	0.48	-11.25	-0.73	-1.76	0.84	13.97

Table 11.4. Comparison of change in coverage (Δ cm^2) between Sites 4 and 9 due to ecological processes during a 16-month exposure.

Taxa/Category	Ecological Process By Site					
	Flow Disruption		Disturbance		Gross Recruitment	
	B4B	B9A1	B4B	B9A1	B4B	B9A1
Stolon	12.79	-14.42	25.14	-10.24	50.20	97.13
Unknown	15.88	-3.94	31.16	-4.03	23.59	55.23
Annelida	-40.72	-0.02	-14.04	6.19	83.42	3.87
Hydroida	-5.07	-31.53	25.87	-19.33	27.49	89.74
Bryozoa	-19.11	2.13	2.21	34.55	51.45	22.56
Rhizopoda	59.24	3.28	18.30	8.31	-12.35	31.03
Mollusca	-11.25	16.67	-1.76	9.45	13.97	18.06
Entoprocta	8.97	-0.22	7.35	-1.77	-7.20	4.37
Anthozoa	0.07	16.03	-0.07	10.67	0.15	-6.00
Ascidiacea	0.00	-0.20	0.22	2.80	0.07	2.38
Cirripedia	0.00	1.76	0.00	1.34	0.00	-1.14

Discussion

The results of the epibenthic recruitment study to date have revealed several interesting points. First, early successional-stage epibenthic communities do not appear to be influenced strongly by ecological processes. During the first 6-month exposure there were no significant differences in coverage within any taxa/category except for Mollusca (Fig. 11.1). This indicates it is solitary organisms which are more susceptible to ecological effects in early successional stages than are colonial organisms. This is in agreement with much of the literature on colonial versus solitary life history strategies

(Jackson 1977; Buss 1979). The other organisms, which dominate the plates and show no differences at an early stage, are largely all colonial or aggregating species. This trend indicates recruitment rates of solitary and colonial organisms are affected by different ecological processes.

Jackson (1977) points out that many early stage communities on coral reefs are dominated by colonial organisms, typically covering more than 95% of the substrata. This can be attributed to their ability to reproduce and grow asexually, which may be a more successful life strategy in a highly dynamic environment. Solitary organisms, if presented with new space to colonize, must typically wait to sexually reproduce and therefore often lose out on the opportunity. Colonial organisms, on the other hand, are better able to colonize empty space almost immediately and can recover quickly from a disturbance event, such as scouring or predation. This is apparently true in the Pinnacle Habitat as well. The most abundant organisms are colonial and are not severely affected by the processes of water flow disruption and disturbance (Tables 11.3 and 11.4).

The organisms found that do have negative effects from water flow disruption are, for the most part, both active and passive suspension feeders (Tables 11.3 and 11.4). Water flow disruption, caused by the cages, may somewhat inhibit feeding rates among these animals and lead to a decrease in mean coverage over time (Table 11.3). This is inconclusive, however, because not all taxa or categories follow the trend towards complete inhibition by disrupted water flow. For instance, processes do not affect densities of bivalves, polychaetes, and barnacles in the early stages of community development when they would seem to have the most impact (Table 11.2).

In the early community, disturbance negatively affects "soft bodied" organisms more than organisms with exoskeletons (Table 11.3). The later community demonstrates an opposite trend, however, leading to a preliminary conclusion that Cnidaria and other stoloniferous organisms have developed defenses to a degree that predation is prevented. Gross recruitment rates are high and generally increase over the 16-month exposure time (Table 11.3). The decrease in stolons over time may be due to changing resource allocation in the colonial organisms. Once coverage approaches 100% of the plate, hydroids, bryozoans, and entoprocts may put more energy into developing reproductive or feeding units (Crisp 1979; Shelton 1979). The decrease in Rhizopoda over time may be due to the interference of resident organisms during the settlement of foraminifers (Table 11.3).

Disturbance effects are largely apparent in organisms with exoskeletons or protective coverings at Site 4 but are more pronounced in organisms without any skeletal protection at Site 9 (Table 11.4). A hypothesis to explain higher disturbance effects on protected taxa at Site 4 is higher predation rates at that site, while higher disturbance effects on organisms without external protection at Site 9 can be explained by higher scouring rates. Part of this hypothesis is supported by evidence that mass sediment flux was much higher at Site 9 than at Site 4 (see Chapter 5). Gross recruitment rates are high at both Sites 4 and 9. There is no definite trend for one site to be more fecund than the other, although there may be more diversity at Site 9 (Table 11.4).

204

Literature Cited

Baker, E.T. and J.W. Lavelle. 1984. The effect of particle size on the light attenuation coefficient of natural suspensions. J. Geophys. Res. 89:8,197-8,203.

Bartz, R., H. Pak, and J.R.V. Zaneveld. 1978. A transmissometer for profiling and moored observations in water. Proc. Soc. Photo-Opt. Instr. Engineers, Ocean Optics V, 160:102-108.

Boehm, P.D. and A.G. Requejo. 1986. Overview of the recent sediment hydrocarbon geochemistry of Atlantic and Gulf Coast over continental shelf environments. Est. Coast. Shelf. Sci. 23:29-58.

Boesch, D.F. and N.N. Rabalais. 1987. Long-term environmental effects of offshore oil and gas development. Elsevier Applied Science Publishers Ltd., England. 708 pp.

Bohnsack, J.A. 1976. An investigation of a photographic method for sampling hard-bottom benthic communities. M.S. Thesis, University of Miami. 188 pp.

Bohnsack, J.A. 1979. Photographic quantitative sampling of hard-bottom communities. Bull. Mar. Sci. 29(2):242-252.

Boland, G.S., B.J. Gallaway, J.S. Baker, and G.S. Lewbel. 1983. Ecological effects of energy development on reef fish of the Flower Garden banks. Final Report to National Marine Fisheries Service, Galveston Laboratory by LGL Ecological Research Associates. 466 pp.

Boothe, P.N. and W.D. James. 1985. Neutron activation analysis of barium in marine sediments from the north central Gulf of Mexico. J. Trace and Microprobe Techniques 3:377-399.

Boothe, P.N. and B.J. Presley. 1987. The effects of exploratory petroleum drilling in the northwest Gulf of Mexico on trace metal concentrations in near rig sediments and organisms. Environ. Geol. Water Sci. 9:173-182.

Brassell, S.C., G. Eglinton, J.R. Maxwell, and R.P. Philip. 1978. Natural background of alkanes in the aquatic environment, pp. 69-86. In: O. Huntzinger, L.H. van Lelyveld, and B.C.J. Zoetman (eds.). Aquatic Pollutants, Transformations and Biological Effects. Oxford, Pergamon Press.

Bray, J.R. and J.T. Curtis. 1957. An ordination of the upland forest communities of southern Wisconsin. Ecological Monographs 27:325-349.

Bright, T.J. and L.H. Pequegnat (eds). 1974. Biota of the West Flower Garden Bank. Gulf Publishing Company, Houston, TX. 435 pp.

Brooks, J.M. (ed.). 1991. Mississippi-Alabama continental shelf ecosystem study: data summary and synthesis, Volume I: Executive Summary; Volume II: Technical Narrative; Volume III: Appendices, Part 1 (Appendices A-D), Volume III: Part 2, (Appendix E). OCS Study MMS 91-0062 (I), 91-0063 (II), 91-0064 (III). U.S. Department of the Interior, Minerals Management Service, Gulf of Mexico OCS Region, New Orleans, LA. 43 pp. (I), 862 pp. (II), 1,001 pp. (III-1), and 1,001 pp. (III-2).

Buss, L.W. 1979. Habitat selection, directional growth, and spatial refuges: why colonial animals have more hiding places, pp. 459-497.. In: G. Larwood and B.R. Rosen (eds.), Systematics Association Special Volume No. 11, *Biology and Systematics of Colonial Organisms*. London, Academic Press.

Carricart-Ganivet, J.P., G. Horta-Puga, M.A. Ruiz-Zarate, and E. Ruiz-Zarate. 1994.
Retrospective determination of growth in the hermatypic coral *Monastrea annularis*
(Scleractinia: Faviidae) in reefs of the Gulf of Mexico. Revista de Biologia Tropical
42(3):515-521.

Cashman, C.W. 1973. Contributions to the ichthyofauna of the West Flower Garden reefs and
other reef sites in the Gulf of Mexico and western Caribbean. Ph.D. Dissertation, Texas
A&M Univ., College Station, TX. 247 pp.

Chow, T.J. and C.B. Snyder. 1981. Barium in marine environment: a potential indicator of
drilling contamination, pp. 691-722. In: Proceedings on Research on Environmental Fate
and Effects of Drilling Fluids and Cuttings Symposia. Lake Buena Vista, Florida, 21-23
January 1980.

Colin, P.L. 1974. Observation and collection of deep-reef fishes off the coasts of Jamaica and
British Honduras (Belize). Mar. Biol. 24:29-38.

Colin, P.L. 1976. Observations of deep-reef fishes in the Tongue-of-the-Ocean, Bahamas. Bull.
Mar. Sci. 26(4):603-604.

Continental Shelf Associates, Inc. 1983. Environmental monitoring program for Exploratory
Well No. 3, Lease OCS-G 3316, Block A-384, High Island Area, South Extension near
the West Flower Garden Bank. Draft Final Report to Union Oil Company. 2 volumes.

Continental Shelf Associates, Inc. 1985a. Live-bottom survey of drillsite locations in Destin
Dome Area Block 617. Report to Chevron U.S.A., Inc. 40 pp. + app.

Continental Shelf Associates, Inc. 1985b. Environmental monitoring program for Platform "A",
lease OCS-G 2759, High Island Area, South Extension, East Addition, Block A-389 near
the East Flower Garden Bank. Final Report to Mobil Producing Texas and New Mexico,
Inc., Houston, TX. 3 volumes.

Continental Shelf Associates, Inc. 1987. Live bottom survey for Destin Dome Area Lease Block
57. A final report prepared for Conoco, Inc.

Continental Shelf Associates, Inc. 1989. Fate and effects of drilling fluid and cutting discharges
in shallow nearshore waters. Prepared for the American Petroleum Institute. 129 pp.

Continental Shelf Associates, Inc. 1992. Mississippi-Alabama Shelf Pinnacle Trend Habitat
Mapping Study. OCS Study MMS 92-0026. U.S. Department of the Interior, Minerals
Management Service, Gulf of Mexico OCS Region, New Orleans, LA. 75 pp. + app.

Continental Shelf Associates, Inc. and Texas A & M University, Geochemical and Environmental
Research Group. 1998. Northeastern Gulf of Mexico Coastal and Marine Ecosystem
Program: Ecosystem Monitoring, Mississippi/Alabama Shelf; Second Annual Interim
Report. U.S. Department of the Interior, U.S. Geological Survey, Biological Resources
Division, USGS/BRD/CR-1998-0002 and Minerals Management Service, Gulf of
Mexico OCS Region, New Orleans, LA. OCS Study MMS 98-0044. 198 pp.

Crisp, D.J. 1979. Dispersal and re-aggregation in sessile marine invertebrates, particularly
barnacles. In: Systematics Association Special Volume No. 11, *Biology and Systematics
of Colonial Organisms*, G. Larwood and B.R. Rosen, eds. London, Academic Press, pp.
319-327.

Darnell, R. 1991. Summary and synthesis, pp. 15-1 to 15-144. In: Brooks, J.M. (ed.),
Mississippi-Alabama Continental shelf ecosystem study: Data Summary and Synthesis.
Vol. II: Technical Narrative. OCS Study MMS 91-0063. U.S. Department of the Interior,
Minerals Management Service, Gulf of Mexico OCS Region, New Orleans, LA. 862 pp.

Dennis, G.D. and T.J. Bright. 1988a. Reef fish assemblages on hard banks in the northwestern Gulf of Mexico. Bull. Mar. Sci. 43(2):280-307.

Dennis, G.D. and T.J. Bright. 1988b. New records of fishes in the northern Gulf of Mexico, with notes on some rare species. N.E. Gulf Sci. 10(1):1-18.

Folk, R.L. 1974. Petrology of sedimentary rocks. Hemphill Publishing Co., Austin, TX. 184 pp.

Gardner, W.D. and I.D. Walsh. 1990. The role of aggregates in horizontal and vertical flux across a continental margin. Deep-Sea Res. 37:401-412.

Gardner, W.D., M.J. Richardson, K.R. Hinga, and P.E. Biscaye. 1983. Resuspension measured with sediment traps in a high-energy environment. Earth Planet. Sci. Lett. 66:262-278.

Gardner, W.D., P.E. Biscaye, J.R.V. Zaneveld, and M.J. Richardson. 1985. Calibration and comparison of the LDGO nephelometer and the OSU transmissometer on the Nova Scotian Rise. Mar. Geol. 66:323-344.

Gardner, W.D., S.P. Chung, M.J. Richardson, and I.D. Walsh. 1995. The oceanic-mixed layer pump. Deep-Sea Res. pt. II 42:757-776.

Genin, A., P.K. Dayton, P.F. Lonsdale, and F.N. Spiess. 1986. Corals on seamount peaks provide evidence of current acceleration over deep-sea topography. Nature 322:59-61.

Gili, J.M., J. Murillo, and J. Ros. 1989. The distribution of benthic cnidarians in the Western Mediterranean. Scientia Marina 53(1):19-35.

Gilmore, R.G., C.J. Donahoe, and D.W. Cooke. 1987. Fishes of the Indian River Lagoon and adjacent waters, Florida. Harbor Branch Foundation Tech. Rep. 41. 68 pp.

Gittings, S., T. Bright , and W. Schroeder. 1991. Topographic features characterization - biological, pp. 13-1 to 13-117. In: J.M. Brooks (ed.), Mississippi-Alabama Continental Shelf Ecosystem Study: Data Summary and Synthesis. Volume II: Technical Narrative. OCS Study MMS 91-0063. U.S. Department of the Interior, Minerals Management Service, Gulf of Mexico OCS Region, New Orleans, LA.

Gittings, S.R., T.J. Bright, W.W. Schroeder, W.W. Sager, J.S. Laswell, and R. Rezak. 1992. Invertebrate assemblages and ecological controls on topographic features in the northeast Gulf of Mexico. Bull. Mar. Sci. 50(3):435-455.

Gordon, H.R., R.C. Smith, and J.R.V. Zaneveld. 1984. Introduction to ocean optics. SPIE Ocean Optics 489:2-41.

Hardin, D.D., E. Imamura, D.A. Coats, and J.F. Campbell. 1993. A survey of prominent anchor scars and the level of disturbance to hard-substrate communities in the Point Arguello region. Report to Chevron U.S.A Production Company, Ventura, CA. 58 pp.

Hardin, D.D., J. Toal, T. Parr, P. Wilde, and K. Dorsey. 1994. Spatial variation in hard-bottom epifauna in the Santa Maria Basin: The importance of physical factors. Marine Environmental Research 37(2):165–193.

Houghton, J.P., D.L. Beyer, and E.D. Thielk. 1981. Effects of oil well drilling fluids on several important Alaskan marine organisms, pp. 1,017-1,043. In: Proceedings on Research on Environmental Fate and Effects of Drilling Fluids and Cuttings Symposia. Lake Buena Vista, Florida, 21-23 January 1980.

Hyland, J., D. Hardin, D. Coats, R. Green, M. Steinhauer, and J. Neff. 1994. Impacts of offshore oil and gas development on the benthic environment of the Santa Maria Basin. Marine Environmental Research 37:195–229.

Jackson, J.B.C. 1977. Competition on marine hard substrata: the adaptive significance of solitary and colonial strategies. The American Naturalist 111(980):743-767.

Jerlov, N.G. 1976. Marine optics. Elsevier Applied Science Publishers Ltd., NY.

Johnson, H.P. and M. Helferty. 1990. The geological interpretation of side-scan sonar. Rev. of Geophys. 28:357-380.

Kelly, F.J. 1991. Physical oceanography/water mass characterization, pp. 10-1 to 10-151. In: Mississippi-Alabama Continental Shelf Ecosystem Study: Data Summaries and Synthesis. Volume II: Technical Narrative. OCS Study MMS 91-0063. U.S. Department of the Interior, Minerals Management Service, Gulf of Mexico OCS Region, New Orleans, LA.

Kendall, J.J. 1990. Detection of effects at long-term production sites, pp. 23-28. In: R.S. Carney (ed.). Northern Gulf of Mexico Environmental Studies Planning Workshop. Proceedings of a workshop held in New Orleans, Louisiana, 15-17 August 1989. Prepared by Geo-Marine, Inc. OCS Study MMS 90-0018. U.S. Department of the Interior, Minerals Management Service, Gulf of Mexico OCS Region, New Orleans, LA. 156 pp.

Kennicutt, M.C., II (ed.). 1995. Gulf of Mexico offshore operations monitoring experiment, Phase I: Sublethal responses to contaminant exposure. Final Report. OCS Study MMS 95-0000. U.S. Department of the Interior, Minerals Management Service, Gulf of Mexico OCS Region, New Orleans, LA. 739 pp.

Kennicutt, M.C. II and P. Comet. 1992. Resolution of sediment hydrocarbon sources: Multiparameter approaches, pp. 308-337. In: J.K. Whelan and J.W. Farrington (eds.), Organic productivity, accumulation, and preservation in recent and ancient sediments. Columbia University Press.

Kennicutt, M.C. II, P.N. Boothe, T.L. Wade, S.T. Sweet, R. Rezak, F.J. Kelly, J.M. Brooks, B.J. Presley, and D.A. Wiesenburg. 1996. Geochemical patterns in sediments near offshore production platforms. Can. J. Fish. Aquat. Sci. 53:2254-2566.

Kindinger, J.L. 1988. Seismic stratigraphy of the Mississippi-Alabama shelf and upper continental slope. Mar. Geol. 83:79-94.

Kindinger, J.L. 1989. Depositional history of the Lagniappe Delta, Northern Gulf of Mexico. Geo-Mar. Lett. 9:59-66.

Lake Buena Vista Symposium. 1981. Research on environmental fate and effects of drilling fluids and cuttings: Volumes 1 and 2. January 21-24, 1980, Lake Buena Vista, FL. 1,122 pp.

Laswell, J.S., W.W. Sager, W.W. Schroeder, K.S. Davis, and R. Rezak. 1992. High-resolution geophysical mapping of the Mississippi-Alabama outer continental shelf, pp. 155-192. In: R. Geyer (ed.), Geophysical Exploration at Sea. CRC Press, Boca Raton, FL.

Lauenstein, G.G., A.Y. Cantillow, and S.S. Dolvin. 1993. Benthic surveillance and mussel watch projects analytical protocols 1984-1992, pp. III-151 to III-185. In: NOAA Technical Memorandum NPS ORCA. NOAA, Silver Spring, MD.

Ludwick, J.C. and W.R. Walton. 1957. Shelf-edge, calcareous prominences in the northeastern Gulf of Mexico. Amer. Assoc. Petrol. Geol. Bull. 41(9):2054-2101.

Ludwig, J. and J. Reynolds. 1988. Statistical ecology: A primer on methods and computing. John Wiley & Sons, NY. 337 pp.

Messing, C.G., A.C. Neumann, and J.C. Lang. 1990. Biozonation of deep-water lithoherms and associated hardgrounds in the northeast Straits of Florida. Palaios 5:15-33.

Middleditch, B.S. 1981. Environmental effects of offshore production. The Buccaneer Gas and Oil Field Study. Plenum Press, New York. 446 pp.

Miller, G.C. and W.J. Richards. 1980. Reef fish habitat, faunal assemblages, and factors determining distributions in the South Atlantic Bight, pp. 114-130. In: Proc. Gulf. Carib. Fish. Inst., 32nd Annual Meeting.

Mitchum, R.M., Jr. and P. R. Vail. 1977. Seismic stratigraphy and global changes of sea level, part 7: seismic stratigraphic interpretation procedure, pp. 135-143. In: C.E. Payton (ed.), Seismic Stratigraphy - Applications to Hydrocarbon Exploration, Memoir 26. Amer. Assoc. Petrol. Geol., Tulsa, OK.

Moody, J.A., B. Butman, and M.H. Bothner. 1986. Estimates of near-bottom suspended-matter concentration during storms. Cont. Shelf Res. 7:609-628.

Morel, A. 1974. Optical properties of pure water and pure sea water, pp. 1-24. In: N. Jerlov and E. Steeman Nielsen (eds.), Optical Aspects of Oceanography. Academic Press, NY.

Mortensen, P.B. and H.T. Rapp. 1998. Oxygen and carbon isotope ratios related to growth line patterns in skeletons of *Lophelia pertusa* (L) (Anthozoa, Scleractinia): Implications for determination of linear extension rates. Sarsia 83(5):433-446.

Pak H., D.A. Kiefer, and J.C. Kitchen. 1988. Meridional variations in the concentration of chlorophyll and microparticles in the North Pacific Ocean. Deep-Sea Res. 35:1,151-1,171.

Parker, R.O., Jr. and R.W. Mays. 1998. Southeastern United States deepwater reef fish assemblages, habitat characteristics, catches, and life history summaries. NOAA Tech. Rep. 138. 41 pp.

Parker, R.O. and S.W. Ross. 1986. Observing reef fishes from submersibles off North Carolina. N.E. Gulf Sci. 8(1):31-50.

Parker, N.R., P.V. Mladenov, and K.R. Grange. 1997. Reproductive biology of the antipatharian black coral *Antipathes fiordensis* in Doubtful Sound, Fiordland, New Zealand. Mar. Biol. 130(1):11-22.

Pequegnat, W.E. 1964. The epifauna of a California siltstone reef. Ecology 45:272-283.

Phillips, N.W., D.A. Gettleson, and K.D. Spring. 1990. Benthic biological studies of the southwest Florida shelf. Am. Zool. 30:65-75.

Philp, R.P. 1985. Fossil fuel biomarkers: Application and spectra. Methods in geochemistry and geophysics. Elsevier, NY. 294 pp.

Riggs, S.R., S.W. Snyder, A.C. Hine, and D.L. Mearns. 1996. Hardbottom morphology and relationship to the geologic framework: Mid-Atlantic continental shelf. Jour. Sediment. Res. 66:830-846.

Rubinstein, N.I., R. Rigby, and C.N. D'Asaro. 1981. Acute and sublethal effects of whole used drilling fluids on representative estuarine organism, pp. 828-846. In: Proceedings on Research on Environmental Fate and Effects of Drilling Fluids and Cuttings Symposia. Lake Buena Vista, Florida, 21-23 January 1980.

Sager, W.W., W.W. Schroeder, J.S. Laswell, K.S. Davis, R. Rezak, and S.R. Gittings. 1992. Topographic features of the Mississippi-Alabama outer continental shelf and their implications for sea level fluctuations during the Late Pleistocene-Holocene transgression. Geo-Mar.Lett. 12:41-48.

Sager, W.W., W.W. Schroeder, K.S. Davis, and R. Rezak. 1999. A tale of two deltas: seismic mapping of near surface sediments on the Mississippi-Alabama outer shelf and implications for recent sea level fluctuations. Mar. Geol. 160:119-136.

Shelton, G.A.B. 1979. Co-ordination of behaviour in cnidarian colonies, pp. 141-154. In: G. Larwood and B.R. Rosen (eds.), Systematics Association Special Volume No. 11, *Biology and Systematics of Colonial Organisms*. London, Academic Press.

Shipp, R.L. and T.S. Hopkins. 1978. Physical and biological observations of the northern rim of the De Soto Canyon made from a research submersible. Northeast Gulf Sci. 2(2):113-121.

Smith, G.B. 1976. The ecology and distribution of the eastern Gulf of Mexico reef fishes. FL Dept. Nat. Res. Mar Res. Pub. 19:1-78.

Smith, G.B., H.M. Austin, S.A. Bortone, R.W. Hastings, and L.H. Ogren. 1975. Fishes of the Florida Middle Ground with comments on ecology and zoogeography. FL Dept. Nat. Res. Mar. Res. Pub. 9:1-14.

Sonnier, F., H.D. Hoese, and J. Teerling. 1976. Observations on the offshore reef and platform fish fauna of Louisiana. Copeia (1):105-111.

Southwest Research Institute. 1978. ecological investigations of petroleum production platforms in the Central Gulf of Mexico. Report Prepared for the U.S. Department of Commerce.

Spinrad R.W., J.R.V. Zaneveld, and J. C. Kitchen. 1983. A study of the optical characteristics of the suspended particles in the benthic boundary layer of the Scotian Rise. J. Geophys. Res. 88:7641-7645.

Swartz, R.C. 1978. Techniques for sampling and analyzing the marine macrobenthos. U.S. Dept. of Commerce Nat. Tech. Info. Service, PB-281 631. Corvallis Env. Res. Lab., OR.

Sydow, J. and H.H. Roberts. 1994. Stratigraphic framework of a late Pleistocene shelf-edge delta, Northeast Gulf of Mexico. Amer. Assoc. Petrol. Geol. Bull. 78:1,276-1,312.

Taylor, B.J. and B.J. Presley. 1998. TERL trace element quantification techniques, pp. 32-73. In: Sampling and Analytical Methods of the National Status and Trends Program, Mussel Watch Project: 1993-1996 update. NOAA Technical Memorandum NOS ORCA 130.

Tornberg, L.D., E.D. Thielk, R.E. Nakatani, R.C. Miller, and S.O. Hillman. 1981. Toxicity of drilling fluids to marine organisms in the Beaufort Sea, Alaska, pp. 997-1,016. In: Proceedings on Research on Environmental Fate and Effects of Drilling Fluids and Cuttings Symposia. Lake Buena Vista, Florida, 21-23 January 1980.

Wade, T.L., E.L. Atlas, J.M. Brooks, M.C. Kennicutt II, R.G. Fox, J. Sericano, B. Garcia-Romero, and D. DeFreitas. 1988. NOAA Gulf of Mexico status and trends program: Trace organic contaminant distribution in sediments and oysters. Estuaries 11:171-179.

Walsh, I.D. 1990. Project CATSTIX: Camera, transmissometer, and sediment trap integration experiment. Ph. D. Dissertation, Texas A&M University, College Station, TX.

Walsh, I.D. and W.D. Gardner. 1992. A comparison of aggregate profiles with sediment trap fluxes. Deep-Sea Res. 39:1817-1834.

Walsh, I., K. Fischer, D. Murray, and J. Dymond. 1988. Evidence for resuspension of rebound particles from near-bottom sediment traps. Deep-Sea Res. 35:59-70.

Walsh, I.D., S.P. Chung, M.J. Richardson, and W.D. Gardner. 1995. The Diel Cycle in the integrated particle load in the equatorial Pacific: a comparison with primary production. Deep-Sea Res. pt. II 42:465-478.

Wessel, P. and W.H.F. Smith. 1995. New version of the Generic Mapping Tools released. EOS, Trans. AGU 76:329.

Zhang, Y. 1997. Sedimentation and resuspension across the central Louisiana inner shelf. Ph.D. Dissertation, Texas A&M University, College Station, TX. 171 pp.

U.S. Department of the Interior
U.S. Geological Survey
Biological Resources Division

As the Nation's principal conservation agency,
the Department of the Interior has responsibility
for most of our nationally owned public lands and
natural resources. This responsibility includes
fostering the sound use of our lands and water
resources; protecting our fish, wildlife, and
biological diversity; preserving the environmental
and cultural values of our national parks and
historical places; and providing for enjoyment of
live through outdoor recreation. The Department
assesses our energy and mineral resources and
works to ensure that their development is in the
best interests of all our people by encouraging
stewardship and citizen participation in their care.
The Department also has a major responsibility
for American Indian reservation communities.